IDENTIFICATION OF POTENTIAL MECHANISMS OF ACTION OF 3′,4′,5′-TRIMETHOXYFLAVONOL IN THE INHIBITION OF PROSTATE CANCER

Thesis submitted for the degree of

Doctor of Philosophy

at the University of Leicester

by

Cordella, Uleta, Fiona, Kelly Hill, BSc, MSc

Department of Cancer Studies

University of Leicester

September 2015

Abstract

Identification of potential mechanisms of action of 3′,4′,5′-trimethoxyflavonol in the inhibition of prostate cancer

C. U. F. Kelly Hill

3′,4′,5′-Trimethoxyflavonol (TMFol), a synthetic analogue of the naturally occurring flavonols quercetin and fisetin, has demonstrated putative anti-cancer activity in the prostate. The mechanisms of action that are engaged are largely unknown. Therefore, the work presented in this thesis investigated the mechanisms used by TMFol to compromise cell proliferation in prostate cell lines 22Rv1, PC-3 and PNT2. Furthermore, it investigated the effect of TMFol on prostate cancer development and progression in two separate transgenic models, $PB^{Cre4}p53^{flox}Rb^{flox}$ and $PB^{Cre4}Pten^{flox}$ mice.

Apoptosis and cell cycle distribution were analysed by flow cytometry, while biochemical assays, Western blots, histological evaluations or qPCR were used to analyse senescence, changes in prostate metabolism and the effect of TMFol on mice.

TMFol inhibited cell proliferation *in vitro* without inducing apoptosis. However the reduction in tumour growth in 22Rv1 xenografts, that were fed a 0.2 % TMFol diet, was associated with a significant increase in cleaved caspase-3 staining, an indicator of apoptosis. There was S phase arrest in the PC-3 and PNT2 cells, while there was an increase in senescence-associated β-galactosidase activity in both 22Rv1 and PC-3 cells. TMFol also caused a significant increase in the protein expression of p21 and p53 in 22Rv1 cells. TMFol significantly inhibited the expression of acetyl-CoA carboxylase at the protein and mRNA levels and the expression and activity of mitochondrial aconitase, which could result in the inhibition of fatty acid synthesis and citrate oxidation, respectively. $PB^{Cre4}p53^{flox}Rb^{flox}$ and $PB^{Cre4}Pten^{flox}$ mice fed a 0.2 % TMFol diet did not display any evidence of tumours in the prostate, but there was no significant difference in the PIN development between the mice on the control diet and those on the TMFol diet.

Taken together, TMFol has the potential to induce cell cycle arrest, apoptosis and senescence and to inhibit fatty acid synthesis and citrate oxidation in prostate cancer cells.

<u>Acknowledgement</u>

List of Contents

Table of Contents

List of Figures

List of Tables

List of Abbreviations

$(NH_4)Fe(SO_4)_2$	Ammonium iron (III) sulphate
4-MU	4-methylumbelliferone
ACC	Acetyl-CoA carboxylase
ACLY	ATP citrate lyase
ACO2	Mitochondrial aconitase
ACTB	Actin gene expression assay
AICAR	5-aminoimidazole-4-carboamide ribonucleotide
AJCC	American Joint Committee on Cancer
AMACR	α-methylacyl-CoA racemase
AMP	Adenosine monophosphate
AMPK	AMP-activated protein kinase
ANOVA	Analysis of variance
APAF1	Apoptosis protease activating factor 1
Apo2L	Apoptosis ligand 2
APS	Ammonium persulphate
AR	Androgen receptor
ATBC	Alpha-Tocopherol and Beta-Carotene
ATP	Adenosine triphosphate
BCA	Bicinchoninic acid
BPH	Benign Prostatic Hypertrophy
BRCA1	Breast cancer 1, early onset
BRCA2	Breast cancer 2, early onset
BSA	Bovine serum albumin
CDK	Cyclin-dependent kinase
CDKI	Cyclin-dependent kinase inhibitor
cDNA	Complementary deoxyribonucleic acid
CHAPS	[(3-cholamidopropyl)dimethylammonio]-1-propanesulfonate
C_{max}	Maximum serum concentration
CO_2	Carbon dioxide
CoA	Coenzyme A
CPT-1	Carnitine palmitoyltransferase 1

C_T	Cycle threshold
CYP3A4	Cytochrome P-450 3A4
DAB	Diaminobenzidine
DHT	Dihydrotestosterone
DIABLO	Direct inhibitor of apoptosis-binding protein with low pI
DISC	Death inducing signalling complex
DLST	Dihydrolipoyl succinyltransferase
DMSO	Dimethyl sulfoxide
DNA	Deoxyribonucleic acid
DPX	Mixture of distyrene, a plasticizer and xylene
DRE	Digital rectal examination
EC	Epicatechin
ECACC	European Collection of Cell Cultures
ECG	Epicatechin-3 gallate
EDTA	Ethylenediaminetetraacetic acid
EGC	Epigallocatechin
EGCG	Epigallocatechin-3-gallate
ER	Oestrogen receptor
ERG	V-ets avian erythroblastosis virus E26 oncogene homolog
ERK	Extracellular signal-regulated kinase
FADD	FAS associated death domain
$FADH_2$	Flavinadenine dinucleotide
FAS	Fatty acid synthase
FasL	First apoptosis signal ligand
FCS	Foetal calf serum
FDA	Food and Drug Administration
FH	Fumarate hydratase
FITC	Fluorescein isothiocyanate
G1	Gap 1
G2	Gap 2
GAPDH	Glyceraldehyde 3-phosphate dehydrogenase
GEMM	Genetically engineered mouse model
GLUT	Glucose transporter protein
H&E	Haematoxylin and eosin

HCAs	Heterocyclic amines
HG-PIN	High-grade prostatic intraepithelial neoplasia
HRP	Horseradish peroxidase
IAP	Inhibitor of apoptosis proteins
IARC	International Agency for Research on Cancer
IC_{50}	Half maximal inhibitory concentration
IgG	Immunoglobulin G
IMS	Industrial methylated spirit
IRP-1	Iron regulatory protein 1
IRP-2	Iron regulatory protein 2
JNK	c-Jun N-terminal kinase
LDHA	Lactate dehydrogenase
LG-PIN	Low-grade prostatic intraepithelial neoplasia
M	Mitosis
MEK	Mitogen-activated protein (MAP) kinase kinase
MRI	Magnetic resonance imaging
mRNA	Messenger ribonucleic acid
mTOR	Mammalian target of rapamycin
MUG	4-methylumbelliferyl-β-D-galactopyranoside
NADH	Reduced nicotinamide adenine dinucleotide
NaOH	Sodium hydroxide
NICE	National Institute for Health and Care Excellence
NPCT	Nutritional Prevention of Cancer Trial
OMe	Methoxy group
pACC	Phosphorylated or phospho-ACC
PAGE	Polyacrylamide gel electrophoresis
PAHs	polycyclic aromatic hydrocarbons
pAMPKα	Activated AMPKα or phosphorylated or phospho-AMPKα
PB	Probasin
PBS	Phosphate buffered saline
PBST	PBS-Tween-20
PCA3	Prostate cancer antigen 3
PCPT	Prostate Cancer Prevention Trial

PCR	Polymerase chain reaction
PDC-E2	E2 subunit of pyruvate dehydrogenase
PDH	Pyruvate dehydrogenase
PDH-E1	E1 component of PDH
PDK	Pyruvate dehydrogenase kinases
PEPCK	Phosphoenolpyruvate carboxykinase
PI	Propidium iodide
PI3K	phosphoinositide-3-kinase
PIN	Prostatic intraepithelial neoplasia
PMSF	Phenylmethanesulfonyl fluoride
PS	Phosphatidylserine
PSA	Prostate specific antigen
Pten	Phosphatase and tensin homolog deleted on chromosome 10
qPCR	Quantitative real-time polymerase chain reaction
Rb	Retinoblastoma
REDUCE	Reduction by Dutasteride of Prostate Cancer Events
RNA	Ribonucleic acid
RPMI	Roswell Park Memorial Institute
RT	Reverse transcription
S	Synthesis
SASP	Senescence-associated secretory phenomenon
SA-β-galactosidase	Senescence-associated-β-galactosidase
SCD	stearoyl-CoA desaturase
SCID	Severe combined immune deficiency
SD	Standard deviation
SDHA	Succinate dehydrogenase flavoprotein subunit A
SDS	Sodium dodecyl sulphate
SEER	Surveillance, Epidemiology and End Results
SELECT	Selenium and Vitamin E Cancer Prevention Trial
Smac	Second mitochondria-derived activator of caspases
SREBP-1	Sterol regulator element binding protein-1
SUCLG1	Succinate-CoA ligase, α subunit
SV40	Human simian virus 40

Tag	Large T antigen
TEMED	N,N,N′,N′-tetramethylethylenediamine
TMFol	3′,4′,5′-trimethoxyflavonol
TMPRSS2	Transmembrane protease, serine 2
TNM	Tumour, nodes, metastasis
TRADD	Tumour necrosis factor receptor associated death domain
TRAMP	Transgenic adenocarcinoma of the mouse prostate
TRUS	Transrectal ultrasound
VDAC	Voltage-dependent anion channel
WCRF	World Cancer Research Fund
X-gal	5 bromo-4-chloro-3-indolyl-β-D-galactopyranoside
ZIP	Zinc transporter

List of Publications and Conference Abstracts

Research Paper

Hill, C. U. F. K., Saad, S. E., Britton, R. G., Gescher, A. J., Sale, S., Brown, K. & Howells, L. M. (2015). Inhibition of prostate cancer cell growth by 3',4',5'-trimethoxyflavonol (TMFol). *Cancer Chemother Pharmacol,* 76**:** 179-85.

Abstract

Hill, C. U. F. K., Rufini, A., Howells, L. M., Sale, S., & Brown, K. Mechanisms of action of 3',4',5'-trimethoxyflavonol in the inhibition of prostate cancer. Poster presentation. European Association for Cancer Research (EACR) − American Association for Cancer Research (AACR) − Società Italiana di Cancerologia (SIC) Special Conference on Anticancer Drug Action and Drug Resistance: from Cancer Biology to the Clinic. Florence, Italy, June 2015.

Chapter 1. Introduction

1.1. Cancer and carcinogenesis

Cancer is a complex disease that is characterised by the development of abnormal cells that grow beyond their usual boundaries to infiltrate and destroy normal tissues. The transformation of a normal cell to a malignant cell is a multistage process involving cellular, genetic and epigenetic changes that culminate in the cell displaying the hallmarks of cancer (Figure 1.1) (Yokota, 2000; Hanahan and Weinberg, 2011).
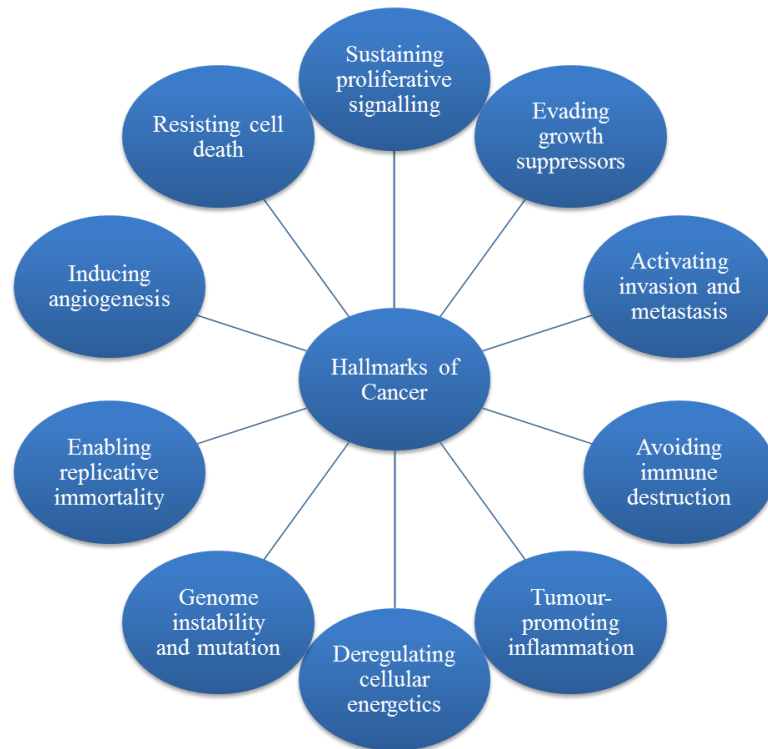
Figure 1.1: Hallmarks of cancer. Schematic representation of the features required for the transformation of a normal cell into a cancer cell. Figure adapted from Hanahan and Weinberg (2011)

The multistage process is referred to as carcinogenesis. Evidence from rodent carcinogenesis studies have identified three distinct stages of carcinogenesis, initiation, promotion and progression and these stages occur over a period of years before the development and expansion of the neoplastic cells (Figure 1.2) (Surh, 1999). Initiation is the induction of irreversible genetic alterations in a cell which could result in the activation of oncogenic pathways and the inactivation of apoptotic pathways and DNA repair mechanisms (Weston and Harris, 2003; Surh, 1999). Initiation can be triggered

by either endogenous or exogenous carcinogenic agents that are capable of inducing DNA damage, including DNA adducts, strand breaks and other lesions caused by reactive oxygen species. Generally, an adduct is formed between a reactive chemical carcinogen and a nucleotide in DNA, and without effective DNA repair, mutations arise during DNA replication (Weston and Harris, 2003). Carcinogens capable of causing or contributing to increased levels of DNA damage include ultraviolet radiation, viruses such as Hepatitis B, bile salts and chemicals found in tobacco smoke (Bernstein et al., 2011; Cooper, 2000; Cunningham et al., 2011; Kanavy and Gerstenblith, 2011). Promotion is the clonal expansion of the initiated cell to produce a preneoplastic tumour population (Surh, 1999). Proliferation of the mutated cells is stimulated by mitogenic agents that are generally nonmutagenic. The artificial sweetener saccharin and the androgens are among several agents that have been shown to have tumour-promoting properties (Weston and Harris, 2003). Progression is the irreversible step during which some of the preneoplastic cells may undergo further genetic and epigenetic changes, transforming them into malignant cells that display an increase in proliferation, invasiveness and metastasis (Weston and Harris, 2003; Surh, 1999).
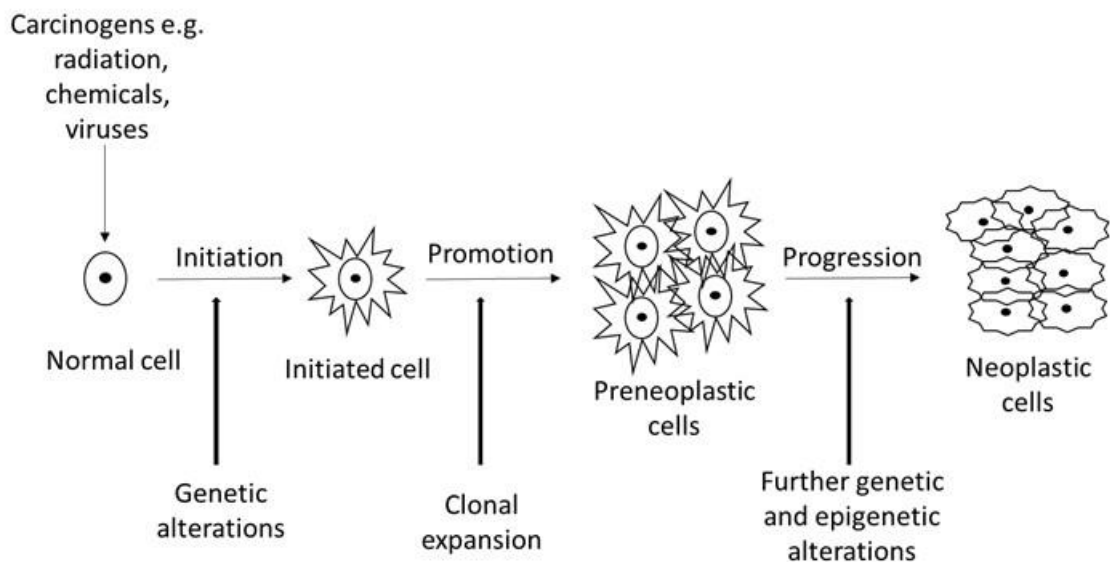
Figure 1.2: Schematic representation of the steps in carcinogenesis

Cancer can develop within any organ site in the body but the most common types include lung, breast, prostate and colorectal cancers. Globally there were 14.1 million new cases and 8.2 million cancer-related deaths in 2012 (Forman and Ferlay, 2014). By 2030 it is estimated that there will be approximately 23.6 million new cases of all

cancer types globally (Cancer Research UK, 2014a). Therefore, to reduce the tremendous health burden associated with cancer, the biomedical community must continue research into efforts that lead to risk reduction, prevention, early detection and effective treatment of cancers.

1.2. Prostate Cancer

Prostate cancer is the second most common cancer in men globally, as approximately 1.1 million men were diagnosed with the disease in 2012, accounting for 15 % of the cancers diagnosed in men during that year (Ferlay et al., 2013). This malignancy is also the 5th leading cause of death from cancer in men throughout the world. However, the mortality rates in the United Kingdom (UK) and the United States of America (USA) make prostate cancer the second leading cause of cancer deaths in the male population in those countries (Cancer Research UK, 2014b; American Cancer Society, 2015). With the high incidence and mortality rates, compounded by a growth in the aging population, prostate cancer is poised to become a major public health burden.

1.2.1. Biology, Diagnosis and Management of Prostate Cancer

1.2.1.1. Anatomy of the human prostate gland

The prostate gland is the largest accessory gland of the male reproductive system and is located just below the bladder in front of the rectum. It is divided into four anatomic zones; peripheral, central, transition and fibromuscular stroma (Figure 1.3). The peripheral zone surrounds the distal urethra and is the largest zone, comprising about 70 % of the glandular tissue (Bhavsar and Verma, 2014). The central zone surrounds the ejaculatory ducts and makes up 25 % of the gland, while the transition zone surrounds the proximal urethra and makes up the remaining 5 % of the glandular tissue. The fibromuscular stroma is the zone without glandular tissue, but is comprised of fibrous and smooth muscle. These four zones are compacted within a pseudo-capsule to form the walnut-shaped structure of the prostate gland, which functions to secrete a thin, alkaline fluid that forms part of the ejaculate, aiding the survival and motility of sperm (Bhavsar and Verma, 2014; Mawhinney and Mariotti, 2013).

Development of the prostate starts before birth and continues until adulthood. The embryology and development of the prostate gland is regulated by male hormones such as testosterone, and any impairment in the hormonal system could lead to abnormalities in sexual development, benign prostatic hypertrophy (BPH) or the more serious condition of prostate cancer, dependent on the stage of prostate development at which hormonal control is impaired (Feldman and Feldman, 2001; Mawhinney and Mariotti, 2013; Wilson et al., 1981). BPH usually develops in the transition zone, while the peripheral zone is the origin of about 70 % of prostatic adenocarcinoma (Bhavsar and Verma, 2014; Applewhite et al., 2001).
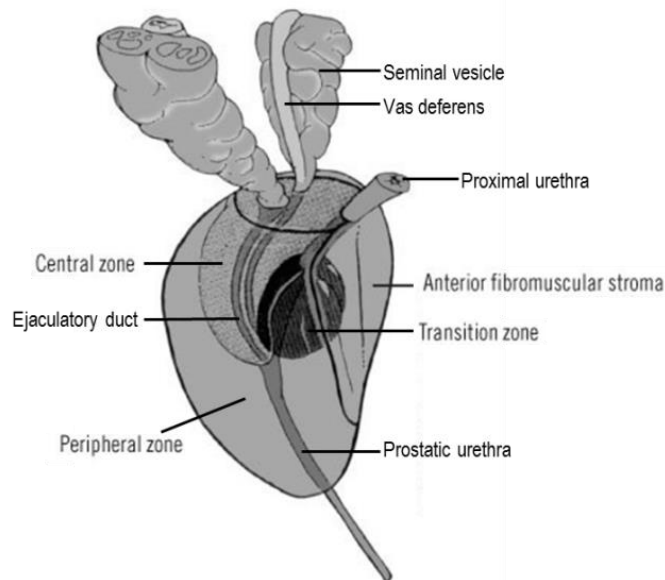
Figure 1.3: Zonal anatomy of the prostate. Figure adapted from Bhavsar and Verma (2014).

1.2.1.2. Risk factors for development of prostate cancer

There are significant variations in the incidence and mortality rates of prostate cancer worldwide. Incidence may vary as much as 25-fold while mortality varies about 10-fold (Ferlay et al 2013) (Figure 1.4). The disparity in incidence rates may be attributed to a combination of genetic, environmental and social factors (Haas and Sakr, 1997). Age, race and a family history of the disease are the most important risk factors, while diet and lifestyle are gaining recognition as potential risk factors.
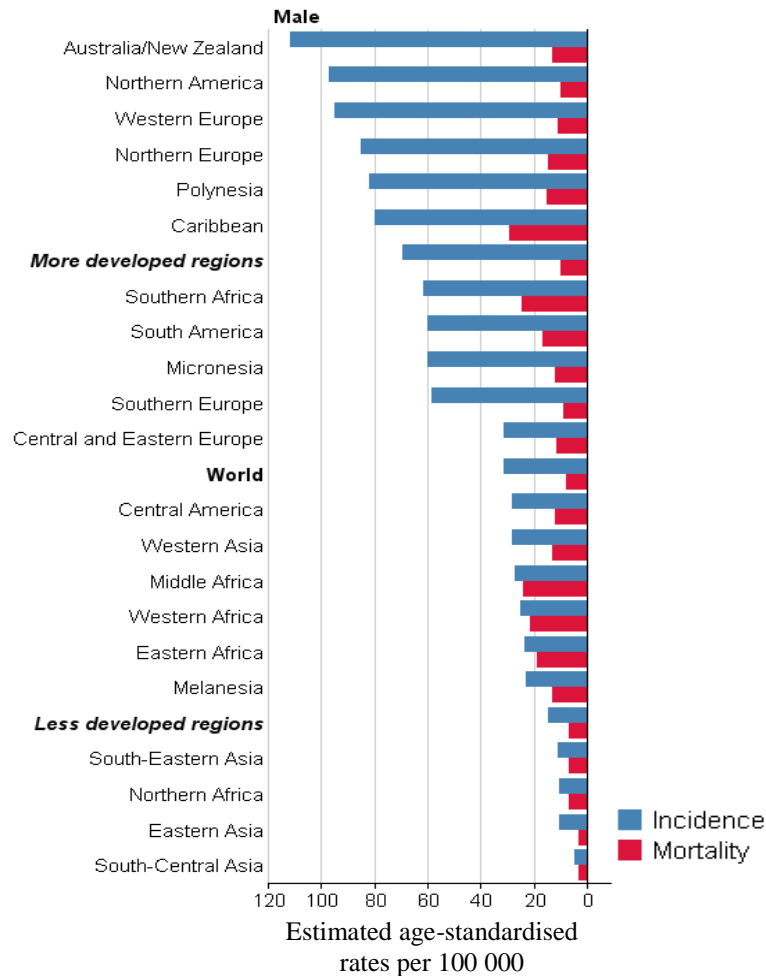
Figure 1.4: Prostate cancer incidence and mortality worldwide in 2012. Incidence rates are much more variable than mortality rates throughout the world. Most of the cases occur in the more developed regions, while mortality rates are highest in predominantly black populations. The average statistics for the regions indicated in bold print are represented on the graph. More developed countries include all regions of Europe plus Northern America, Australia/New Zealand and Japan, while less developed countries include all regions of Africa, Asia (excluding Japan), Latin America and the Caribbean, Melanesia, Micronesia and Polynesia. Figure adapted from Ferlay *et al* (2013).

<u>Age:</u> Prostate cancer is considered to be a disease of older men as it is extremely rare in men younger than 40 years of age and then rapidly increases in incidence with each decade of life (Figure 1.5). In the UK, the average age at diagnosis is over 75 years (Cancer Research UK, 2014b), while in the USA the average age is between 65 and 74 years (Surveillance, Epidemiology and End Results [SEER] 18, 2014). Since prostate cancer can take decades to progress from the premalignant stage to the invasive form of

5

the disease, it should be noted that as countries introduce a prostate cancer screening programme, the age of diagnosis is likely to fall as the disease may be detected at a much earlier stage. This probably accounts for the difference in the average age of diagnosis between the UK and USA. In the USA 75 % of men aged 50 and older have been screened at least once for prostate cancer (Sirovich et al., 2003) compared to about 10-20 % of men in Europe (Bray et al., 2010).

Estimated Incidence By Age

Figure showing rate per 100 000 males on the y-axis (0 to 500) against Age at diagnosis on the x-axis (0-14, 15-39, 40-44, 45-49, 50-54, 55-59, 60-64, 65-69, 70-74, 75+), with an increasing dashed curve.
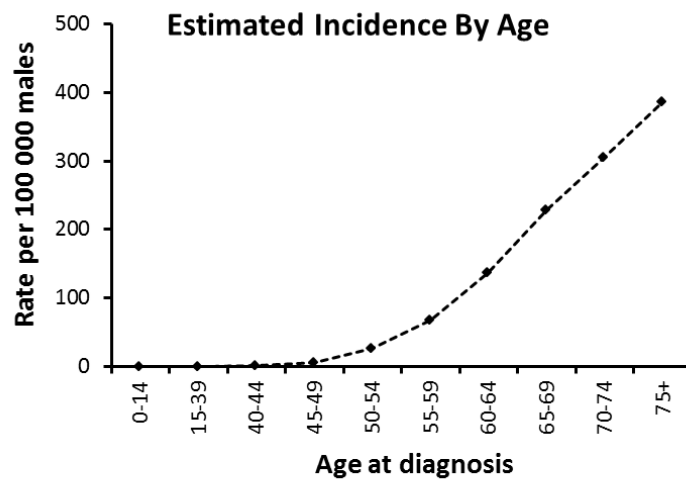
Figure 1.5: Incidence rate worldwide for prostate cancer by age. Very few cases of prostate cancer are detected between the ages 40-44 but it increases rapidly for each subsequent age group, peaking in the 75+ age group. Graph generated from GLOBOCAN 2012 v 1.2. (International Agency for Research on Cancer (IARC), 2015)**.**

Race: Race is the second most common risk factor for developing prostate cancer. Regardless of their origin, black men are most likely to develop and die from prostate cancer compared to other ethnic groups. In the UK, black men have a 3-fold higher risk of developing prostate cancer than white men (Ben-Shlomo et al., 2008), while Asian men have the lowest risk (National Cancer Intelligence Network and Cancer Research UK, 2009; Metcalfe et al., 2008). Furthermore, black men are also diagnosed at a younger age than their white counterparts (Ben-Shlomo et al., 2008; Swords et al., 2010). This disparity is also quite evident in the USA as the incidence rate is about 60 % higher in black men than Caucasians (SEER 18, 2014). Studies investigating the racial disparity have observed marked differences in testosterone metabolism, evident by the elevated 5-alpha reductase activity and dihydrotestosterone levels in black men

when compared to white men (McIntosh, 1997; Litman et al., 2006). Additionally, the variations in the androgen receptor that have been observed among African-American, whites and Asian-Americans may also play a role in the frequency of prostate cancer in black men (McIntosh, 1997). Nevertheless, these and other factors that could influence the link between race and prostate cancer remain to be clearly determined. The importance of 5-alpha reductase, dihydrotestosterone and the androgen receptor in prostate carcinogenesis is described in a later section.

Family history of prostate cancer: A family history of prostate cancer is another common risk factor for the development of prostate malignancies. It is estimated that 5-10 % of prostate cancer cases are linked to family history and the inheritance of genes that predispose to prostate cancer (Carter et al., 1992; Elo et al., 2001; Hemminki and Czene, 2002). The risk of prostate cancer is greater for men who have a brother with the disease than for men with affected fathers (Kiciński et al., 2011). The risk becomes even higher if the affected first degree relative was diagnosed at an age younger than 65 years and if more than one first degree relative has been diagnosed at any age (Kiciński et al., 2011) (Table 1.1). Additionally, there is evidence to support an increased risk of prostate cancer among men whose biological mother had breast cancer (Chen et al., 2008; Hemminki and Chen, 2005). This association between prostate and breast cancers within the same family may be attributable to the increased risk of prostate cancer among men with BRCA1/ BRCA2 mutations (Edwards et al., 2003; Gayther et al., 2000; Thompson and Easton, 2002). Mutations that inactivate the *ribonuclease L* or *RNASEL* gene on chromosome 1 have also been observed in some cases of inherited prostate cancer (Carpten et al., 2002).

Diet and lifestyle: Comparative epidemiological studies show that prostate cancer incidence is higher in Japanese and Chinese male immigrants to the USA than in their native countries, suggesting that diet or lifestyle may influence prostate cancer incidence (Shimizu et al., 1991; Yu et al., 1991). The high fat Western diet has been implicated to play a role in prostate carcinogenesis. Some *in vitro* and *in vivo* studies have demonstrated enhanced proliferation of prostate cancer cells as a consequence of exposure to a high fat diet (Huang et al., 2012; Park et al., 2013). Case control and prospective cohort studies have also supported the association between high dietary fat consumption and prostate cancer (Fleshner et al., 2004; Pelser et al., 2013).

Additionally, the type of fatty acid content of the diet may also be relevant as a few studies have shown an increased risk of prostate cancer with higher intakes of alpha-linolenic acid (De Stéfani et al., 2000; Giovannucci et al., 2007; Pelser et al., 2013). It has also been suggested that a diet high in calcium from dairy products or a diet high in cadmium appears to increase prostate cancer risk, but no underlying mechanisms of action have been proposed (Gao et al., 2005; Julin et al., 2012). More recently, selenium has been added to the list of substances that can increase prostate cancer risk (Kristal et al., 2014).

Heterocyclic amines (HCAs) and polycyclic aromatic hydrocarbons (PAHs) are formed when meats are cooked at high temperatures, such as when frying, grilling and barbecuing (Cross et al., 2004; Jägerstad and Skog, 2005). The HCAs and PAHs are genotoxic carcinogens, damaging DNA and resulting in the development of different types of cancer, including prostate cancer, in animal models (Shirai et al., 1997; Sugimura et al 2004). Epidemiological studies also suggest that consumption of meats cooked at high temperatures is associated with an increased risk of advanced prostate cancer (Cross et al., 2005; Joshi et al., 2012; Sinha et al., 2009).

The risks of prostate cancer posed by the aforementioned diets are further compounded by obesity, as obesity is linked to an increased risk of advanced prostate cancer and increased prostate cancer mortality (Cao and Ma, 2011; Discacciati et al., 2012; Gong et al., 2007). The World Cancer Research Fund (WCRF), a recognised authority on the relationship between diet and cancer risk, have reiterated the link between obesity and an increased prostate cancer risk but has concluded that there is insufficient evidence linking specific dietary consumption with increased risk of prostate cancer (WCRF, 2014).

1.2.1.3. Screening for prostate cancer

The aim of any cancer screening programme is to detect the cancer in the early stages before it metastasises, and thus reduce the overall disease-specific mortality. Screening methods for prostate cancer include:

Prostate specific antigen (PSA) test: PSA is a component of seminal fluid produced by the prostate epithelium to facilitate the motility of sperm (Roth-Kauffman, 2011). Levels of this protein tend to be elevated (i.e. exceeding 4 ng/mL) in prostate cancer (Simmons et al., 2011), as the malignant cells secrete PSA into the bloodstream. However, PSA is not tumour specific in the prostate (Hamdy, 2001) as elevated PSA can be caused by BPH, prostatitis, trauma and lower urinary tract infection. Also, levels of PSA can remain elevated up to 48 hours after ejaculation. Approximately 70 % of men with an abnormal PSA show no histological evidence of prostate cancer upon biopsy (Selley et al., 1997; Thompson et al., 2005). Furthermore, among the men with normal PSA levels, as many as 15 % may have prostate cancer (Thompson et al., 2004). In the cases where prostate cancer is accurately identified, the PSA test cannot distinguish between a cancer that will become clinically significant during the man's lifetime and a clinically insignificant cancer. Despite these limitations, the PSA test currently remains the best and most widely used method of identifying the early stages of prostate cancer. Therefore, to improve the reliability of the PSA test it should be repeated at regular intervals to first establish the normal range and subsequently detect any changes that could indicate the presence of prostate cancer.

Digital rectal examination (DRE): DRE is a diagnostic tool to detect nodules and abnormal prostate symmetry. It involves inserting the index finger into the rectum to feel the prostate for lumps, soft or hard spots or any other irregular features. Only the posterior and lateral aspects of the prostate gland can be felt via the rectum. Therefore, DRE is capable of detecting tumours mainly in the peripheral zone, in which 70 % of prostatic adenocarcinomas develop (Bhavsar and Verma, 2014; Applewhite et al., 2001). Nevertheless the usefulness of DRE as a screening method has been questioned since 40-50 % of men with unusual findings showed no pathological evidence of prostate cancer, while approximately 40 % of those who had a normal prostate on DRE were found to have prostate cancer upon pathological analysis (Philip et al. 2005). Consequently DRE is used in conjunction with the PSA test to detect the presence of prostate cancer and also to determine the extent of the cancerous mass.

Many Western countries, including the USA and some European countries have been screening for prostate cancer for decades but recent studies have raised concerns about the risks of over-diagnosis with screening (Draisma et al., 2009; Etzioni et al., 2002;

Pashayan et al., 2009). Additionally some studies have concluded that there are no benefits to be derived from prostate cancer screening (Andriole et al., 2009; Djulbegovic et al., 2010), while others have observed a significant reduction in mortality from prostate cancer when screening programmes are in place (Bokhorst et al., 2014; Schröder et al., 2009 and 2012). In the United States there are conflicting guidelines on screening for prostate cancer. The American Cancer Society recommends that screening should begin at 50 years of age for average-risk men but at 40-45 years of age for high-risk men, while the American Urological Association only recommends routine screening between 55-69 years of age every two years for average-risk men, but should be individualised for high-risk men (Wolf et al., 2010; Carter et al., 2013). These guidelines are in sharp contrast to that of the United States Preventive Services Task Force which does not recommend screening for prostate cancer at any age (Moyer, 2012). The UK has always advised against any routine screening programme, leaving it to the men to request screening if they have any concerns about their prostate health (NHS, 2015).

The concerns over limitations of the current screening methods for prostate cancer have highlighted the need for newer and more clinically reliable biomarkers for prostate cancer. In recent years, biomarkers including the prostate cancer antigen 3 (*PCA3*) gene and transmembrane protease, serine 2 (*TMPRSS2*) gene with the transcription factor v-ets avian erythroblastosis virus E26 oncogene homolog (*ERG*) have generated much interest (de Kok et al., 2002; Hessels et al., 2007). PCA3 is now approved by the Food and Drug Administration (FDA) in the USA as a diagnostic test for prostate cancer in cases of prior negative prostate biopsy (Prensner et al., 2012). Nevertheless, none of the current biomarkers of prostate cancer are yet suitable to replace PSA and DRE prostate cancer screening.

1.2.1.4. Diagnosis of prostate cancer

If the screening results suggest prostate cancer a transrectal ultrasound (TRUS)-guided prostate biopsy is recommended. TRUS-guided prostate biopsy is crucial in identifying the presence of prostate cancer and also in identifying the stage of tumour development. During this procedure, a transrectal ultrasound is used to determine the sections of the prostate gland that should be biopsied. Then a biopsy needle-gun is used to obtain two

to three tissue core samples in a systematic way from every region, especially the peripheral zone. If the ultrasound detects lesions, additional samples for biopsy analysis would be taken from those locations. Histological evaluation of the core samples would then determine the presence and stage of any tumours. It should be noted that between 20-30 % of tumours are missed at biopsy (Rabbani et al., 1998; Simmons et al., 2011). However, the diagnostic reliability of the biopsy increases with the number of samples taken, as the cancer may be small and is more likely to be missed from the sample pool if too few sections are taken. Those men with a negative biopsy, but a persistently high or rising PSA upon follow-up evaluations, are likely to require another biopsy with a higher core sample size. A positive biopsy is further evaluated to determine the extent of the cancer development.

Approximately 5-16 % of men who undergo prostate biopsies are diagnosed with prostatic intraepithelial neoplasia (PIN), a precursor to some forms of adenocarcinoma (cancer that starts in the gland cells) (Montironi et al., 2011). PIN is a condition in which epithelial cells within the small glandular units (acini) and ducts of the prostate gland become atypical, growing larger than the normal cells with a larger nucleus and more prominent nucleoli (Brawer, 2005). It can be further classified as either low-grade PIN (LG-PIN) or high-grade PIN (HG-PIN). Only HG-PIN is associated with an increased risk of prostate cancer (Bishara et al., 2004) and hence diagnosis of HG-PIN may require follow-up biopsies within a year.

If a tumour is detected in the biopsy samples, then the Gleason Scoring system is applied to determine the degree of tumour differentiation and aggressiveness of the cancer (Epstein et al., 2005). In each biopsy sample a grade range from 1 (well-differentiated) to 5 (poorly differentiated) is assigned, based on the glandular differentiation at low magnification (Gleason, 1992). As there may be more than one grade of cancer in the biopsy samples, an overall Gleason score is calculated by adding the most common Gleason grade in all of the samples to the highest grade found among the remaining samples (Pan et al., 2000). For example, a Gleason grade of 4+3=7 means that grade 4 tumours are most abundant, while there are fewer cases of grade 3 tumours. Tumours with a Gleason score of 6 or less are classified as low risk, while at 7 the tumours are classified as intermediate risk. A Gleason score between 8 and 10, inclusive, are high risk tumours and tend to be more aggressive.

After the diagnosis of prostate cancer in biopsy samples it is critical to determine the extent of the cancer within the prostate gland and to identify any possible metastasis, if present. This is referred to as prostate cancer staging and is determined based on PSA values, DRE findings, prostate biopsy results and Gleason score. The most widely used staging system for prostate cancer is the TNM system developed by the American Joint Committee on Cancer (AJCC). It describes the extent of the primary tumour (T), involvement of the regional lymph nodes (N) and the presence of distant metastasis (M) (Falzarano and Magi-Galluzzi, 2010) (Table 1.1). The TNM system allows for both clinical and pathologic staging. Clinical staging is based on the clinical findings such as PSA, DRE, biopsy results and imaging, but pathologic staging is based on gross and microscopic examination after a radical prostatectomy. After defining the T, N and M of the disease, a stage of I, II, III or IV is assigned, with stage I being the least advanced and stage IV being the most advanced form of prostate cancer (Table 1.2).

Primary tumour (T)	
TX	Primary tumour cannot be assessed
T0	No evidence of primary tumour
T1	Clinically inapparent tumour neither palpable nor visible by imaging
T1a	Tumour incidental histologic finding in ≤5% of tissue resected
T1b	Tumour incidental histologic finding in >5% of tissue resected
T1c	Tumour identified by needle biopsy (e.g. because of elevated PSA)
T2	Tumour confined within prostate
T2a	Tumour involves one-half of one lobe or less
T2b	Tumour involves more than one-half of one lobe but not both lobes
T2c	Tumour involves both lobes
T3	Tumour extends through the prostate capsule
T3a	Extracapsular extension (unilateral or bilateral)
T3b	Tumour invades seminal vesicle(s)
T4	Tumour is fixed or invades adjacent structures other than seminal vesicles such as external sphincter, rectum, bladder, levator muscles, and/or pelvic wall
Regional lymph nodes (N)	
NX	Regional lymph nodes were not assessed
N0	No regional lymph node metastasis
N1	Metastasis in regional lymph node(s)
Distant metastasis (M)	
M0	No distant metastasis
M1	Distant metastasis
M1a	Non-regional lymph node(s)
M1b	Bone(s)
M1c	Other site(s) with or without bone disease

Table 1.1: Prostate cancer TNM staging. The definitions of TNM are based on AJCC 7th edition implemented for use in 2010. Table taken from Falzarano and Magi-Galluzzi (2010).

Group	T	N	M	PSA	Gleason score (GS)
I	T1a–c	N0	M0	PSA < 10	GS ≤ 6
	T2a	N0	M0	PSA < 10	GS ≤ 6
	T1–2a	N0	M0	PSA X	GS X
IIA	T1a–c	N0	M0	PSA < 20	GS 7
	T1a–c	N0	M0	PSA ≥ 10 < 20	GS ≤ 6
	T2a	N0	M0	PSA ≥ 10 < 20	GS ≤ 6
	T2a	N0	M0	PSA < 20	GS 7
	T2b	N0	M0	PSA < 20	GS ≤ 7
	T2b	N0	M0	PSA X	GS X
IIB	T2c	N0	M0	Any PSA	Any GS
	T1–2	N0	M0	PSA ≥ 20	Any GS
	T1–2	N0	M0	Any PSA	GS ≥ 8
III	T3a–b	N0	M0	Any PSA	Any GS
IV	T4	N0	M0	Any PSA	Any GS
	Any T	N1	M0	Any PSA	Any GS
	Any T	Any N	M1	Any PSA	Any GS

Table 1.2: Prostate cancer staging. The classifications of the stages of prostate cancer are based on AJCC 7th edition. X means not assessable. Stage I is the least nocuous with a good prognosis while stage IV is the advanced stage of the cancer and has a poor prognosis. Table adapted from Falzarano and Magi-Galluzzi (2010).

1.2.1.5. Treatment of prostate cancer

The treatment options for men diagnosed with prostate cancer vary depending on the stage of the cancer, plus the age and overall health of the affected man. In the UK, men with a low or intermediate risk for prostate cancer, who also have a reduced life expectancy as a consequence of more immediate life threatening health conditions, are advised to engage in watchful waiting. Watchful waiting involves regular PSA tests and DRE to monitor the disease progression. Any change to indicate growth of the cancer is followed by palliative treatment only to control the cancer rather than to cure it.

The 2014 prostate cancer treatment guidelines by the National Institute for Health and Care Excellence (NICE) in the UK recommend active surveillance as a suitable alternative to radical treatment for men with low risk localised prostate cancer. Furthermore, active surveillance can be offered to men with intermediate risk localised prostate cancer who do not want radical treatment. Active surveillance involves regular assessment of the cancer using PSA tests, DRE, prostate biopsies and magnetic resonance imaging (MRI). Any sign of disease progression would lead to radical treatment for a curative outcome.

Radical prostatectomy (open, laproscopic and robotic) removes the entire prostate gland and seminal vesicles to cure the disease. In the USA it is the most popular treatment across the prostate cancer risk groups, as described by Gray and colleagues (2014) who identified a significant increase in the use of radical prostatectomy among 823,977 men diagnosed with localised prostate cancer between 2004 and 2011 in the USA. Major complications of this surgical intervention include erectile dysfunction and urinary incontinence. Approximately 20-40 % of men who opt for radical prostatectomy develop biochemical recurrence of the disease and hence should be committed to at least 10 years of follow-up evaluations to facilitate early intervention upon cancer recurrence (Amling et al., 2000; Freedland et al., 2005; Roehl et al., 2004). Biochemical recurrence is indicated by rising levels of PSA and it usually predates the clinical progression of prostate cancer, metastasis and death by several years (Paller and Antonarakis, 2013).

Radiotherapy (external beam and brachytherapy) applies a curative dose of radiation to the prostate gland. It is suitable for localised and advanced disease but its use has been declining in popularity (Gray et al., 2014). Side effects are similar to those of a radical prostatectomy. Recurrence rate is also comparable to that of a radical prostatectomy. However, follow-up evaluations would be necessary for up to 15 years after treatment (Critz et al., 2013).

Androgen deprivation therapy (medical castration by hormone therapy) is used in conjunction with the surgical procedures (Messing et al., 2006; D'Amico et al., 2008). Evidence suggests that high levels of androgens enhance the development of prostate cancer (Yu and Berkel, 1999). Therefore, the lack of androgen stimulation could

potentially slow progression of the disease. Treatment involves administering drugs like Degarelix and Bicalutamide that either prevent the synthesis of testosterone or prevent testosterone from getting to the cancer cells. Androgen deprivation is indicated as an adjuvant treatment when the grade and staging of the cancer suggest a high possibility of recurrence. Those cancers that respond to androgen deprivation therapy are referred to as androgen-dependent, while those that do not respond are androgen-independent. By itself androgen deprivation therapy in men with localised prostate cancer provides no added survival advantage (D'Amico et al., 1998), but as an adjuvant therapy there are significant survival benefits irrespective of the many side effects of therapy (Kumar et al., 2006; Bolla et al., 2010). Other treatment methods, such as cryotherapy and high intensity focused ultrasound are used minimally, generally in a clinical trial setting, to treat localised and advanced prostate cancer, as the long-term efficacy of these methods is yet to be determined.

Chemotherapy is used as the last line of defence to treat the metastatic form of the disease, which tends to be androgen-independent. Docetaxel is the most commonly used chemotherapeutic drug. It may slow the growth of the cancer and reduce symptoms, adding a few more months of life, but it is unlikely to cure prostate cancer. Recently, a randomised clinical trial showed that administration of docetaxel in conjunction with androgen deprivation therapy extended survival by 17 months when compared to men on androgen deprivation therapy only (Sweeney et al., 2015).

In the USA and UK, the five-year relative survival by stage at the time of diagnosis ranges from nearly 100 % at Stages I − III, to approximately 30 % at Stage IV (American Cancer Society, 2015; Cancer Research UK, 2014b). Stage IV is treated with chemotherapy. Hence there is still a need for more efficacious and less noxious therapeutic protocols to treat metastatic prostate cancer.

1.2.2. Prostate cancer metabolism

Cancer cells reprogram their metabolic pathways, including glycolysis, the Krebs cycle and fatty acid metabolism, to satisfy their need to proliferate, survive and metastasise (Dang, 2012; Dang and Samenza, 1999; Modica-Napolitano and Singh, 2004). However, the extent of the role of an altered metabolism in the pathogenesis of prostate

cancer is still being deciphered, to facilitate an improvement in the chemoprevention, diagnosis and treatment of prostate cancer.

1.2.2.1. Pyruvate metabolism

In typical mammalian cells, glucose utilisation via glycolysis produces pyruvate. The fate of pyruvate is determined primarily by the availability of oxygen. Under normoxic conditions the pyruvate enters the mitochondria to be oxidised by pyruvate dehydrogenase (PDH) to acetyl-coenzyme A (acetyl-CoA), which is subsequently used in the Krebs cycle. Hypoxic conditions cause pyruvate to remain in the cytosol where it is converted by lactate dehydrogenase to lactate (Roudier and Perrin, 2009). Pyruvate metabolism is often altered in cancer. PDH activity is suppressed in many cancer types, either as a result of a decrease in PDH expression or an increase in PDH kinases (PDKs), which are inhibitors of PDH (Kim et al., 2006; Koukourakis et al., 2005). The PDKs inhibit the activity of PDH by phosphorylating PDH. As a consequence, the energy demands of the rapidly proliferating cancer cells is satisfied by aerobic glycolysis or the Warburg effect, where pyruvate is converted to lactate in the presence of oxygen (Vander Heiden et al., 2009). Although aerobic glycolysis provides less energy to satisfy the high energy demands of the cancer cell, it produces the energy at a faster rate than oxidative phosphorylation via the Krebs cycle. Additionally, it provides the necessary nutrients required to synthesise new cells. A concomitant increase in the rate of glucose uptake usually accompanies the switch to aerobic glycolysis (Liu, 2006; Pelicano et al., 2006). Therefore, in many tumours there tends to be a higher expression of the glucose transporter proteins (GLUTs) (Kurata et al., 1999; Suganuma et al., 2007). Prostate cancer cells are different to the typical mammalian cells in that PDH is over-expressed and aerobic glycolysis has only been demonstrated in advanced stages of prostate cancer (Effert et al., 2004; Lexander et al., 2005; Vaz et al., 2012). On the other hand, the primary stages of the disease display low glycolysis and expression of the GLUTs (Chandler et al., 2003; Zadra et al., 2013).

1.2.2.2. Citrate metabolism

In mammalian cells, citrate is synthesised in the mitochondria where it can either enter the Krebs cycle for oxidation, generating energy and intermediates for other metabolic pathways, or be exported to the cytosol (Franklin and Costello, 2009; Mycielska et al.,

2009). Once in the cytosol, citrate is converted to acetyl-CoA and used in fatty acid and cholesterol synthesis. This form of citrate metabolism is common in most mammalian cells except for prostate cells. Instead, in normal prostate epithelial cells there is very little citrate oxidation as the citrate is exported to the cytosol and then secreted into the prostatic fluid. These normal prostate epithelial cells are specialised to accumulate and secrete citrate (Costello et al., 1999, 2005) (Figure 1.6).

The secretion of high levels of citrate requires a high rate of citrate synthesis. In typical mammalian cells citrate is synthesised by the condensation of acetyl-CoA (a product of glucose oxidation) and oxaloacetate (a product of citrate oxidation). In normal prostate cells the precursor requirements for citrate synthesis remain the same, but there are some differences in the derivation of the precursors. Glucose oxidation is still responsible for the generation of acetyl-CoA but the glucose is oxidised by aerobic glycolysis (Costello and Franklin, 1989). Conversely, oxaloacetate is derived by transamination of aspartate which is allowed to accumulate in the prostate cells by active uptake from the plasma via specific high affinity aspartate transporters (Franklin et al., 2006).
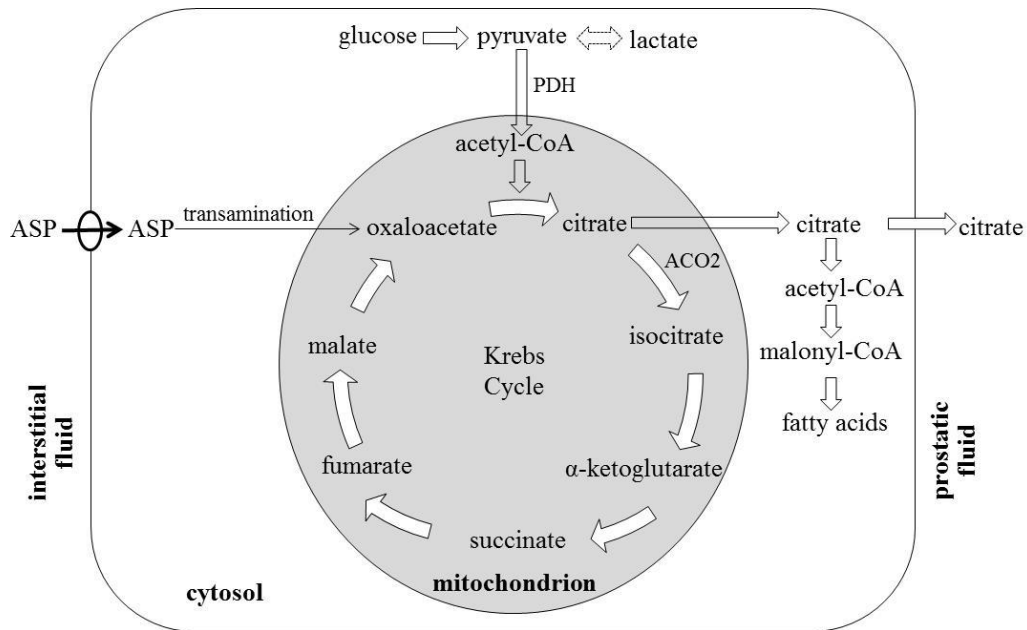
Figure 1.6: Citrate metabolism in normal mammalian prostate cells. Citrate is synthesised in the mitochondria from acetyl-CoA and oxaloacetate. In normal prostate cells the citrate is exported from the mitochondria into the cytosol for secretion into the prostatic fluid, rather than being used up in the Krebs cycle or fatty acid synthesis, as is the case in most other normal mammalian cells. PDH: pyruvate dehydrogenase, ACO2: mitochondrial aconitase; ASP: aspartate. Figure adapted from Costello and Franklin (2006).

To ensure that high citrate levels are maintained, the prostate epithelial cells must prevent the utilisation of citrate by inhibiting citrate oxidation. Citrate oxidation occurs in the Krebs cycle and mitochondrial aconitase (ACO2) regulates the entry of citrate into the Krebs cycle, by catalysing the interconversion of citrate to isocitrate. In typical mammalian cells ACO2 is expressed at very high levels and is not rate limiting. Interestingly, normal prostate cells have similar levels of ACO2, thus suggesting that the activity of ACO2 must be inhibited to prevent citrate oxidation in the prostate (Costello et al., 1996; Liu et al 1996). It was soon realised that the activity of ACO2 is under the regulation of zinc (Singh et al., 2006). Normal prostate cells contain higher levels of mitochondrial zinc compared to other typical mammalian cells (Liu et al., 1997). Costello and colleagues (1997) demonstrated that zinc is an inhibitor of ACO2 activity and citrate oxidation. This inhibition of ACO2 short circuits the Krebs cycle and consequently reduces the amount of energy the Krebs cycle could potentially generate (Costello et al., 2005). Additionally, the high levels of zinc inhibit terminal oxidation to help create the low respiration environment that defines the normal prostate

(Costello et al., 2004), and zinc can stimulate the release of proteins from the mitochondria that can trigger apoptosis (mitochondrial apoptogenesis) and inhibit cell growth (Feng et al., 2000, 2002; Liang et al., 1999). The inhibition of ACO2 and citrate oxidation is lethal in all other mammalian cells but the prostate has adapted to this low energy environment by also generating additional energy during the aerobic glycolysis required for citrate synthesis.

Alterations in citrate metabolism are implicated in tumorigenesis of the prostate. The citrate content of malignant prostate tissue is markedly lower than that of normal prostate tissue (Costello et al., 1999). The zinc levels are also much lower in malignant prostate tissue (Costello et al., 2005) (Table 1.3). The significant decline in zinc levels implies that the inhibitory effect on the activity of ACO2 is removed, thus allowing citrate to enter the Krebs cycle for oxidation. This restores the Krebs cycle and significantly increases the amount of energy that is available for the malignant cells to utilise. Furthermore, the growth restrictive effect of mitochondrial apoptogenesis is lost with a decline in zinc levels. The drop in zinc and citrate levels precedes the malignant transformation of the normal prostate cells (Costello et al., 1999; Habib et al., 1979). Since the levels of zinc determine the levels of citrate, the decrease in zinc levels is most likely to precede the decrease in citrate production (Costello et al., 2004).

	Citrate (nmol/g wet weight)	Zinc (nmol/g wet weight)
Normal peripheral zone	12 000 – 14 000	3 000 – 4 500
Prostate cancer malignant tissue	200 – 2 000	400 – 800
Other tissues	250 – 450	200 – 400
Normal prostatic fluid	40 000 – 150 000	8 000 – 10 000
Prostate cancer prostatic fluid	1 000 – 30 000	250 – 1 000
Blood plasma	100 - 200	15

Table 1.3: Citrate and zinc levels in the human prostate. Citrate and zinc levels are much higher in the prostatic fluid than in the prostate tissue. Additionally the levels of citrate and zinc are dramatically lower in the prostate cancer prostatic fluid and malignant tissue than in the normal prostatic fluid and tissue, respectively. Table adapted from Franklin and Costello (2009).

Down-regulation of zinc transporters has been identified as the cause for the decline in zinc levels in prostate cancer cells. Malignant prostate tissues have a notable lower expression of zinc transporters, ZIP1, ZIP2 and ZIP3, than normal prostate tissue and downregulation of these transporters leads to a 70-80 % decrease in the uptake of zinc by prostate cells (Desouki et al., 2007; Franklin et al., 2005; Rishi et al., 2003). Furthermore, black males have been found to have a much lower expression of zinc transporters in their normal peripheral zone than white males and this could be a factor for the race-associated higher incidence of prostate cancer in black men (Rishi et al., 2003). Despite the established relationship between the zinc transporters and zinc levels in the prostate, the genetic transformation that triggers downregulation of the zinc transporters in prostate cells remains unknown.

1.2.2.3. Fatty acid metabolism

1.2.2.3.1. Fatty acid synthesis

Living cells require fatty acids to help satisfy their energy and new membrane biogenesis demands (Ramírez de Molina et al., 2002; Zadra et al., 2013). These fatty acids can either be obtained from the diet (exogenous) or synthesised by the cells (endogenous). Apart from a few exceptions, including the brain, liver, adipose and lung tissues, normal mammalian cells use exogenous fatty acids to satisfy their metabolic demands, and as a consequence, expression of the enzymes involved in fatty acid synthesis are maintained at low levels (Jayakumar et al., 1995). In contrast, cancer cells synthesise most of their fatty acids, irrespective of the levels of exogenous fatty acids, resulting in an upregulation of the enzymes involved in fatty acid synthesis (Menendez and Lupu, 2007; Tennant et al., 2010). Prostate cancer cells also display this altered fatty acid metabolism.

Fatty acid synthesis (Figure 1.7) occurs in the cytosol and is initiated when citrate is released into the cytosol and is converted to acetyl-CoA and oxaloacetate by ATP citrate lyase (ACLY). The oxaloacetate is converted to either malate or pyruvate for re-entry into the Krebs cycle. The acetyl-CoA undergoes carboxylation by acetyl-CoA carboxylase (ACC). This is the rate-limiting and committing step of fatty acid synthesis which results in the production of malonyl-CoA. Subsequently, fatty acid synthase (FAS) synthesises palmitate from the condensation of one molecule of acetyl-CoA and

seven molecules of malonyl-CoA. Palmitate is the main enzymatic product of FAS but other fatty acids such as myristate and stearate are produced in a lesser quantity (Jayakumar et al., 1995; Kuhajda et al., 1994). These saturated fatty acids are further modified by elongases or desaturases to form longer saturated fatty acids or monounsaturated fatty acids, respectively, before forming lipids for energy production and cell membrane biosynthesis (Zadra et al., 2013).
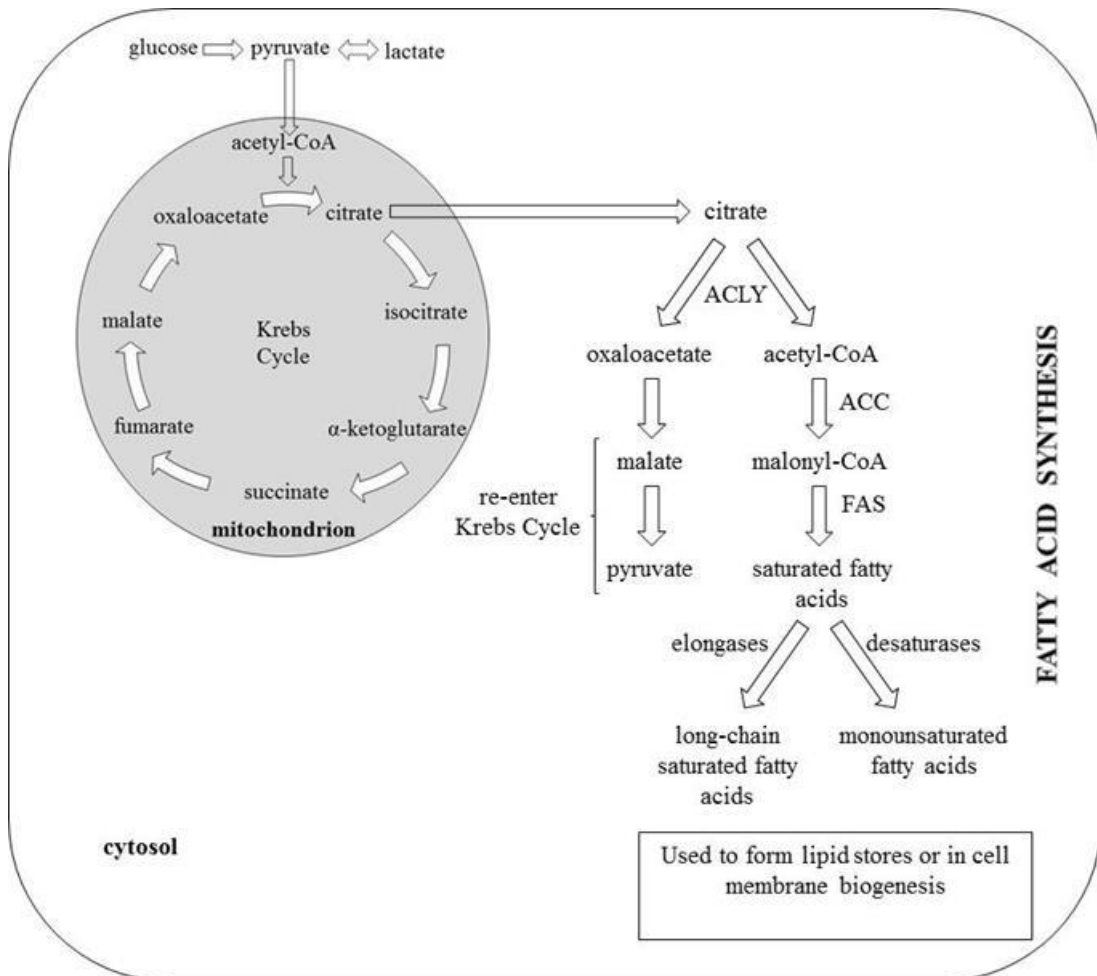
Figure 1.7: Fatty acid synthesis pathway. Citrate from the Krebs cycle enters the cytosol where it goes through a series of enzyme-catalysed reactions to form saturated fatty acids for use in cell membrane biogenesis or lipid storage. ACLY: ATP citrate lyase, ACC: acetyl-CoA carboxylase, FAS: fatty acid synthase. Figure adapted from Zadra *et al*., (2013).

In prostate cancer, the enzymes involved in fatty acid synthesis tend to be over-expressed (Rossi et al., 2003; Swinnen et al., 2000, 2002). ACLY is considered a key player in cancer metabolism as it is either upregulated or activated in many human

cancer types including prostate cancer (Bauer et al., 2005; Swinnen et al., 2000). Inhibition of ACLY has been shown to inhibit the proliferation of prostate cancer cells *in vitro*, suppress tumour growth in xenograft mice and induce apoptosis (Gao et al., 2014). Therefore, it appears that ACLY plays an important role in the progression of prostate cancer, but the mechanisms behind its oncogenic ability still need to be elucidated (Gao et al., 2014).

ACC, a highly regulated enzyme in the fatty acid synthesis pathway, is over-expressed in prostate cancer (Swinnen et al., 2000). Over-expression of ACC usually occurs together with an over-expression of FAS, most likely to prevent the accumulation of malonyl-CoA, which is cytotoxic in high quantities (Swinnen et al., 2000). Knockdown or pharmacological inhibition of ACC using soraphen A is cytotoxic to prostate cancer cells, inducing growth arrest and apoptosis (Beckers et al., 2007; Brusselmans et al., 2005b). This chemical inhibition of ACC obstructs the fatty acid synthesis pathway and decreases the amount of phospholipids in prostate cancer cells (Beckers et al., 2007). While the extent of the role of ACC in the pathogenesis of prostate cancer remains to be determined, the limited evidence in the literature indicates that ACC is critical for the proliferation of prostate cancer cells (Beckers et al., 2007; Brusselmans et al., 2005b; Swinnen et al., 2000).

The overexpression of FAS occurs early in the pathogenesis of prostate cancer and has been associated with a poor prognosis, with the highest levels of FAS evident in androgen-independent bone metastases (Rossi et al., 2003). Pharmacological inhibition of FAS using orlistat is selectively cytotoxic to prostate cancer cells, with no effect on the normal prostate cells, and causes a reduction in prostate cancer tumour volume in xenograft models (Kridel et al., 2004). Silencing of the FAS gene by RNA interference causes apoptosis, suggesting that the inhibition of apoptosis may be a potential mechanism of FAS oncogenicity (De Schrijver et al., 2003). Additionally, FAS has been shown to activate the Wnt/β-catenin pathway (Fiorentino et al., 2008) and inhibit endoplasmic reticulum stress (Little et al., 2007) in prostate cancer, further demonstrating the need for endogenous fatty acids in the development and progression of prostate cancer.

Endogenous fatty acid synthesis is under the control of transcriptional regulators and metabolic enzymes that act as oncogenes and tumour suppressors (Cantor and Sabatini, 2012; Zadra et al., 2013). Among these regulators, AMP-activated protein kinase (AMPK) has a major influence on fatty acid metabolism with diverse roles ranging from energy conservation to growth regulation (Luo et al., 2010). The protein exists as a heterotrimeric complex composed of a catalytic α subunit and regulatory β and γ subunits, each with at least two isoforms. AMPK becomes activated when Thr172 in the AMPKα subunit of the complex is phosphorylated (Flavin et al., 2011). Pharmacologically activated AMPK can inhibit fatty acid synthesis by targeting several of the enzymes in the pathway. It can directly inhibit ACC through phosphorylation, or indirectly inhibit FAS and ACLY via phosphorylation of SREBP-1 (sterol regulator element binding protein-1), a transcriptional regulator (Flavin et al., 2011). Consequently, the cancer cells would undergo apoptosis and growth inhibition (Fogarty and Hardie, 2010; Shaw, 2009). In prostate cancer the direct activation of AMPK induces growth arrest and apoptosis (Chen et al., 2012; Lin et al., 2012; Zadra et al., 2014). Furthermore, pharmacologic activation of AMPK in LNCaP prostate cancer cells using metformin and 5-aminoimidazole-4-carboamide ribonucleotide (AICAR) resulted in downregulation of genes that are overexpressed in prostate cancer, indicating the potential role of AMPK in tumour growth inhibition (Jurmeister et al., 2014). *In vivo* studies show that loss of the catalytic subunit of AMPK promotes the development of prostate cancer (Faubert et al., 2013; Zadra et al., 2014). Nevertheless, the extent of the role of AMPK in prostate cancer metabolism still requires clarification, as some studies suggest that the activation of AMPK is involved in the growth and survival of human prostate cancer (Chhipa et al., 2010; Frigo et al., 2011; Park et al., 2009).

1.2.2.3.2. Fatty acid oxidation

In malignant cells, the saturated fatty acids produced during fatty acid synthesis, which are not utilised in cell membrane biosynthesis or in lipid stores, are catabolised by the fatty acid oxidation (β-oxidation) pathway. It occurs predominantly in the mitochondria and is initiated when the fatty acids are activated and transported by carnitine palmitoyltransferase1 (CPT-1) from the cytosol into the mitochondria (Biswas et al., 2012). Once in the mitochondria, fatty acids go through several cycles of a series of four reactions (two separate dehydrogenation reactions, hydration and thiolysis) to

produce acetyl-CoA along with reduced nicotinamide adenine dinucleotide (NADH) and the reduced form of flavin adenine dinucleotide (FADH$_2$) during each cycle (Carracedo et al., 2013). The NADH and FADH$_2$ enter the electron transport chain to produce ATP, while the acetyl-CoA condenses with oxaloacetate to form citrate for entry into the Krebs cycle for efficient ATP production.

As previously indicated, an increase in citrate oxidation via the Krebs cycle is a requirement for the progression of prostate cancer (Costello and Franklin, 2000; Costello et al., 2005), and so a continuous supply of acetyl-CoA is required to ensure citrate oxidation. Since prostate cancer cells display a low rate of glycolysis, fatty acid oxidation is the most likely source of acetyl-CoA, and by extension, ATP (Liu, 2006; Liu et al., 2010). α-Methylacyl-CoA racemase (AMACR), an enzyme involved in fatty acid oxidation, is consistently overexpressed in human prostate cancer (Jiang et al., 2001; Kumar-Sinha et al., 2004; Luo et al., 2002; Rubin et al., 2002). Additionally, the loss of stearoyl-CoA desaturase (SCD) expression, a key enzyme involved in the modification of saturated fatty acids, is a common occurrence in prostate cancer and results in the elevation of palmitate levels, which subsequently enhance fatty acid oxidation (Moore et al., 2005). Malonyl-CoA acts as an allosteric inhibitor of fatty acid oxidation by inhibiting CPT-1 (Eaton et al., 1996), so as the levels of malonyl-CoA are kept low due to the high rate of fatty acid synthesis in prostate cancer, allosteric inhibition is lost and fatty acid oxidation can readily occur (Biswas et al., 2012; Currie et al., 2013). Taken together, the evidence in the literature implies a role for citrate oxidation in prostate cancer tumorigenesis. However the direct effect of fatty acid oxidation on prostate cancer metabolism, growth and survival remains unclear.

1.3. *In vitro* and *in vivo* models of prostate cancer

Pre-clinical models of prostate cancer have advanced the biological understanding of human prostate cancer and led to the development of therapeutic agents such as docetaxel (Ahmad et al., 2008; Jennings et al., 2002). Among these pre-clinical models, immortalised cell lines and mouse models are widely used.

1.3.1. Prostate cancer cell lines

Prostate cancer cell lines are critical in the identification of potential gene or protein targets and molecular mechanisms involved in the development and treatment of prostate cancer. There are a number of well-established human prostate cancer cell lines available for use in prostate cancer research (Table 1.4). Almost all of the cell lines have been established from metastatic sites and thus limit studies to the metastatic form of prostate cancer (Peehl, 2005; Wang et al., 2005). Among these cell lines, the most commonly used are PC-3, DU145 and LNCaP (Pienta et al., 2008; Toivanen et al., 2012). Only a few cell lines have been developed from the localised tumour and among them 22Rv1 is widely used in prostate cancer studies (Pienta et al., 2008). Therefore, no single cell line can depict the heterogeneous features of prostate cancer and so multiple cell lines should be included in any study to determine the effects of a therapy at various stages in the pathogenesis of prostate cancer. Several immortalised non-tumorigenic cell lines, including RWPE and PNT2, have been developed and can be used to compare the normal prostate response with the prostate cancer cell lines. However it is imperative to note that the immortalised prostate cell lines may possess genetic features derived from the immortalisation process, such as the human simian virus 40 (SV40), that are not representative of the human prostate cell *in vivo* (Peehl, 2005) and hence should be considered when interpreting data using these cell lines.

Model	Source	Androgen receptor (AR) status
PC-3	Cell line from bone metastasis	AR-
LNCaP	Cell line from lymph node metastasis	Mutated AR
DU145	Cell line from dural metastasis	AR-
22Rv1	Primary prostate tumour	AR+
PC-82	Primary prostate tumour	AR+
PrEC	Non-immortalised prostate epithelial cells	AR+
RWPE	Immortalised prostate epithelial cells	AR+
PNT2	Immortalised prostate epithelial cells	Mutated AR

Table 1.4: Human prostate cancer cell lines. These cell lines are obtained from different sources. The AR status indicates the presence or absence of the AR but it does not indicate if the specific cell lines require androgens for growth. Table based on information gathered from van Bokhoven *et al* (2003) and Pienta *et al* (2008).

1.3.2. Mouse models of prostate cancer

Mouse models have made a significant contribution to the knowledge and understanding of prostate cancer biology. However, there are some anatomical differences between the mouse and humans. As previously described, the human prostate is a single gland made up of zones which demonstrate differences in disease susceptibility. In the mouse there are four distinct lobes, anterior, ventral, lateral and dorsal. The dorsal and lateral (dorso-lateral) lobes are considered anatomically similar to the peripheral zone in humans (Powell et al., 2003) but there is no molecular evidence to support any direct link between the lobes of the mice and the zones of the human prostate (Shappell et al., 2004). Furthermore, mice are unable to develop spontaneous cases of cancer in the prostate (Shappell et al., 2004). Despite these challenges, the mouse is the most widely used animal model of human prostate cancer and a few of the models are described below.

1.3.2.1. Xenograft models of prostate cancer

The mouse is used as a xenograft model for *in vivo* analysis of immortalised prostate cancer cell lines and human tumour tissues. The mice used in xenograft studies are

immunodeficient and are therefore unable to mount an immunologic response to the human tissues or cells that are implanted. Consequently, the human tumours are able to grow without interference from the host/mouse microenvironment (Toivanen et al., 2012).

When developing human prostate cancer xenografts, the tissue source, the host mice and the graft site must be carefully considered, in order to ensure that the xenografts adequately recapitulate the progression of the disease in a microenvironment that mimics that of prostate cancer (Figure 1.8). So far, human prostate cancer xenografts have successfully demonstrated that tumours which are subjected to androgen deprivation therapy are capable of synthesising androgens *de novo*, thus accounting for the development of androgen independent prostate cancer following hormone therapy (Locke et al., 2008). Additionally, these xenografts have been used to identify many potential prostate cancer preventive or therapeutic agents (Singh and Agarwal, 2006). Despite the range of applications of human prostate cancer xenografts, there are a number of limitations that contribute to the relatively low success of the xenograft-tested agents later in the clinic (Toivanen et al., 2012). These limitations include omission of the normal process of tumour initiation and elimination of the interaction between immune and tumour cells, which have some influence on metastasis (Valkenburg and Williams, 2011). Nevertheless, within the boundaries of their limitations, mouse xenografts are still essential in prostate cancer research.
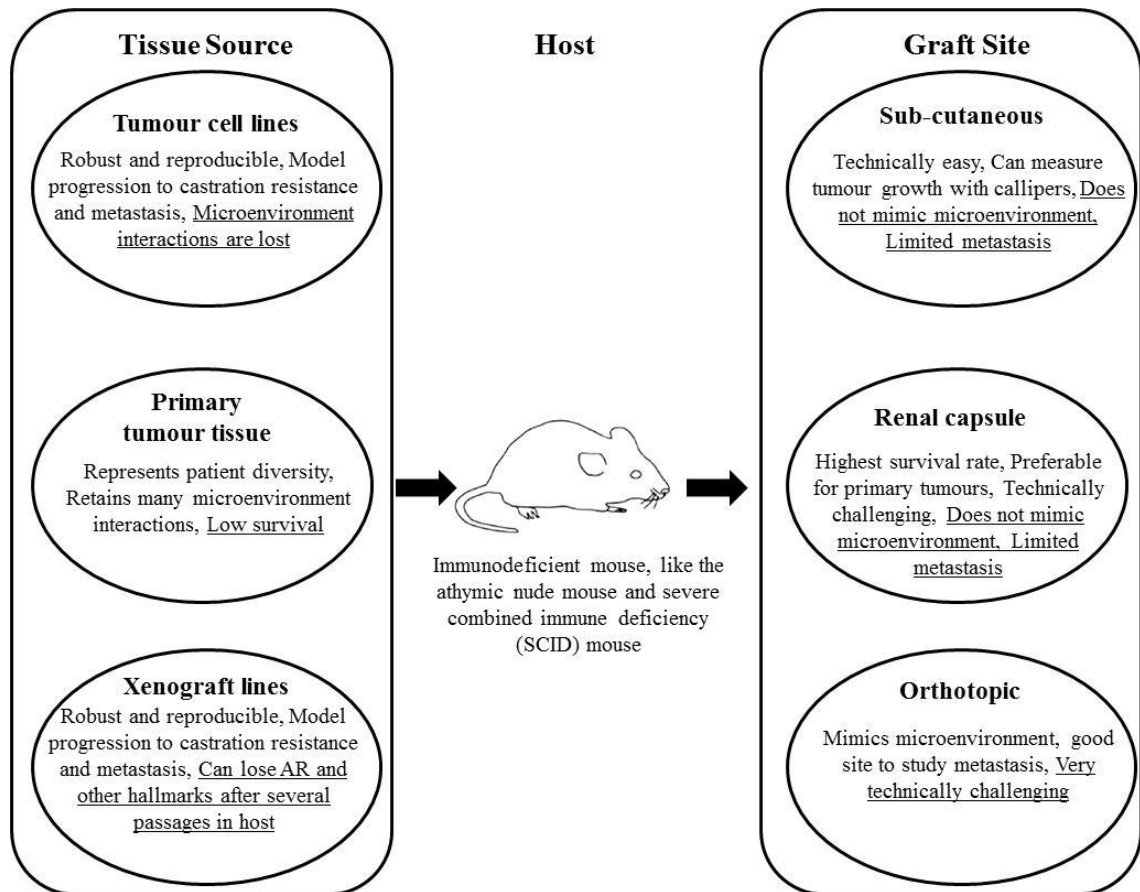
Figure 1.8: Human prostate cancer xenograft systems. Schematic diagram of the main xenograft systems, highlighting the advantages and the disadvantages (underlined) of each system. Established immortalised prostate cancer cell lines can be implanted into the host or primary human tissues can be implanted for study in a single host without passaging. The xenograft lines are human prostate cancer tissues created from a human tumour that has been serially transplanted in a mouse without any *in vitro* culturing. The host mice are all immunodeficient but have different genetic and morphological features. Therefore, host mice must be carefully selected to prevent these features from altering the xenograft study. The choice of graft site depends on the technical expertise available, the tissue source, the desired endpoint, the suitability of the host and the type of microenvironment required for the study. Figure adapted from Toivanen *et al.* (2012).

1.3.2.2. Genetically engineered mouse models of prostate cancer

Genetically engineered mouse models (GEMMs) circumvent many of the limitations associated with the mouse xenografts since the tumours are allowed to arise *in situ* and to progress through the stages of tumorigenesis in an environment that closely mimics that of human prostate cancer. Several GEMMs of prostate cancer are being utilised in

research to further the understanding of prostate cancer biology and to test the efficacy of preventive and therapeutic agents (Table 1.5). Only a few of the more common models are included here.

Model	Genetic manipulation	Phenotype
Pten	Traditional/germline knockout	Homozygous deletion-embryonic lethality; Heterozygotes-develop PIN, dysplasia
PB^{Cre4}*Pten^{flox}*	Conditional knockout	Homozygous deletion-develop PIN which progress to metastatic adenocarcinoma; Metastatic sites: lymph node, lung
Nkx3.1	Traditional/germline knockout	Homozygous deletion-prostatic hyperplasia and neoplasia; Heterozygotes-similar to above but less severe
Pten/*Nkx3.1*	Compound deletion (*Pten$^{+/-}$,Nkx3.1$^{-/-}$*) by traditional/germline knockout	Develop PIN which progress to metastatic adenocarcinoma; Metastatic site: lymph node
PB^{Cre4}*p53^{flox}Rb^{flox}*	Conditional knockout	Develop PIN which progress to metastatic adenocarcinoma; Metastatic sites: lymph node, lung, liver, adrenal gland
TRAMP	SV40 transgene expression	Develop PIN which progress to metastatic neuroendocrine carcinoma; Metastatic sites: lymph node, lung, adrenal gland, bone
LADY	SV40 transgene expression	Develop PIN and progress to adenocarcinoma with neuroendocrine differentiation; Metastatic sites: lymph node, liver, lung

Table 1.5: Genetically engineered mouse models of prostate cancer. The models are created either by the whole body deletion (traditional/germline knockout) or prostate-specific deletion (conditional knockout) of genes that are important in the development of prostate cancer. Additionally, some may be produced by integrating a transgene that upon expression, allows for the development of prostate cancer. Each model exhibits phenotypes that mimic various aspects of human prostate cancer, but there is no model that accurately depicts the entire spectrum of the human disease. Table adapted from Hensley and Kyprianou (2012) and Parisotto and Metzger (2013).

1.3.2.2.1. Transgenic T antigen models

Transgenic T antigen models were the first-generation of GEMMs developed. These allowed for the prostate-specific expression of the viral oncogene, SV40 Large T antigen (Tag), which inactivates the tumour suppressor proteins p53 and retinoblastoma (Rb) to induce the oncogenic process (Ahuja et al., 2005; Parisotto and Metzger, 2013). The TRansgenic Adenocarcinoma of the Mouse Prostate (TRAMP) model, one of the most widely used and highly characterised models, expresses both the large-T and small-t SV40 antigens under the control of the prostate-specific rat probasin promoter (PB) (Greenberg et al., 1995). The T antigen oncoprotein is expressed in the dorso-lateral and ventral lobes of the TRAMP mice. These mice develop PIN between 8-12 weeks of age, which progresses to a poorly differentiated invasive neuroendocrine carcinoma by 16-28 weeks (Gingrich et al., 1996; Kaplan-Lefko et al., 2003). The cancer generally metastasises to the liver, kidney and adrenal glands by 16-36 weeks. There is also metastasis to the bone, albeit at a very low frequency, if the C57BL/6/FVBn genetic background is used, as opposed to the pure C57BL/6 (Gringrich et al., 1996). The progression from PIN to metastatic disease, along with the display of many of the morphological, genetic and metabolic changes observed in human prostate cancer, makes the TRAMP model highly suitable for cancer prevention studies (Costello et al., 2011; Gupta et al., 2001; Klein, 2005). However, its use is also heavily criticised as there is no evidence to support the role of SV40 in the development of prostate cancer in humans, so the clinical relevance of the TRAMP model is questionable. Furthermore, most of the TRAMP mice develop neuroendocrine prostate cancer, which occurs in very few human prostate cancer cases, so again any study findings in the TRAMP model have limited application in the clinical setting (Abrahamsson, 1999). Despite these cautions, the TRAMP model remains popular and has been used in chemoprevention studies with agents such as green tea polyphenols (McCarthy et al., 2007) and genistein (Wang et al., 2007).

1.3.2.2.2. Traditional knockout models

Traditional or germline knockout models are used to investigate the roles of specific genes, namely tumour suppressor genes or oncogenes, in the pathogenesis of prostate cancer and subsequently to evaluate preventive or therapeutic strategies against those genetically-driven prostate cancers. Mutations that reduce or eliminate the function of

tumour suppressors are often evident in the human disease (Berger and Pandolfi, 2011). Therefore, in these models the gene of interest is deleted/silenced or mutated in all cells in the mice (Capecchi, 1994). Phosphatase and tensin homolog deleted on chromosome 10 (*Pten*) is a tumour suppressor gene that is often mutated in metastatic prostate cancers and has been implicated in the resistance seen by these cases to chemotherapy (Priulla et al., 2007) and radiotherapy (Anai et al., 2006). Therefore, *Pten* knockout mice have been generated to establish the importance of Pten in prostate cancer development. Homozygous deletion of *Pten* alleles caused embryonic lethality (Di Cristofano and Pandolfi, 2000; Suzuki et al., 1998) while heterozygotes (*Pten* $^{+/-}$) developed PIN within 8-10 months with no evidence of metastasis (Podsypanina et al., 1999). Neoplasia was also detected in a number of distant tissues including intestines, thyroid and adrenal glands (Di Cristofano et al., 1998, Podsypanina et al., 1999). Hence, Pten is critical to the development of prostate cancer, but its loss from the genome is not sufficient to cause prostate cancer, and so other genes including *p27* or *Nkx3.1* have been knocked out along with the *Pten* gene (compound deletion or double knockout) to improve the model. Since these knockout models eliminate the gene of interest from the entire animal, the prostate-specific role of the gene cannot be determined and is not a real reflection of human prostate cancer where prostate-specific mutations are believed to be triggers in the initiation and development of prostate cancer (Hanahan and Weinberg, 2000). Therefore, prostate-specific gene knockout models are of greater translational value.

1.3.2.2.3. Conditional knockout models

A conditional knockout model is a biological model in which the gene of interest is inactivated in a specific tissue but remains functionally expressed in all other tissues. Therefore, in the conditional knockout models described below, the genes of interest are inactivated in the prostate only. The Cre-lox P system is widely used for the generation of conditional knockout models. In the model described by Abremski and Hoess (1984) Cre recombinase catalyses recombination in genes that are engineered with flanking (floxed) lox P sites. Mouse lines expressing Cre recombinase in the prostatic epithelial cells carry the *Cre* gene under the control of the -426/+28 PB promoter or ARR$_2$PB promoter, which is made of the -426/+28 PB promoter linked to two androgen-responsive regions (Maddison et al., 2000; Wu et al., 2001). These mouse lines are

known as PB-*Cre* and PB-*Cre4*, respectively. The specificity of the promoter is critical for the success of the Cre-lox P system and so a number of promoters have been generated. For example, attachment of the *Cre* gene to a ligand-binding domain of the human oestrogen receptor (ER) to form a tamoxifen activated Cre recombinase (Cre-ER^T) (Feil et al., 1996) offers even greater possibilities as the target genes can be knocked out at specific time points rather than from birth. Nevertheless, the PB-*Cre* and PB-*Cre4* are widely used, with PB-*Cre4* showing more specificity for the prostate epithelial cells, thus eliminating tumours with a neuroendocrine differentiation (Wu et al., 2001). Genes including *Pten* (Trotman et al., 2003; Wang et al., 2003), *Rb* (Maddison et al., 2004) and *p53* (Zhou et al., 2006) have been conditionally knocked out using the PB-*Cre* and PB-*Cre4* promoters.

Conditional knockout models have made it possible to observe the role of genes whose homozygous loss in the traditional models resulted in embryonic lethality. Furthermore, the conditional models provide a more accurate depiction of the disease since in the human condition the genetic mutations are usually confined to the prostate rather than a whole body event. Hence, the traditional *Pten* knockout model caused PIN only, while PB^{Cre4}*Pten^{flox}* caused adenocarcinoma and metastasis (Podsypanina et al., 1999; Wang et al., 2003). Conditional knockouts can also knockout more than one gene. The prostate-specific conditional knockout of *Rb* only or *p53* only led to PIN with no progression to adenocarcinoma (Zhou et al., 2006). However, when both were lost from the prostate (PB^{Cre4}*p53^{flox}Rb^{flox}*), metastatic disease developed and was found to exhibit some important molecular features of advanced human prostate cancer (Zhou et al., 2006). In addition to deleting/inactivating genes, the Cre-lox P system can be used to activate target genes leading to the overexpression of the gene product. This is crucial in investigating genes that are overexpressed. Taken together, conditional knockout mouse models of prostate cancer provide a wide opportunity to investigate the roles of the multiple genes that are deregulated in human prostate cancer (Bradford et al., 2006; Hughes et al., 2005; Mazaris and Tsiotras, 2013).

1.4. Chemoprevention in prostate cancer

Chemoprevention is the use of natural or synthetic compounds with the ability to prevent, arrest or reverse cancer before the development of metastatic disease (Lippman

et al., 1994). It can be further classified into three different categories as primary, secondary and tertiary chemoprevention (Kelloff et al., 1995). Primary chemoprevention is the use of chemical agents to prevent the onset of the disease in persons who are healthy but may have certain risk factors for developing the disease (Steward and Brown, 2013). With regards to prostate cancer, the primary chemopreventive agents aim to prevent the development of PIN in men who exhibit the risk factors previously described. Secondary chemoprevention, on the other hand, involves the administration of chemical agents to persons with premalignant lesions, in order to arrest the progression to the invasive form of the disease, while tertiary chemoprevention aims to prevent the relapse of cancers and the formation of new primary cancers in persons who previously were successfully treated (Steward and Brown, 2013). Therefore, secondary chemoprevention could delay or arrest the progression of PIN to adenocarcinoma, while tertiary chemoprevention could prevent or delay the biochemical recurrence of prostate cancer, which usually occurs in men who have been previously treated for localised prostate cancer.

Prostate cancer is an excellent clinical model for chemoprevention because of its high incidence and its tendency to progress slowly, sometimes over decades, to the invasive form of the disease (Djavan et al., 2004). Furthermore, watchful waiting or active surveillance is recommended for men with low risk localised prostate cancer, and the administration of a chemopreventive agent at this stage could potentially prevent or delay the onset of advanced cancer.

At the preclinical level, potential chemopreventive agents should show high efficacy and low toxicity in animal studies before clinical chemoprevention trials can be considered (Greenwald, 2002). Currently clinical trials to test the efficacy of chemopreventive agents are costly and require large populations (Steward and Brown, 2013). This is mainly due to the fact that the end point in clinical chemoprevention trials is overt cancer, which takes many years to develop (Greenwald, 2002). Hence the use of biomarkers for cancer as surrogate end points has generated a lot of interest as they would facilitate shorter-term trials at a much reduced cost (Crowell, 2005; Gerhauser et al., 2006; Greenwald, 2002). Suitable biomarkers are yet to be validated as surrogate end points for prostate cancer (Trock, 2001).

Bioactive food components such as genistein and green tea catechins have been the focus of recent prostate cancer chemoprevention trials, as these dietary agents are inexpensive and convenient to administer and also have excellent safety profiles, preclinical efficacy and epidemiological observations suggesting a reduction in prostate cancer incidence (Parnes et al., 2013). Drugs, such as the widely prescribed metformin, which is used by diabetics to control their blood sugar, have been repurposed for prostate cancer chemoprevention as retrospective studies have linked metformin with a reduced incidence of prostate cancer (Margel et al., 2013). As a consequence, metformin is now the subject of many prostate cancer chemoprevention clinical trials (Azvolinsky, 2014). New synthetic drugs may first be utilised as adjuvant treatments to facilitate a better understanding of their safety and efficacy profiles before they are considered for chemoprevention in healthy populations that do not have detectable cancer. Ultimately, the aim of chemoprevention is to provide natural or synthetic agents with low toxicity that will reduce the incidence and mortality of cancer.

1.4.1. Molecular targets in the management of prostate cancer

There are a number of biochemical and molecular pathways that become aberrant during the development and progression of prostate cancer. Therefore, these may present suitable targets for chemoprevention or treatment protocols against prostate cancer. Abnormalities in the metabolism of prostate cancer were highlighted earlier, but deregulated cell cycle progression and apoptosis are also common. Moreover, the role of cellular senescence in the chemoprevention and treatment of prostate cancer must also be given some consideration.

1.4.1.1. Cell Cycle Progression

Cell cycle is the sequence of events that lead to the duplication and subsequent division of cells into daughter cells. There are four phases to the cell cycle: Gap 1 (G1), DNA synthesis (S), Gap 2 (G2) and mitosis (M) (Norbury and Nurse, 1992) (Figure 1.9). The cell cycle is tightly regulated by cyclin-dependent kinases (CDKs), which are activated by binding to specific cyclins (Michalides, 1999). The transition from one phase to the next requires specific CDK/cyclin interactions. The levels of CDKs remain constant throughout the cell cycle but those of cyclins vary according to the phase of the cell cycle. Growth factors or other stimuli trigger the cell cycle by stimulating the

production of D cyclins, which activate CDK4 and CDK6 (Sherr, 1994). Upon activation, these kinases cause the phosphorylation of Rb, resulting in the release of E2F transcription factors. The transcription factors regulate the transcription of genes, including cyclin A and cyclin E, which are required for progression of the cell cycle (Brehm et al., 1998). CDK2 is activated by cyclin E for the G1/S transition (Sherr, 1994). CDK2-cyclin A complex is required for S-phase progression while CDK1-cyclin A complex is required for G2/M transition (Grana and Reddy, 1995). CDK1-cyclin B regulates mitosis (Arellano and Moreno, 1997).

CDK activity is negatively regulated by CDK inhibitors (CDKI), which are able to inactivate CDK-cyclin complexes or prevent activation of CDKs by binding to these proteins. There are two families of CDKI, the INK4 family and the Cip/Kip family (Sherr and Roberts, 1995). Together, these CDKIs help to restrict the cell cycle, thus preventing excessive cell growth. To ensure that the genetic integrity of a cell is preserved as it goes through the cell cycle, checkpoints are established at G1/S, S and G2/M phases. The detection of aberrations at these checkpoints leads to cell cycle arrest until the damage is repaired or the cell undergoes apoptosis. The *p53* tumour suppressor gene plays a critical role at these checkpoints (el-Deiry et al., 1993). *Rb*, *p53* and some of the CDKIs, including *p27*, *p16* and *p14* are often mutated in prostate cancer (Guo et al., 1997; Navone et al., 1993; Phillips et al., 1994; Konishi et al., 2002; Badal et al., 2008). Additionally, the loss of expression of *p21* from the Cip/Kip family of CDKIs, is often associated with a poor prognosis in prostate cancer (Aaltomaa et al., 1999). Therefore, any chemopreventive agents that can upregulate CDKIs can potentially inhibit the development and progression of prostate cancer.
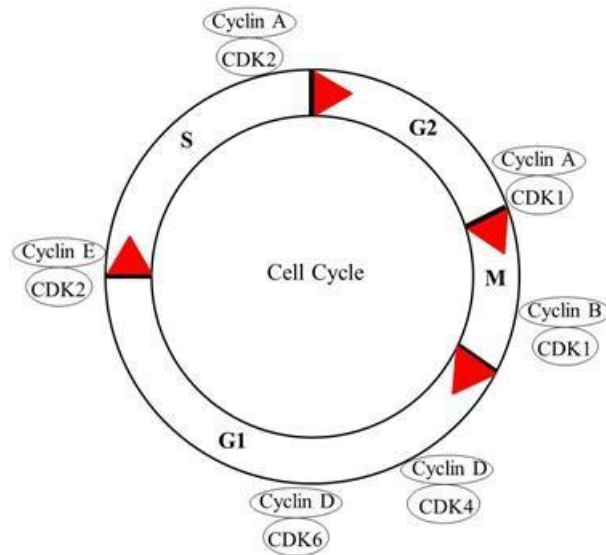
Figure 1.9: Phases of the cell cycle. The cell cycle starts at G1 and proceeds through to M. Each phase is under the regulation of the CDK-cyclin complexes indicated. If aberrations are detected in any of the phases then cell cycle arrests occurs and cell growth will come to a halt. G1: Gap 1, S: synthesis, G2: Gap 2, M: mitosis, CDK: cyclin-dependent kinase.

1.4.1.2. Apoptosis

The induction of apoptosis is considered to be the most important defence mechanism against the development and progression of cancer. Extracellular or intracellular signals trigger the extrinsic or intrinsic apoptotic pathways, respectively (Figure 1.10). In the extrinsic pathway, pro-apoptotic ligands, such as first apoptosis signal ligand (FasL) and Apo2 ligand (Apo2L), bind to the death receptor, resulting in formation of the death inducing signalling complex (DISC) and activation of caspase-8. The activated caspase-8 then activates the executioner caspases, caspase-3, -6, and -7, to bring about degradation of the cell (Kuno et al., 2012). Furthermore, active caspase-8 can cleave Bid (a pro-apoptotic protein), thus allowing its active fragment to become attached to the mitochondrial membrane. This would then initiate the intrinsic apoptotic pathway, in a bid to amplify the apoptotic effect (Kuno et al., 2012). In addition to the 'cross-talk' between the two pathways, the intrinsic pathway is initiated by non-receptor mediated stimuli (for example, DNA damage, oxidative stress and chemotherapeutic drugs) that cause the release of pro-apoptotic proteins such as cytochrome c from the

mitochondria into the cytoplasm. This leads to the activation of caspase-9, which in turn activates the executioner caspases to bring about cell degradation. Smac/DIABLO [the second mitochondria-derived activator of caspases (Smac) and direct inhibitor of apoptosis-binding protein with low pI (DIABLO)] is also released from the mitochondria to help facilitate caspase activation by removing the inhibitory action of the inhibitor of apoptosis proteins (IAPs) (Khan et al., 2010). The Bcl-2 family of proteins, made up of anti-apoptotic, (Bcl-2 and Bcl-xL), and pro-apoptotic, (Bax and Bad) proteins is a major regulator of the intrinsic pathway (Iannalo et al., 2008). The anti-apoptotic proteins are located in the outer mitochondria and function to inhibit cytochrome c release. The pro-apoptotic proteins are present in the cytosol, but translocate to the mitochondria following stimulation, where they facilitate the release of cytochrome c. In cancer cells the anti-apoptotic proteins are predominantly expressed, making the cell resistant to apoptosis (Catz and Johnson, 2003). Histological studies have demonstrated the over-expression of Bcl-2 in approximately 30 % of prostate cancers, which correlates with a more aggressive form of the disease and poorer prognosis (McCarthy, 2004). Hence, any potential chemopreventive agents that can modulate the ratio of pro-apoptotic to anti-apoptotic proteins in a manner that favours apoptosis could be effective in inhibiting prostate cancer.
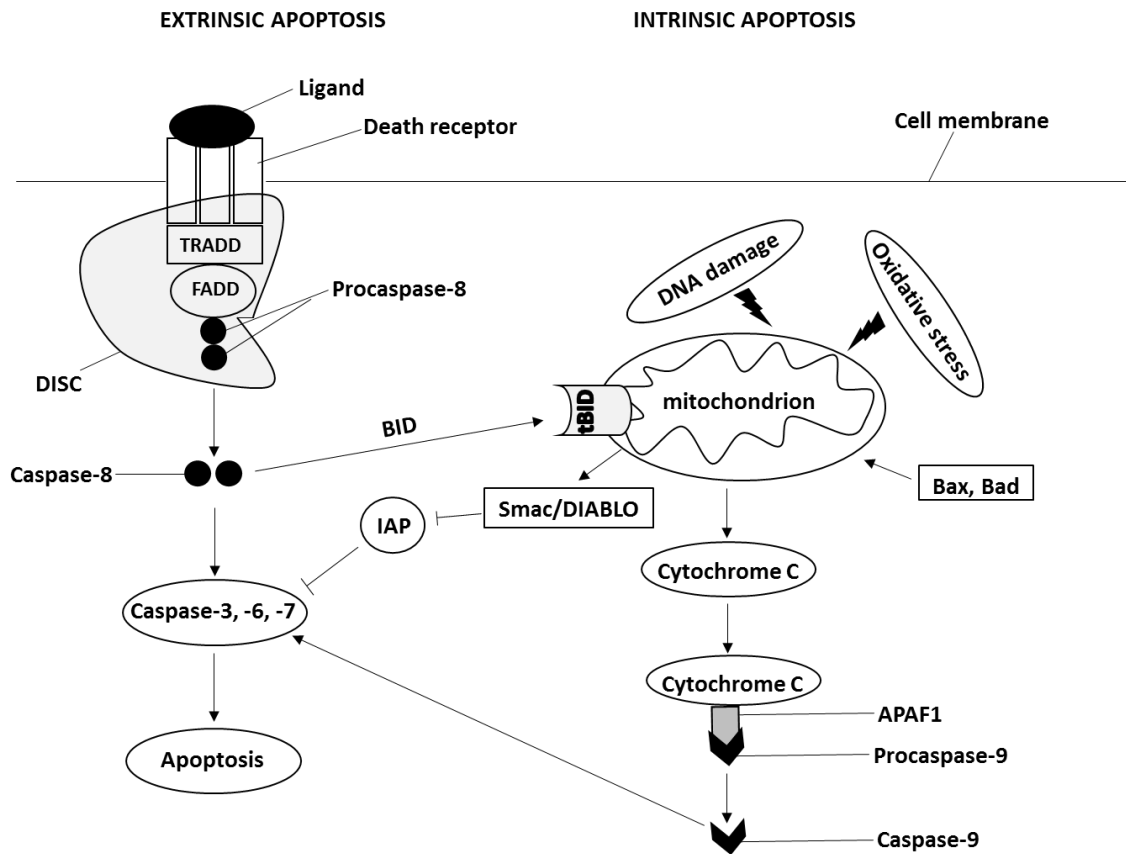
Figure 1.10: Schematic diagram of the intrinsic and extrinsic pathways of apoptosis. The pathways are activated by different stimuli but both lead to the activation of caspases. The caspases initiate degradation of the cell and eventually the apoptotic cell is ingested by phagocytes. TRADD: tumour necrosis factor receptor associated death domain, FADD: FAS associated death domain, Smac: the second mitochondria-derived activator of caspases, DIABLO: direct inhibitor of apoptosis-binding protein with low pI, APAF1: apoptosis protease activating factor 1, DISC: death-inducing signalling complex, IAP: inhibitor of apoptosis protein

1.4.1.3. Senescence

Cellular senescence is the irreversible growth arrest of cells which are still metabolically active (Campisi and d'Adda di Fagagna, 2007). It can be induced by several factors including telomere shortening, DNA double strand breaks, oncogenic factors and chemotherapy and radiation (Collado et al., 2005; DiLeonardo et al., 1994;

Mathon and Lloyd, 2001; Roninson, 2003). Growth arrest generally occurs in either the G1 or G2/M phase of the cell cycle as a consequence of an increase in CDKIs, including p16, p21 and p27 (Bringold and Serrano, 2000). Both p53 and Rb are also involved in the induction of senescence (Beausejour et al., 2003; Campisi and d'Adda di Fagagna, 2007). Induction therefore can follow different pathways depending on the cell type. However, most senescent cells express high levels of p16 (Ben-Porath and Weinberg, 2005; Stein et al., 1999). Cells with or without functional p53 and Rb can readily be induced to senesce (Beausejour et al., 2003; Campisi and d'Adda di Fagagna, 2007; Chang et al., 1999; Schwarze et al., 2005). Senescent cells usually display an enlarged and flattened morphology with an increase in cytoplasmic granularity (Campisi, 2001). They can be distinguished from the non-senescent cells by measuring senescence-associated β-galactosidase (SA-β-galactosidase) activity at pH 6 (Debacq-Chainiaux et al., 2009; Gary and Kindell, 2005). The senescent cells have a higher SA-β-galactosidase activity because of their much larger lysosomal mass (Lee et al., 2006).

Malignant transformations tend to be associated with the inhibition of senescence. For example, senescence is evident in benign prostatic hyperplasia and the premalignant prostatic intraepithelial neoplasia but absent from the adenocarcinomas isolated from humans (Chen et al., 2005; Choi et al., 2000; Majumder et al., 2008). Hence, senescence appears to play a role in restricting tumorigenesis. Nevertheless, the malignant cells do not lose the ability to senesce, since chemotherapy and re-activation of the *p53* gene can subsequently induce senescence in these malignant cells, resulting in tumour regression (Coppé et al., 2010; Ventura et al., 2007; Xue et al., 2007). Consequently, the induction of senescence is considered to be a crucial anticancer mechanism since it can prevent the growth of cells at risk for malignant transformation and also stop the growth of malignant cells.

A cursory glance at the relationship between senescence and malignancy would suggest that the induction of cellular senescence is a beneficial outcome for chemopreventive/chemotherapeutic agents, but many studies are suggesting otherwise. A key feature of senescent cells is the ability to secrete growth factors, cytokines and other proteins, referred to as senescence-associated secretory phenomenon (SASP) (Coppé et al., 2006, 2010). These SASP proteins have now been found to stimulate the growth and migration of malignant cells (Bartholomew et al., 2009; Coppé et al., 2008;

Krtolica et al., 2001). More recently, androgen deprivation-induced senescent prostate cancer cells were found to stimulate the proliferation of the incurable androgen-independent prostate cancer cells (Burton et al., 2013). Only a few of the SASP proteins are unable to stimulate cancer growth (Nickoloff et al., 2004). Hence, despite the immediate benefits of therapy-induced senescence in cancer management, particularly prevention, the long term effects of its induction may revert these benefits and as a consequence therapy-induced senescence remains an active area of research.

1.4.2. Potential chemopreventive agents for prostate cancer

1.4.2.1. 5-Alpha reductase inhibitors

5-Alpha reductase is required to convert testosterone into its more potent form of dihydrotestosterone, which regulates normal and hyperplastic growth of the prostate gland (Brawley & Barnes, 2001; Hsing et al., 2002) (Figure 1.11). There are three isoforms of 5-alpha reductase and they are expressed in a wide range of tissues, but the expression of types 1 and 2 are altered in prostate cancer (Azzouni et al., 2012; Thomas et al., 2008). Therefore, 5-alpha reductase inhibitors can potentially inhibit androgen-stimulated growth in the normal and malignant prostate, thus resulting in a reduction of BPH and prostate cancer incidence. Hence, the development of finasteride and dutasteride, which are both 5-alpha reductase inhibitors, provided the opportunity to determine the efficacy of this class of drugs in the chemoprevention of prostate cancer.
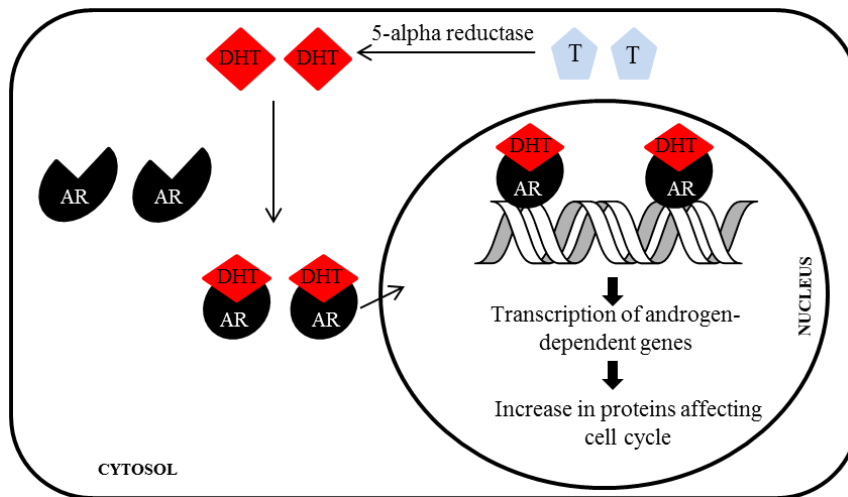
Figure 1.11: 5-Alpha reductase in androgen-induced gene expression. Testosterone (T) diffuses into the cell and if 5-alpha reductase is present it is converted into dihydrotestosterone (DHT). DHT interacts with the androgen receptor (AR), then translocates to the nucleus where the DHT-AR complex binds to the DNA of the target genes. The genes are then transcribed and translated into proteins that may influence cell growth and differentiation.

Finasteride: Finasteride, a Food and Drug Administration (FDA) approved drug treatment for BPH, inhibits the type 2 isoform of 5-alpha reductase. It was used in the Prostate Cancer Prevention Trial (PCPT) to determine whether it could reduce the risk of prostate cancer (Goetzl and Holzbeierlein, 2006; Thompson et al., 2014). Approximately 18 800 men, aged 55 and older, with a PSA of less than 3.0 ng/mL and a normal DRE, were randomly selected to receive 5 mg of finasteride or placebo daily for 7 years. At the end of the study there was a 24.4 % reduction in the prevalence of prostate cancer. However, there was a higher proportion of high-grade tumours in the finasteride group compared to the placebo group (Goetzl and Holzbeierlein, 2006; Thompson et al., 2014). High-grade tumours are more aggressive and result in higher mortality (Zhou et al., 2005). As a consequence, finasteride has not been approved for preventing prostate cancer. However, subsequent analyses of the PCPT data concluded that the higher risk of high-grade tumour in the finasteride group was due to improved detection, facilitated by the finasteride treatment (Redman et al., 2008). Furthermore, twenty years after the study started, no difference was observed in the fifteen-year survival rates for the finasteride and placebo groups, and the survival rates for low-grade and high-grade tumours were similar between the groups (Thompson et al., 2014).

Therefore, it can be concluded that finasteride significantly reduces the risk of prostate cancer but with no added advantage to life expectancy (LeFevre, 2013).

Dutasteride: Dutasteride inhibits both the type 1 and type 2 isoforms of 5-alpha reductase. In the Reduction by Dutasteride of Prostate Cancer Events (REDUCE) trial, men aged 50-75 years with a PSA of between 2.5-10 ng/mL and a negative prostate biopsy 6 months prior to enrolment, were given either 0.5 mg of dutasteride or placebo daily for 4 years to determine whether dutasteride was capable of reducing the incidence of disease in these men who were at a high risk for prostate cancer (Andriole et al., 2010). It was found that dutasteride reduced the risk of biopsy-detectable prostate cancer by approximately 23 % and that it also reduced the risk of progression of benign prostatic hyperplasia (Andriole et al., 2010; Roehrborn et al., 2011). However, similarly to finasteride, there was an increased incidence of high-grade tumours amongst the dutasteride group (Andriole et al., 2010). As a consequence, dutasteride remains approved for the treatment of BPH but is not approved as a prostate cancer chemopreventive agent.

1.4.2.2. Selenium and Vitamin E

Selenium is an essential trace element found at varying concentrations in many plants, such as garlic and onions, and also in a variety of sea animals, including tuna. It can exist in different forms with variable effects on prostate cancer and normal cells (Pinto et al., 2007). Most of the selenium chemoprevention studies have used either sodium selenite or selenomethionine (Shukla and Gupta, 2005). Preclinical investigations using LNCaP, DU145 and PC-3 cell lines demonstrated that selenium in the form of sodium selenite inhibited growth through the induction of apoptosis (Ghosh, 2004; Menter et al., 2000; Zhong and Oberley, 2001). Additionally, selenite caused mitochondrial injury and cell death (Zhong and Oberley, 2001) and activation of *p53*, leading to p53-mediated apoptosis (Sarveswaran et al., 2010) in LNCaP cells. Several epidemiological studies further suggest a role for selenium as a potential chemopreventive agent for prostate cancer, as higher levels of selenium in the plasma and toenail samples of men appear to be associated with a lower risk of prostate cancer (Li et al., 2004; Nomura et al., 2000; van den Brandt et al., 2003). More convincingly, a randomised placebo-controlled trial, the Nutritional Prevention of Cancer Trial (NPCT) in which participants

were given a daily dose of 200 μg of selenised yeast for approximately 5 years, revealed a 63 % reduction in incidence of prostate cancer in comparison to the placebo group (Clark et al., 1998). Further analysis of NPCT data revealed that selenium supplementation had no effect among men with a high baseline of plasma selenium (Duffield-Lillico et al., 2003). Despite the encouraging preclinical and epidemiological evidence in support of selenium as a potential chemopreventive agent for prostate cancer, more recent studies have created significant doubt. The randomised, controlled Selenium and Vitamin E Cancer Prevention Trial (SELECT) revealed that selenium supplementation in the form of L-selenomethionine (200 μg/day) had no effect on prostate cancer incidence (Lippman et al., 2009). Furthermore, in men with a high baseline of plasma selenium there was an increased risk of high-grade prostate cancer (Kristal et al., 2014). Most recently, Kenfield *et al*. (2015) found that selenium supplementation (140 μg/day) after diagnosis of localised prostate cancer, may increase risk of prostate cancer mortality. Therefore, the clinical trials have largely failed to demonstrate any chemopreventive effects of selenium and supplementation at doses that exceed the recommended dietary intakes would be unwise.

Vitamin E is a group of naturally occurring lipid-soluble antioxidants found in a variety of plants. α-Tocopherol is the most active form and has been found to significantly inhibit the growth and stimulate apoptosis of LNCaP cells (Gunawardena et al., 2000). Vitamin E succinate treatment of PC-3 cells also resulted in apoptosis, which was enhanced when vitamin E succinate was given in combination with selenium (Shiau et al., 2006; Zu and Ip, 2003). When vitamin E was administered together with selenium and lycopene to LADY transgenic mice there was a dramatic reduction in prostate cancer incidence (Venkateswaran et al., 2004) and the chemopreventive effect was most evident when the supplementation commenced within 8 weeks of age (Venkateswaran et al., 2009). Supplementation with vitamin E and selenium was less effective in decreasing prostate cancer incidence, thus suggesting that lycopene is critical for the efficacy of the vitamin E, selenium and lycopene combination supplementation (Venkateswaran et al., 2009). Vitamin E supplementation by itself or in combination with lycopene has been found to cause necrosis in the tumours of Dunning rats, but in this study the vitamin E only supplementation was more effective (Siler et al., 2004). In the Alpha-Tocopherol and Beta-Carotene (ATBC) cancer prevention trial, designed primarily to investigate chemoprevention in lung cancer, male smokers were given

vitamin E (50 mg/day) and/or β-carotene (20 mg/day). As a secondary endpoint, the incidence of prostate cancer was significantly reduced by 32 % and there was a 41 % reduction in prostate cancer mortality in the men receiving vitamin E compared to the control group (Heinonen et al., 1998). The encouraging results of the ATBC and preclinical studies, in support of vitamin E as a potential chemopreventive agent, prompted the SELECT trial mentioned earlier. Unfortunately, in this trial vitamin E supplementation significantly increased the risk of prostate cancer (Klein et al., 2011). It should be noted that the ATBC study was evaluating lung cancer and that prostate cancer was a secondary endpoint and so the prostate cancer findings are not as reliable as that of the SELECT study. Moreover, in the ATBC study all the men were long-term smokers while in the SELECT study 43 % never smoked and only 8 % were current smokers at the time of the study (Klein et al., 2011), and vitamin E supplementation has been shown to reduce the risk of prostate cancer in smokers but has no effect in non-smokers (Chan et al., 1999). Therefore, like selenium, vitamin E supplementation is not recommended as a prostate cancer chemopreventive agent.

1.4.3. Flavonoids in prostate cancer chemoprevention

1.4.3.1. Classification of flavonoids

Flavonoids are a group of naturally occurring polyphenols in plants that are ubiquitously found in fruits, vegetables, wine and tea. The typical molecular structure of flavonoids includes two aromatic rings (A and B) linked via a three-carbon bridge (Corcoran et al., 2012). These flavonoids are divided into six classes, to include flavonols, flavones, flavanones, flavanols, isoflavones and anthocyanins (Table 1.6). Many of the dietary sources of flavonoids have been identified. Epidemiological studies have shown that the consumption of flavonoids is associated with a reduced risk for developing various cancers, including prostate cancer (Hsing et al., 2002; Knekt et al., 2002; Rossi et al., 2010) and several *in vitro* studies using cultured cells have demonstrated cytotoxicity of the dietary flavonoids on different cancers (Ben Sghaier et al., 2011; Chiu and Lin, 2008; Gálvez et al., 2003). Therefore, flavonoids could play a key role as potential agents for the prevention and treatment of prostate cancer.

Flavonoid subclass	Basic structure	Major dietary flavonoids	Major food sources
Flavones		Apigenin, luteolin	Celery, parsley, thyme, red pepper
Flavonols		Quercetin, fisetin, myricetin, kaempferol	Onions, kale, broccoli, apples, cherries, sorrel, tea
Flavanones		Hesperedin, naringenin	Citrus, prunes
Flavanols		Catechins, epigallocatechin-3-gallate	Tea, apples, cocoa
Isoflavones		Genistein, daidzein,glycitein	Soya beans, legumes
Anthocyanidins		Cyanidin, delphinidin, malvidin	Cherries, grapes
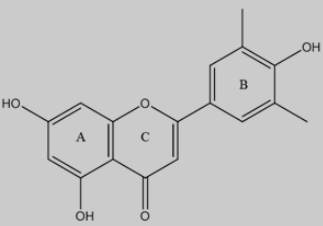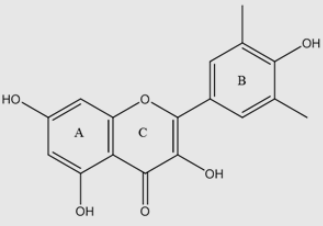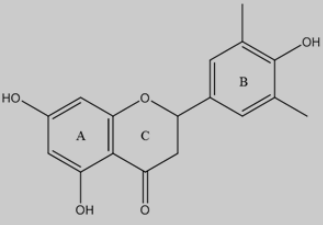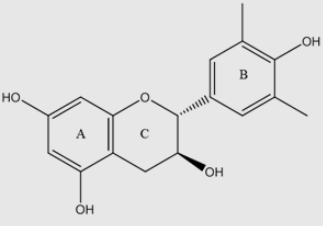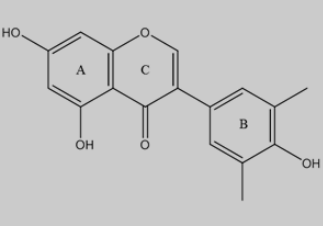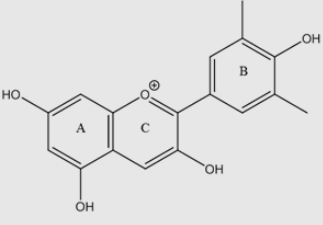
Table 1.6: Major subclasses of flavonoids found in the human diet

1.4.3.2. Bioavailability, metabolism and safety of flavonoids

The daily human intake of flavonoids varies in amount and class, depending on the dietary sources and habits of people from different demographic regions. Therefore, in the Japanese diet the soy isoflavones, mainly daidzein and genistein, would be the predominant class of flavonoids ingested because the Japanese usually consume a diet high in soy (Messina et al., 1994; Tsugane and Sawada, 2014). Meanwhile, in the United States the average consumption of flavonoids would be relatively low and consist mainly of flavonols (Messina et al., 1994; Corcoran et al., 2012). Flavonoids exist as glycosides (attached to sugar moieties) or aglycones (not attached to any sugar moieties). Within plants most flavonoids, except for isoflavones, are in the form of glycosides (Kumar and Pandey, 2013). Upon consumption, the aglycones are absorbed in the small intestine where they can be metabolised to form methylated, glucuronidated or sulfated metabolites (Manach et al., 2004). After oral absorption the metabolites, may undergo further hepatic metabolism in the liver, and can be transported to target cells via the blood before eventual elimination in the urine or faeces (Thilakarathna and Rupasinghe, 2013). The majority of flavonoids which exist as glycosides must first be hydrolysed in the small intestines by the enzyme lactase phloridzin hydrolase to release the sugar and aglycone, which can subsequently be metabolised. Glycosides that reach the colon are hydrolysed by specific bacteria before further metabolism in the liver. The absorption and metabolism of flavonoids is a complex process that varies depending on their structure. It is also influenced by intestinal microflora (Hur et al., 2000; Nurmi et al., 2009), the rate of gastrointestinal transport of the flavonoids (Mizuma et al., 1993) and how the food is processed before consumption (Gennaro et al., 2002; Nemeth and Piskula, 2007). In general, the absorption of flavonoids is relatively low, with the isoflavones being the most readily absorbed compared to the flavanols and anthocyanins which are poorly absorbed (Manach et al., 2005).

Dietary intake of flavonoids, even at high levels, is not associated with any direct adverse effects, possibly as a consequence of their low absorption. However, consumption of some, such as naringenin, present in high concentrations in grapefruit juice, is contraindicated when using certain medications (Dahan and Allman, 2004). Naringenin, an inhibitor of cytochrome P-450 3A4 (CYP3A4), could increase the concentration of drugs that are metabolised by cytochrome P-450 3A4 (Ho et al., 2001).

Furthermore, consumption of flavonoids with a meal can impair iron absorption from food, which could increase the risk of iron deficiency in vulnerable populations (Zijp et al., 2000). Although high levels of flavonoids in the diet through the consumption of plants and plant-derived foods and beverages are not linked to any toxicity, the effects of long-term consumption of supra-physiological doses in the form of supplements are unknown.

1.4.3.3. Chemoprevention activity of flavonoids in prostate cancer

The efficacy of any chemopreventive agent is dependent on its ability to reduce or eliminate those features that drive the development and progression of the disease. Several mechanisms of action have been proposed for the effect of flavonoids on cancer. A few of the major molecular mechanisms, along with the flavonoids involved are highlighted in Table 1.7.

Mechanism	Flavonoid	Cell line	Reference
Cell cycle arrest	Apigenin, Quercetin, Fisetin, Luteolin	PC-3, LNCaP	Gupta et al., 2000; 2003; Haddad et al., 2006; Hagen et al., 2013; Shen et al., 2000; Shukla & Gupta, 2007
	Genistein, EGCG	PC-3, LNCaP, DU145	
Apoptosis	Genistein	DU145	Ahmad et al., 1997; Brusselmans et al., 2005a; Khan et al., 2008; Paschka et al., 1998; Xu et al., 2013; Yuan-Jing et al., 2009
	Myricetin	PC-3	
	Luteolin, Quercetin, Kaempferol, Fisetin	LNCaP	
	EGCG	PC-3, LNCaP, DU145	
FAS inhibition	Luteolin, Quercetin, Kaempferol, EGCG	LNCaP	Brusselmans et al., 2005a

Table 1.7: Selected mechanisms of action of flavonoids in prostate cancer. The flavonoids are able to cause cell cycle arrest, apoptosis and FAS inhibition in *in vitro* models of prostate cancer. The effects may be cell type dependent and may be achieved through the modulation of different molecular pathways. This list is by no means exhaustive for the flavonoids or the potential chemopreventive mechanisms in prostate cancer. EGCG: epigallocatechin-3-gallate.

1.4.3.3.1. Green tea polyphenols

A high intake of green tea has been linked to a reduction in the development of prostate cancer (Johnson et al., 2010; Zheng et al., 2011). This health benefit associated with green tea has been attributed to certain polyphenols called catechins. The catechins belong to the flavanol subclass and the main catechins found in green tea are epicatechin (EC), epigallocatechin (EGC), epicatechin-3 gallate (ECG) and epigallocatechin-3-gallate (EGCG). EGCG is the predominant form, making up approximately 50 % of the total catechins. As a consequence, EGCG has been used in many studies to determine the health benefits of green tea. *In vitro* studies have demonstrated a growth inhibitory effect on DU145, LNCaP and PC-3 cells treated with EGCG at concentrations up to 80 µM (Adhami et al., 2007; Ahmad et al., 1997; Gupta et al., 2000 and 2003; Hagen et al., 2013; Siddiqui et al., 2006 and 2008). In these

studies, the growth inhibitory effects were associated with the induction of apoptosis and cell cycle arrest. EGCG-mediated apoptosis is primarily activated via the p53-dependent pathway, requiring upregulation of p21 and Bax (Hastak et al., 2005). EGCG is capable of increasing extracellular signal-regulated kinase (ERK) 1/2 activity via a mitogen-activated protein (MAP) kinase kinase (MEK)-independent and phosphoinositide-3-kinase (PI3K)-dependent signalling pathway in order to inhibit the growth of PC-3 cells (Albrecht et al., 2008). The ERK 1/2 signalling pathway is often dysregulated in prostate cancer (Paweletz et al., 2001).

The results of several studies in animal models have created an encouraging profile for the green tea catechins as potential chemopreventive agents of prostate cancer. In one study, 80 % of TRAMP mice exposed to water containing 0.3 % green tea catechin solution (equivalent to about 6 cups of green tea per day by an average human) for 16 weeks only developed PIN lesions, while the remaining 20 % along with the water-fed control group developed prostate cancer (McCarthy et al., 2007). This suggested that the green tea catechins are capable of delaying the development of prostate cancer. Furthermore, intraperitoneal administration of 1 mg EGCG in xenograft mice with implanted prostate cancer cells resulted in reductions of tumour volume, serum PSA and AR protein expression when compared to control mice (Chuu et al., 2009; Siddiqui et al., 2011). It is also important to note that the duration and time of exposure to the green tea polyphenols influences the effectiveness of the treatment. A number of studies involving oral administration of EGCG or the whole green tea polyphenols in TRAMP mice at different ages revealed that intervention at an earlier age had a greater protective effect (Adhami et al., 2009, Harper et al., 2007).

In a double-blind, placebo-controlled study, 600 mg/day of green tea catechins was given in capsule form to men with high-grade PIN for 1 year. At the end of the study there was only a 3 % incidence of prostate cancer in the treated group compared to 30 % in placebo-treated men (Bettuzzi et al., 2006). This finding suggests that prostate cancer chemoprevention may be possible and that the green tea polyphenols are promising natural chemopreventive compounds. A follow-up of the patients in this study approximately two years after, revealed that the low incidence of prostate cancer in the treated group was maintained when compared to the placebo-treated men (Brausi et al., 2008), suggesting a long term chemopreventive effect for the polyphenols.

However, this study was small scale, with only 60 men, and must be confirmed by larger clinical trials. An earlier short-term study using a lower dose of green tea catechins and men with hormone refractory prostate cancer showed that green tea catechins were ineffective against androgen-independent prostate cancer (Choan et al., 2005). Therefore, further studies are required before the green tea catechins can be considered as chemopreventive agents for prostate cancer.

1.4.3.3.2. Fisetin

Fisetin, a flavonol found in many fruits and vegetables including strawberries, kiwi and cucumber, exhibits chemopreventive properties against prostate cancer. It is a potent growth inhibitor of prostate cancer cells in culture. Treatment of LNCaP, PC-3 and 22Rv1 cells with fisetin at concentrations ranging from 10-60 μM for 48 hours caused significant growth inhibition, while normal prostate epithelial cells remained largely unaffected (Haddad et al., 2006; Khan et al., 2008 and 2010). The IC_{50} values in these cells ranged between 23-33 μM, with LNCaP exhibiting the highest sensitivity (Britton et al., 2012; Haddad et al., 2006). At these concentrations, fisetin caused cell cycle arrest and apoptosis. Cell cycle arrest was induced in the G1 phase of LNCaP cells, but in the G2/M phase of PC-3 cells (Haddad et al., 2006). The G1 arrest was associated with changes in cyclins and cyclin-dependent kinases, leading to the induction of p21 and p27 (Syed et al., 2008). Apoptosis occurred via the intrinsic or mitochondrial pathway since it was associated with the release of mitochondrial cytochrome c into the cytosol, activation of caspases-3, -8 and -9, downregulation of IAPs and upregulation of Smac and DIABLO (Syed et al., 2008).

Fisetin is a potent inhibitor of 5-alpha reductase (type 1) activity (Hiipakka et al., 2002), thus possessing the ability to inhibit androgen-stimulated growth. Furthermore, Khan *et al* (2008) demonstrated that fisetin can interact with the ligand binding site of the AR, thus competing with the natural ligand DHT and any other AR ligands. Once bound to the AR, fisetin prevents the transcription and subsequent translation and protein synthesis of AR target genes. Therefore, in this study, fisetin treatment inhibited the protein and mRNA expression of PSA, an AR target gene. In AR-positive 22Rv1 xenografts, fisetin inhibited tumour growth and also reduced the levels of PSA (Khan et al., 2008). In PC-3 cells fisetin inhibited growth through the inactivation of the

PI3K/Akt and c-Jun N-terminal kinase (JNK) signalling pathways (Chien et al., 2010). Additionally, Suh *et al*. (2010) found that fisetin can inhibit the complexes of mammalian target of rapamycin (mTOR), mTORC1 and mTORC2 in PC-3 cells. This resulted in the induction of autophagic cell death. So far, these limited studies have presented a favourable chemopreventive profile for fisetin but it is important to note that fisetin exhibits some signs of mutagenicity in *in vitro* assessments (López-Lázaro et al., 2010; Resende et al., 2012) which could limit its use as a human supplement. Therefore, it is pertinent that further studies are conducted to determine the feasibility of using fisetin in prostate cancer chemoprevention.

1.4.3.4. Synthetic flavonol, 3′,4′,5′-trimethoxyflavonol (TMFol), in the management of cancer

1.4.3.4.1. Structural features of TMFol

In addition to the general low absorption of flavonoids (Manach et al., 2005), some of the flavonols with encouraging *in vitro* and *in vivo* chemopreventive properties display signs of mutagenicity (Resende et al., 2012). Therefore, with the aim of eliminating the mutagenic features of flavonols and improving their efficacy, TMFol was synthesised (Britton et al., 2009). The hydroxyl groups on the A and B rings of flavonols have been implicated in their mutagenic effects at specific concentrations (Rietjens et al., 2005), while the presence of methoxy groups on the rings improved the efficacy of another subclass of flavonoids called flavones (Walle et al., 2007; Cai et al., 2009). Furthermore, Britton *et al*. (2012) demonstrated that the presence of methoxy groups (OMe) at the 3′, 4′, 5′ positions of the B ring appears to improve the growth inhibitory activity of TMFol when compared to those with methoxy groups in other positions, and those with hydroxyl groups at the 3′, 4′, 5′ positions. Thus, TMFol possesses the typical flavonol structure but there are no hydroxyl groups on the A ring and the hydroxyl groups on the B ring have been replaced by methoxy groups (Figure 1.12).
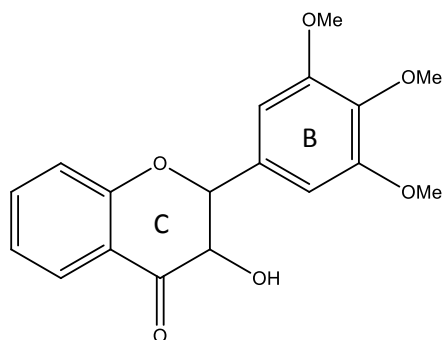
Figure 1.12: Chemical structure of TMFol. There are no OH groups on the A and B rings. There are methoxy (OMe) groups at the 3′, 4′ and 5′ positions of the B ring.

1.4.3.4.2. Molecular action of TMFol

The high levels of TMFol that reach the intestinal and prostate tissue of mice that were given a single intra-gastric dose of TMFol (240 mg/kg) suggest that it could be a useful agent in the inhibition of colorectal and prostate cancers (Britton et al., 2009; Saad et al., 2012). Subsequently, it was found that TMFol (0.1-10 μM) was capable of inhibiting the proliferation of colorectal Apc10.1 mouse adenoma cells and human HCT116 cancer cells, where IC_{50} values of 1.3 and 3.3 μM, respectively, made TMFol more potent than the naturally occurring flavonols, fisetin and quercetin, in the same cells (Howells et al., 2010). Furthermore in Apc^{Min} mice, TMFol reduced the adenoma burden in the small intestine, but not the colon, by approximately 50 %, while in HCT116 adenocarcinoma-bearing nude mice, early administration of a diet containing TMFol (0.2 %), led to a significant reduction in tumour growth. Subsequent evaluation of the tumour tissues from these mice showed an increase in apoptosis and an upregulation of p53 expression relative to the control. The expression of p21 and Bax, p53 target proteins, was also increased by TMFol (Howells et al., 2010). The lack of mutagenic activity of TMFol at the concentrations used in the Howells *et al*. (2010) study further demonstrated the superior anticancer qualities of TMFol compared to the naturally occurring quercetin.

Saad *et al*. (2010) demonstrated the anti-proliferative effect of TMFol in prostate cancer cell lines, TRAMP C2, LNCaP and PC-3, with IC_{50} values ranging from 1.3-5 μM. This potent growth inhibitory effect was later demonstrated in the 22Rv1 human-

derived prostate cancer cells, where TMFol was considered one of the most potent, based on the IC_{50} values, when compared to an array of natural and synthetic flavonols (Britton et al., 2012). Cell cycle arrest was induced at the S phase for PC-3 and at G2/M for LNCaP and TRAMP C2 cells and there were also significant increases in the number of apoptotic cells in both LNCaP and TRAMP C2 (Saad, 2011). Downregulation of AR and PSA was also observed in the prostate cell lines studied (Saad, 2011; Britton et al., 2012). Hence modulation of the AR, which can lead to cell cycle arrest and apoptosis could be a mechanism engaged by TMFol to elicit anti-proliferative activity in prostate cancer (Saad, 2011). Expression of p53 and its target gene, *p21*, were elevated in the LNCaP and TRAMP C2 cells after TMFol intervention. Since p53 is involved in cell cycle arrest and apoptosis (Giono and Manfredi, 2006), TMFol may be utilising the p53 pathway to induce its potent anti-proliferative effects in the colorectal and prostate cancer cell lines studied. However, other mechanisms must be involved since TMFol had similar anti-proliferative effects on PC-3 cells, which lack both AR and p53.

The metabolism and subsequent bioavailability of TMFol has been studied in mice. The C_{max} of TMFol in the prostate of mice given a single oral dose (240 mg/kg) was 18.4 nmol/g and this was achieved 6 hours after administration (Saad et al., 2012). However, no TMFol was detected in the murine plasma, which is not unusual as some flavonols, such as quercetin, are often found in association with the red blood cells which would limit concentrations of the free compound in plasma (Fiorani et al., 2003). Six metabolites of TMFol were identified in mice fed a single intra-gastric dose of TMFol (240 mg/kg); TMFol-3-*O*-glucuronide, three TMFol-*O*-desmethyl glucuronides and two unconjugated *O*-desmethyl TMFol species, but their concentrations were negligible compared to the parent TMFol. Therefore, the TMFol metabolites may not be important contributors to the anti-prostate cancer effects of TMFol (Saad et al., 2012).

The effect of dietary TMFol (0.2 % TMFol) on prostate tumour growth in nude mice bearing the TRAMP C2 cells showed that TMFol caused a significant decrease in tumour volume by 42 % and a decrease in the tumour weight by 15 % (Saad, 2011). When the concentrations of TMFol in the tumour and prostate tissue were assessed TMFol was more abundant in the prostate and the concentrations in both tissues were

similar to or exceeded the IC$_{50}$ values previously obtained in prostate cancer cells, thus accounting for the significant decrease in tumour volume. Administration of the 0.2 % TMFol-containing diet to TRAMP C2 prostate cancer xenograft nude mice also led to a 40 % reduction in the Ki-67 labelling index (Saad, 2011), indicating a significant reduction in proliferation of the tumour cells.

In an unpublished study conducted in this laboratory tumour tissues from another xenograft model bearing 22Rv1 prostate cancer cells were subjected to proteomic analysis and 700 proteins were found to be significantly upregulated following TMFol intervention. These proteins were identified as mainly components of the Wnt and Krebs cycle and also the focal adhesion complex (Dr. Leonie Norris, unpublished data). Therefore, the proteomic data along with the consistent modulation of p53, suggest that TMFol may be exerting its anti-cancer ability by altering the metabolism of prostate cancer. Thus, the challenge remains to determine the mechanisms or signalling pathways through which TMFol fully exerts its effect so as to facilitate a better understanding of this putative prostate cancer chemopreventive agent.

1.5. Aims and Objectives

The mechanisms of action of TMFol are largely unknown. Therefore, the overall aim of this research was to determine the essential mechanisms of action of TMFol as a putative agent in the management of prostate cancer and further assess its *in vivo* efficacy. This overall aim was achieved by:

   i.   investigating the effect of TMFol on the proliferation of human-derived prostate cancer cell lines, 22Rv1 and PC-3 and also a normal immortalised prostatic epithelial cell line, PNT2.

  ii.   determining if TMFol can activate apoptosis.

 iii.   determining if TMFol can cause cell cycle arrest.

 iv.   checking if TMFol can cause the induction of senescence.

  v.   determining if TMFol can alter the expression and activity of metabolic proteins that may play a role in the development and progression of prostate cancer.

 vi.   investigating the *in vivo* chemopreventive efficacy of a dietary intake of TMFol on tumour development and survival in two transgenic mouse models of prostate cancer, PB^{Cre4}*p53*^{flox}*Rb*^{flox} and PB^{Cre4}*Pten*^{flox}.

The overall outcome of this research will determine the ability of TMFol to modulate molecular targets involved in prostate carcinogenesis and subsequently guide the optimisation of any future preclinical assessments to ascertain the potential value of TMFol in the management of prostate cancer.

Chapter 2. Materials and Methods

2.1. Materials

2.1.1. Chemicals and reagents

For cell culture, the growth medium, trypsin and foetal calf serum were obtained from Life Technologies (Paisley, UK). Buffers used in Sodium Dodecyl Sulphate Polyacrylamide Gel Electrophoresis (SDS-PAGE), 10X TRIS/Glycine SDS Running Buffer, 10X TRIS/Glycine Transfer Buffer, ProtoGel (30%) 37.5:1 Acrylamide to Bisacrylamide Stabilised Solution, 4X ProtoGel Resolving Buffer and ProtoGel Stacking Buffer, were all purchased from Geneflow (Lichfield, UK). Antibodies were obtained from Sigma (Dorset, UK), Santa Cruz (Heidelberg, Germany) or Cell Signaling (Hertfordshire, UK) as indicated in Table 2.4. All other chemicals and reagents were purchased from Sigma (Dorset, UK), unless stated otherwise.

2.1.2. Polyacrylamide gel composition

Table 2.1: Composition of the polyacrylamide gels used in Western blotting.

Gel Components	5 % Stacking	8 % Resolving	10 % Resolving	12 % Resolving
Water (mL)	5.7	9.5	8.1	6.8
4X ProtoGel Resolving Buffer (mL)	-	5	5	5
ProtoGel Stacking Buffer (mL)	2.5	-	-	-
ProtoGel 30 % Acrylamide (mL)	1.7	5.3	6.7	8
10 % APS (mL)	0.100	0.200	0.200	0.200
TEMED (mL)	0.015	0.015	0.015	0.015

The above volumes were sufficient for 2 gels. The stacking gel was poured onto the set resolving gel in the gel cassettes and 10 or 15 well combs inserted in the stacking gel before setting. APS – ammonium persulphate, TEMED - N,N,N′,N′ - Tetramethylethylenediamine

2.1.3. Buffers

Table 2.2: Buffers and their constituent ingredients

Buffer	Composition
Annexin V Binding Buffer	1X working solution of Annexin V Binding Buffer (BD Biosciences, Oxford, UK) in distilled water (dH$_2$O) contained 10 mM HEPES/NaOH (pH 7.4), 140 mM sodium chloride (NaCl) and 2.5 mM calcium chloride (CaCl$_2$)
Blocking Buffer	Contained 5 % milk (Marvel dried skimmed milk, Spalding, UK) dissolved in 1X PBST (see below)
Citrate Buffer	Contained 10 mM citric acid monohydrate in dH$_2$O and pH adjusted to 6.0 with 2 M sodium hydroxide (NaOH) solution
Complete Cell Lysis Buffer	Contained 1 complete mini protease inhibitor cocktail tablet and 1 PhosStop phosphatase inhibitor cocktail tablet dissolved in 10 mL of complete lysis – M reagent. Items supplied by Roche Diagnostics (Sussex, UK).
Phosphate Buffered Saline (PBS)	1X working solution contained 10 PBS tablets (Oxoid, Hampshire, UK) dissolved in 1000 mL dH$_2$O
PBS-Tween-20 (PBST)	1X working solution contained 10 PBS tablets dissolved in 1000 mL dH$_2$O with 1 mL Tween-20
Running Buffer	1X working solution contained 25 mM Tris, 192 mM glycine and 0.1 % w/v sodium dodecyl sulphate (SDS)
Sample Buffer, Laemmli 2X concentrate	Contained 4 % SDS, 20 % glycerol, 10 % 2 – mercaptoethanol, 0.004 % bromophenol blue and 0.125 M Tris HCl, pH adjusted to 6.8
Transfer Buffer	1X working solution contained 25 mM Tris, 192 mM glycine and 20 % v/v methanol (Fisher Scientific, Loughborough, UK)

2.2. Methods

2.2.1. Cell Culture

Human derived prostate cancer cell lines, 22Rv1 and PC-3, and the human derived normal prostatic epithelial cells, PNT2, were utilised in the *in vitro* studies of this research. The 22Rv1 cells were derived in 1999 from a human prostate cancer xenograft serially propagated in mice after castration-induced regression and relapse of the parental CWR22 xenograft (Sramkoski et al., 1999). The PC-3 cells were derived in 1979 from a grade IV bone prostate cancer metastasis in a 62 year old Caucasian (Kaighn et al., 1979). The PNT2 cells were derived from normal prostatic epithelial cells obtained from the prostate of a 33 year old male at post mortem and immortalised with SV40 (Berthon et al., 1995). The cells were sourced from the European Collection of Cell Cultures (ECACC), except for 22Rv1 cells, which were kindly provided by Dr. Imran Ahmad (Beatson Institute for Cancer Research, Glasgow, UK). All of the cells were cultured in Roswell Park Memorial Institute (RPMI) 1640 containing L-glutamine and supplemented with 10 % foetal calf serum (FCS). The cells were incubated at 37 ˚C in 5 % carbon dioxide (CO_2). The doubling times of the cells were 40 h for 22Rv1, 25 h for PC-3 and 36 h for PNT2. Throughout the research period, the cells were tested for mycoplasma at 6 monthly intervals.

2.2.1.1. Maintenance of cells

Once the cells were resuscitated from liquid nitrogen, they were cultured at a required density in 75 cm^2 flasks in 12 mL of FCS-supplemented growth medium and were not used in any experiment beyond passage 30. For routine maintenance, the cells were grown to approximately 80-90 % confluency before passaging. To passage, the growth medium was removed and the cells were washed twice with 5 mL of PBS. The cells were then trypsinised with 5 mL of 1X trypsin/EDTA for approximately 5 minutes at 37 ˚C. To facilitate cell detachment, the flask was gently tapped before the trypsin was neutralised with 5 mL of the growth medium containing FCS. The cell suspension was centrifuged at 350 x g for 3 minutes and the cell pellet formed was resuspended at the required dilution in fresh growth medium.

2.2.1.2. Cell treatment preparation

TMFol was synthesised by Dr. Robert Britton (Department of Cancer Studies, University of Leicester, UK) as described in Britton *et al.* (2009). The stock solution of TMFol was prepared at a concentration of 20 mM in dimethyl sulfoxide (DMSO) and stored at -20 ˚C. As recommended in Britton *et al*. (2009), the stock solution was used in experiments up to 3 months after its preparation and then discarded. Since DMSO was the solvent for TMFol, all treatments and controls contained the same concentration of DMSO, which did not exceed 0.1 % v/v.

2.2.2. Cell proliferation assay

The cells were seeded at a density of 1×10^4 cells/well in 1 mL of growth medium, onto 24-well plates, in three replicates. The cells were allowed to adhere overnight before treatment with 1, 2.5, 5 or 10 µM TMFol or DMSO control in a final volume of 2 mL. Following 72 or 144 h incubation at 37 ˚C, the growth medium was removed from the wells and the cells were washed twice with 1 mL PBS. Trypsin/EDTA (0.5 mL) was added to each well and the plates incubated at 37 ˚C for 5 minutes to detach the cells. Once the cells were detached the trypsin/EDTA was neutralised by adding 0.5 mL of growth medium. The cell suspension from each well was added to a coulter counter cup with 9 mL ISOTON® II diluent (Beckman Coulter, High Wycombe, UK). The number of cells present was determined by passing the diluted cell suspension through a Z2 Coulter Particle Counter with Size Analyser (Beckman Coulter, High Wycombe, UK). Cell numbers were calculated as percentage of the DMSO control and plotted against TMFol concentration. To determine the 50 % inhibitory concentration (IC_{50}), the cell number as percentage of the DMSO control was plotted against the log concentration at 72 or 144 h in Microsoft Excel 2013. A linear trend-line was plotted and the linear equation generated was used to calculate the log concentration at 50 % of cell number. The antilog concentration was subsequently calculated to give the IC_{50} value. Each cell proliferation assay was performed independently at least three times and the graphs and IC_{50} values are the means ± the standard deviation (SD).

2.2.3. Measurement of apoptosis using annexin V and flow cytometry

The earliest feature of apoptosis is the translocation of plasma membrane phosphatidylserine (PS) from the inner side of the plasma membrane to the outer layer

(Martin et al., 1995). Annexin V binds to the PS that is now exposed on the external surface of the cell, distinguishing the apoptotic cell from the healthy. When using flow cytometry, annexin V conjugated to fluorochromes such as fluorescein isothiocyanate (FITC) is used as a probe to identify apoptotic cells. The translocation of PS to the external surface of the cell also occurs during cell necrosis, but during early apoptosis the cell membrane remains intact, whilst the cell membrane is disrupted in the necrotic cell. Hence to distinguish between early apoptosis and necrosis the annexin V-FITC staining must be undertaken in conjunction with a DNA-intercalating dye such as propidium iodide (PI), which can only enter the cell following membrane disruption. Healthy intact cells are annexin V-FITC and PI negative, apoptotic cells are annexin V-FITC positive and PI negative and necrotic cells are annexin V-FITC and PI positive (Vermes et al., 1995). The annexin V-FITC and PI staining is a highly sensitive and easy to perform method to quantitatively determine the percentage of cells within a population undergoing apoptosis.

A FITC-Annexin V Apoptosis Detection kit (BD Biosciences, Oxford, UK) was used to detect apoptosis. 22Rv1 and PC-3 cells were seeded at a density of 5×10^5 while PNT2 cells were seeded at 3×10^5 in 75 cm^2 flasks in 12 mL of growth medium. Cells were allowed to adhere overnight before the growth medium was removed and replaced with medium containing TMFol (10 μM) or DMSO control for 24, 48 or 72 h. Fifty μM etoposide was used as the positive control in the PNT2 cells while 20 μM sorafenib tosylate was the positive control in the PC-3 and 22Rv1 cells. The cells that detached in the medium during the incubation time were removed and reserved. The adherent cells were washed twice with PBS, trypsinised and then pooled with the detached cell medium. The cells were centrifuged at 350 x g for 5 min and the pellet was resuspended in 10 mL fresh growth medium supplemented with FCS. The cells were incubated for 30 min at 37˚C before being re-centrifuged. The cell pellet formed was then resuspended in 500 μL 1X Annexin V Binding Buffer. Then 5 μL of FITC-Annexin V and 5 μL of PI (0.05 μg/test) were added to the cells. The cells were gently vortexed and incubated at room temperature in the dark for 15 min. The percentage of cells undergoing apoptosis was determined by flow cytometry using a FACS Aria II (Becton Dickinson, New Jersey, USA) with the BD FACS Diva analysis software (version 6.1.2).

2.2.4. Evaluation of specimens from xenograft study

The paraffin-embedded slides of the prostate tumour sections and tumour lysates from 22Rv1 xenografts were available for Western blot and immunohistochemical analyses. The xenograft study was previously performed in this laboratory. The procedure followed for the xenograft study is included in section 2.2.4.1 below for clarity on the source of the specimens.

2.2.4.1. Xenograft study and lysate preparation

Male MF-1 outbred nude mice (30-40 g, 6 weeks of age) were obtained from Harlan UK (Bicester, Oxon, UK) and ear-punched for identification. Mice were kept in the Leicester University Biomedical Services facility at 20-23 °C under conditions of 40-60 % relative humidity and a 12 h light/dark cycle. Experiments were carried out under animal project license PPL 80/2167, granted to Leicester University by the UK Home Office. The experimental design was vetted by the Leicester University Local Ethical Committee for Animal Experimentation and met the standards required by the UKCCCR guidelines (Workman et al., 2010). 22Rv1 cells (2×10^6) suspended in matrigel:serum-free medium (1:1; 100 μL; Becton-Dickinson, Worthing, UK) were injected subcutaneously into the right flank of male nude mice of 8 weeks of age under light halothane anaesthesia. Mice received standard powdered AIN93G diet (controls) or powdered AIN93G diet supplemented with 0.2 % w/w TMFol. Each group consisted of 10 animals. Mice commenced diet seven days prior to cell inoculation. Mice were weighed weekly, and tumour size was measured twice per week using callipers. Animals were culled approximately 7 weeks after tumour cell inoculation, when tumours in untreated mice reached the maximal size (~17 mm in length) permissible under UK animal welfare stipulations. Tumour tissue samples were snap-frozen (liquid nitrogen) and stored at -80 °C until analysis by Western blotting or fixed in 10 % formalin and histologically processed until analysis by immunohistochemistry.

Tumour tissue from control mice or mice which received TMFol was homogenized with lysis buffer (1:4, w:v. PBS, 1 % NP-40, 0.5 % sodium deoxycholate, 0.1 % SDS, with protease inhibitors PMSF 1 mM, aprotinin 2 μg/ml, leupeptin 5 μg/ml and phosphatase inhibitors sodium vanadate 1 mM and sodium fluoride 1 mM). The homogenate was

placed on ice for 15 min and centrifuged (20 min, 10 000 x g, 4 ℃). The protein concentrations of the tumour lysates were measured as described in section 2.2.6 below.

2.2.4.2. Immunohistochemical analysis of cleaved caspase-3

Formalin-fixed 22Rv1 tumour tissues were stained for cleaved caspase-3 using cleaved caspase-3 Asp 175 polyclonal antibody from Cell Signaling Technology (Hertfordshire, UK). The paraffin-embedded sections (4 μm) mounted on polysine-coated slides were de-waxed by incubating at 65 °C for 20 min. The sections were hydrated by first immersing the slides in xylene (Genta Medical, York, UK) for 3 min (2X), followed by immersion in a graded series of industrial methylated spirit (IMS) (Genta Medical, York, UK) rinses (99 % - 2X for 3 min and 95 % - 2X for 3 min). The slides were then washed in running tap water for 5 min. The antigen was unmasked by microwaving the slides on high power in 10 mM citrate buffer (pH 6.0) for 20 min. A Novocastra™ Novolink™ Polymer Detection System (Leica Biosystems, Newcastle Upon Tyne, UK) was subsequently used in the staining. The endogenous peroxidase activity was inactivated by adding 100 μL of the peroxidase block directly on the sections for 10 min. The slides were washed in PBS (2X for 5 min) before adding 100 μL of the protein block directly on the sections for 10 min to block nonspecific binding. The slides were washed in PBS as before and the sections incubated with the cleaved caspase-3 antibody (dilution 1:200) overnight at 4 ˚C. The antibody diluent was 3 % w/v bovine serum albumin and 1 % v/v Triton X - 100 in PBS. The negative control was rabbit immunoglobulin fraction (normal) (Dako, Ely, UK). After washing the sections in PBS (2X for 5 min), 100 μL of the post primary block was added for 5 min to detect the mouse antibodies. This was followed by PBS washing (2X for 5 min) and the addition of 100 μL of the Novolink™ Polymer for 30 min to detect the rabbit immunoglobulins. While washing in PBS, 3,3′-diaminobenzidine (DAB) was prepared by adding 5 μL DAB chromogen to 100 μL Novolink™ DAB substrate buffer and this DAB working solution (100 μL) was added to the sections for 5 min to react with the peroxidase to produce a brown stain. Following a 5 min wash with running tap water the sections were counterstained with Mayer's Haematoxylin for 1 min and washed again for another 5 min in running tap water. The sections were finally dehydrated back through the graded IMS and xylene. Coverslips were added to the slides with the help of the DPX (mixture of distyrene, a plasticizer and xylene) mountant. The slides were

visualised under a microscope (Leica DM 2500 with Leica digital camera, Leica Microsystems, Milton Keynes, UK) at a magnification of x 40 and images were taken of 10 random fields of view for each section. The Leica Application Suite (version 2.8.1) was used to acquire the images. The slides were scored by two independent observers blinded to the treatment group. Representative fields were selected for each image and the total number of epithelial cells and the number of positively stained epithelial cells were counted. The apoptotic index was calculated as the percentage of epithelial cells from the 10 random fields of view per section which stained positive for cleaved caspase-3.

2.2.5. Cell cycle analysis

Cell cycle distribution can be determined by measuring the DNA content of the cells. A fluorescent dye is used to stain the DNA quantitatively so that the fluorescence intensity of the stained cells at certain wavelengths correlates with the amount of DNA. Hence, the fluorescence of cells in the G2/M phase would be twice as high as that of cells in the G1 phase, while the fluorescence of cells in the S phase would lie somewhere between that of G1 and G2/M. The fluorescence intensity is measured by flow cytometry.

22Rv1 cells were seeded at a density of 1 x 10^6, while PC-3 and PNT2 cells were seeded at 8 x 10^5 in 75 cm^2 flasks in 12 mL of media. After allowing 24 h for cell adherence the cells were treated with 10 μM TMFol or DMSO control for 24, 48 or 72 h. The cells were washed twice with 5 mL PBS and harvested by trypsinisation. The resulting cell suspension was centrifuged for 5 min at 400 x g. The supernatant was discarded and the cells were fixed in 2 mL of ice-cold 70% ethanol (Fisher Scientific, Loughborough, UK) overnight or up to one week at 4 °C. After fixation, the cell suspension was centrifuged at 400 x g for 10 min and the cells were resuspended overnight at 4 °C in 800 μL of PBS and RNase A at a final concentration of 10 μg/mL. PI, at a final concentration of 20 μg/mL, was subsequently added and incubated for a minimum of 2-3 h at 4 °C before FACS analysis on a FACS Aria II (Becton Dickinson, New Jersey, USA). Data were analysed using the ModFit software version LT3.3.

2.2.6. Bicinchoninic acid (BCA) Protein Assay

The Pierce BCA protein assay kit (Thermo Scientific, Loughborough, UK) was used to determine the concentration of proteins in lysates. Serial dilutions of BSA ranging from 0 to 1 mg/mL were used to prepare a standard curve. Then the lysates of unknown concentration were serially diluted with distilled water (for example, 1:10, 1:50, 1:100) to ensure that the absorbance of the lysates was within the linear range of the BSA standard curve. Ten µL of the distilled water, BSA standard solutions and serially diluted lysates was added to separate wells on a 96 well microplate in triplicate. Two hundred µL of the BCA working solution, prepared by mixing 50 parts of BCA Reagent A with 1 part of BCA Reagent B, was added to each well and mixed thoroughly. The microplate was covered and incubated at 37 °C for 30 min. Subsequently, the microplate was cooled to room temperature before reading the absorbance at 595 nm on a Fluostar Optima plate reader (BMG Labtech Ltd, Aylesbury, UK). The standard curve generated was used to determine the protein concentration of the unknown lysates.

2.2.7. Quantitative assay of senescence-associated β-galactosidase activity

SA-β-galactosidase activity is the classical biomarker for determining cellular senescence in mammalian cells. Measurement of activity is generally by staining cells with the chromogenic substrate 5 bromo-4-chloro-3-indolyl-β-D-galactopyranoside (X-gal) at pH 6.0 to give a blue colouration to the senescent cells, and the percentage of positively stained cells determined. Since 22Rv1 cells tend to grow in clusters it was decided that the quantitative assay previously described by Gary and Kindell (2005) would give a more accurate analysis of SA-β-galactosidase activity. This assay determines SA-β-galactosidase activity by measuring the conversion rate of 4-methylumbelliferyl-β-D-galactopyranoside (MUG) to 4-methylumbelliferone (4-MU) at pH 6.0, which is highly fluorescent in alkaline solution.

PNT2 and PC-3 cells were seeded at a density of 8×10^5, while 22Rv1 cells were seeded at 1×10^6 in 10 cm plates in 12 mL of growth medium. The cells were allowed to adhere over 24 h before treating with 10 µM TMFol or DMSO control for 24, 48 or 72 h. At the end of the treatment period the plates were washed six times with PBS, and 450 µL of 1X lysis buffer (Table 2.3) was added to each plate. The cells were scraped

and transferred to a 1.5 mL tube. The cells were vortexed vigorously and then centrifuged for 5 min at 12 000 x g. The supernatant, now referred to as the clarified lysate, was collected and kept on ice. The protein concentration of the clarified lysate was determined using the BCA protein assay as outlined in 2.2.6 above. Then 150 µL of 2X reaction buffer (Table 2.3), 100 µL of the clarified lysate and 50 µL of a pH 6.0-adjusted solution of 200 mM sodium phosphate with 200 mM citric acid were mixed together and placed into a 37 °C water bath for a 2 h incubation period. To determine the optimal incubation period for each cell type several incubation periods from 1 to 3 h were used and it was found that the rate of 4-MU formation was linear over the first two hours for all of the clarified lysates. As a positive control, 150 µL of 2X reaction buffer, 50 µL of clarified lysate, 50 µL of 1X lysis buffer and 50 µL of a pH 4.0-adjusted solution of 200 mM sodium phosphate with 200 mM citric acid were mixed together and incubated in a 37 °C water bath for 2 h. At the end of the incubation period, 500 µL of 400 mM sodium carbonate stop solution was added to 50 µL of the reaction mix. Then 150 µL of the carbonate stopped reaction mix was added to triplicate wells in a 96-well microplate. The fluorescence was measured using a Fluostar Optima plate reader (BMG Labtech Ltd, Aylesbury, UK) with excitation at 360 nm, emission at 465 nm and gain held constant at 800. The SA-β-galactosidase activity was normalised for total protein (4-MU fluorescence/µg protein/hour) and then finally expressed as a percentage of the DMSO control.

Table 2.3: Composition of buffers used in the quantitative assay of SA-β-galactosidase activity

Buffer	Composition
1X Lysis buffer	5 mM 3-[(3-cholamidopropyl)dimethylammonio]-1-propanesulfonate (CHAPS), 4 mM citric acid, 4 mM sodium phosphate, 0.5 mM benzamidine and 0.25 mM phenylmethanesulfonyl fluoride (PMSF) {added immediately before use}, pH 6.0
2X Reaction buffer	4 mM citric acid, 4 mM sodium phosphate, 300 mM sodium chloride, 10 mM β-mercaptoethanol, 4 mM magnesium chloride and 1.7 mM MUG {added immediately before use}, pH 6.0

2.2.8. Gel Electrophoresis and Western blotting

2.2.8.1. Preparation of whole cell lysate

22Rv1 cells were seeded at a density of 1 x 10^6, while PC-3 and PNT2 cells were seeded at 8 x 10^5 in 75 cm^2 flasks in 12 mL of media. After allowing 24 h for cell adherence the cells were treated with 10 µM TMFol or DMSO control for 24, 48 or 72 h. The cells were washed twice in 5 mL PBS and harvested by trypsinisation. The cell suspension was centrifuged at 350 x g for 3 min and the cell pellet formed was resuspended in 800 µL PBS. The cell suspension was centrifuged at 17 000 x g for 3 min. The supernatant was discarded and the cell pellet stored on ice and used to form the whole cell lysate. The cell pellet was resuspended in complete cell lysis buffer (2X volume displaced by the cell pellet) and incubated on ice for 20 min. The cell suspension was centrifuged at 17 000 x g at 4 ˚C for 20 min. The supernatant containing the proteins from the cell lysis was collected as the whole cell lysate. The protein concentration of the lysate was determined using the BCA protein assay described above (section 2.2.6) and then stored at -20 ˚C.

2.2.8.2. Modulation of glucose composition in cell culture medium

22Rv1 cells were seeded at a density of 1 x 10^6 in 75 cm^2 flasks in 12 mL of RPMI-1640 medium and incubated for 48 h. The medium was removed and replaced with glucose-free RPMI-1640 containing 10 % FCS for 8 h. Then the cells were treated for 24 h with 10 µM TMFol or DMSO control in glucose-free RPMI-1640 medium containing 0, 5 or 11 mM glucose supplementation. The cells were washed twice in 5 mL PBS and harvested by trypsinisation. The whole cell lysates were then prepared as described above.

2.2.8.3. SDS-PAGE and Western Blotting

To prepare the whole cell lysates for SDS-PAGE an appropriate volume of the lysate was mixed with an equivalent volume of sample buffer 2X Laemmli concentrate to obtain 20 µg of protein. This mixture was boiled at 100 ˚C for 5 min and then briefly centrifuged before loading 20 µL/well on a polyacrylamide gel. The percentage resolving buffer used in the gel was dependent on the molecular weight of the protein of interest. A pageruler prestained protein ladder (Thermo Scientific, Loughborough,

UK) was added to the first and last wells in each gel to indicate the relative sizes of the separated proteins in the cell lysate.

The Bio-Rad mini gel electrophoresis system (Hertfordshire, UK) was used for the SDS-PAGE. All gels were placed in the running buffer and electrophoresis was performed at 120 V until the dye front was approximately 5-10 mm from the end of the gel. The gels were then removed from the plates and allowed to equilibrate in transfer buffer for 10 min before being assembled in the transfer cassette. The separated proteins were transferred in transfer buffer for 90 min onto a nitrocellulose membrane of pore size 0.2 μM (GE Healthcare, Buckinghamshire, UK) at 100 V.

Upon completion of the transfer, the nitrocellulose membrane was placed in the blocking buffer for 2 h on a rocking platform at room temperature. The membrane was then incubated with the primary antibody of interest at the concentrations indicated in Table 2.4. Incubation was carried out overnight in the cold room on a rocking platform. Following the incubation period the nitrocellulose membrane was washed in PBST (1X for 10 min and 2X for 5 min). The corresponding secondary antibody (Table 2.4) was then added to the membrane for 1 h at room temperature on a rocking platform. The secondary antibody was then removed and washed with PBST (1X for 10 min and 1X for 5 min). The last wash was with water for 5 min. Equal volumes of EZ-ECL solution A and EZ-ECL solution B from the EZ-ECL chemiluminescence detection kit for HRP (Biological Industries, Israel) were mixed together and allowed 5 min to equilibrate. The membrane was subsequently incubated with the EZ-ECL mixture for 1-2 min at room temperature. The excess mixture was drained away and the membrane wrapped in cling film and placed with the protein side up in the film cassette. In a dark room the membrane was exposed to an ECL hyperfilm (GE Healthcare, Buckinghamshire, UK) for an appropriate time based on signal intensity and then developed using a Curix 60 Agfa-Gevaert (Germany). The membranes were re-probed for actin, the house-keeping protein used as the loading control. For re-probing, the nitrocellulose membrane was first washed in PBST for 10 min on a rocking platform at room temperature, followed by incubation in stripping buffer (ThermoScientific, Loughborough, UK) at room temperature for 10 min on a rocking platform. The stripped membrane was then washed once in PBST for 10 min before repeating the

Western blotting procedure as outlined earlier in this paragraph. The protein band densities were determined using ImageJ software version 1.47.

Table 2.4: Antibodies for Western Blotting

Antibody		Supplier	Host	Dilution
Acetyl-CoA carboxylase (C83B10)		Cell Signaling	Rabbit	1:1000
ACO2 (A-22)		Santa Cruz	Rabbit	1:1000
Actin (1-19)		Santa Cruz	Goat	1:1000
AMPKα (23A3)		Cell Signaling	Rabbit	1:1000
Anti-DLST		Sigma	Rabbit	1:1000
Anti-FH		Sigma	Rabbit	1:1000
Anti-SUCLG1		Sigma	Rabbit	1:1000
ATP-citrate lyase		Cell Signaling	Rabbit	1:1000
Fatty acid synthase (C20G5)		Cell Signaling	Rabbit	1:1000
IRP-1 (N-17)		Santa Cruz	Goat	1:1000
LDHA (C4B5)		Cell Signaling	Rabbit	1:1000
P16 INK4A		Cell Signaling	Rabbit	1:1000
p21 Waf1/Cip1(12D1)		Cell Signaling	Rabbit	1:1000
p53 (DO-1)		Santa Cruz	Mouse	1:1000
PDC-E2		Santa Cruz	Mouse	1:1000
PDH-E1α (9H9)		Santa Cruz	Mouse	1:1000
PEPCK (H-300)		Santa Cruz	Rabbit	1:1000
Phospho-acetyl-CoA carboxylase (Ser 79) (D7D11)		Cell Signaling	Rabbit	1:1000
Phospho-AMPKα (Thr172)(40H9)		Cell Signaling	Rabbit	1:1000
SDHA (H-204)		Santa Cruz	Rabbit	1:1000
VDAC (D73D12)		Cell Signaling	Rabbit	1:1000
Secondary Antibodies	Anti-mouse IgG-HRP	Santa Cruz	Goat	1:20000
	Anti-goat IgG-HRP	Santa Cruz	Donkey	1:20000
	Anti-rabbit IgG-HRP	Santa Cruz	Goat	1:20000

ACO2: mitochondrial aconitase; AMPKα: AMP-activated protein kinase α; DLST: dihydrolipoyl succinyltransferase; FH: fumarate hydratase; SUCLG1: succinate-Co A ligase, α subunit; IRP-1: iron regulatory protein 1; LDHA: lactate dehydrogenase; PDC-E2: E2 subunit of pyruvate dehydrogenase; PDH-E1α: E1α subunit of pyruvate dehydrogenase; PEPCK: phosphoenolpyruvate carboxykinase; SDHA: succinate dehydrogenase flavoprotein subunit A; VDAC: voltage-dependent anion channel; HRP: horseradish peroxidase; IgG: immunoglobulin G

2.2.9. Mitochondrial aconitase activity

In mammalian cells, aconitase, an iron-sulphur protein, is found in both the mitochondria and cytosol. The mitochondrial aconitase (ACO2) functions in the Krebs cycle, where it catalyses the reversible interconversion of citrate and isocitrate, via the cis-aconitate intermediate. The cytosolic aconitase exists in two forms, iron regulatory proteins 1 and 2 (IRP-1 and IRP-2). When there is an abundance of iron in the cell IRP-1 acts like ACO2 but when the iron level is low it regulates intracellular iron homeostasis. IRP-2 is only involved in iron homeostasis. There are antibodies that can identify each form of aconitase but in order to monitor the activity of mitochondrial aconitase it is necessary to separate the mitochondria from the cytosol.

2.2.9.1. Isolation of mitochondria from cultured cells

22Rv1, PC-3 and PNT2 cells were seeded at a density of 1×10^6 in 175 cm^2 flasks in 24 mL of media. After allowing 24 h for cell adherence, the cells were treated with 10 μM TMFol or DMSO control for 24 h. The cells were washed twice in 10 mL PBS and harvested by trypsinisation. The cell suspension was centrifuged at 350 x g for 3 minutes and the cell pellet formed was resuspended in 800 μL PBS. The cell suspension was centrifuged at 17 000 x g for 3 min. The supernatant was discarded and the cell pellet was either stored at -20 ˚C or used immediately to isolate the mitochondria.

To separate the mitochondrial and cytosolic fractions, differential centrifugation with a bench-top microcentrifuge was performed, as outlined in the mitochondrial isolation kit for cultured cells (Thermo Scientific, Loughborough, UK). Immediately before performing the test, 10 μL of Thermo Scientific™ Halt™ Protease Inhibitor Cocktail, EDTA-free (Loughborough, UK) was added to 1 mL of the mitochondria isolation Reagents A and C from the kit. The cell pellet was resuspended in 800 μL of Reagent A and vortexed at medium speed for 5 sec, followed by incubation on ice for exactly 2 min. The cell suspension was then transferred to a cold Dounce Homogeniser. The cells were homogenised on ice. The cells required between 200-250 strokes to achieve approximately 80 % lysis efficiency. The cell lysis efficiency was checked by comparing a sample of the homogenate under a microscope with a sample of whole cells. The lysed cells were returned to the original tube and 800 μL of Reagent C was

added. The Dounce Homogeniser was rinsed with 200 µL of Reagent A which was added to the lysed cells in the tube. The tube was inverted several times to ensure mixing and was then centrifuged at 700 x g for 10 min at 4 ˚C. The supernatant was collected and centrifuged at 3000 x g for 15 min. The supernatant now containing the cytosol was collected and kept on ice. The pellet containing the mitochondria was resuspended in 500 µL of Reagent C and centrifuged at 12 000 x g for 5 min. The supernatant was discarded and the mitochondrial pellet was placed on ice. Both mitochondrial and cytosolic fractions were stored at -80 ˚C until ready for use.

2.2.9.2. Purity of mitochondrial fraction

To determine the purity of the mitochondrial fraction, the mitochondrial pellet was resuspended in cold assay buffer (2X the volume displaced by the pellet) from the aconitase activity assay kit (Sigma-Aldrich, Dorset, UK). The mitochondria were sonicated on ice four times for 20 sec, with a 1 min interval between each sonication. The protein concentration was then determined using the BCA protein assay (section 2.2.6). For completeness the purity of the mitochondrial fraction was compared to the cytosolic fraction and untreated whole cell lysate. The proteins in the cytosolic fraction were already in a soluble state and therefore required no further processing prior to measuring the protein concentration. The untreated whole cell lysate was prepared by the sonication method used with the mitochondrial fraction. Samples for SDS-PAGE and Western blotting were removed and processed as described in section 2.2.8.2 while the rest was stored at -80 ˚C for use in the activity assay. The antibodies used in Western blotting were VDAC, LDHA, ACO2 and IRP-1 (Table 2.4).

2.2.9.3. Mitochondrial aconitase activity assay

The activity of aconitase in the mitochondrial fraction from each cell type was determined using the aconitase activity assay kit supplied by Sigma-Aldrich (Dorset, UK). This assay measured aconitase activity spectrophotometrically at 450 nm by following the conversion of citrate to isocitrate.

The mitochondria were activated on ice for 1 h by adding 10 µL of aconitase activation solution to 100 µL of mitochondrial sample. The aconitase activation solution was freshly prepared each time by mixing 100 µL each of cysteine (reconstituted with assay

buffer) and $(NH_4)Fe(SO_4)_2$ (also reconstituted with assay buffer). In the meantime the isocitrate standards for colorimetric detection were prepared. A 2 mM isocitrate standard solution was made by diluting 10 µL of the 100 mM standard solution with 490 µL of the assay buffer. Increasing aliquots (0, 2, 4, 6, 8 and 10 µL) of the 2 mM isocitrate standard solution was added to duplicate wells onto a 96-well plate. Assay buffer was added to each well to make a final volume of 50 µL. Hence the final concentration of the isocitrate standards generated were 0 (blank), 4, 8, 12, 16 and 20 mmole/well standards.

Upon completion of aconitase activation, several dilutions of the activated mitochondrial fraction were prepared to ensure the readings were within the linear range of the standard curve. No more than 50 µL of the activated mitochondrial fraction was added to duplicate wells and made to a final volume of 50 µL with assay buffer. Additional duplicate wells for each dilution were prepared to be used as a background control. The assay reaction mixes were as per Table 2.5 below.

Table 2.5: Aconitase activity assay reaction mixes

Reagent	Samples and standards	Sample blank
Assay buffer	46 µL	48 µL
Enzyme mix	2 µL	2 µL
Substrate	2 µL	-

Fifty µL of the sample blank (Table 2.5) was added to the wells for the background control while 50 µL of the reaction mix for samples and standards were added to the appropriate wells. The solutions in the wells were mixed thoroughly by pipetting. The plate was wrapped in aluminium foil to exclude light and then incubated at 25 °C for 45 min. Then 10 µL of the developer was added to each well, mixed and incubated at 25 °C for 10 min. The absorbance was measured at 450 nm.

To calculate the aconitase activity, the isocitrate standard curve was plotted by first correcting for the background control (i.e. subtracting the absorbance value obtained for 0 mM isocitrate standard from all the other absorbance readings for the isocitrate standard). For the mitochondrial samples, the absorbance value was corrected by

subtracting the absorbance readings of the sample blank from that of its corresponding sample dilution. Then the amount of isocitrate generated by the aconitase in the mitochondrial fraction was determined from the standard curve.

The aconitase activity was then calculated using the equation:

Aconitase activity (milliunit/mL or nmole/min/mL) $= \frac{B \times sample\ dilution\ factor}{T \times V}$

B = amount (nmole) of isocitrate generated

T = time reaction incubated in minutes

V = pretreated sample volume (mL) added to well

One unit of aconitase was the amount of enzyme that converted 1.0 µmole of citrate to isocitrate per min at pH 7.4 at 25 °C. For each cell line, the mitochondrial aconitase activity from the TMFol treated cells was normalised to that of the control.

2.2.10. Pyruvate dehydrogenase (PDH) activity assay

PDH is the key enzyme that links glycolysis to the Krebs cycle by catalysing the oxidative decarboxylation of pyruvate to acetyl-CoA (Patel and Korotchkina, 2006; Vander Heiden et al., 2009). To measure PDH activity, the PDH enzyme activity microplate assay kit supplied by Abcam (Cambridge, UK) was utilised. The wells of the microplate were pre-coated with PDH antibody so that upon addition of the cell lysate the PDH enzyme in the lysate was immunocaptured within the wells. Then the PDH activity was measured by following the reduction of nicotinamide adenine dinucleotide (NAD^+) to reduced nicotinamide adenine dinucleotide (NADH), coupled to the reduction of a reporter dye to produce a yellow product that was monitored by measuring absorbance at 450 nm.

22Rv1, PC-3 and PNT2 cells were seeded at a density of 1 x 10^6 in 175 cm^2 flasks in 24 mL of media. After allowing 24 h for cell adherence, the cells were treated with 10 µM TMFol or DMSO control for 24 h. The cells were washed twice in 10 mL PBS and harvested by trypsinisation. The cell suspension was centrifuged at 350 x g for 3 min and the cell pellet formed was resuspended in 800 µL PBS. The cell suspension was

centrifuged at 17 000 x g for 3 min. The supernatant was discarded and the cell pellet was stored at -20 ˚C until ready for use.

The cell pellet was resuspended in PBS (2X the volume displaced by the cell pellet). The protease inhibitor, phenylmethylsulfonylfluoride (PMSF) (1 mM) was added to the resuspended cell pellet before solubilisation with the Detergent ($\frac{1}{10}$ the cell suspension volume) supplied with the kit. This was followed by a 10 min incubation period on ice. The cells were centrifuged at 1000 x g for 10 min at 4 °C. The supernatant which now contains the cell extracts was collected and the protein concentration was determined by the BCA protein assay (section 2.2.6) and immediately used in the activity assay. The concentration of the cell extract was adjusted with 1X Buffer to a concentration within the working range of each cell type extract to facilitate direct comparison of individual experimental samples. To obtain this working range the PDH activity was measured for a control cell extract that was serially diluted across the linear working range for the assay (100 – 1000 µg/200 µL/well). Two hundred µL of the concentration-adjusted cell extract was added to the microplate wells. A buffer control was used as a negative control while bovine heart mitochondrial lysate (Abcam, Cambridge, UK) was used as a positive control.   The microplate was subsequently incubated for 3 h at room temperature. Following the incubation, the wells of the microplate were emptied and rinsed twice with 300 µL of 1X Stabiliser. Two hundred µL of Assay Solution was then added to each well and the kinetic absorbance of each well was measured at 450 nm at room temperature for 15 min in a Fluostar Optima plate reader (BMG Labtech Ltd, Aylesbury, UK).   PDH activity was calculated from the curves generated by determining the initial rate of reaction using the following equation:

$$\Delta mOD_{450 \text{ nm/min}} = 1000 \text{ x } \frac{(OD \text{ at time } T2 - OD \text{ at time } T1)}{T2 - T1}$$

where mOD is milli optical density and the change in OD with time follows linear dependence between times T1 and T2 (min). PDH activity was finally recorded as the change in mOD per minute per µg of PDH ($\Delta mOD_{450 \text{ nm/min/µg}}$).

2.2.11. mRNA expression in cultured cells

To determine if TMFol has an effect on the transcription of the *ACC* gene in the prostate cancer cells, the mRNA expression of ACC in the DMSO control cells and the TMFol treated cells was compared. 22Rv1 cells were seeded at a density of 1×10^6, while PC-3 and PNT2 cells were seeded at 8×10^5 in 75 cm^2 flasks in 12 mL of media. After allowing 24 h for adherence, the cells were treated with 10 μM TMFol or DMSO control for 24, 48 or 72 h. The cells were washed twice in 5 mL PBS and harvested by trypsinisation. The cell suspension was centrifuged at 350 x g for 3 minutes and the cell pellet formed was resuspended in 800 μL ice-cold PBS. The cell suspension was centrifuged at 17 000 x g for 3 min at 4 ˚C. The supernatant was discarded and the cell pellet was stored at -80 ˚C until ready for use.

2.2.11.1. RNA extraction

RNeasy Mini Kit (Qiagen, Manchester, UK) was used according to the manufacturer's protocol to isolate total RNA from the cell pellet. Approximately 3×10^6 pelleted cells were used for the RNA extraction. RLT Buffer (350 μL) was added to the cell pellet and mixed thoroughly by vortexing to ensure efficient lysis. The lysate was homogenised in a QIAshredder homogeniser by centrifugation for 2 min at 11000 x g. An equal volume of 70 % ethanol was added to the homogenised lysate and mixed thoroughly by pipetting. This sample was then transferred to an RNeasy spin column for centrifugation at 8000 x g for 15 sec. The RNA, which was now attached to the membrane of the spin column, was washed with 350 μL Buffer RW1, followed by incubation with DNaseI solution for 15 min at room temperature. The DNaseI solution was used to digest any contaminating DNA in the lysates. The RNA on the membrane of the spin column was then subjected to 15 sec spin buffer washes at 8000 x g with 350 μL and 500 μL of Buffer RW1 and Buffer RPE, respectively. The final spin wash was with 500 μL of Buffer RPE for 2 min at 8000 x g before the RNA was eluted by adding 40μL RNase-free water to the spin column and centrifuging for 1 min at 8000 x g. The RNA extract was kept on ice and the quantity of the RNA was assessed spectrophotometrically using a Nanodrop Spectrophotometer ND-1000 (Labtech, Sussex, UK). Only RNA extracts with A260/280 ratio of 2.0 and over were used in the reverse transcription procedure described below. The RNA extracts were stored at -80°C until ready for use.

2.2.11.2. Reverse transcription

One µg of extracted RNA was reverse-transcribed into complementary DNA (cDNA) according to the protocol of QuantiTect Reverse Transcription Kit (Qiagen, Manchester, UK). Any contaminating genomic DNA was eliminated from the RNA extracts by incubating with a gDNA Wipeout Buffer for 2 min at 42 °C, then by immediate storage on ice. This was followed by reverse transcription using a master mix containing equal volumes of the Quantiscript Reverse Transcriptase and RT Primer Mix prepared in a Quantiscript RT Buffer. The reverse transcription reaction was carried out at 42 °C for 15 min and then terminated by a 3 min incubation at 95 °C. The cDNA formed was diluted with RNase-free water and stored at -20 °C until ready for use. To verify that all genomic DNA was effectively eliminated prior to reverse transcription, a no reverse transcription control for each sample was prepared at the same time and in a similar manner as the cDNA, except that Quantiscript Reverse Transcriptase was omitted. Therefore, reverse transcription was prevented and any DNA present was due to contaminating genomic DNA.

2.2.11.3. Quantitative real-time polymerase chain reaction (qPCR)

qPCR was performed on an Applied Biosystems Step One Plus^{TM} Real-time PCR System (Life Technologies, Paisley, UK). In 96-well plates, a mixture of 5 µL of Taqman Fast Universal PCR Master Mix (Life Technologies, Paisley, UK), 0.5 µL of the relevant Taqman gene expression assay and 4.5 µL of the cDNA or no reverse transcription control, was added in triplicate. A no template control was also included for each gene expression assay where nuclease-free water was substituted for the cDNA. Two reference Taqman gene expression assays were used, actin [ACTB: Hs 99999903_m1; Assay ID 16584474] and glyceraldehyde 3-phosphate dehydrogenase [GAPDH: Hs 03929097_g1; Assay ID 16451489]. The gene of interest was acetyl-CoA carboxylase or ACC [ACACA: Hs 01046070_m1; Assay ID 16431762]. The thermal cycling parameters for the qPCR were: holding stage – 95 °C for 20 sec and the cycling stage for 40 cycles – 95 °C for 1 sec followed by 60 °C for 20 sec. The comparative C_T (cycle threshold) method was used to determine the fold change in the expression of the ACC mRNA relative to the control after normalisation to the reference genes.

2.2.12. *In vivo* efficacy studies

The *in vivo* efficacy studies were conducted in two different conditional knockout mouse models of prostate cancer, PB^{Cre4}*p53^{flox}Rb^{flox}* and PB^{Cre4}*Pten^{flox}*. As a result of collaboration, all animal work was performed in the animal facility at the Cancer Research UK Cambridge Institute, University of Cambridge, UK under the supervision of Dr. Antonio Ramos-Montoya, Dr. Sérgio Felisbino and Dr. Chiranjeevi Sandi. As part of the collaborative effort, I was involved in harvesting of organs from the PB^{Cre4}*p53^{flox}Rb^{flox}* mice, enrolment of the PB^{Cre4}*Pten^{flox}* mice in the study and all histological analysis of the harvested tissues.

2.2.12.1. Mouse models

PB^{Cre4}*p53^{flox}Rb^{flox}* mice were the kind donation of Dr. Andrea Flesken-Nikitin, Cornell University (Ithaca, New York). The PB^{Cre4}*Pten^{flox}* mice were generated at Cancer Research UK, Cambridge Institute by crossing FVB.B6(D2)-Tg(Pbsn-cre)4Prb N11 and FVB.C(129S4)-*Pten*^{tm1Hwu}/J N11 strains. Primer sequences for PB^{Cre4}, *p53^{flox}*, *Rb^{flox}* and *Pten^{flox}* were used in the screening of DNA, from punch biopsies of the earlobes from each animal, by PCR to authenticate the genotypes of the animals. The mice were housed in a climate-controlled environment with a 12 h light/dark cycle. Experiments were kept within the limits of the animal project license PPL 80/2435.

2.2.12.2. PB^{Cre4}*p53^{flox}Rb^{flox}* study design

At the age of 4 weeks, 40 male PB^{Cre4}*p53^{flox}Rb^{flox}* mice were weighed and randomised into 4 groups. There were 2 control groups with 10 mice in each group, where the animals were fed the control diet of AIN93G from the age of 4 weeks until the age of 27 weeks (a 23-week study) or until moribund (survival study). In the remaining 2 groups, with 10 mice in each group, the animals were fed pellets of the treatment diet (AIN93G supplemented with 0.2% w/w TMFol) from the age of 4 weeks until the age of 27 weeks (a 23-week study) or until moribund (survival study). The diets were manufactured by LabDiet (International Product Supplies, London, UK). The diet and water were supplied *ad libitum*.

The body weight of the animals was recorded weekly. Additionally the animals were palpated and had ultrasound weekly. From the age of 30 weeks, the general health

status of the animals in the survival study was determined by daily manual assessment. The animals in the 23-week study were sacrificed at age 27 weeks by inhalation of isoflurane followed by cervical dislocation. Blood was collected by means of cardiac puncture prior to the cervical dislocation. After opening of the abdomen, the prostate lobes, seminal vesicles, bladder, urethra, liver and any other organs that visually reflected tumour metastasis were harvested. Tissue samples for histological and immunohistochemistry evaluation were fixed in 10 % neutral-buffered formaldehyde for 24 h and then paraffin-embedded. Samples intended for biochemical analysis were snap frozen in liquid nitrogen and stored at -80 ˚C. The animals in the survival study were similarly sacrificed when they were moribund. The animals were considered to be moribund when they showed signs of ill health, such as piloerection and hunched posture, inactivity or loss of appetite for a period of 48 h. Additionally, if an animal lost more than 20 % of its body weight or developed more serious clinical signs such as diarrhoea or dyspnoea it was sacrificed.

2.2.12.3. PB^{Cre4}Pten^{flox} study design

At an average age of 3.5 months, 20 male PB^{Cre4}Pten^{flox} mice were weighed and randomised into 2 groups. Each group consisted of 10 animals and they were fed the AIN93G diet or the 0.2 % TMFol diet for 12 weeks. The diet and water were supplied *ad libitum*. The body weight of the animals was recorded weekly. Additionally, the animals were palpated and had ultrasound weekly. At the end of the study the animals were sacrificed by inhalation of isoflurane followed by cervical dislocation. All tissue samples were collected and stored as described in section 2.2.12.2 above.

2.2.12.4. Histopathological evaluation of animal tissues

The paraffin-embedded tissues were sectioned at 3 – 4 μm thickness for haematoxylin and eosin (H&E) staining. The H&E slides were digitally scanned using Aperio Digital Pathology (Milton Keynes, UK) while Aperio ImageScope (version 11.1.2.760) was used to view the scanned slides. The H&E sections of the prostates, urethra, liver, kidney, spleen and pancreas were evaluated for the incidence and burden of prostate cancer pathologies. The histopathological evaluation was performed in a blinded manner to the treatment status by one pathologist or in collaboration with a morphologist.

2.2.13. Statistical analysis

Data from all *in vitro* studies are presented as the mean of at least 3 independent experiments ± standard deviation (SD). Student's T-test in Excel 2013 was used for all *in vitro* data when comparing the treatment group to the control group only. Survival curves generated from the animal survival study were compared by the log-rank test (Prism 6), while the body weights were compared by a mixed effects linear regression (performed by Dr. Maria Viskaduraki, a biostatistician at the University of Leicester). Data were considered to be statistically significant if $p < 0.05$.

Chapter 3. Investigation of the mechanisms of action of TMFol in prostate cancer

3.1. Introduction

The anti-proliferative effect of TMFol in prostate cancer cells has been previously demonstrated in both murine-derived and human-derived prostate cancer cell lines (Britton et al., 2012; Saad, 2011). The mechanisms driving the anti-proliferative activity have not been characterised in detail. Cell cycle arrest in the S and G2/M phases seem to be an important mechanism, while apoptosis appears to be a relevant mechanism in the androgen-dependent prostate cancer cells only (Saad, 2011). These two mechanisms of action of TMFol may be partially mediated through the modulation of AR and p53, but other mechanisms must be involved, since TMFol is also a potent inhibitor of prostate cancer cells that are deficient in AR and p53.

The overall focus of this chapter was to investigate the strategies utilised by TMFol in the growth inhibition of prostate cancer cells. This required verifying the anti-proliferative effect of TMFol in prostate cancer cells, to facilitate a comparison with the growth effect on normal prostate epithelial cells. Subsequently, the role of cell cycle arrest and apoptosis in the activity of a potentially pharmacologically-achievable concentration of TMFol was studied in all cell lines. Eventually, a range of biochemical assays, flow cytometry, immunohistochemistry, qPCR and Western blots were used to detect the cell signalling or metabolic pathways that were modulated and could be effective strategies in the growth inhibitory effects of TMFol.

3.2. Effect of TMFol on the proliferation of 22Rv1, PC-3 and PNT2 cells

Uncontrolled cell proliferation is one of the hallmarks of cancer (Hanahan and Weinberg, 2000 and 2011). Hence, chemopreventive or chemotherapeutic drugs must have the capacity to reduce or eliminate aberrant cellular proliferation. None of the studies published to date on the putative prostate cancer chemopreventive/chemotherapeutic properties of TMFol have considered the effect of TMFol on normal prostate epithelial cells. Therefore, in this study the ability of TMFol to alter the proliferation of two prostate cancer cell lines, 22Rv1 and PC-3 and an immortalised normal prostate epithelial cell line, PNT2, was assessed. To perform this study, the cells were exposed to TMFol (1, 2.5, 5 or 10 µM) or to DMSO (vehicle control) for up to 144 h. The cells were harvested at specific times and counted using a Z2 Coulter Particle Counter with Size Analyser (Beckman Coulter, High Wycombe, UK)). Cell numbers were expressed as a percentage relative to the vehicle control.

TMFol had a dose-dependent growth inhibitory effect at 72 h (Figure 3.1 A) and 144 h (Figure 3.1 B) on the androgen responsive 22Rv1 cells. Exposure of these cells to 5 and 10 µM TMFol for 144 h significantly reduced the cell numbers by more than 50%, relative to the control population. The androgen independent PC-3 cells also had a dose-dependent response to TMFol with high sensitivity to 5 and 10 µM at 144 h (Figures 3.2 A and B). TMFol also modulated the growth of the normal prostatic epithelial cells. At 72 h there was a dose-dependent response, with 5 and 10 µM causing a significant reduction in cell number when compared to the vehicle control (Figure 3.3 A). Then at 144 h, concentrations of TMFol less than 2.5 µM did not exert any growth inhibitory effect on the PNT2 cells (Figure 3.3 B). However, the inhibitory effect observed at 72 h for the higher concentrations was maintained at 144 h. The IC_{50} values at 144 h for 22Rv1 (3.7 ± 0.5 µM), PC-3 (4.1 ± 0.4 µM) and PNT2 (4.5 ± 0.8 µM) are relatively similar, reflecting a general growth inhibitory response to TMFol for both cancer cell lines and the normal prostatic epithelial cells. However, the results also indicate that at longer exposure times the 22Rv1 cells were more sensitive to the growth inhibitory effect of TMFol than the PC-3 and PNT2 cells.

(A)

$IC_{50} = 9.8 \pm 5.0\ \mu M$

(B)

$IC_{50} = 3.7 \pm 0.5\ \mu M$

(C)

Linear equation
$y = -70.502x + 89.981$
$Log\ IC_{50} = 0.57$
$IC_{50} = 3.7\ \mu M$
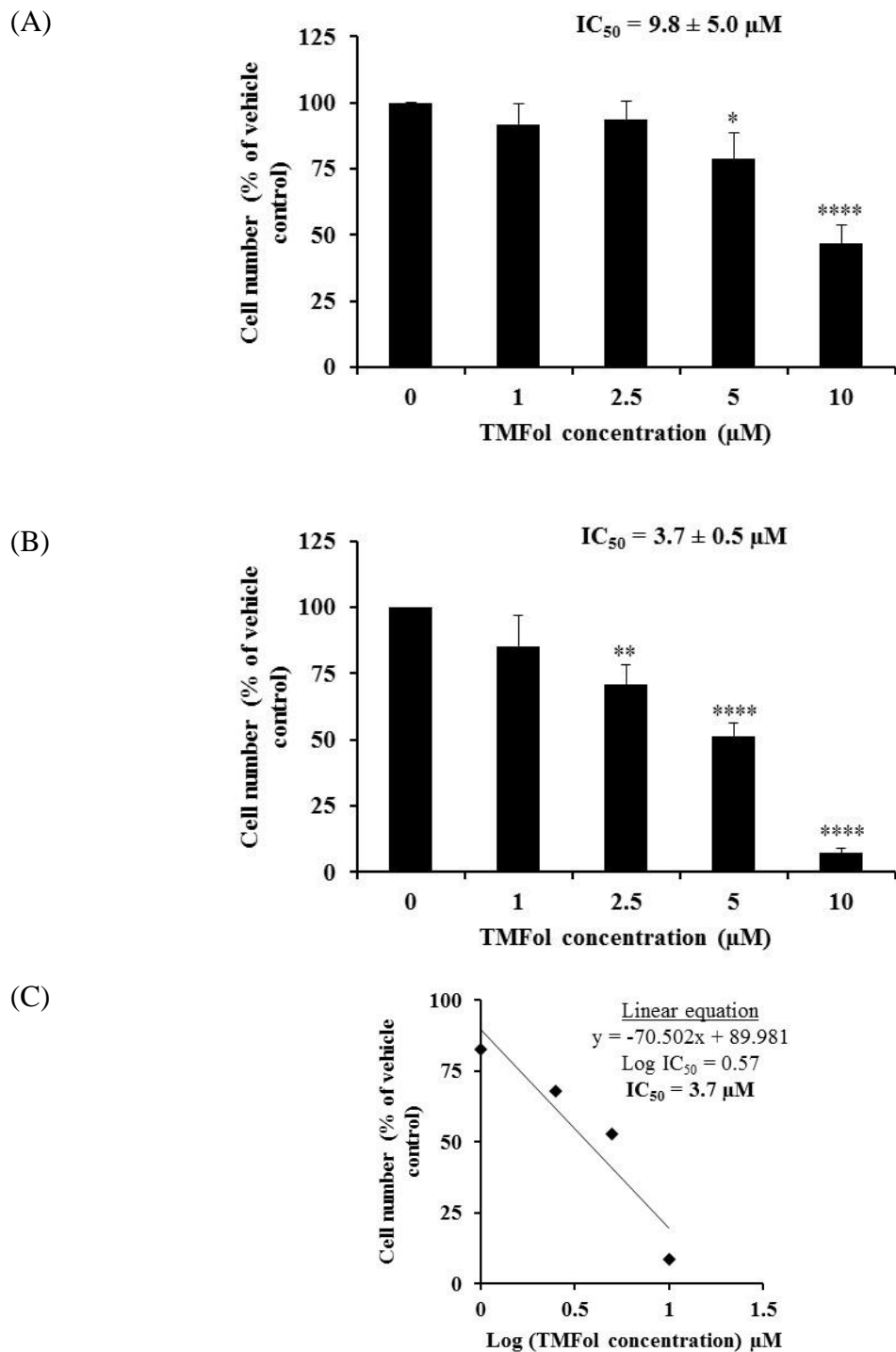
Figure 3.1: Effect of TMFol on the growth of 22Rv1 prostate cancer cells. The cells were counted following treatment with TMFol for 72 h (**A**) and 144 h (**B**). Each column represents the mean ± SD of three independent experiments, each performed in triplicate. Statistical comparison between the control and TMFol treatment was by Student's T-test. Statistically significant differences are indicated as * ($p < 0.05$), ** ($p < 0.01$) and **** ($p < 0.001$). (**C**) shows how the IC_{50} value was calculated for the 144 h time point, as outlined in chapter 2.

(A)

(B)

(C)
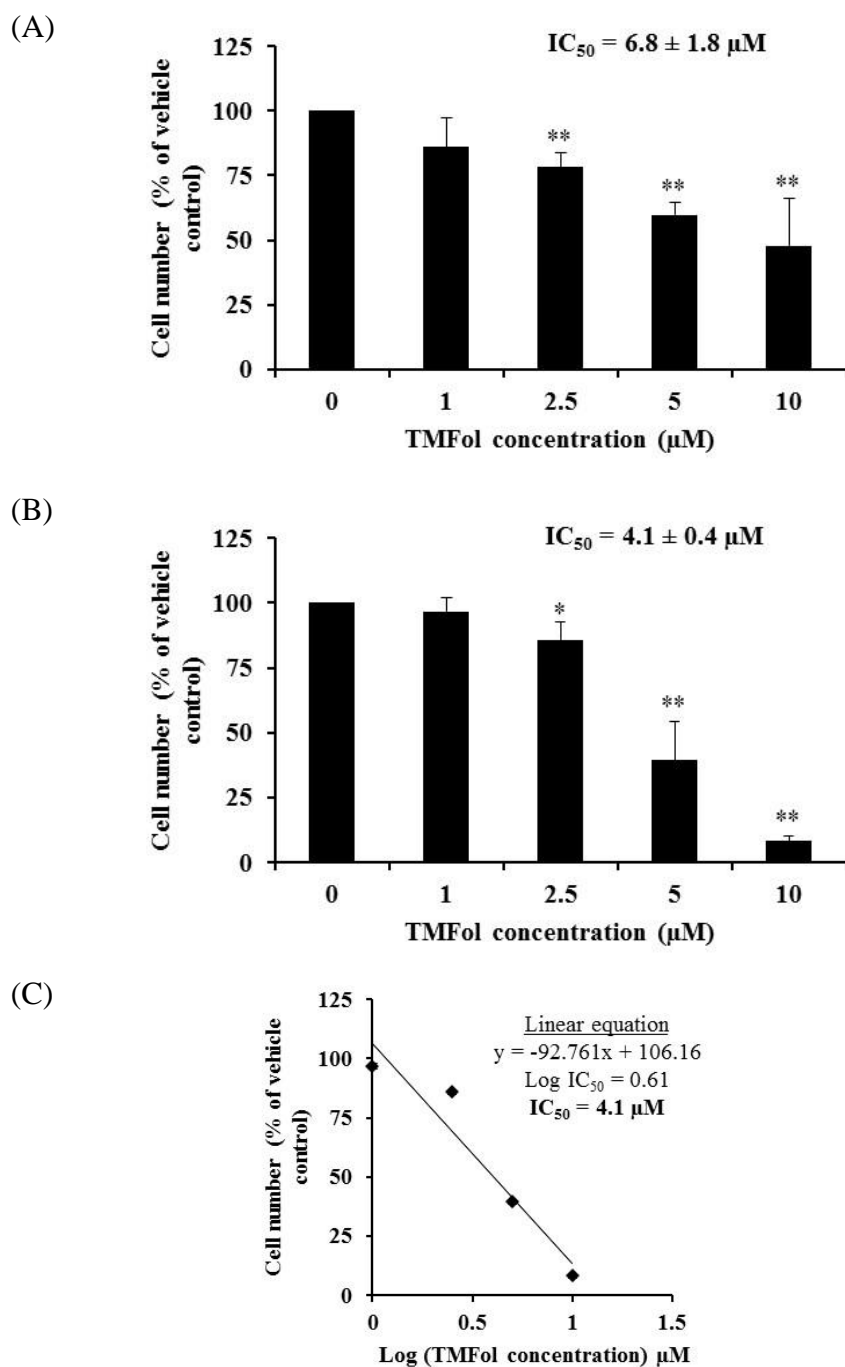
Figure 3.2: Effect of TMFol on the growth of PC-3 prostate cancer cells. The cells were counted following treatment with TMFol for 72 h (A) and 144 h (B). Each column represents the mean ± SD of three independent experiments, each performed in triplicate. Statistical comparison between the control and TMFol treatment was by Student's T-test. Statistically significant differences are indicated as * ($p < 0.05$) and ** ($p < 0.01$). (C) shows how the IC_{50} value was calculated for the 144 h time point, as outlined in chapter 2.

(A)

(B)

(C)
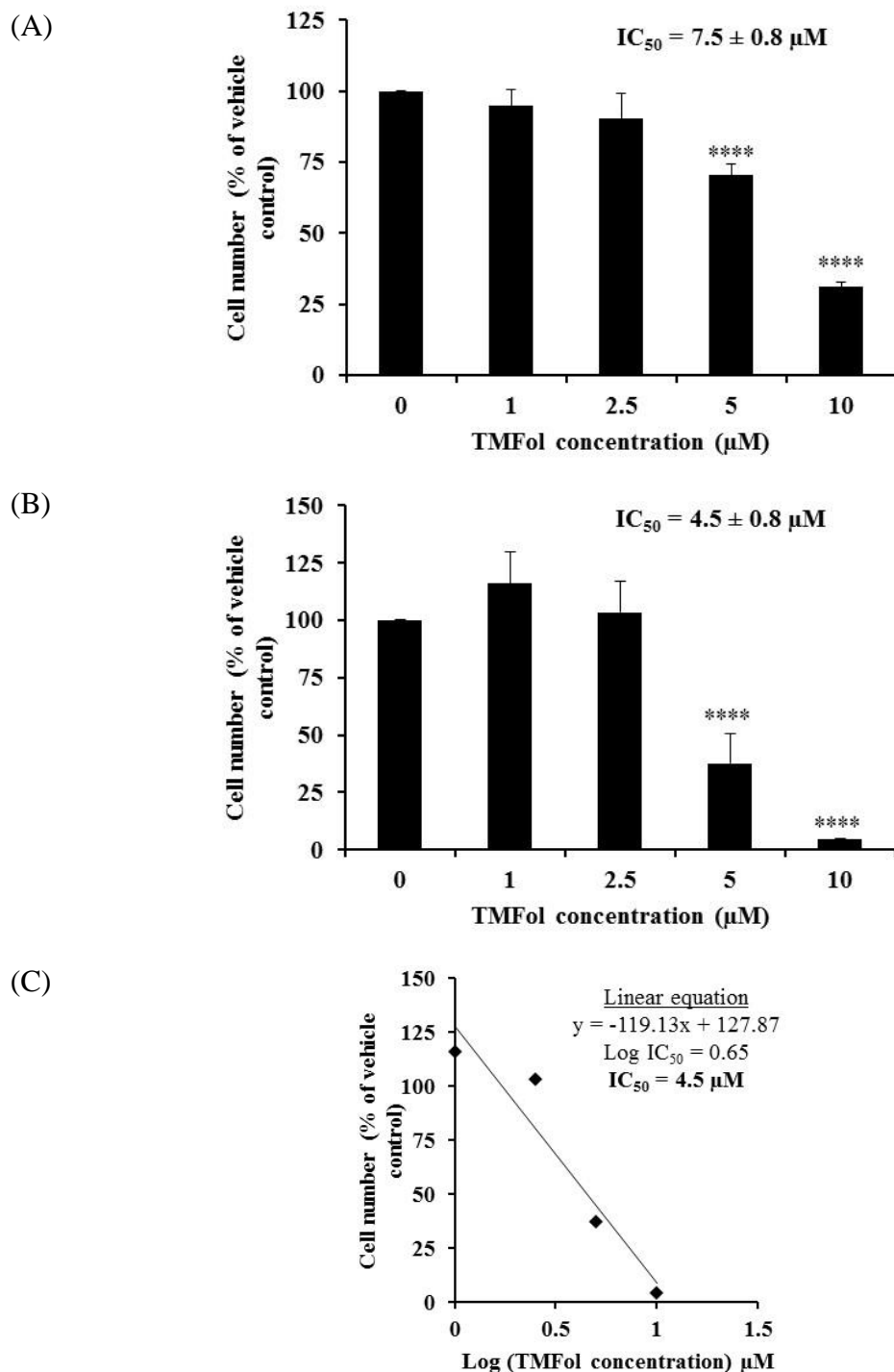
Figure 3.3: Effect of TMFol on the growth of PNT2 prostate cells. The cells were counted following treatment with TMFol for 72 h (A) and 144 h (B). Each column represents the mean $\pm$ SD of three independent experiments, each performed in triplicate. Statistical comparison between the control and TMFol treatment was by Student's T-test. Statistically significant differences are indicated as **** ($p < 0.001$). (C) shows how the IC_{50} value was calculated for the 144 h time point, as outlined in chapter 2.

3.3. Effect of TMFol on cell cycle distribution in prostate cancer cells

Aberrations in the cell cycle have been implicated in the development of cancers (Meeran and Katiyer, 2008). Many flavonoids cause cell cycle arrest to inhibit the development and progression of prostate cancer (Gupta et al., 2003; Haddad et al., 2006). Hence, TMFol was examined for its effect on the cell cycle profiles of 22Rv1, PC-3 and PNT2 cells.

The cells were treated for 24, 48 and 72 h with TMFol, and flow cytometry, using propidium iodide, was performed to assess cell cycle events. In 22Rv1 cells there was no significant increase in the cell numbers in the G1, S or G2/M phases at any of the time points studied (Figures 3.4 and 3.5). At 72 h there was only a slight increase in the fraction of cells in G2/M, with a corresponding small decrease in the proportions of cells in the G1 and S phases (Figures 3.4 and 3.5 C). TMFol caused S phase arrest in PC-3 cells, as the population of cells in the S phase increased, becoming significant at 48 and 72 h (Figures 3.6 and 3.7). This was accompanied by a decrease in the G1 population at all of the time points, but the effect was only statistically significant at 48 and 72 h. Interestingly, the normal prostate epithelial cells, PNT2, were arrested at G1 after 24 h, as evidenced by a significant increase in the proportion of cells in G1, with a significant decrease in S phase cells (Figures 3.8 and 3.9 A). However at 48 h there was a significant rise in the S phase population, with a corresponding significant decrease in G1 (Figures 3.8 and 3.9 B). Eventually, at 72 h the cells were all in S phase (Figures 3.8 and 3.9 C). In comparison to PC-3 cells, the S phase arrest was more prominent in PNT2 cells, which had the greater increase in the S phase population. Hence, TMFol is capable of inducing cell cycle arrest in *in vitro* models of prostate cancer and normal prostate epithelial cells.
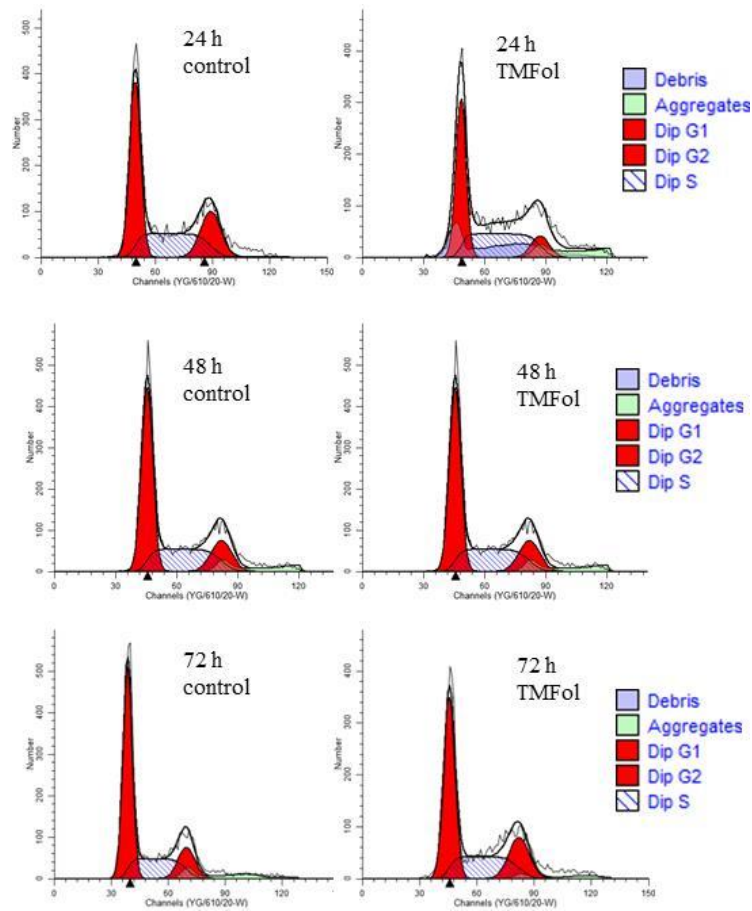
Figure 3.4: Representative flow cytometry profiles for cell cycle distribution in 22Rv1 cells following exposure to 10 µM TMFol for 24 h (A), 48 h (B) and 72 h (C). The profiles were generated by the ModFit LT 3.3 software and used to determine the following cell cycle distribution graph. Dip: diploid

(A)

(B)

(C)
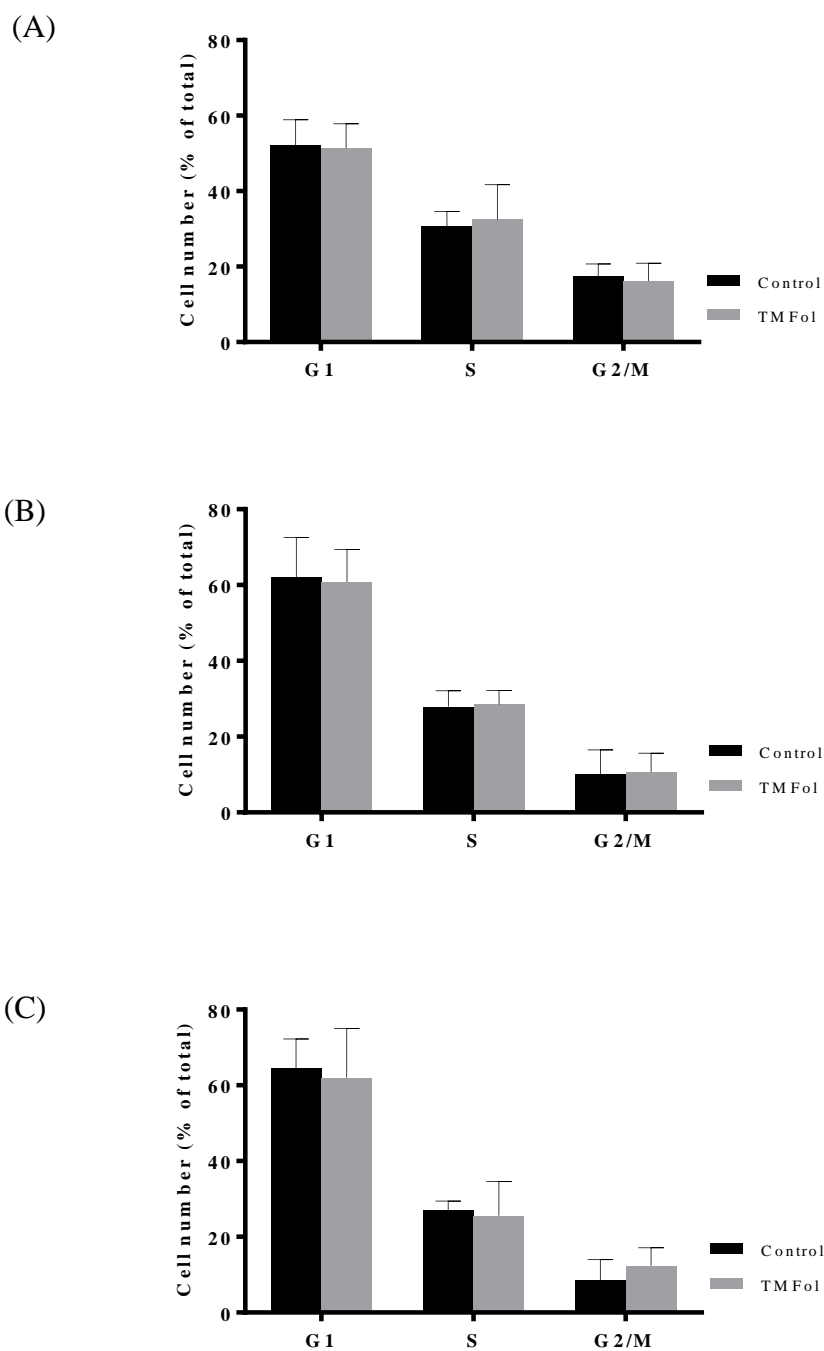
Figure 3.5: Cell cycle distribution in 22Rv1 cells following exposure to 10 µM TMFol for 24 h (A), 48 h (B) and 72 h (C). Following treatment, the cells were harvested and stained with PI. The DNA content was analysed by flow cytometry and the ModFit LT 3.3 software was used to determine the cell cycle profile. The values represent the percent of cell population in each phase. Each column represents the mean ± SD of three independent experiments. No statistically significant difference was observed between the control and TMFol treated cells.
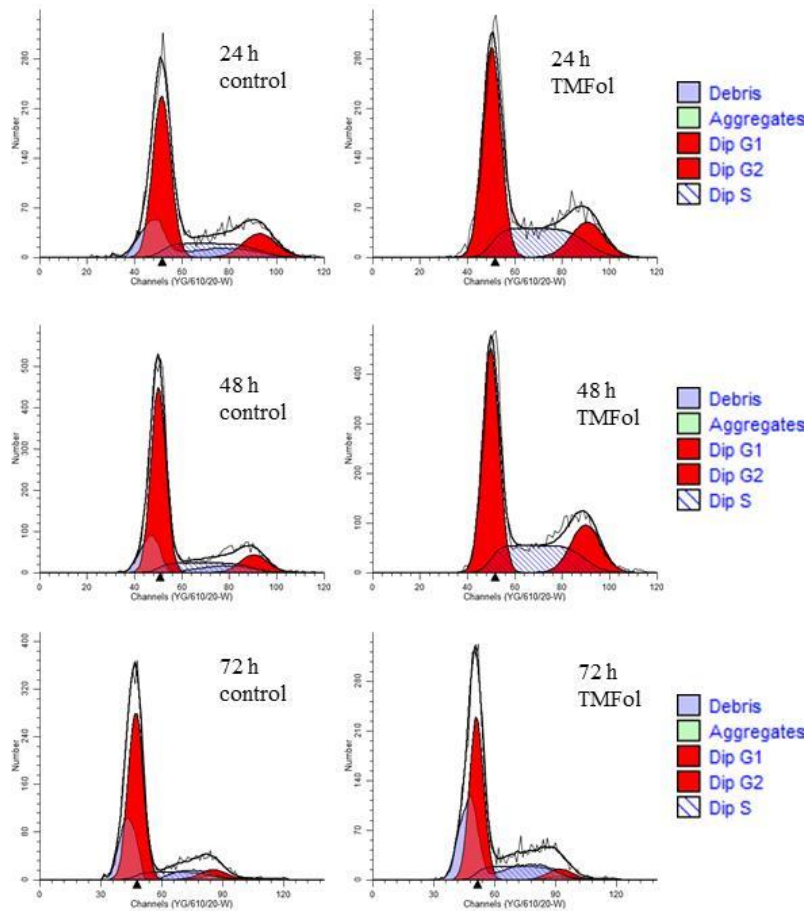
Figure 3.6: Representative flow cytometry profiles for cell cycle distribution in PC-3 cells following exposure to 10 μM TMFol for 24 h (A), 48 h (B) and 72 h (C). The profiles were generated by the ModFit LT 3.3 software and used to determine the following cell cycle distribution graph. Dip: diploid
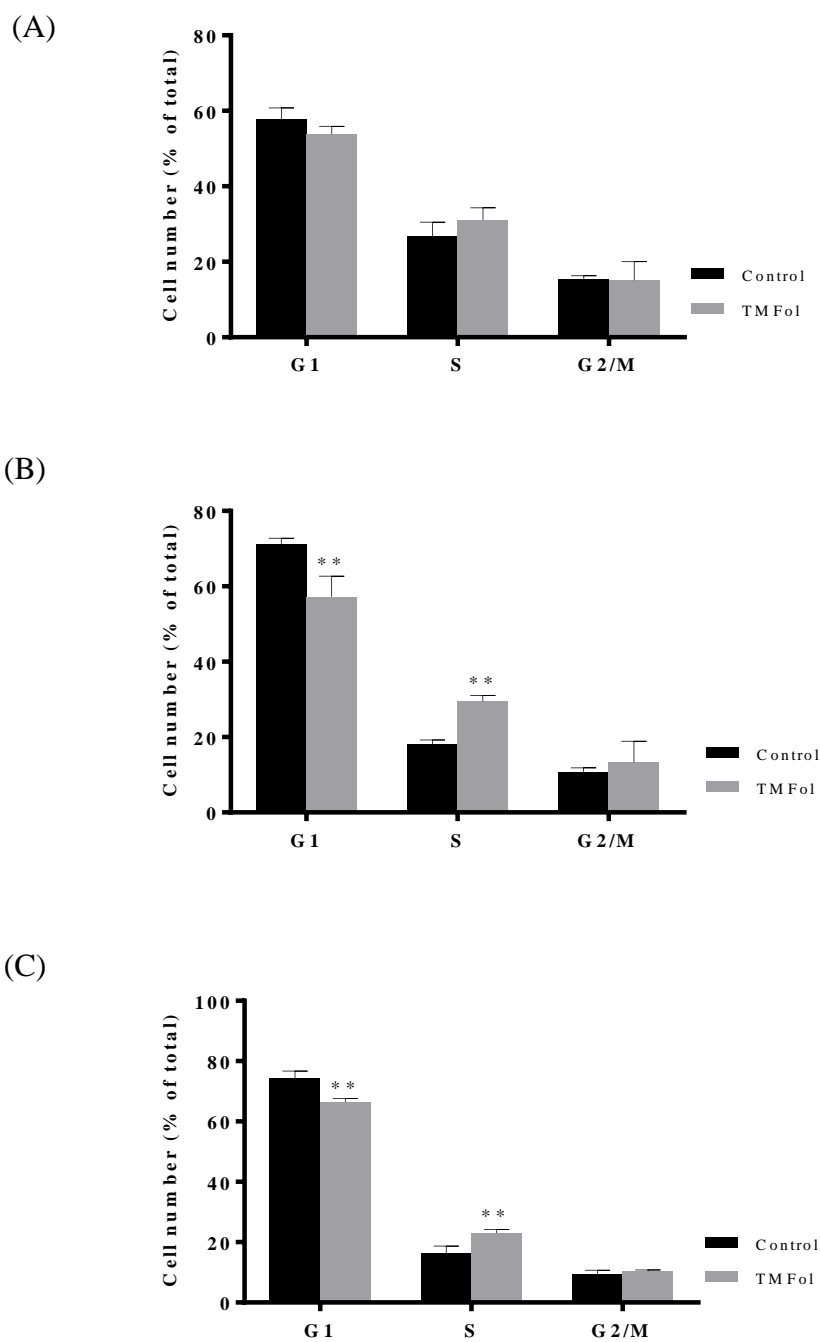
Figure 3.7: Cell cycle distribution in PC-3 cells following exposure to 10 µM TMFol for 24 h (A), 48 h (B) and 72 h (C). Following treatment, the cells were harvested and stained with PI. The DNA content was analysed by flow cytometry and the ModFit LT 3.3 software was used to determine the cell cycle profile. The values represent the percent of cell population in each phase. Each column represents the mean ± SD of three independent experiments. Statistical comparison between the control and TMFol treatment was by Student's T-test. Statistically significant differences are indicated as ** (p< 0.01).
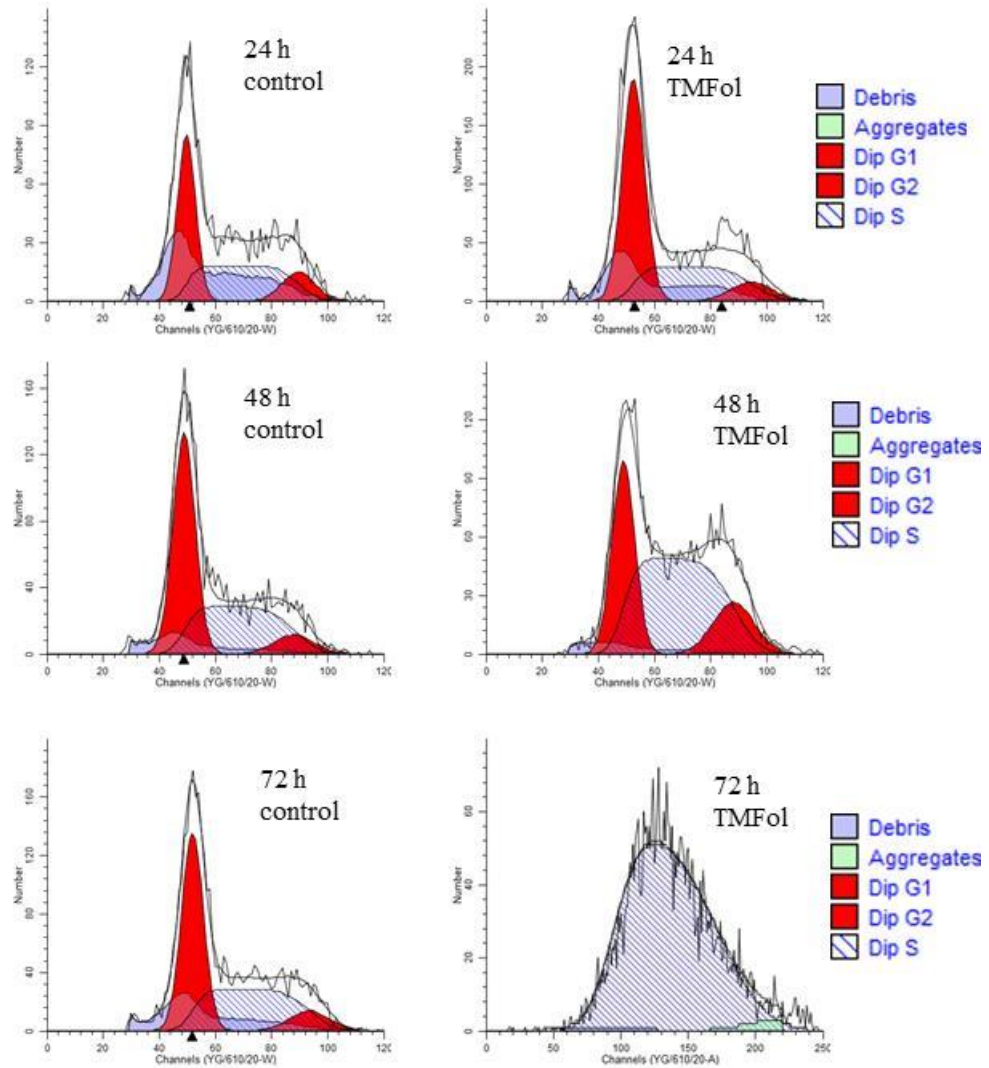
Figure 3.8: Representative flow cytometry profiles for cell cycle distribution in PNT2 cells following exposure to 10 μM TMFol for 24 h (A), 48 h (B) and 72 h (C). The profiles were generated by the ModFit LT 3.3 software and used to determine the following cell cycle distribution graph. Dip: diploid

(A)

(B)

(C)
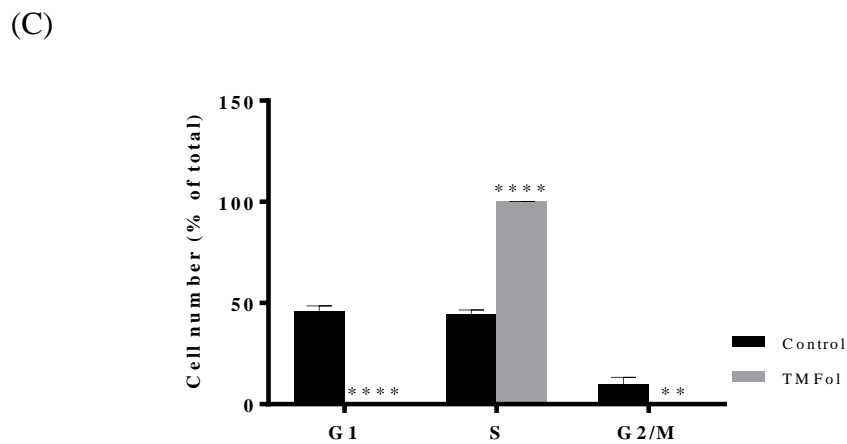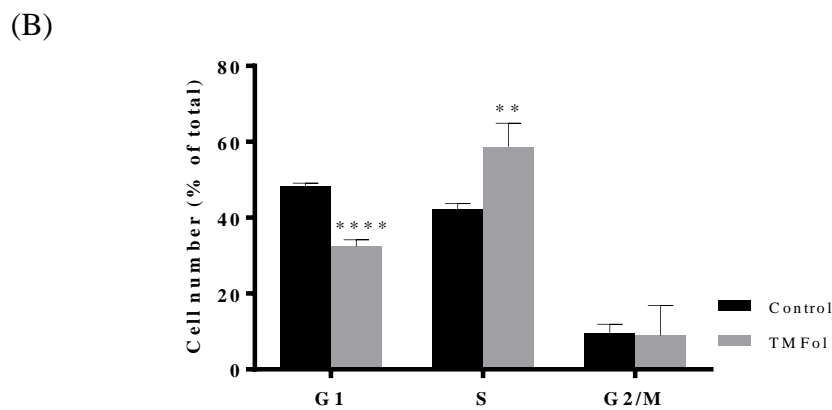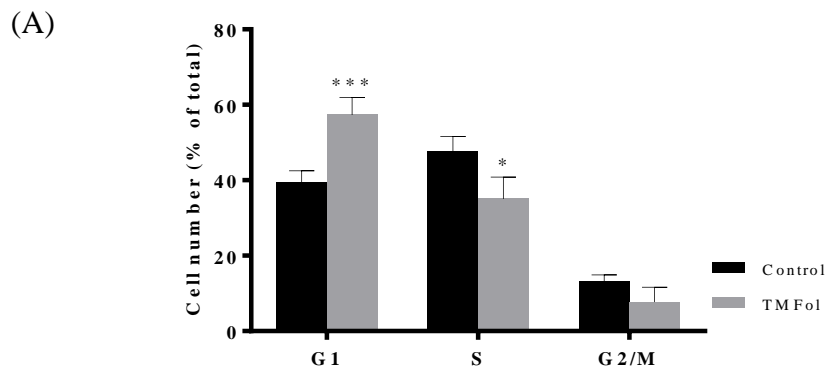
Figure 3.9: Cell cycle distribution in PNT2 cells following exposure to 10 µM TMFol for 24 h (A), 48 h (B) and 72 h (C). Following treatment, the cells were harvested and stained with PI. The DNA content was analysed by flow cytometry and the ModFit LT 3.3 software was used to determine the cell cycle profile. The values represent the percent of cell population in each phase. Each column represents the mean ± SD of three independent experiments. Statistical comparison between the control and TMFol treatment was by Student's T-test. Statistically significant differences are indicated as * (p< 0.05), ** (p< 0.01), *** (p< 0.005) and **** (p< 0.001).

3.4. Effect of TMFol on apoptosis in 22Rv1, PC-3 and PNT2 cells

The inhibition of apoptosis is critical in the development and progression of cancers (Zhivotovsky and Orrenius, 2006). Therefore, the activation of apoptosis to eliminate pre-cancerous/cancerous cells is a potent mechanism for chemotherapeutic and potentially chemopreventive agents. *In vitro* and animal studies have demonstrated the induction of apoptosis as the most potent defence against cancer for several putative chemopreventive agents (Hail, 2005; Sun et al., 2004). Flavonols, such as quercetin and fisetin, have been shown to mediate their anti-prostate cancer effects via apoptosis (Khan et al., 2008; Lee et al., 2008). Therefore, it was necessary to determine if apoptosis contributed to the anti-proliferative effects of TMFol in 22Rv1, PC-3 and PNT2 cells.

Flow cytometry was used to determine the apoptotic profile of the cell lines, 22Rv1, PC-3 and PNT2, when treated with 10 μM TMFol. At all of the time points studied 10 μM TMFol did not cause a significant change in the extent of apoptosis above background levels measured in control 22Rv1 cells (Figures 3.10 and 3.11). There was also no evidence of apoptosis activation in the PC-3 cells (Figures 3.12 and 3.13) and PNT2 cells (Figures 3.14 and 3.15) at 24, 48 and 72 h. However, the PNT2 cells showed significant increase in the percentage of necrotic cells after exposure to 10 μM TMFol for 72 h (Figure 3.15 C).
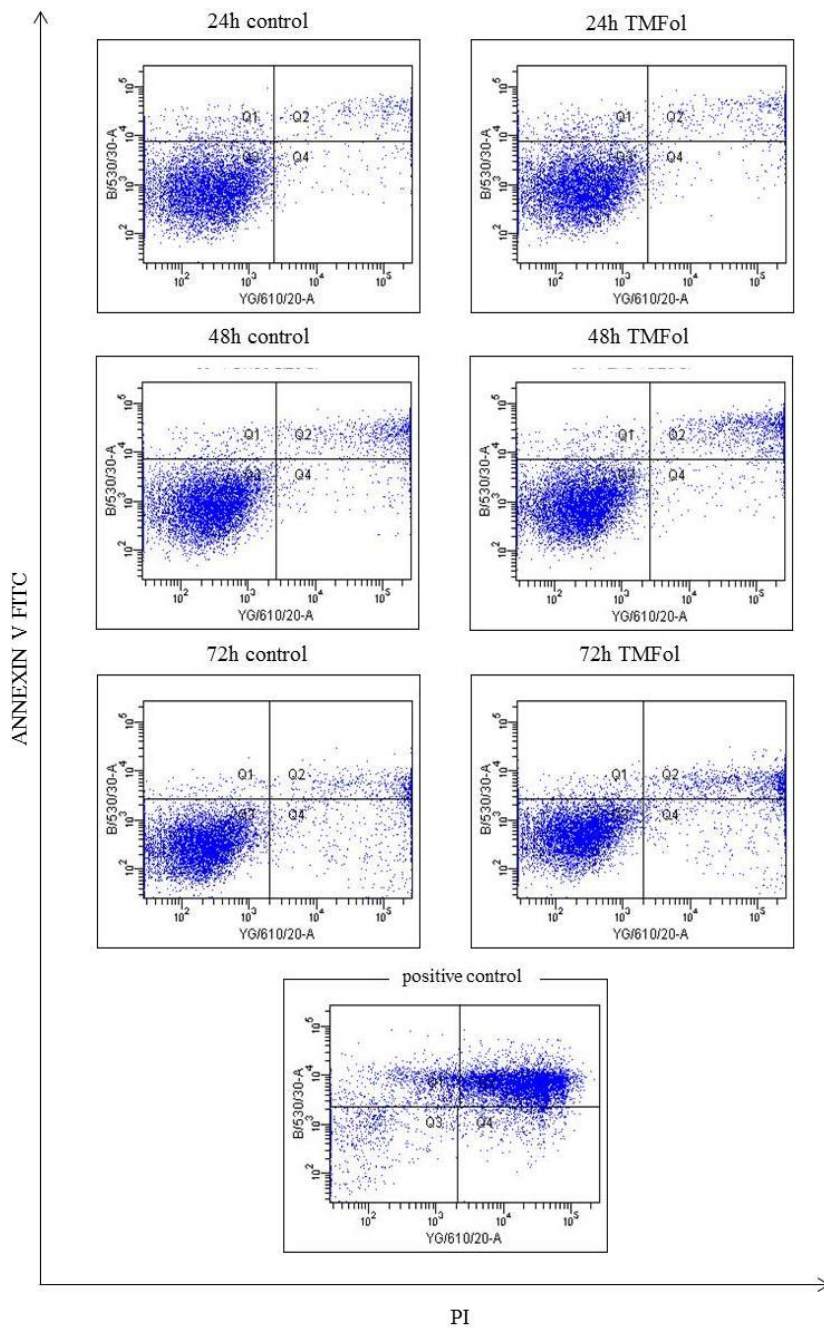
Figure 3.10: Representative flow cytometry scatter plots for the Annexin V assay in 22Rv1 cells treated with 10 μM TMFol for 24, 48 and 72 h. After treatment, the cells were trypsinised and stained with Annexin V – FITC and PI. The early apoptotic cells are stained with Annexin V only and are localised to Q1, while the late apoptotic or necrotic cells are stained with both dyes and are in Q2. The viable cells do not take up any of the dyes and are confined to Q3. The non-viable cells take up PI only and are located in Q4. A representative scatter plot of the positive control (cells treated with 20 μM sorafenib tosylate) is included.

(A)

(B)

(C)
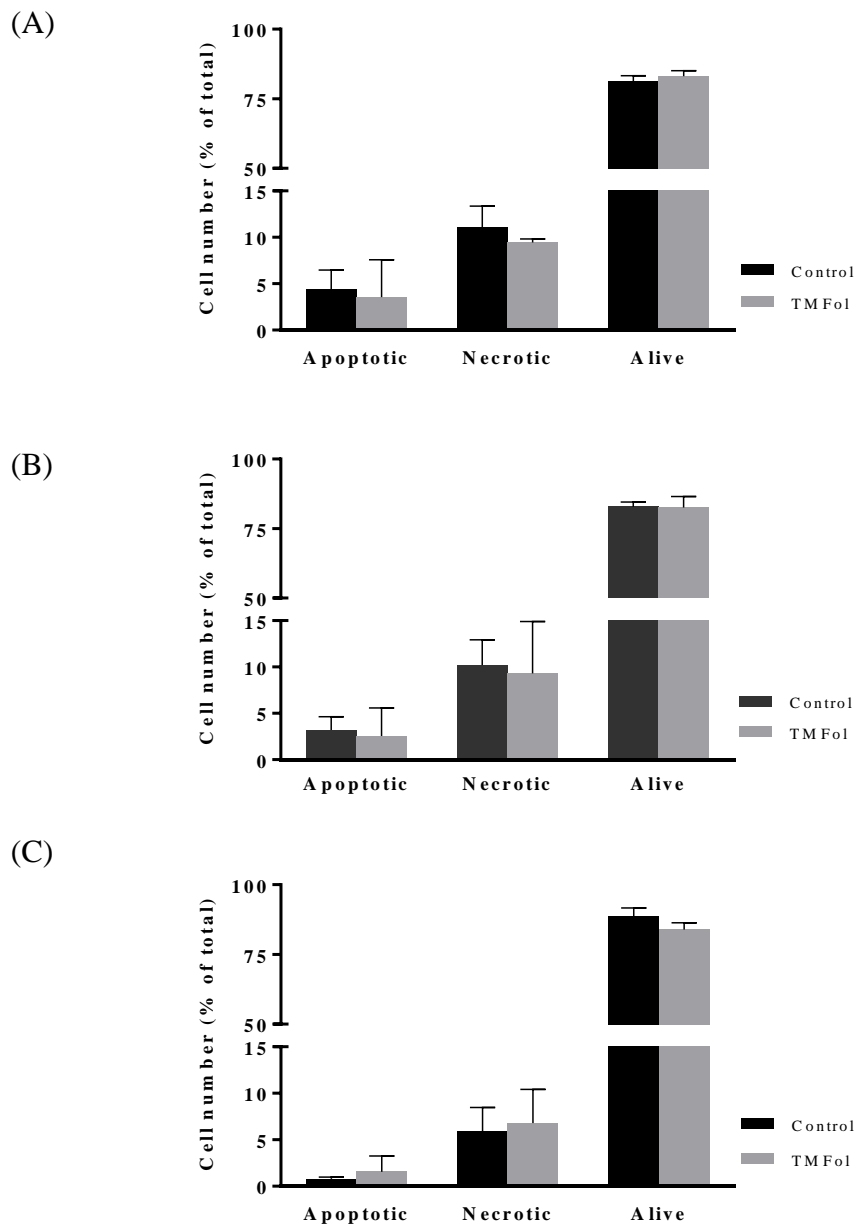
Figure 3.11: Percentage distribution of apoptotic, necrotic and live 22Rv1 cells following exposure to 10 μM TMFol for 24 h (A), 48 h (B) and 72 h (C). Each column represents the mean ± SD of three independent experiments. The break in the Y-axis has been included for clarity. No statistically significant difference was observed between the control and TMFol treated cells.
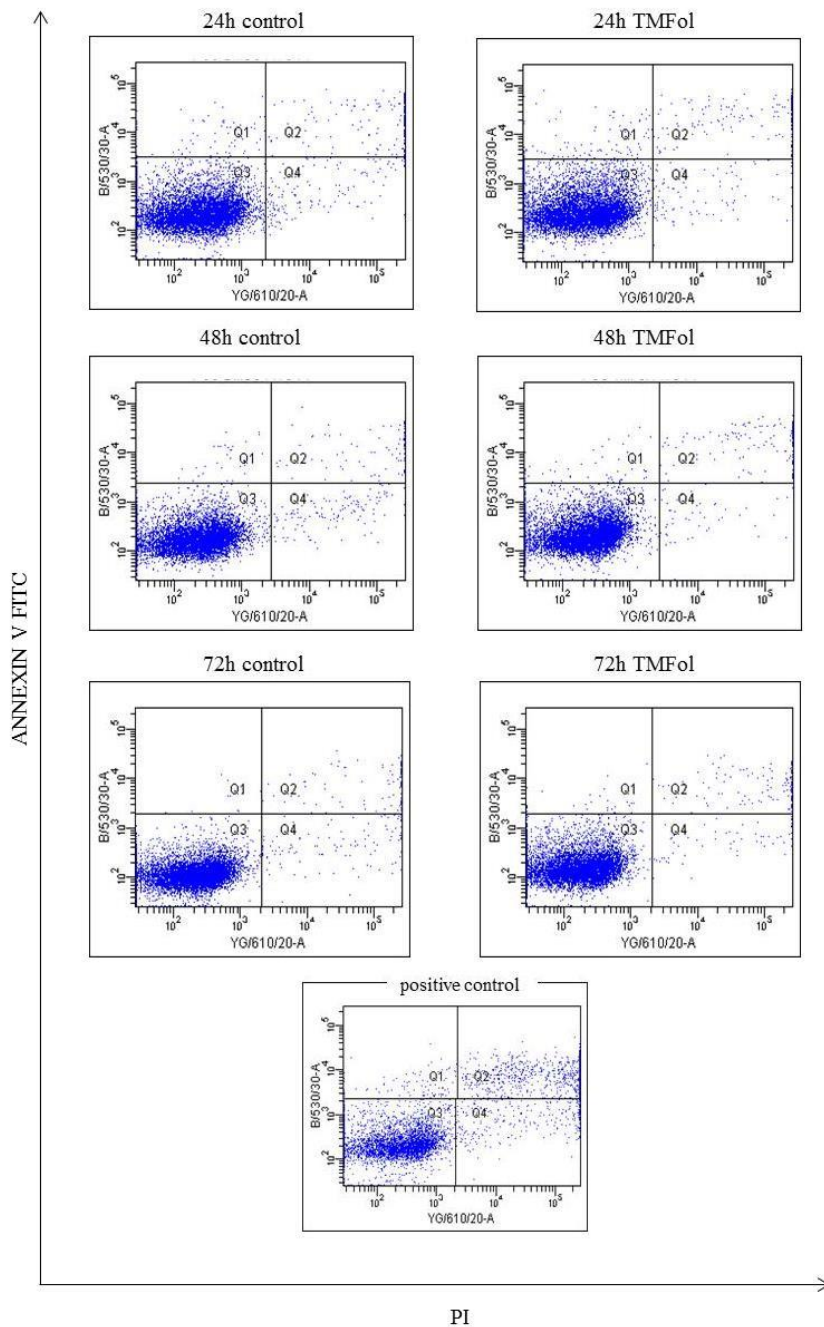
Figure 3.12: Representative flow cytometry scatter plots for the Annexin V assay in PC-3 cells treated with 10 μM TMFol for 24, 48 and 72 h. After treatment, the cells were trypsinised and stained with Annexin V – FITC and PI. The early apoptotic cells are stained with Annexin V only and are localised to Q1, while the late apoptotic or necrotic cells are stained with both dyes and are in Q2. The viable cells do not take up any of the dyes and are confined to Q3. The non-viable cells take up PI only and are located in Q4. A representative scatter plot of the positive control (cells treated with 20 μM sorafenib tosylate) is included.
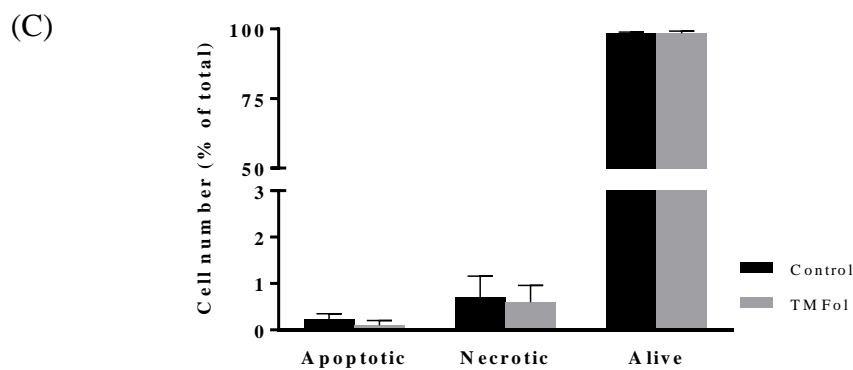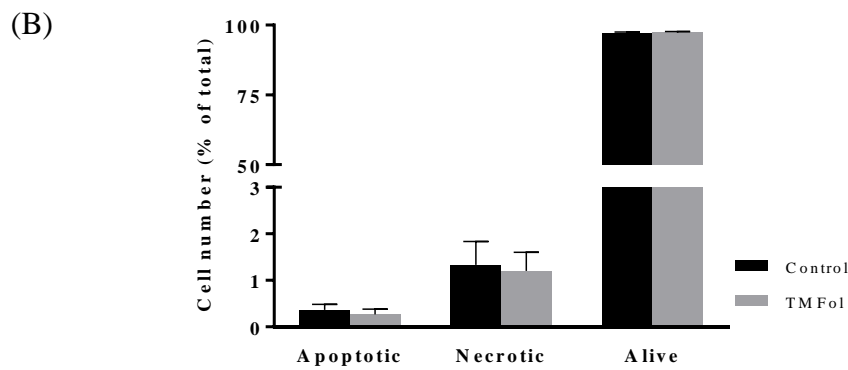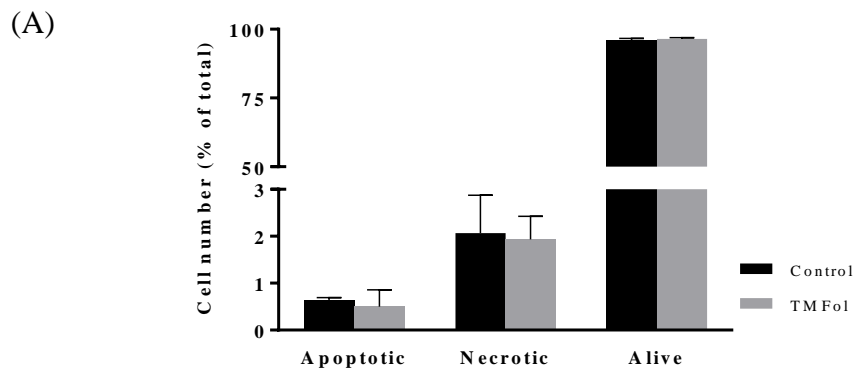
Figure 3.13: Percentage distribution of apoptotic, necrotic and live PC-3 cells following exposure to 10 μM TMFol for 24 h (A), 48 h (B) and 72 h (C). Each column represents the mean ± SD of three independent experiments. The break in the Y-axis has been included for clarity. No statistically significant difference was observed between the control and TMFol treated cells.
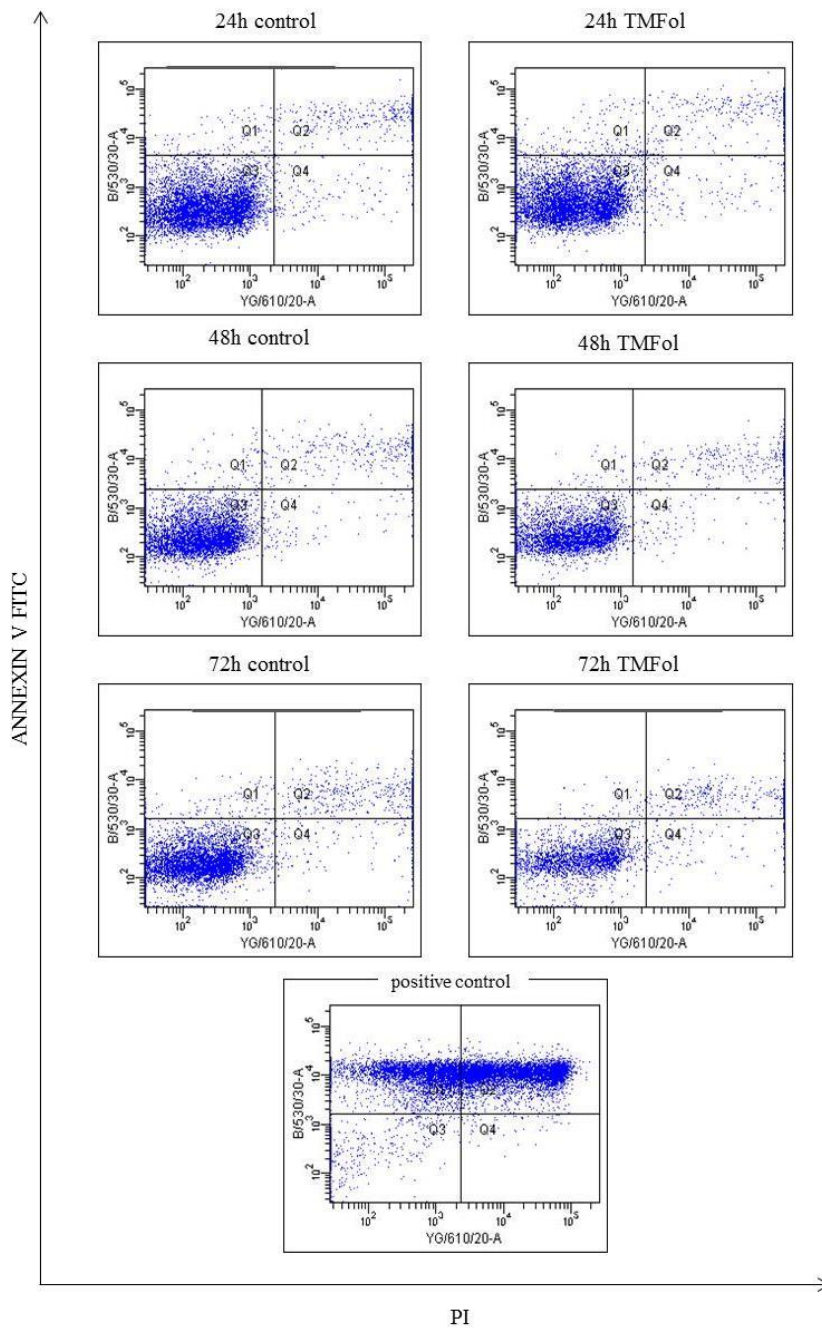
Figure 3.14: Representative flow cytometry scatter plots for the Annexin V assay in PNT2 cells treated with 10 μM TMFol for 24, 48 and 72 h. After treatment, the cells were trypsinised and stained with Annexin V – FITC and PI. The early apoptotic cells are stained with Annexin V only and are localised to Q1, while the late apoptotic or necrotic cells are stained with both dyes and are in Q2. The viable cells do not take up any of the dyes and are confined to Q3. The non-viable cells take up PI only and are located in Q4. A representative scatter plot of the positive control (cells treated with 50 μM etoposide) is included.

99
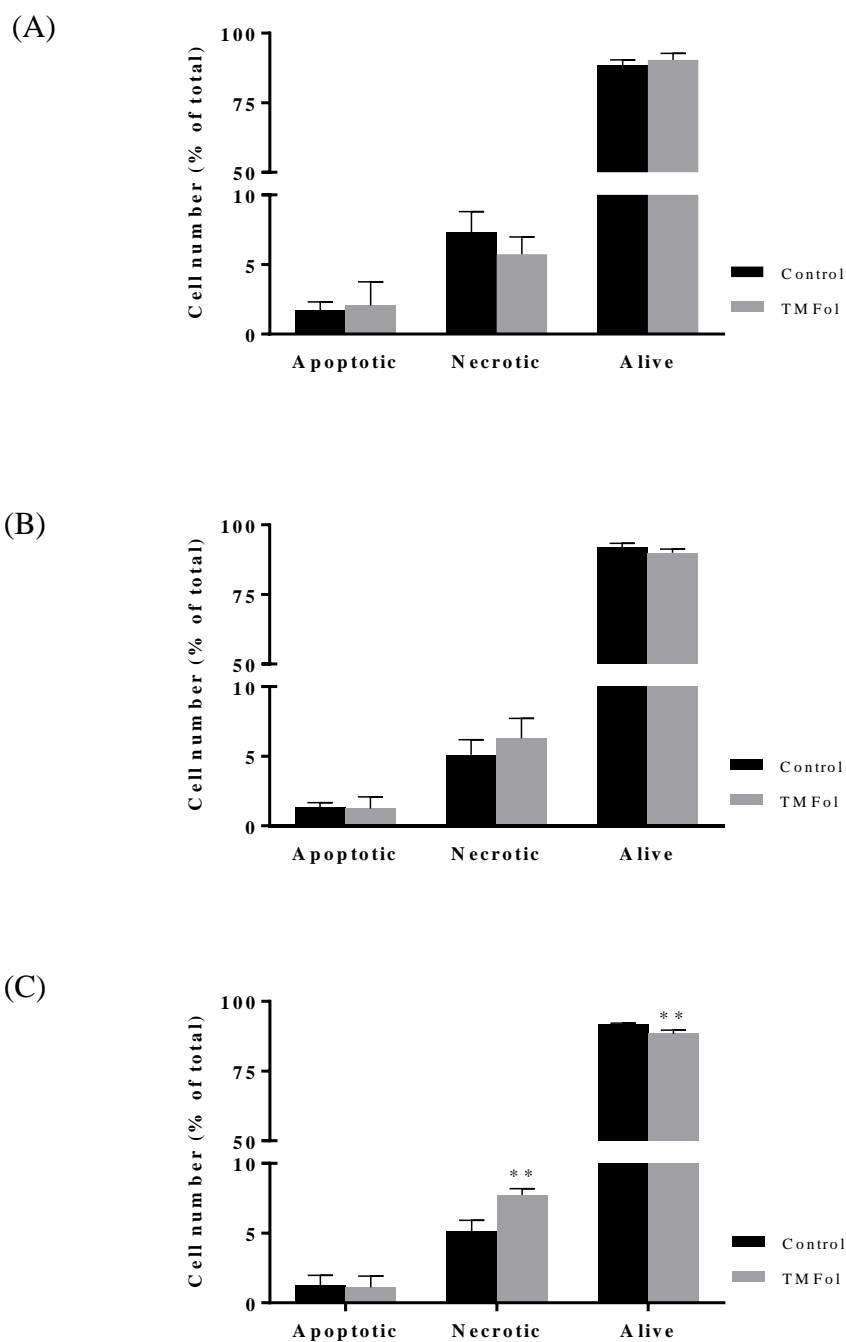
Figure 3.15: Percentage distribution of apoptotic, necrotic and live PNT2 cells following exposure to 10 μM TMFol for 24 h (A), 48 h (B) and 72 h (C). Each column represents the mean ± SD of three independent experiments. The break in the Y-axis has been included for clarity. Statistical comparison between the control and TMFol treatment was by Student's T-test. Statistically significant differences are indicated as ** ($p < 0.01$).

3.5. Effect of a 0.2 % TMFol diet on apoptosis in 22Rv1 xenografts

Previous unpublished work from this laboratory, performed by Dr Stewart Sale, demonstrated the growth inhibitory effect of a 0.2 % TMFol diet administered to xenograft mice for approximately 7 weeks, on tumours derived from 22Rv1 prostate cancer cells. TMFol reduced tumour development modestly, but significantly by 35 % in the treated mice when compared to the control. The paraffin-embedded slides of the prostate tumour sections from these 22Rv1 xenografts were made available in this current study for assessment of apoptosis. To determine apoptosis, the tumour sections from the mice on the control and TMFol diets were immunostained for cleaved caspase-3, a well-known apoptotic marker (Gown and Willingham, 2002). There was a significant increase in the number of cleaved caspase-3 stained cells in the TMFol-fed mice compared to those in the control group (Figure 3.16), indicating an approximate 1.5-fold increase in apoptosis. The percentage of cells positive for cleaved caspase-3 in the tumours from the control mice (62 %) appeared unusually high. This could mean that there were factors, such as inadequate access to nutrients by the tumours, in the tumour environment of these mice, which could potentially stimulate apoptosis. However, follow up analysis were not possible within the scope of this current research. Nevertheless, it appears that TMFol (10 µM) does not induce significant apoptosis in prostate cancer and normal prostate epithelial cells *in vitro*, but a dietary intake of 0.2% TMFol triggered apoptosis in 22Rv1 xenografts.
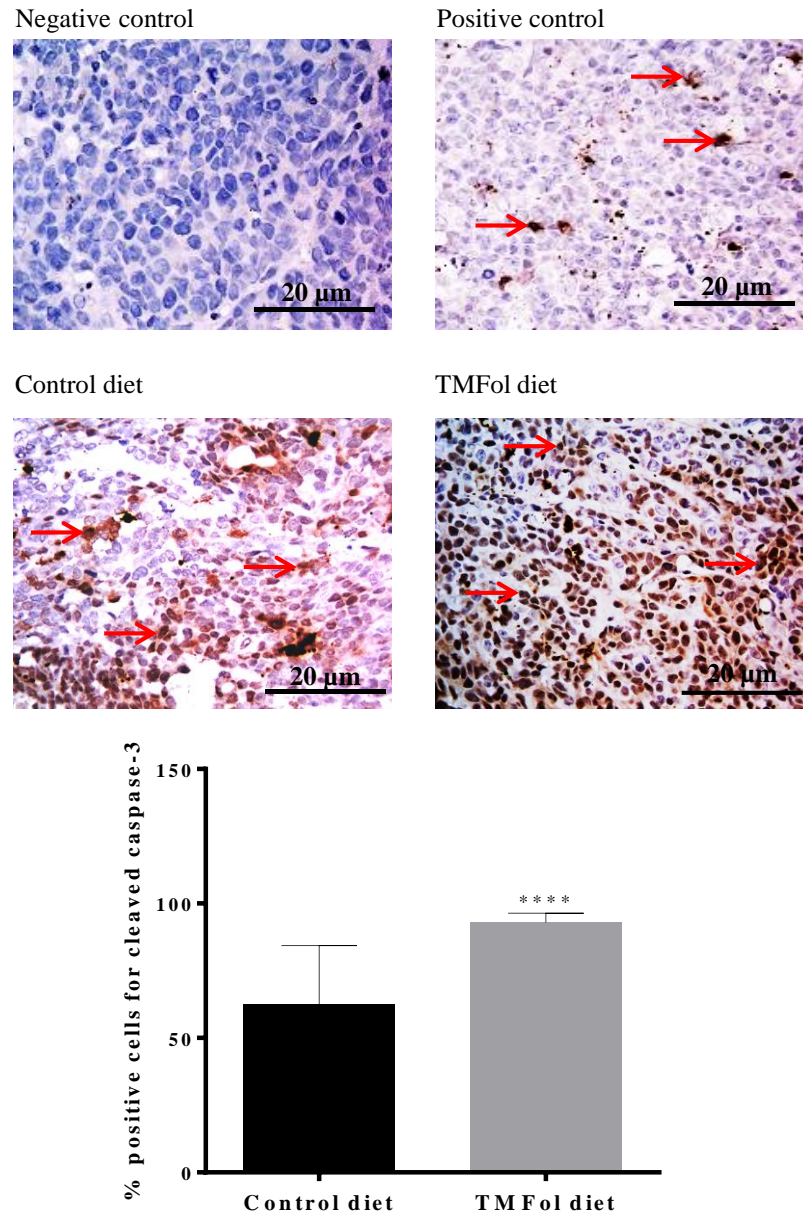
Figure 3.16: Effect of 0.2% TMFol diet on cleaved caspase-3 expression in prostate tumour tissue from mice bearing 22Rv1 tumours. Immunostaining was performed on paraffin-embedded tumour sections (n = 10 mice per group). The photomicrographs are representative of samples from the TMFol-fed and the control-fed groups, along with a positive control (human tonsil) and a negative control (tumour tissue without antibody). The cytoplasmic and perinuclear immunoreactions (brown) were regarded as positive for cleaved caspase-3 (red arrows) and counted at x40 magnification in 10 randomly selected areas in each tumour sample. The bar chart represents the mean of the positively stained cells ± SD as a percentage of the total number of cells. **** indicates data is statistically significant from the control (p < 0.001). Statistical comparision was by Student's T-test.

3.6. Effect of TMFol on senescence in prostate cancer cells

Cellular senescence is a potent anticancer mechanism that indefinitely suppresses the growth of cells (Rodier and Campisi, 2011). In the literature there is limited knowledge available about the effect of flavonoids on the mechanisms of cellular senescence. Of the dietary flavonols, fisetin has been shown to be incapable of inducing cellular senescence in prostate cancer cells (Haddad et al., 2010). As described in section 3.3 above, cell cycle arrest occurred in two of the three cell types, so it was considered worthwhile to assess whether TMFol was able to induce cellular senescence in prostate cancer. The gold standard for detecting cellular senescence is measurement of SA-β-galactosidase activity at pH 6.0. As described in the Methods chapter (section 2.2.7), SA-β-galactosidase activity was determined by fluorescence spectroscopy, by measuring the conversion rate of MUG to its fluorogenic substrate, 4-MU, at pH 6.0.

When the 22Rv1 cells were treated with TMFol (10 μM) there was a significant increase in SA-β-galactosidase activity for all time points (Figure 3.17 A). TMFol caused an 11-30 % increase in SA-β-galactosidase activity over the background levels, with the magnitude of effect increasing with time. PC-3 cells also showed an increase in SA-β-galactosidase activity at all of the time points but it was only statistically significant at 48 h (Figure 3.17 B). In contrast, the PNT2 normal prostate epithelial cells displayed reduced SA-β-galactosidase activity at 48 and 72 h in response to TMFol exposure, with the effect reaching significance at the later time point (Figure 3.17 C). Therefore, TMFol appears to activate cellular senescence at the dose and time points tested in 22Rv1 and PC-3 cancer cells.

Increased levels of p21, p16 and p53 are often observed in cellular senescence (Bernardes de Jesus and Blasco, 2012). Therefore, to further explore the effects of TMFol on pathways involved in cellular senescence in prostate cancer cells, the expression of p21, p16 and p53 were assessed by Western blotting. In 22Rv1 cells there was an increase in both p53 and p21 at the time points indicated in Figure 3.18, supporting the induction of cellular senescence, while there was a decrease in p16 (Figures 3.18 A and B). From the graphs (Figure 3.18 B) it is evident that the expression of p53 in the 22Rv1 cells increased in magnitude from 24 to 72 h, while the expression of p21 reached a maximum of approximately 40% increase at 48h. PC-3

cells lack detectable p53 and p16, and there was generally a decrease in the expression of p21 when compared to the control (Figures 3.18 A and C). PNT2 cells do not express detectable levels of p21 or p16, and the expression of p53 was largely constant, except at 72 h where there was a significant decrease in expression compared to the control (Figures 3.18 A and D).

(A)

(B)

(C)
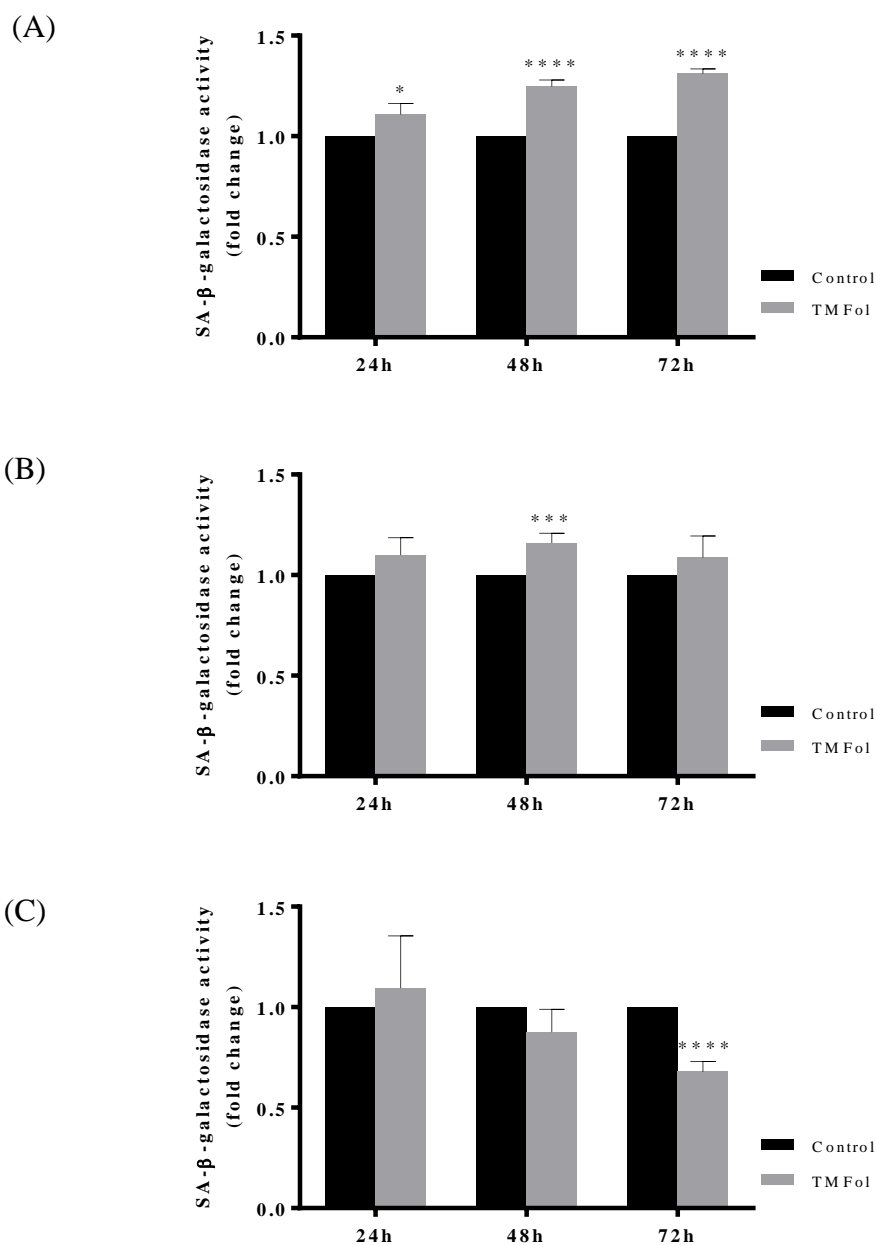
Figure 3.17: Quantitative SA-β-gal activity in 22Rv1 (A), PC-3 (B) and PNT2 (C) cells following exposure to 10 μM TMFol. After treatment (24, 48 or 72 h) the cell lysates were incubated with MUG fluorogenic substrate and the fluorescence intensity of the product, 4-MU, was determined. Readings were normalised for protein concentration and expressed as fold change compared to vehicle control. Each column represents SA-β-gal activity as the mean of the fold change ± SD of three independent experiments. Statistical comparison between the control and TMFol treatment was by Student's T-test. Statistically significant differences are indicated as * ($p < 0.05$), *** ($p < 0.005$) and **** ($p < 0.001$).
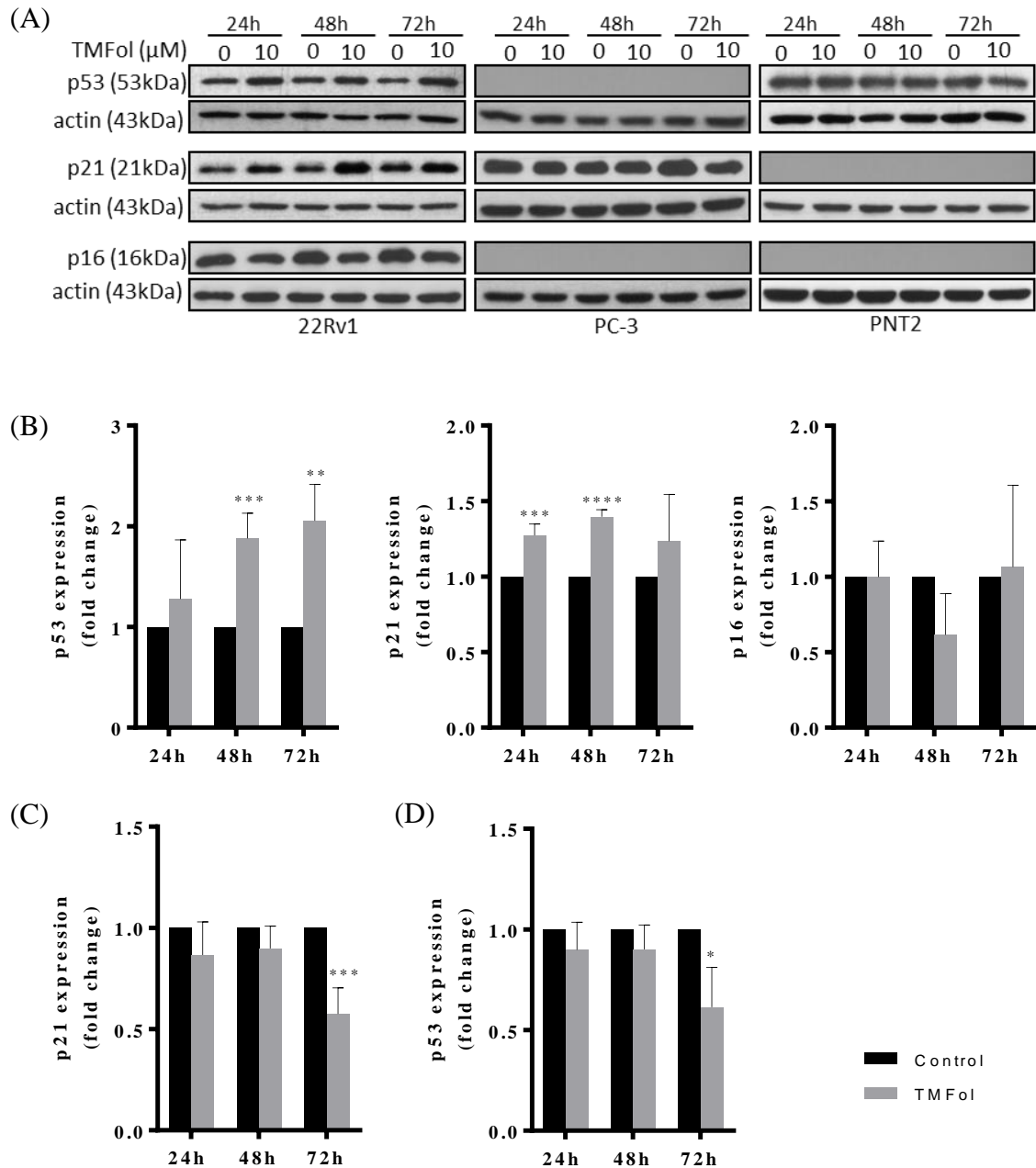
Figure 3.18: Expression of senescence biomarkers p53, p21 and p16 in 22Rv1, PC-3 and PNT2 cells following exposure to 10 μM TMFol. Representative western blots (**A**) showing the expression in all the cell lines while the graphs show the expression of p53, p21 and p16 in 22Rv1 cells (**B**), p21 in PC-3 cells (**C**) and p53 in PNT2 cells (**D**). Each graph is based on densitometric analysis of Western blots after normalisation to actin. Each column represents mean ± SD of three independent experiments. Statistical comparison between the control and TMFol treatment was by Student's T-test. Statistically significant differences are indicated as * (p< 0.05), ** (p< 0.01), *** (p< 0.005) and **** (p< 0.001).

3.7. Discussion

The primary focus of the work described in this chapter was to identify the potential mechanisms engaged by TMFol to inhibit the growth of prostate cancer cells. To facilitate this process it was necessary to evaluate the effects of TMFol in both prostate cancer cell lines, 22Rv1 and PC-3, and normal prostatic epithelial cells, PNT2. All cell types showed sensitivity to the growth inhibitory effects of TMFol with IC_{50} values in the low micromolar range (Figures 3.1, 3.2 and 3.3) and within the concentration range previously shown to be achievable in the prostate tissue of mice by Saad *et al*, 2012. A desirable feature of a chemopreventive /chemotherapeutic agent would be to inhibit and eliminate the growth of premalignant/malignant cells with little to no negative effect on the healthy cells. The ability of TMFol to exert a growth inhibitory effect on the normal prostate epithelial cells at such low concentrations may create doubt as to the potential usefulness of TMFol in the management of prostate cancer. However, the growth inhibitory effect on the normal prostate epithelial cells may have some clinical relevance since TMFol could reduce the cell turnover in the prostate, making it less likely for the development of benign prostatic hyperplasia and ultimately preventing the initiation of prostate cancer (Pannek et al., 1999). Additionally, to date TMFol has not been shown to cause any signs of toxicity in medium term mouse studies (Howells et al., 2010; Saad, 2011).

It is well documented that flavonoids can cause apoptosis in prostate cancer cell lines, but in this study FACS analysis revealed there was no induction of apoptosis by TMFol in the prostate cancer cells or normal prostate cells *in vitro* (Figures 3.10–3.15). However a 0.2 % TMFol diet triggered a 1.5–fold increase in apoptosis in 22Rv1 xenografts, as measured by cleaved caspase-3 expression (Figure 3.16). While there is no precedence in the literature for this differential induction of apoptosis by flavonoids, there is evidence of this type of contrasting response, as the mTOR inhibitor temsirolimus (CCI – 779) is a chemotherapeutic agent capable of inducing apoptosis in multiple myeloma – bearing mice *in vivo* but not in myeloma cells *in vitro* (Frost et al., 2004). Unlike the cell line model, there are more options in the *in vivo* environment for complex interactions with TMFol that could stimulate the induction of apoptosis. The repeated daily dosing and longer exposure time to TMFol in the *in vivo* study, which lasted for a maximum of about 7 weeks, could be a significant factor in triggering

apoptosis. Additionally, in the animals on the control diet there was a high level of cleaved caspase-3 staining (62 %, Figure 3.16), suggesting that the tumours had a relatively high sensitivity to apoptosis, which was further induced when exposed to TMFol. Anti-angiogenic compounds have been found to induce apoptosis in prostate cancer (Huss et al., 2003) and quercetin is capable of inhibiting angiogenesis in prostate cancer cells (Pratheeshkumar et al., 2012). Therefore, one could speculate that in the 22Rv1 xenograft mice that TMFol, a congener of quercetin, could potentially inhibit angiogenesis and induced the apoptosis observed.

As previously demonstrated by Saad (2011), cell cycle analysis confirmed the significant accumulation of PC-3 cells in the S phase, following 48 h exposure to TMFol. Furthermore, this current study demonstrated that the S phase arrest was sustained at the 72 h time point (Figures 3.6 and 3.7). In the PNT 2 cells TMFol caused G1 phase arrest within 24 h, but further exposure at 48 and 72 h resulted in a significant S phase arrest (Figures 3.8 and 3.9). It is unknown at this point if the dramatic accumulation of PNT2 cells in S phase at 72 h was sustained beyond that time point. The effect of TMFol on the expression of cell cycle checkpoint proteins was not assessed in this study so the biological pathways responsible for S phase arrest in the PC-3 and PNT2 cells are currently unknown. However, it could be assumed that different pathways are involved as the two cell types display distinct biological features that could impact on the cell cycle process. The most notable difference is the absence of the cell cycle regulator, p53, in the PC-3 cells (Figure 3.18). The lack of cell cycle arrest in the 22Rv1 cells throughout the study time points may be attributed to the slower growth rate of the 22Rv1 cells. These cells have a population doubling time of about 40 hours and so would have completed approximately 2 cell cycles, rather than the 3 completed by the other cell lines, during the 72 h exposure time to TMFol. Therefore, the marginal increase in the percentage of cells in G2/M with the corresponding decrease in the percentage of cells in both S and G1 phases at 72 h (Figures 3.4 and 3.5) could be an early indicator of a possible G2/M arrest if exposure to TMFol were to be extended beyond 72 h.

The induction of cellular senescence is an important anticancer mechanism as it limits the proliferative ability of cells (Ewald et al., 2010; Rodier and Campisi, 2011). The role of senescence in the growth inhibitory effect of dietary flavonoids and their

synthetic derivatives on prostate cancer cells has not been well elucidated. This study demonstrates a significant increase in SA-β-galactosidase activity in the prostate cancer cells, 22Rv1 and PC-3 upon treatment with 10 µM TMFol (Figure 3.17), indicating that TMFol is capable of inducing senescence. Furthermore, the induction of senescence was associated with increased expression of p53 and p21 in the 22Rv1 cells (Figure 3.18). It must be noted here that despite the evidence for senescence in the 22Rv1 cells as a result of TMFol intervention, there was no evidence of cell cycle arrest in these cells for the same time period. While the increase in expression of the senescence biomarkers p53, p21 and p16 can act as confirmation of senescence, Prieur *et al* (2011) recently demonstrated the lack of involvement of p53, p21 and p16 in the induction of senescence *in vitro* despite the increase in expression of these proteins. Additionally, the group observed that p21 and p16 accumulated mainly in the cytoplasm of the cells, suggesting that the induction of these proteins was not involved in regulation of the cell cycle. Therefore, additional confirmatory test for senescence, for example, the formation of senescence-associated heterochromatic foci (SAHF) would be required. As a consequence, it is difficult to interpret the increase in SA-β-galactosidase activity in PC-3 cells as definitive proof of senescence. The PC-3 cells lack p53 and p16 expression (Jarrard et al., 1999), hence TMFol induced senescence would be independent of these proteins, but as for the 22Rv1 cells it would be best to confirm senescence independently by assessing the formation of SAHF. Interestingly, in the PNT2 cells there was a downward trend in the SA-β-galactosidase activity, significant at 72 h only. Given the fact that TMFol was capable of inhibiting the growth and stimulating S phase arrest of PNT2 cells, the relevance of this decrease in SA-β-galactosidase activity is currently unknown.

Taken together, the growth inhibitory effect of TMFol on prostate cancer cells can be partially explained by cell cycle arrest. Potentially, the induction of senescence may contribute to growth inhibition but as indicated earlier, further experiments are required for verification. TMFol is also capable of causing apoptosis but this was only observed in the *in vivo* environment. Other mechanisms of action are likely to be involved; hence, the effects of TMFol on the metabolic profiles of these cells were assessed and are presented in the following chapter.

Chapter 4. Investigation of the effects of TMFol on prostate cancer metabolism

4.1. Introduction

Understanding the role of an altered metabolism in the pathogenesis of prostate cancer offers the possibility of utilising chemopreventive/chemotherapeutic agents to modulate features of prostate cancer metabolism that can attenuate cancer progression. As described earlier in the Introduction chapter, alterations in pyruvate, citrate and fatty acid metabolic pathways have been implicated in the progression of prostate cancer (Costello et al., 1999; Lexander et al., 2005 and Rossi et al., 2003). Therefore, in this chapter, a range of biochemical assays, qPCR and Western blots were used to assess the ability of TMFol to alter the expression and activity of metabolic proteins that may play a role in the development and progression of prostate cancer.

4.2. Effect of TMFol on the expression of selected Krebs cycle proteins in prostate cancer cells

Malignant transformation of the prostate glandular epithelial cells is accompanied by an increase in activity of the Krebs cycle (Dakubo et al., 2006). As previously mentioned in the Introduction chapter, unpublished mass spectrometry-based proteomic analysis of 22Rv1 xenografts treated with TMFol showed that several Krebs cycle proteins were significantly differentially expressed compared to levels in tumours arising in untreated control mice. Included among these proteins were ACO2, dihydrolipoyl succinyltransferase (DLST), fumarate hydratase (FH), phosphoenolpyruvate carboxykinase (PEPCK), succinate dehydrogenase flavoprotein subunit A (SDHA) and succinate-Co A ligase, α subunit (SUCLG1) (Norris *et al.* unpublished data). Whole cell lysates from the prostate cancer cell lines, 22Rv1 and PC-3 treated with 10 μM TMFol for 24, 48 and 72 h were analysed by Western blotting to determine the expression of the above-mentioned Krebs cycle proteins. This was to gain insight into how TMFol may be modulating the Krebs cycle to inhibit prostate cancer growth. Furthermore, tumour lysates from the 22Rv1 xenografts were made available in this current study for Western blot analysis to facilitate a comparison between the *in vitro* and *in vivo* data.

In the 22Rv1 cells treated with TMFol, there was a significant decrease in ACO2 expression at 24 and 48 h (Figure 4.1 A). The expression was approximately 16 % less than the expression in the control cell population. The expression of FH was significantly increased at 72 h (Figure 4.1 C), while the expressions of DLST and SDHA remained mostly unchanged in the 22Rv1 cells (Figures 4.1 B and E). PEPCK was significantly upregulated at 48 h (Figure 4.1 D) while SUCLG1 was significantly downregulated at 72 h (Figure 4.1 F).

The changes in expression of the above-mentioned Krebs cycle proteins were more pronounced in the PC-3 cells when compared to those in the 22Rv1 cells. There was a significant decrease in the expression of ACO2 at all of the time points (Figure 4.2 A). The downregulation was time-dependent, ranging from approximately 19 % at 24 h to 70 % at 72 h less than the expression in the control cell population. This downregulation by far exceeds that observed in the 22Rv1 cells (Figure 4.1 A). There was a time-dependent decrease in DLST expression in the PC-3 cells, becoming

significant at 48 and 72 h (Figure 4.2 B). A change in FH expression was only evident at 72 h and this was a significant downregulation (Figure 4.2 C), which is opposite to the effects observed on the expression of this protein in 22Rv1 cells (Figure 4.1 C). Similar to the 22Rv1 cells, PC-3 cells, in response to 10 μM TMFol, showed an increase in PEPCK expression at 48 h, but in the case of PC-3 cells, the expression was not statistically significant (Figure 4.2 D). SDHA expression was upregulated at all the time points, and was approximately 40 % higher than the control cells (Figure 4.2 E). SUCLG1 expression was significantly decreased at 72 h only in the PC-3 cells (Figure 4.2 F), a pattern of expression previously observed in the 22Rv1 cells (Figure 4.1 F).
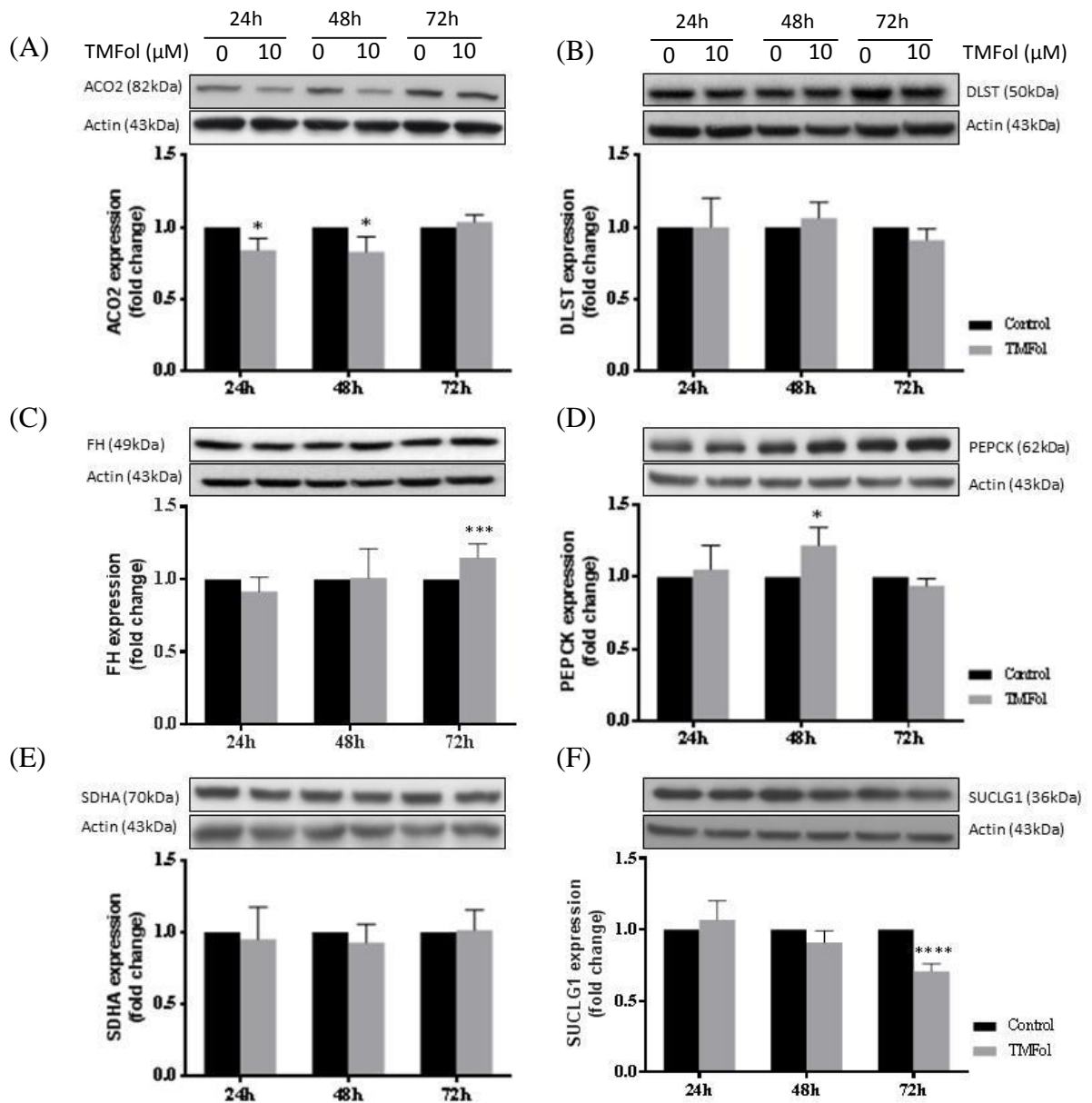
Figure 4.1: Expression of Krebs cycle related proteins in 22Rv1 cells treated with 10 µM TMFol. The expression of ACO2 (**A**), DLST (**B**), FH (**C**), PEPCK (**D**), SDHA (**E**) and SUCLG1 (**F**) was analysed by Western blotting. Each graph is based on densitometric analysis of Western blots after normalisation to actin. Each column represents mean ± SD of three independent experiments. Statistical comparison between the control and TMFol treatment was by Student's T-test. Statistically significant differences are indicated as * (p< 0.05), *** (p< 0.005) and **** (p< 0.001).
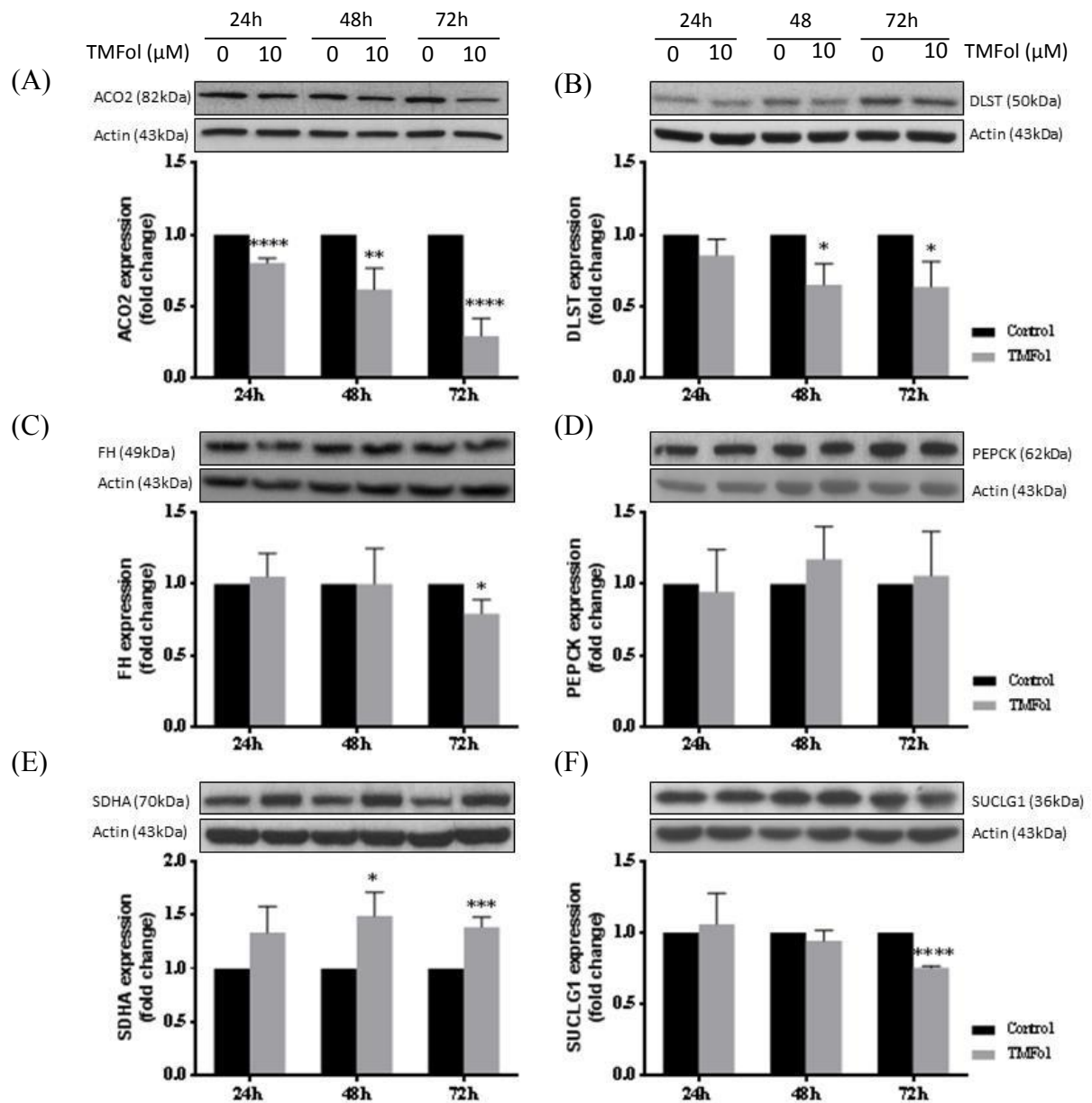
Figure 4.2: Expression of Krebs cycle related proteins in PC-3 cells treated with 10 μM TMFol. The expression of ACO2 (**A**), DLST (**B**), FH (**C**), PEPCK (**D**), SDHA (**E**) and SUCLG1 (**F**) was analysed by Western blotting. Each graph is based on densitometric analysis of Western blots after normalisation to actin. Each column represents mean ± SD of three independent experiments. Statistical comparison between the control and TMFol treatment was by Student's T-test. Statistically significant differences are indicated as * (p< 0.05), ** (p< 0.01), *** (p< 0.005) and **** (p< 0.001).

The availability of the tumour lysates from the 22Rv1 xenografts provided the opportunity to assess the *in vivo* expression of the Krebs cycle proteins of interest and compare the expression to the 22Rv1 *in vitro* analysis. The expression levels of DLST and FH were significantly increased in the 22Rv1 tumour xenografts taken from mice on the TMFol diet compared to the control (Figure 4.3). For the remaining proteins, there was a non-significant decrease in the expression of ACO2, PEPCK and SDHA, while SUCLG1 showed a negligible increase (Figure 4.3). FH was the only protein that was significantly increased in the xenografts and the 22Rv1 cell lines, while ACO2 was decreased in both, albeit in a non-significant way in the xenografts. Although there were contrasting changes in the expression of some of the Krebs cycle proteins, both *in vitro* and *in vivo* data suggest that TMFol is capable of modulating metabolic pathways in prostate cancer models.
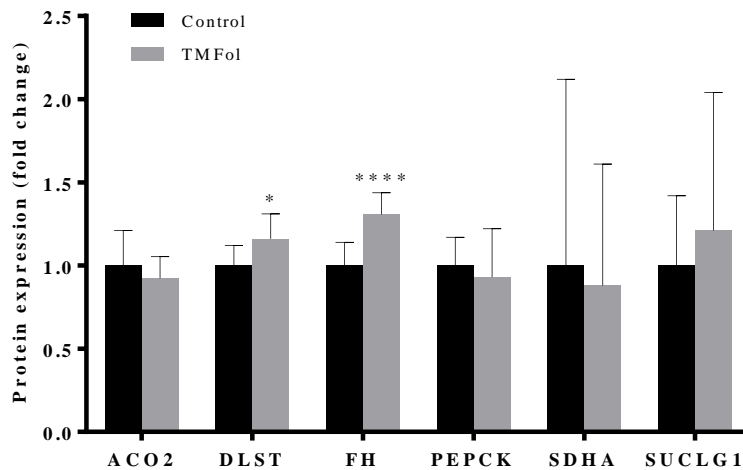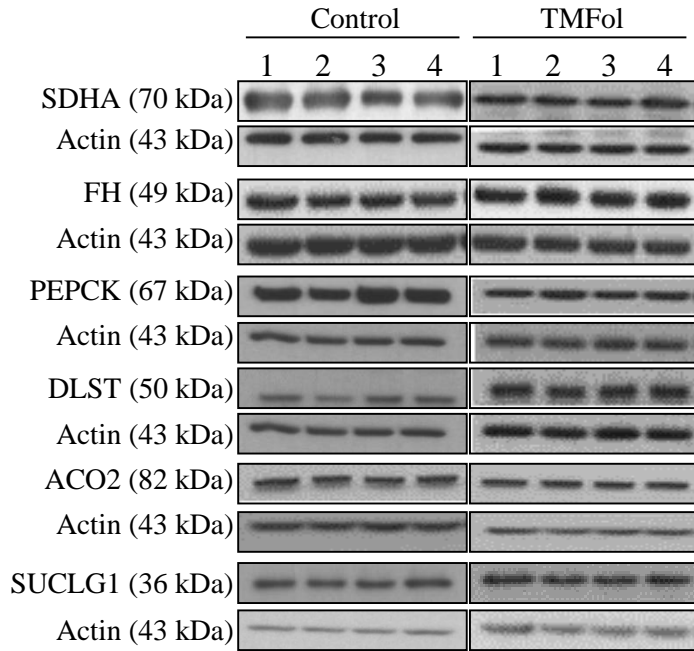
Figure 4.3: Expression of Krebs cycle related proteins in tumour lysates from 22Rv1 xenograft mice on either a control or 0.2% TMFol-containing diet. Analysis was by Western blotting. The blots illustrate representative results for randomly selected tumour lysates from 4 mice per treatment group. The graph is based on densitometric analysis of Western blots after normalisation to actin. Each column represents the mean ± SD for each animal group (n = 13 mice for control and n = 15 for TMFol). Statistical comparison between the control and TMFol treatment was by Student's T-test. Statistically significant differences are indicated as * (p< 0.05) and **** (p< 0.001).

4.3. Effect of TMFol on citrate oxidation in prostate cancer cells

From the Western blot analysis for the Krebs cycle proteins of interest in the 22Rv1 cells, PC-3 cells and 22Rv1 xenograft tumours, ACO2 emerged as the protein that was consistently decreased. ACO2 plays a highly critical role in the development and progression of prostate cancer. ACO2 is required for citrate oxidation as it regulates the entry of citrate into the Krebs cycle. Often the levels of ACO2 remain unchanged in the normal and malignant prostate but the activity of ACO2 is higher in prostate cancer (Costello et al., 1996; Liu et al., 1996; Singh et al., 2006). Given the importance of ACO2 in prostate cancer pathogenesis and the evidence that TMFol is capable of modulating ACO2 in a manner that could inhibit the progression of the disease, it was selected for further investigation. To ascertain whether the effects observed in the 22Rv1 and PC-3 models translate to normal prostate cells the expression of ACO2 in PNT2 cells following TMFol intervention was determined. Furthermore, the mitochondria were isolated from 22Rv1, PC-3 and PNT2 cells treated with TMFol for 24 h and used to determine the level of ACO2 activity within these cells. At 24 h the expression of ACO2 was significantly lower than that of the control in all three cell lines, but still high to facilitate the detection of ACO2 activity. At longer time points the expression of ACO2 could potentially be too low to be detected by the activity assay.

In the PNT2 cells, ACO2 expression was significantly downregulated at all the time points (Figure 4.4). The expression was reduced to approximately 62-81 % of the control levels. To ensure that the aconitase activity was due to ACO2 and not influenced by the aconitase activity of IRP-1, which is cytosol specific, the purity of the mitochondrial fraction isolated was determined. For all three cell lines the VDAC indicated that the mitochondria were confined to the mitochondrial fractions obtained from the differential centrifugation (Figure 4.5). However, the faint protein bands for LDHA in the mitochondrial fractions suggested that there were some cytosolic components within the mitochondrial fractions. Therefore, the fractions were checked to determine if IRP-1 proteins were among the contaminating cytosolic components. In the 22Rv1 cells there was no IRP-1 detected in the mitochondrial fractions but there were weak bands observed in the mitochondrial fractions of the PC-3 and PNT2 cells, making it possible for IRP-1 to contribute to a small percentage of the aconitase activity

measured in the mitochondria of PC-3 and PNT2 cells. ACO2 activity was found to be 53 %, 72 % and 68 % of the control in the mitochondria of 22Rv1, PC-3 and PNT2 cells, respectively, and significantly lower than the control for each cell line (Figure 4.6). Therefore, TMFol had the greatest effect on ACO2 activity in the 22Rv1 cells.
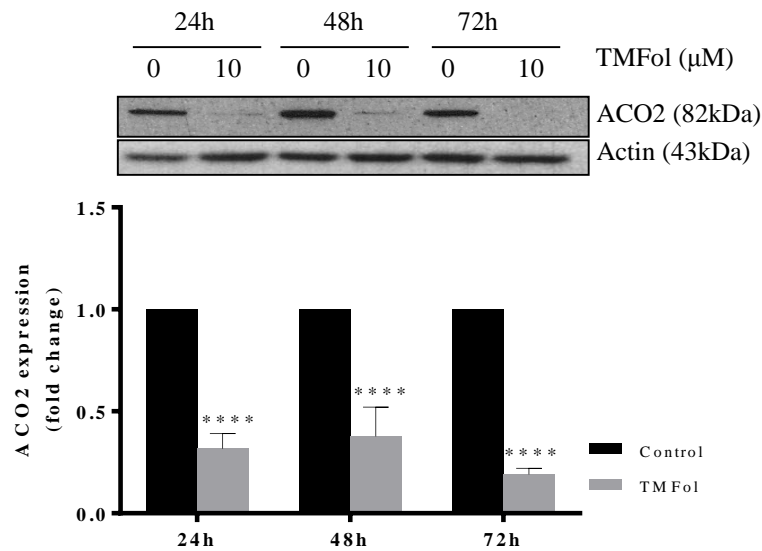
Figure 4.4: Expression of ACO2 in PNT2 cells following exposure to 10 μM TMFol. Analysis was by Western blotting and the blots shown are representative results. The graph is based on densitometric analysis of Western blots after normalisation to actin. Each column represents the mean ± SD of three independent experiments. Statistical comparison between the control and TMFol treatment was by Student's T-test. Statistically significant differences are indicated as **** (p< 0.001).
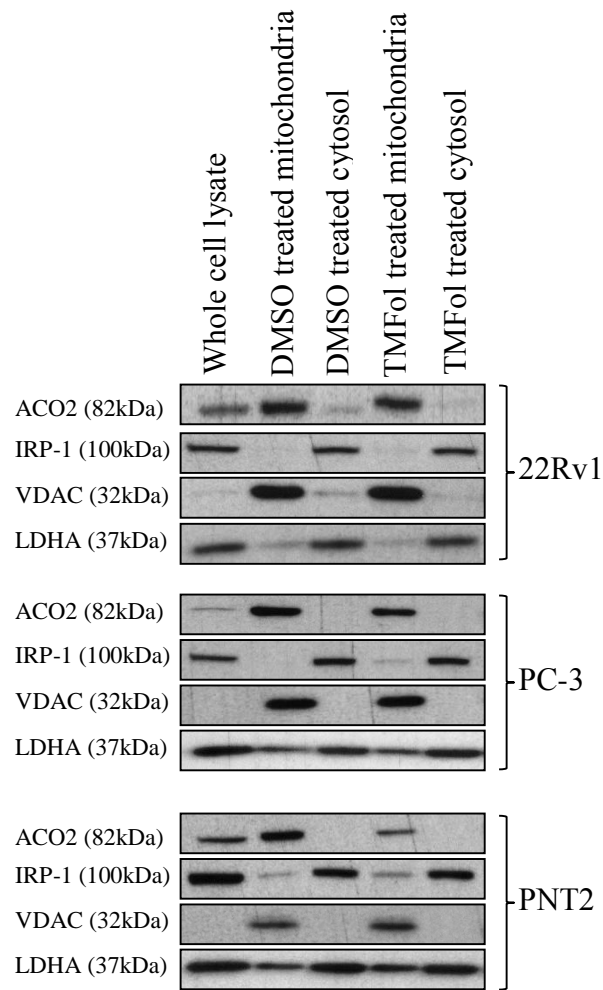
Figure 4.5: Protein components of mitochondrial and cytosolic fractions from 22Rv1, PC-3 and PNT2 cells treated with 10 μM TMFol or DMSO alone (vehicle control) for 24 h. Validation of the purity of the mitochondrial fraction was by Western blotting analysis. Antibodies for ACO2 and VDAC were used to detect the mitochondrial fraction while antibodies for IRP-1 and LDHA were used to detect the cytosolic fraction.
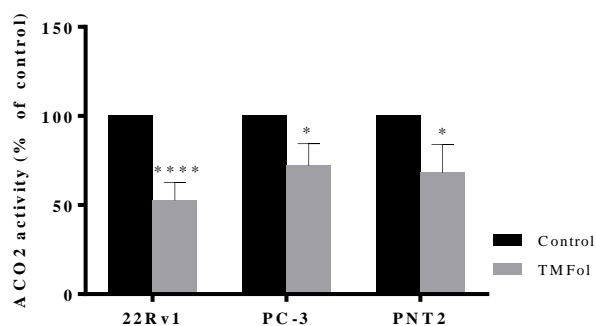
Figure 4.6: Effect of TMFol on ACO2 activity in the mitochondrial fraction of 22Rv1, PC-3 and PNT2 cells following treatment with 10 µM TMFol or DMSO alone (vehicle control) for 24h. The mitochondria were isolated and the activity of ACO2 was determined by measuring the formation of isocitrate from citrate using a colorimetric assay. The activity was recorded as a percentage of the control. Each column represents the mean ± SD of three independent experiments. Statistical comparison between the control and TMFol treatment was by Student's T-test. Statistically significant differences are indicated as * ($p < 0.05$) and **** ($p < 0.001$).

4.4. Effect of TMFol on pyruvate metabolism in prostate cancer

Pyruvate is critical to operation of the Krebs cycle and pyruvate dehydrogenase (PDH) is the key enzyme in pyruvate metabolism that tends to be over-expressed in prostate cancer (Lexander et al., 2005). PDH catalyses the irreversible oxidative decarboxylation of pyruvate to acetyl-CoA (Patel and Korotchkina, 2006; Vander Heiden et al., 2009). During this reaction the E1 component of PDH (PDH-E1) transfers acetate from pyruvate to the E2 subunit of PDH (PDC-E2), which then transfers it to coenzyme A, ultimately converting pyruvate to acetyl-CoA (Chueh et al., 2011). Therefore, the aim was to determine if TMFol could modulate PDH expression and activity by assessing its influence on the expression of PDH components. TMFol had no effect on PDH-E1α expression (Figure 4.7) but caused a significant upregulation in the expression of PDC-E2 for all three cell lines at 24 and 48 h (Figure 4.7). In 22Rv1 cells, PDC-E2 expression was approximately 280 % higher than the expression in the control cells at 24 and 48 h (Figure 4.7 A). There was a time-dependent increase in PDC-E2 expression in PC-3 and PNT2 cells between 24 and 48 h. The change in PDC-E2 expression in the PC-3 cells far exceeded that occurring in PNT2 cells at all of the time points. Generally, the rank order of PDC-E2 expression was 22Rv1 > PC-3 > PNT2 cells, for 24 and 48 h.
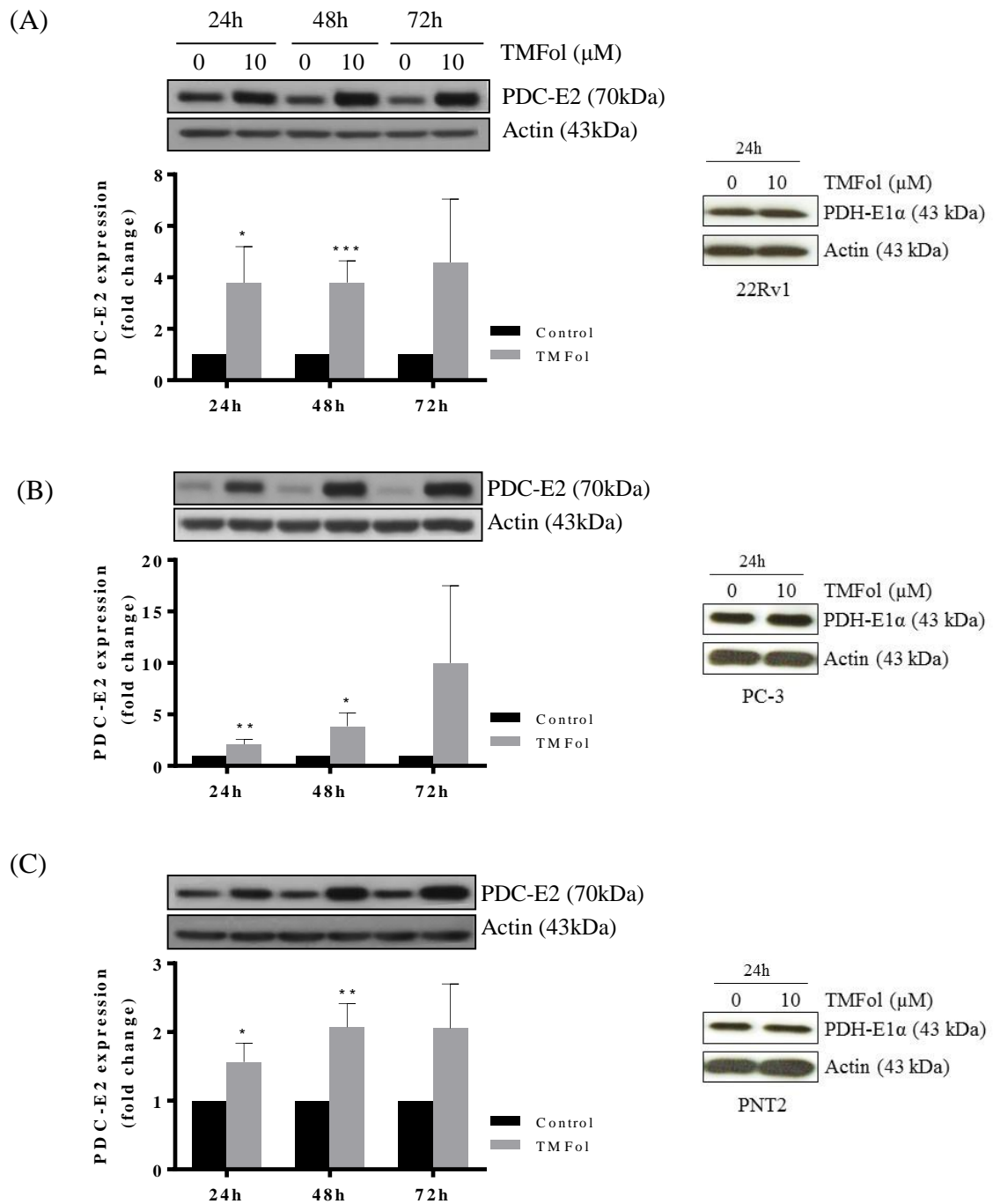
Figure 4.7: Expression of PDC-E2 and PDH-E1α in 22Rv1 (A), PC-3 (B) and PNT2 (C) cells following exposure to 10 μM TMFol or DMSO (vehicle control) only. Analysis was by Western blotting and representative blots are shown for each cell line. The graphs are based on densitometric analysis of Western blots after normalisation to actin and represent the mean ± SD of three independent experiments. Statistical comparison between the control and TMFol treatment was by Student's T-test. Statistically significant differences are indicated as * (p< 0.05), ** (p< 0.01) and *** (p< 0.005).

Given the dramatic increase in PDC-E2 expression, it was thought that the glucose concentration in the culture medium could have influenced the effect of TMFol on PDC-E2 expression. High glucose levels can cause an upregulation in PDH activity (Harris et al., 2002). Therefore, to test this hypothesis, 22Rv1 cells were exposed to 10 μM TMFol or DMSO alone for 24 h in medium consisting of 0, 5 and 11 mM glucose. 11 mM is the concentration of glucose in the standard RPMI-1640 growth medium used in all the cell culture experiments throughout this study. In all medium, PDC-E2 expression was still significantly higher in TMFol-treated cells compared to control cells in the same growth medium (Figure 4.8). However, a comparison across the various growth media indicated a non-significant difference in PDC-E2 expression. Therefore, the level of glucose in the growth medium had no direct influence on PDC-E2 expression.
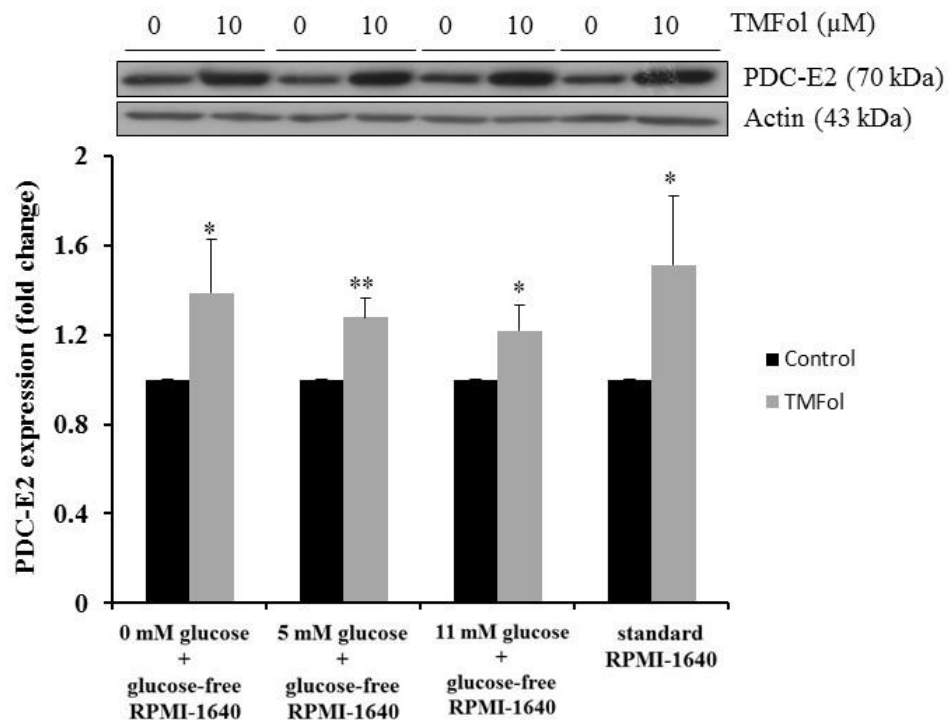
Figure 4.8: Expression of PDC-E2 in 22Rv1 cells following exposure to 10 μM TMFol or DMSO (vehicle control) only, in growth medium with varying glucose concentrations for 24 h. Analysis was by Western blotting and representative blots are shown. The graph is based on densitometric analysis of Western blots after normalisation to actin and represents the mean ± SD of three independent experiments. Statistical comparison between the control and TMFol treatment was by Student's T-test. Statistically significant differences are indicated as * ($p < 0.05$).

PDC-E2 is the core catalytic component of PDH. Therefore, to determine if the activity of PDH was altered by upregulation of PDC-E2, the PDH protein in whole cell lysates from treated and control cells were used in an activity assay. There was a trend towards decreased PDH activity in both 22Rv1 and PC-3 cells at 24 h, but this was not statistically significant (Figure 4.9). The level of PDH activity in the normal cells, PNT2, was not detectable within the limits of the activity assay; therefore, these data are not shown.
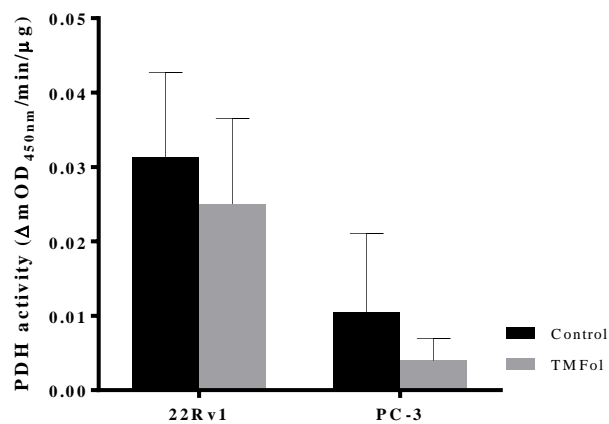
Figure 4.9: Pyruvate dehydrogenase activity in 22Rv1 and PC-3 prostate cancer cells following exposure to 10 μM TMFol or DMSO (vehicle control) only for 24 h. The PDH enzyme in the lysates was immunocaptured in the microplate wells by adding fixed concentrations of whole cell lysates to microplate wells pre-bound with an anti-PDH monoclonal antibody for 3 h. PDH activity was determined by following the reduction of NAD+ to NADH, which was coupled to the reduction of a reporter dye to produce a yellow product that was monitored by measuring kinetic absorbance at 450 nm. PDH activity was recorded as the change in OD per minute per μg of PDH. Each column represents the mean ± SD of three independent experiments. Statistical comparison was by Student's T-test and no significant differences were detected.

4.5. Effect of TMFol on fatty acid synthesis in prostate cancer

Thus far, TMFol has demonstrated its ability to differentially alter the expression of metabolic proteins in a manner that potentially inhibits the development and progression of prostate cancer. Since fatty acid synthesis is often de-regulated in prostate cancer, the effect of TMFol on this metabolic pathway was assessed by first determining the effect of TMFol on ACLY expression. In 22Rv1 cells, there was a time-dependent increase in ACLY expression, which was statistically significant at 24 and 48 h (Figure 4.10 A). In contrast, there was a non-significant decrease in ACLY expression at all of the time points (Figure 4.10 B). No measurable expression of ACLY was detected in the PNT2 cells.

As previously described in the Introduction chapter, AMPK has a major influence on fatty acid metabolism (Luo et al., 2010), therefore, the effect of TMFol on the level of activated AMPKα (pAMPKα) was assessed. There was only a non-significant small increase in pAMPKα at 72 h in 22Rv1 cells (Figure 4.11 A and B). In PC-3 cells the level of pAMPKα was significantly increased by 2-3 fold, relative to the solvent control (Figure 4.11 A and C). No measurable pAMPKα was detected in the PNT2 cells and the total AMPKα protein levels remained relatively unchanged for all cell lines (Figure 4.11 A).

pAMPKα directly phosphorylates ACC on Ser 79 leading to its inactivation (Park et al., 2009), meaning that an increase in phosphorylated ACC (pACC) is indicative of AMPK activation. Therefore, the level of pACC in response to TMFol intervention was assessed. In the 22Rv1 cells there was only a non-significant increase in pACC at 48 and 72 h, while ACC remained relatively unchanged (Figure 3.27 A). The PC-3 cells at 24 h showed a significant increase in pACC but eventually at 72 h, the level of pACC was significantly decreased compared to the control. Interestingly, the total protein levels of ACC were significantly altered in a manner that mimicked the changes in pACC at corresponding time-points (Figure 4.12 B). For the PNT2 cells, both pACC and ACC were altered in a similar manner, showing a significant decrease at 72 h (Figure 4.12 C). Any alteration in the total protein could be responsible for the change

in levels of the phosphorylated protein, so the ratio of pACC to ACC was also determined. The subsequent 1:1 ratio that was obtained indicated that there was no true change in the phosphorylation state of ACC, so the levels of pACC only changed because the levels of the total protein changed. Therefore, TMFol may be engaging other mechanisms to induce the alterations observed in ACC expression.

(A)

(B)
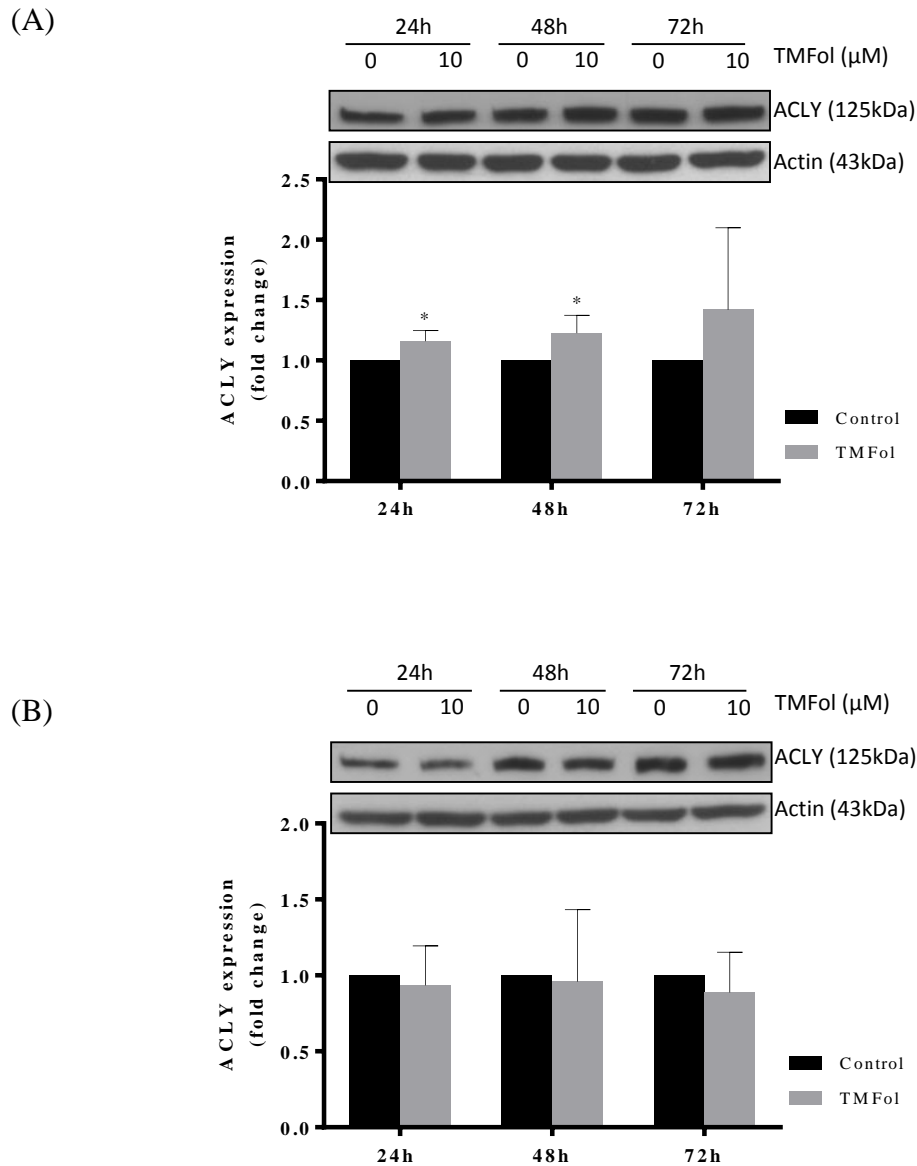
Figure 4.10: Expression of ACLY in 22Rv1 (A) and PC-3 (B) cells following exposure to 10 μM TMFol or DMSO (vehicle control) only. Analysis was by Western blotting and representative blots are shown for each cell line. The graphs are based on densitometric analysis of Western blots after normalisation to actin and represent the mean ± SD of three independent experiments. Statistical comparison between the control and TMFol treatment was by Student's T-test. Statistically significant differences are indicated as * ($p < 0.05$).

(A)

	24h	48h	72h	24h	48h	72h	24h	48h	72h
TMFol (µM) 0 10 0 10 0 10 | 0 10 0 10 0 10 | 0 10 0 10 0 10

pAMPKα (62kDa)

Actin (43kDa)

AMPKα (62kDa)

Actin (43kDa)

22Rv1   PC-3   PNT2

(B)

(C)
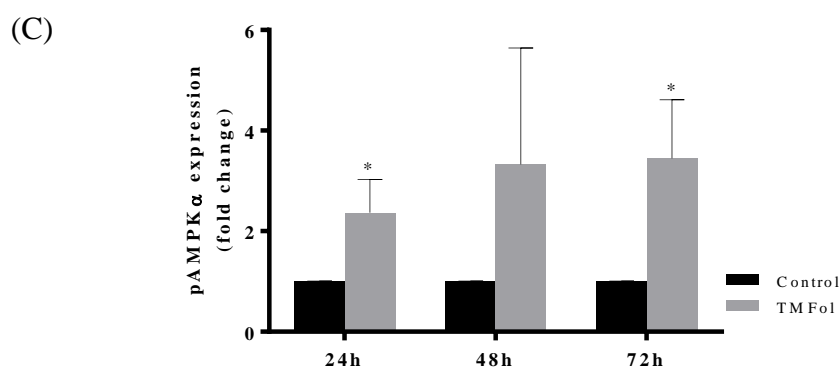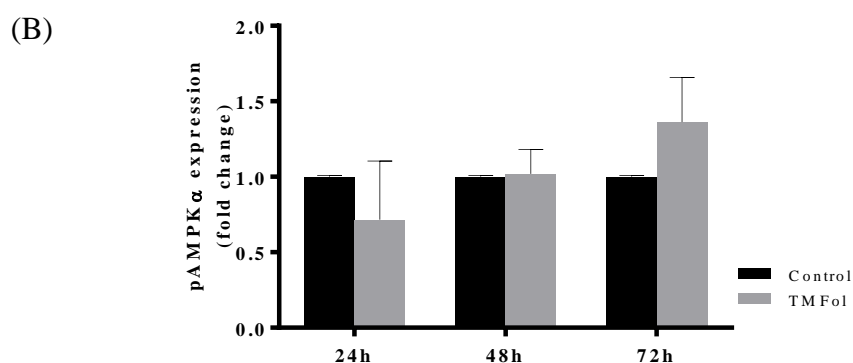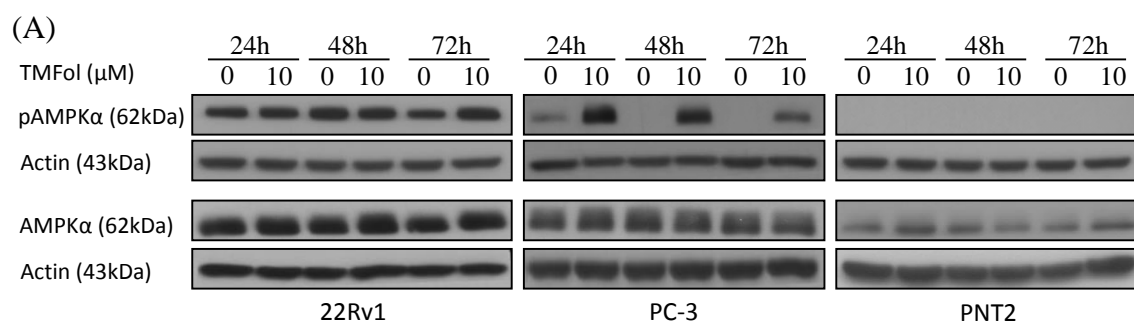
Figure 4.11: Expression of pAMPKα and AMPKα in 22Rv1, PC-3 and PNT2 cells following exposure to 10µM TMFol or DMSO only (solvent control). Analysis was by Western blotting and representative blots are shown for each cell line (A). The graphs show the fold change of pAMPKα in 22Rv1 (B) and PC-3 (C) cells. The graphs are based on densitometric analysis of Western blots after normalisation to actin. Each column represents mean ± SD of three independent experiments. Statistical comparison between the control and TMFol treatment was by Student's T-test. Statistically significant differences are indicated as * (p< 0.05).
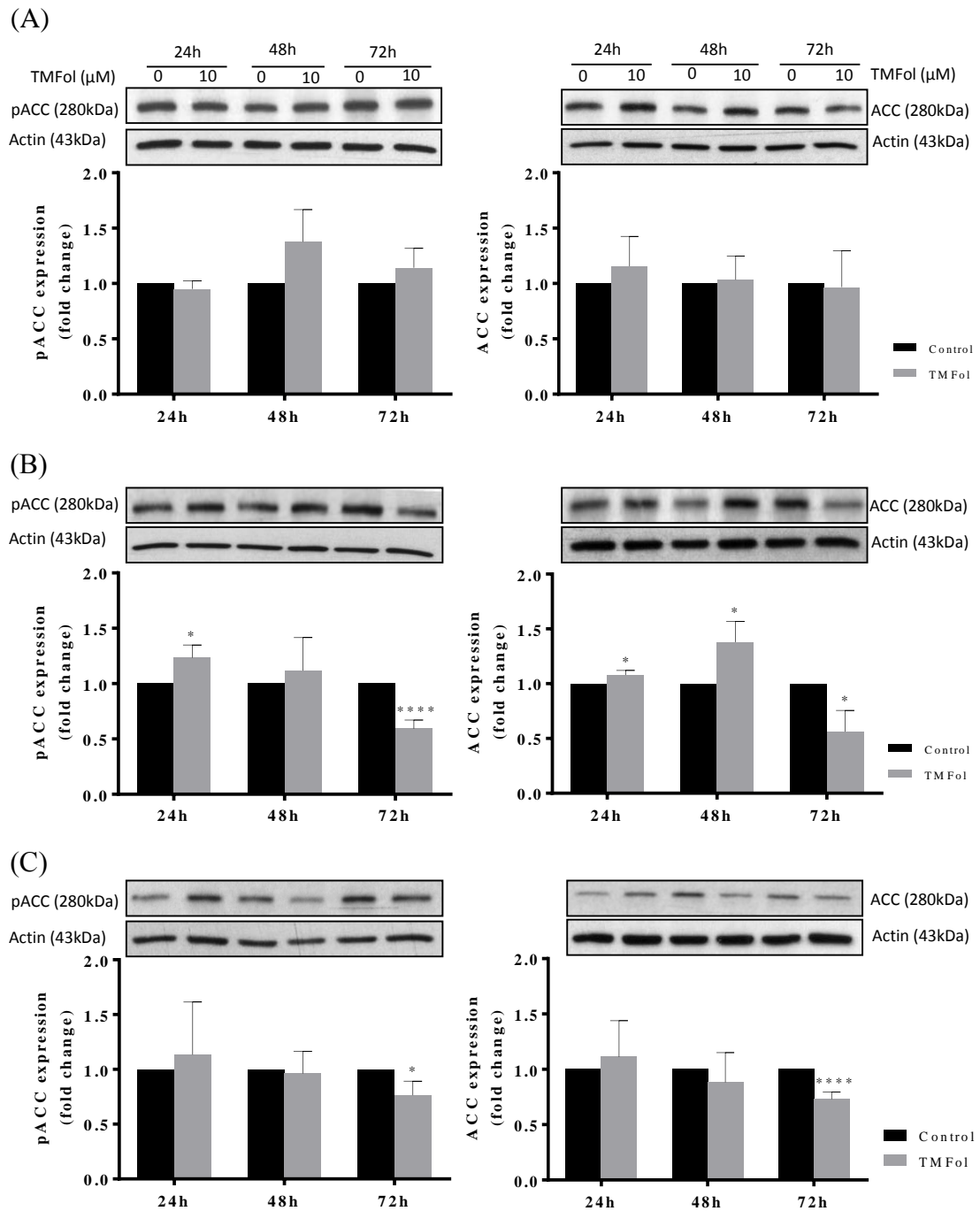
Figure 4.12: Levels of pACC and ACC in 22Rv1 (A), PC-3 (B) and PNT2 (C) cells following exposure to 10µM TMFol or DMSO only (solvent control). Analysis was by Western blotting and representative blots are shown. The graphs are based on densitometric analysis of Western blots after normalisation to actin. Each column represents mean ± SD of three independent experiments. Statistical comparison between the control and TMFol treatment was by Student's T-test. Statistically significant differences are indicated as * (p< 0.05) and **** (p< 0.001).

To determine if TMFol had any effect on the transcription of ACC, RNA was extracted from each of the treated cell lines and used in qPCR to assess the level of ACC mRNA expression. The changes in ACC mRNA expression for all time points in 22Rv1 cells were non-significant (Figure 4.13 A). In PC-3 cells ACC mRNA dropped significantly at 72 h (Figure 4.13 B), while in PNT2 cells there was a significant reduction in ACC mRNA at all of the time points (Figure 4.13 C). The changes in ACC mRNA expression for all cell lines basically correlated with the changes in ACC protein expression.

FAS, which is often over-expressed in prostate cancer and is indirectly inhibited by activated AMPK (Flavin et al., 2011; Rossi et al., 2003), is a critical enzyme in fatty acid synthesis. The effect of TMFol on FAS was assessed to determine the extent of TMFol's influence on fatty acid synthesis. In the 22Rv1 cells, there was no significant difference in FAS expression between the control and treated groups for the various time points (Figure 4.14 A). There was a statistically non-significant decrease in FAS expression at 48 and 72 h in the PC-3 cells (Figure 4.14 B), while a significant downregulation of FAS was observed in PNT2 cells, starting from 24 h (Figure 4.14 C).
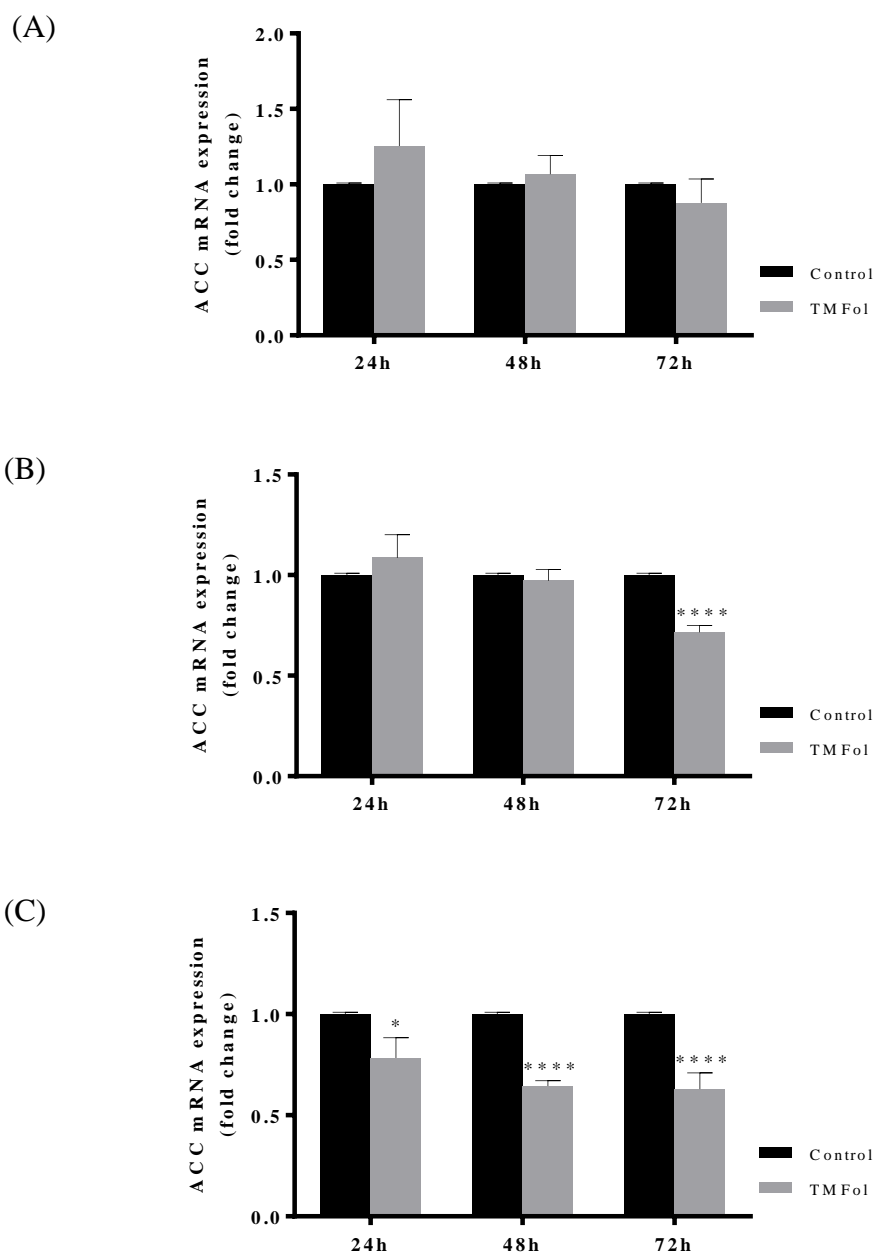
Figure 4.13: Expression of ACC mRNA in 22Rv1 (A), PC-3 (B) and PNT2 (C) cells following exposure to 10 μM TMFol or DMSO only (solvent control). RNA was extracted from the treated cells and reversed transcribed before performing qPCR. The ACC mRNA levels were normalised to two reference genes, GAPDH and actin, and compared with the control by using the comparative C_T (cycle threshold) method. Each column represents mean ± SD of three independent experiments each performed in triplicate. Statistical comparison between the control and TMFol treatment was by Student's T-test. Statistically significant differences are indicated as * (p< 0.05) and **** (p< 0.001).
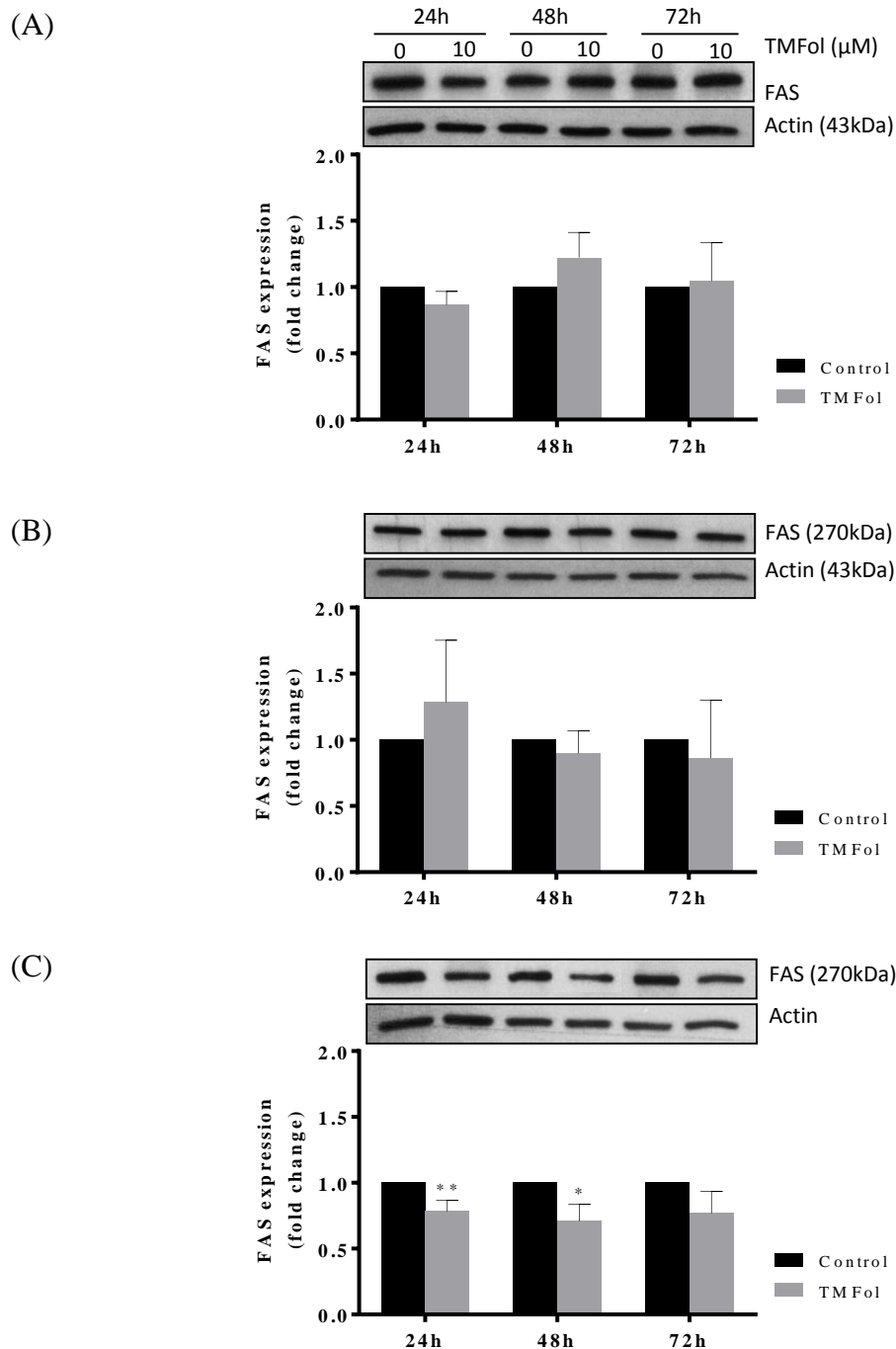
Figure 4.14: Expression of FAS in 22Rv1 (A), PC-3 (B) and PNT2 (C) cells following exposure to 10µM TMFol or DMSO only (solvent control). Analysis was by Western blotting and representative blots are shown for each cell line. The graphs are based on densitometric analysis of Western blots after normalisation to actin. Each column represents mean ± SD of three independent experiments. Statistical comparison between the control and TMFol treatment was by Student's T-test. Statistically significant differences are indicated as * ($p < 0.05$) and ** ($p < 0.01$).

4.6. Discussion

Normal prostate glandular epithelial cells have a truncated Krebs cycle, during which there is low citrate oxidation and low respiration, resulting in citrate secretion into the semen (Dakubo et al., 2006). Therefore, the significant alterations in the Krebs cycle observed here, presented an excellent opportunity to determine the extent of TMFol's involvement in modulating the metabolic features of prostate cancer. FH is the only protein that was significantly increased in both the 22Rv1 cell line and xenograft tumours (Figures 4.1 and 4.3). Mutations in FH or loss of function of FH have been linked to cases of renal cancer (Tomlinson et al., 2002) but there is no evidence to indicate that mutations in FH are associated with prostate cancer (Lehtonen et al., 2003). The disparity in the expression of the other Krebs cycle proteins in the 22Rv1 cell line and 22Rv1 xenografts is a reminder that *in vitro* targets can sometimes be over or under expressed when tumour cells become adapted to the *in vivo* environment. Hence, any significant change in either environment should warrant more than a cursory glance. Generally, the effects of TMFol on the selected Krebs cycle proteins were more prominent in the PC-3 cells than in the 22Rv1 cells (Figures 4.1 and 4.2). Additionally, opposite effects were observed for FH, DLST and SDHA, whereby the expression levels increased in one cell line and decreased in the other, indicating that the effect of TMFol is cell line specific. Except for ACO2, the importance of the alterations in the expression of the remaining Krebs cycle proteins in inhibiting prostate cancer is relatively unknown and the changes in expression could be unrelated or coincidental to the inhibitory action of TMFol on prostate cancer.

ACO2, the critical enzyme in citrate metabolism in human prostate epithelial cells, has been implicated in prostate malignancy (Costello and Franklin, 1998). Analysis of normal and malignant prostate tissue taken from prostate cancer patients has shown that the expression levels of ACO2 are not significantly different (Singh et al., 2006). However, the expression of ZIP1 zinc transporter is downregulated in malignant tissues. In normal prostate epithelial cells, ACO2 activity is inhibited by the high intracellular levels of zinc in the normal tissue, while in the malignant prostate the inhibitory effect is removed as there is a dramatic drop in intracellular zinc in the malignant prostate (Singh et al., 2006). Hence, in this project it was necessary to establish the effect of TMFol on both the expression and activity of ACO2 in the *in vitro* models of prostate

cancer. Consistent among all the cell lines, TMFol caused a significant decrease in ACO2 expression at most of the time points studied (Figures 4.1 A, 4.2 A and 4.4). This decrease in expression correlated with the significant decrease in ACO2 activity following 24 h exposure to TMFol (Figure 4.6). The reduction of ACO2 expression could have been caused by increased degradation of the ACO2 protein and/or by reduced transcription of the *ACO2* gene. p53 has been shown to alter the gene expression of ACO2 in human prostate cancer cells (Tsui et al., 2011). An increase in p53 expression downregulated *ACO2* gene expression in wild-type p53-expressing LNCaP cells and the p53-deficient PC-3 cells that were transiently transfected with a p53 expression vector (Tsui et al., 2011). In chapter 3, TMFol significantly upregulated p53 expression in the 22Rv1 cells (Figures 3.15 A and B) and hence it is possible that TMFol could have downregulated the expression of ACO2 via a p53-mediated mechanism. However, other methods of regulating *ACO2* gene expression would be required in the case of the p53-deficient PC-3 cells and the PNT2 cells, in which p53 expression remained relatively unchanged (Figure 3.15 A).

While it is logical to assume that the decrease in ACO2 activity is directly related to the decrease in ACO2 expression, it is quite possible that TMFol could be modulating the expression and activity of the zinc transporters, such as ZIP 1, that regulate the uptake of zinc by cells. Human ZIP1 is expressed in LNCaP and PC-3 human prostate cancer cells and these lines also have the ability to accumulate zinc (Franklin et al., 2003). Experiments involving the overexpression and knockdown of human ZIP1 in PC-3 cells demonstrated that overexpression of human ZIP1 is associated with higher zinc intake and growth inhibition of PC-3 cells (Franklin et al., 2003), leading to inhibition of ACO2 activity (Singh et al., 2006). Downregulation of the zinc transporter produced opposite effects (Franklin et al., 2003; Singh et al., 2006). Therefore, the effect of TMFol on the expression of zinc transporters and subsequently on zinc accumulation in the prostate cells would offer new insights into the mechanisms used by TMFol to modulate ACO2 activity and also inhibit growth. The accumulation of zinc in prostate cancer cells induces apoptosis (Feng et al., 2000 and 2002; Liang et al., 1999). Hence, if TMFol is capable of altering the zinc transporters in prostate cells to cause intracellular accumulation of zinc, this could be a possible reason for the induction of apoptosis in the 22Rv1 xenografts and its absence *in vitro*. The developing tumours within the mice are most likely to have zinc available through the blood supply, in a

form and concentration that is suitable for uptake and accumulation in the prostate cancer cells, subsequently inducing the apoptosis observed *in vivo*. Therefore, follow-up studies involving immunohistochemical analysis of the xenograft tumours for ZIP 1 expression would be required to determine if TMFol has the ability to modulate the zinc transporter and subsequently alter the intracellular levels of zinc. In the cell line studies the level of zinc in the growth medium was not adjusted. RPMI-1640 medium with FCS has approximately 0.05 µg zinc/mL, which is less than the 1 µg zinc/mL required to cause intracellular accumulation and apoptosis (Costello et al., 1999; Feng et al., 2002). Both PC-3 and 22Rv1 have been shown to express ZIP 1 (Costello et al., 1999; Holubova et al., 2014) and so future studies to determine if TMFol is modulating ZIP 1, and subsequently intracellular zinc levels, in these cell lines should be conducted.

To determine the effects of ACO2 inhibition in prostate cancer, Juang (2004) used a human ACO2 antisense vector to block the endogenous ACO2 expression in several human prostate cancer cells, including LNCaP, PC-3 and DU145 and found that a reduction in the expression of ACO2 correlated with a reduction in ACO2 activity, a reduction in ATP content, an increased citrate secretion and growth inhibition. The ATP content and the levels of citrate secreted were not analysed in the present study but it would be interesting to determine the effect of TMFol on these parameters to firmly establish the link between growth inhibition and loss of aconitase activity. There is no evidence in the literature indicating that flavonoids have the ability to modulate the expression and activity of ACO2 in prostate cells to inhibit growth. Fluoroacetate is a known ACO2 inhibitor but it is not prostate specific and the inhibition of ACO2 activity in any other cell type tends to be lethal (Costello and Franklin, 2006). Therefore, TMFol demonstrates a unique ability to significantly reduce ACO2 expression and activity in the 22Rv1 and PC-3 cells and this could very likely be its major mechanism to bring about the growth inhibition observed in these prostate cancer cell lines.

A review of the literature on whether PDH is a rate-limiting step in cancer would indicate that it is dependent on the cancer cell type. Generally, malignant cells demonstrate an increase in glucose consumption which is accompanied by a switch to aerobic glycolysis (DeBerardinis et al., 2008). As a consequence, PDH activity would be inhibited as the pyruvate from glycolysis would be used to produce lactic acid rather than be used in mitochondrial oxidation. In sharp contrast, there is a relatively low level

of aerobic glycolysis in malignant prostate cells as the pyruvate can now be utilised in the Krebs cycle for efficient ATP production (Costello and Franklin, 2000). Furthermore, PDH is often over-expressed in human prostate cancer (Lexander et al., 2005). Hence, reducing PDH activity in prostate cancer would be a desirable feature of any prostate cancer chemopreventive or chemotherapeutic agent.

All of the cell lines in this current study responded to TMFol exposure with a significant upregulation of PDC-E2, the core catalytic component of PDH (Figure 4.7). However, this did not cause an increase in PDH activity after 24 h incubation with TMFol (Figure 4.9). Rather, there was a dramatic but statistically non-significant decrease in PDH activity in both 22Rv1 and PC-3 cells (Figure 4.9). The decrease in PDH activity could be a direct effect of TMFol on PDH or could be as a result of the inhibition of ACO2 activity by TMFol. Inhibition of ACO2 activity is likely to induce a dependency on aerobic glycolysis as the Krebs cycle becomes truncated and the reliance on PDH activity is now minimal. There does not appear to be any published evidence to indicate that modulation of the expression of the main catalytic component of PDH affects enzyme activity. Hence, experiments involving the over-expression of PDC-E2 in prostate cancer cells would be necessary to determine the effect on PDH activity. Furthermore, it would be beneficial to establish if the decrease in PDH activity caused by TMFol is associated with the expected decrease in oxidative phosphorylation and increase in aerobic glycolysis in these prostate cancer cells. In this study it would have been most expedient if the PDH activity was measured in the cells that were incubated with TMFol for longer than 24 h. No PDH activity was detected in the PNT2 cells as enzymatic activity is generally low in the normal prostate cells, in this case, below the limit of detection for the PDH activity assay used.

Upregulation of endogenous fatty acid synthesis is a common feature of prostate cancer and as a consequence several of the enzymes involved in this process are over-expressed (Rossi et al., 2003). Therefore, inhibition of the over-expressed enzymes in fatty acid synthesis could be useful in the management of prostate cancer. The downregulation of ACLY in PC-3 and LNCaP cells is associated with inhibition of growth in these cells (Gao et al., 2014). The effect of TMFol on ACLY expression was cell line specific (Figure 4.10). The contrasting changes in ACLY expression induced by TMFol could be unrelated to the growth inhibitory action of TMFol.

AMPK has the unique ability to inhibit fatty acid synthesis by targeting several of the enzymes in the pathway. Hence, AMPK activators are potentially beneficial for prostate cancer prevention and treatment. In the PC-3 cells AMPK was activated by TMFol, as evident by the significant increase in pAMPKα (Figure 4.11). With this capability TMFol behaves much like the dietary flavonol, fisetin, which also activates AMPK in PC-3 cells, albeit at much higher concentrations ranging from 40–120 μM (Suh et al., 2010). The modest, but non-significant increase in pAMPKα at 72 h in 22Rv1 cells may indicate that TMFol is unable to activate AMPK in these p53-positive cell types or could have occurred earlier than 24 h. Future studies with these slower growing cells should consider assessment for shorter time points to ascertain the true response profile.

Activation of AMPK should lead to increased levels of pACC as activated AMPK directly inhibits ACC through phosphorylation (Flavin et al., 2011). The expected increase in the proportion of pACC in PC-3 cells was not apparent from the data, since the levels of total protein (ACC) varied in a similar manner to pACC (Figure 4.12). The outcome was similar in the other cell lines. Hence TMFol appears to be exerting a direct effect on ACC rather than modulating its phosphorylation. This effect appears to be at the transcriptional level, as the changes observed in expression of ACC over the 72 h period were in general, similar to the changes in the levels of mRNA for this protein (Figure 4.13).

Since downregulation of ACC expression and mRNA occurred in all of the cell lines, it appears that TMFol may be acting as an inhibitor of ACC transcription. The extent of the inhibitory effect may also be cell line specific as the degree of inhibition varied among the cell lines. Similar to TMFol, quercetin also has the ability to downregulate ACC at the transcriptional level in PC-3 cells, but at concentrations ranging from 100 – 150 μM (Noori-Daloii et al., 2011). Inhibition of ACC decreases malonyl-CoA, attenuates endogenous fatty acid synthesis and induces fatty acid oxidation. Therefore, further study should identify changes in the expression of proteins involved in fatty acid oxidation or the rate of the overall process. Additionally, the phospholipid content of the cells could be analysed since phospholipids are the major end product of fatty acid synthesis and their levels are likely to decrease if TMFol is acting as an inhibitor of ACC transcription.

TMFol caused non-significant changes in FAS expression in both 22Rv1 and PC-3 cells (Figure 4.14). The expression in PC-3 cells at 48 and 72 h was lower than that of the control cells. Activated AMPK can inhibit FAS expression by inhibiting the transcription of its gene (Flavin et al., 2011), but the TMFol-induced activation of AMPK was unable to significantly inhibit FAS expression in the PC-3 cells. It should be noted that downregulation of FAS would not be required here to inhibit endogenous fatty acid synthesis, since TMFol downregulated the synthetic process upstream of FAS by inhibiting the transcription of ACC.

Throughout the investigation into the metabolic features of the cells, PNT2 cells also proved very sensitive to the effects of TMFol. There was a significant inhibition of ACO2 expression and activity and a significant inhibition of the expression of ACC and FAS. In normal prostate cells ACO2 is inhibited and the expression of ACC and FAS would be extremely low as a consequence of little to no endogenous fatty acid synthesis in the normal cells. Hence, any further inhibition triggered by TMFol would have little to no effect on the normal cells since their growth and survival are not dependent on the activities of these enzymes. Therefore, it may be speculated that the growth inhibitory effect of TMFol on PNT2 cells may be largely due to the induction of S phase cell cycle arrest.

Prostate cancer is a multigenic disease, therefore, to determine the mechanism of action engaged by TMFol to inhibit the growth of prostate cancer, two prostate cancer cell lines with different genetic profiles were utilised and compared with a normal prostate cell line. TMFol at a concentration of 10 µM was capable of inhibiting ACO2 expression and activity, potentially inhibiting citrate oxidation. Endogenous fatty acid synthesis is required for the growth of prostate cancer cells and TMFol has the ability to inhibit the transcription of ACC, a key regulatory enzyme in the synthesis pathway, which could ultimately switch off fatty acid synthesis. Additionally, TMFol was able to cause a significant increase in pAMPK in the PC-3 cells only, the importance of its increase in the inhibition of fatty acid synthesis is not clear. Although TMFol increased the expression of the main catalytic component of PDH, TMFol reduced PDH activity, which could lead to less energy for the cancer cells to grow. While further work would be required to determine the importance of each mechanism in the growth inhibitory action of TMFol in prostate cancer, taken together, the body of work

presented here is consistent with the notion that TMFol is a multi-targeted agent that may be efficacious in the management of prostate cancer.

Chapter 5. *In vivo* efficacy of TMFol in PB^{Cre4}*p53^{flox}Rb^{flox}* and PB^{Cre4}*Pten^{flox}* mouse models of prostate cancer

5.1. Introduction

A prerequisite for clinical development of any potential chemopreventive or chemotherapeutic agent is a demonstration of its *in vivo* efficacy in suitable animal models. Previous *in vivo* studies with TMFol utilised mouse xenografts but in this study it was important to determine the extent of TMFol's effect on the very early events occurring after loss of key tumour suppressor genes and subsequent progression of prostate cancers that arise *in situ*. Therefore, two conditional knockout mouse models of prostate carcinogenesis, PB^{Cre4}*p53^{flox}Rb^{flox}* and PB^{Cre4}*Pten^{flox}*, were utilised. The genetic heterogeneity of prostate cancer has made it difficult for the generation of a mouse model that accurately depicts the entire spectrum of human prostate cancer. The choice of these two animals models not only presented the opportunity to monitor the effects of TMFol in models that closely mimic the multiple stages of human prostate cancer from changes occurring immediately after initiation to metastasis (albeit lacking skeletal metastasis), but also provided the opportunity for research collaboration with Professor David Neal's uro-oncology research group at Cancer Research UK Cambridge Institute, University of Cambridge, United Kingdom. It is worth mentioning that this was the first complete descriptive chemoprevention study in the recently generated PB^{Cre4}*p53^{flox}Rb^{flox}* prostate cancer model. An important advantage was the reasonable time frame (approximately 12 months) both models allowed to complete the chemoprevention studies.

5.2. Effect of TMFol consumption on PB^{Cre4}p53^{flox}Rb^{flox} mice

To investigate the effect of TMFol on the growth of prostate cancer in the PB^{Cre4}p53^{flox}Rb^{flox} model, the mice were enrolled in either a 23-week monitoring study or a survival study. The objectives were to evaluate the efficacy of TMFol against the development of prostate cancer and to determine if long-term consumption of the TMFol diet provided any survival benefits. All animals were started on the AIN93G control diet or the AIN93G diet supplemented with 0.2 % TMFol at the age of 4 weeks. Diets were consumed *ad libitum* until the age of 27 weeks for those animals that were enrolled in the 23-week study. For animals in the survival study the mice were culled when they showed signs of illness, as designated in the Home Office Project Licence under which this study was performed, or when the study was terminated as mice reached the age of 44 weeks.

Over the course of the 23-week study the animals on the TMFol diet maintained a significantly higher body weight ($p = 0.008$) than those on the control diet (Figure 4.1). The mice on the TMFol diet were on average 12.7 ± 3.5 % heavier than those on the control diet. Additionally there was a significant increase in the body weights of the animals over time ($p < 0.001$). Unfortunately, body weight data were not available prior to the mice reaching 13 weeks of age, therefore it is not possible to ascertain exactly when this difference in body weight first becomes apparent. The amount of food consumed by each animal was not measured in this study, but one possible explanation is that the mice on the TMFol-containing diet consumed more food per day compared to those on standard control diet. Alternatively, TMFol may alter metabolic factors in a way that results in weight gain. Differences in the presence of tumours or degree of PIN may also influence weight gain and body weight, however, histological analysis described later show that this is not a reason. The possible reasons could be narrowed down by measuring food consumption of the individual mice in each group, in future studies.
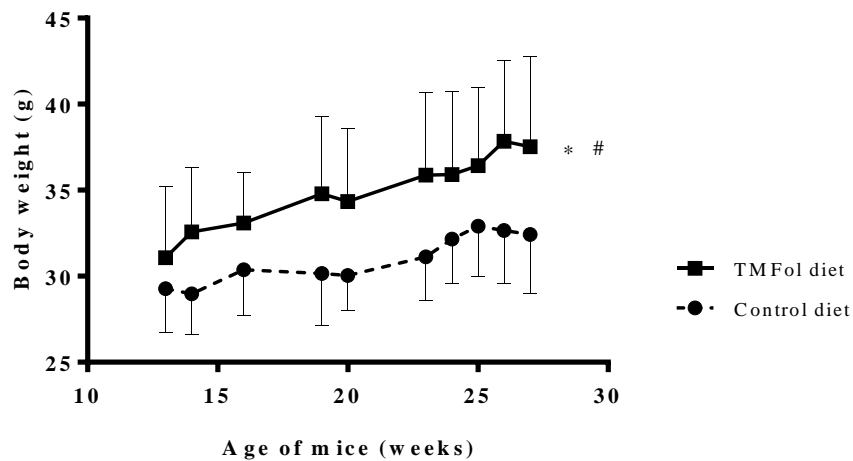
Figure 5.1: Body weight of PB^{Cre4}p53^{flox}Rb^{flox} mice on 0.2% TMFol diet or control diet from age 4 weeks to age 27 weeks. Values represent the mean ± SD (N=10 for each group). * indicates that the difference between mice on the control and TMFol diets was statistically significant (p < 0.05), while # indicates that the difference between the body weights over time was statistically significant (p < 0.05). Statistical comparison was by a mixed effects linear regression. Body weight data were not available prior to the mice reaching 13 weeks of age.

Following 23 weeks on diet, animals were culled by cervical dislocation under terminal anaesthesia, and prostates, seminal vesicles, bladder, urethra and liver were removed for histological assessment. The histological appearance of the animal tissues was reviewed and analysed with the assistance of Dr. Sérgio Felisbino, a morphologist. The assessment of PIN was according to the consensus report from the Bar Harbor meeting, where it was recommended to evaluate the area of the prostate involved (Shappell et al., 2004), but since this was the first complete descriptive chemoprevention study in this model, further evaluation of the cell differentiation pattern as described by Park *et al.* (2002) was included to determine the levels of PIN development. PIN lesions were found in all of the prostatic lobes for all mice in both the control and TMFol groups (Figures 4.2 and 4.3). The percentage of area within the prostatic lobes occupied by PIN was slightly higher in the mice consuming the TMFol diet compared to those on the control diet (Figure 4.3). Furthermore, the area covered by PIN was highest in the dorsal prostate in both the control and TMFol groups with 63.5 % and 67 %, respectively (Figure 4.3). Three levels of PIN development, PIN 1, PIN 2 and PIN 3, were identified in both groups of animals, and the number of animals displaying each grade of PIN was similar for the control and TMFol groups (Figure 4.4 and Table 4.1). Histological analysis revealed no presence of adenocarcinoma in the prostatic lobes of any of the PB^{Cre4}p53^{flox}Rb^{flox} mice, regardless of the intervention.
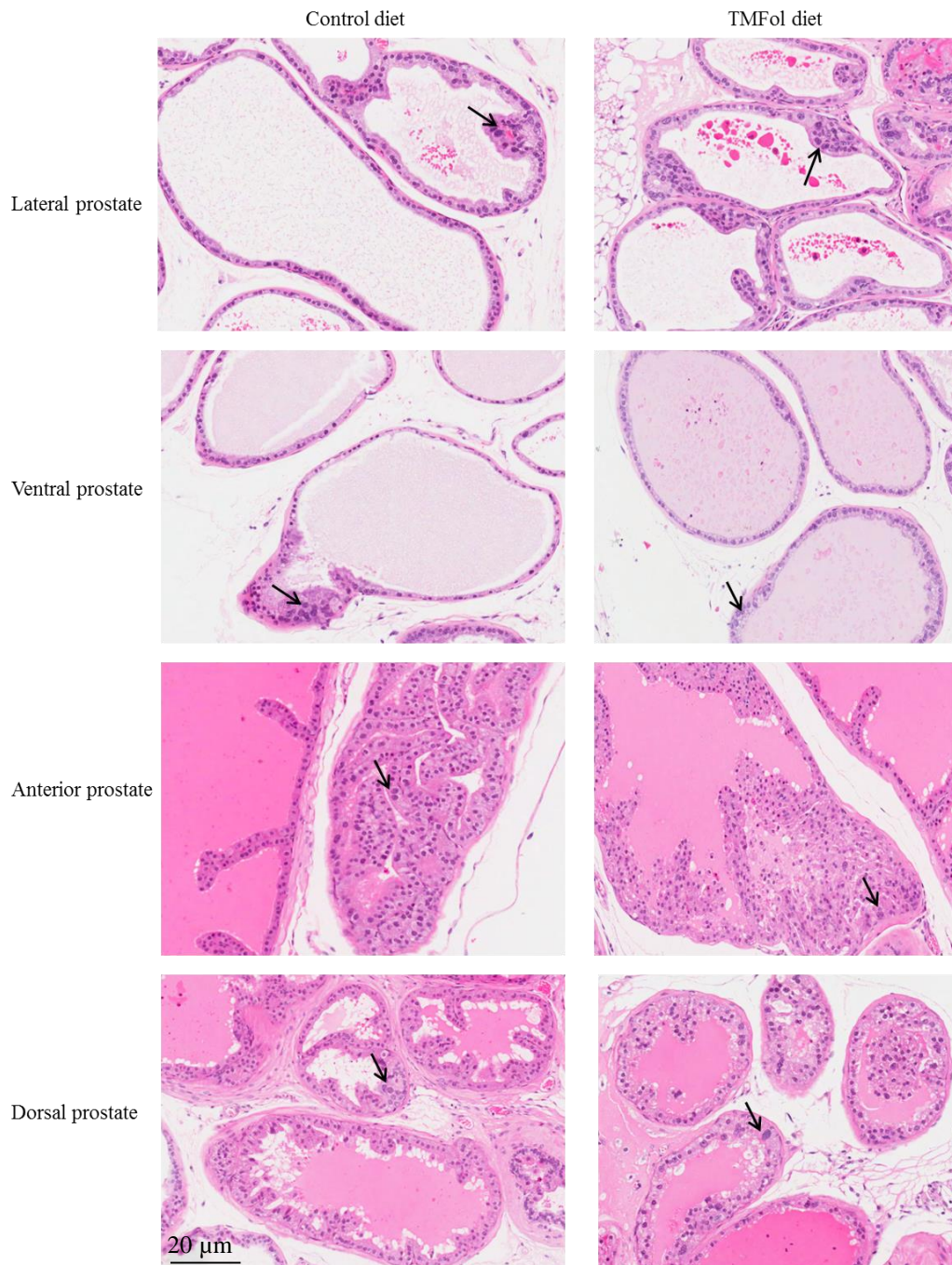
Figure 5.2: Histological appearance of prostatic lobes (H&E stain) in representative PB^{Cre4}p53^{flox}Rb^{flox} mice on 0.2 % TMFol diet or control diet from age 4 to 27 weeks. Magnification x20. Arrows indicate a region of PIN within the prostatic lobe.
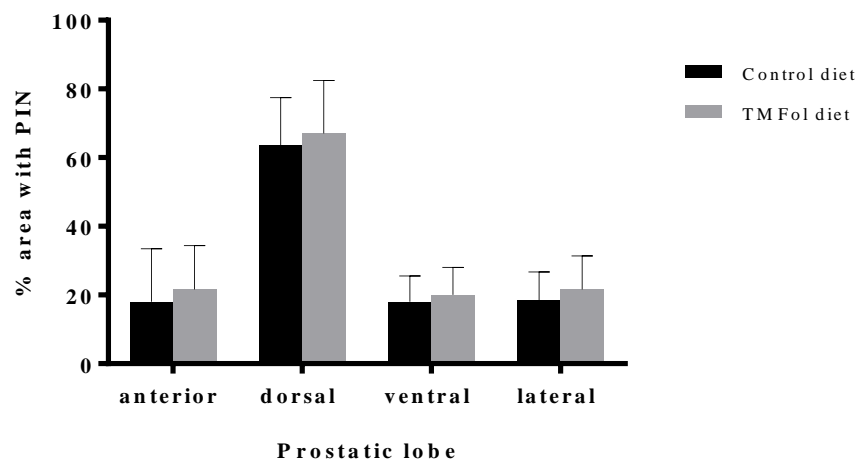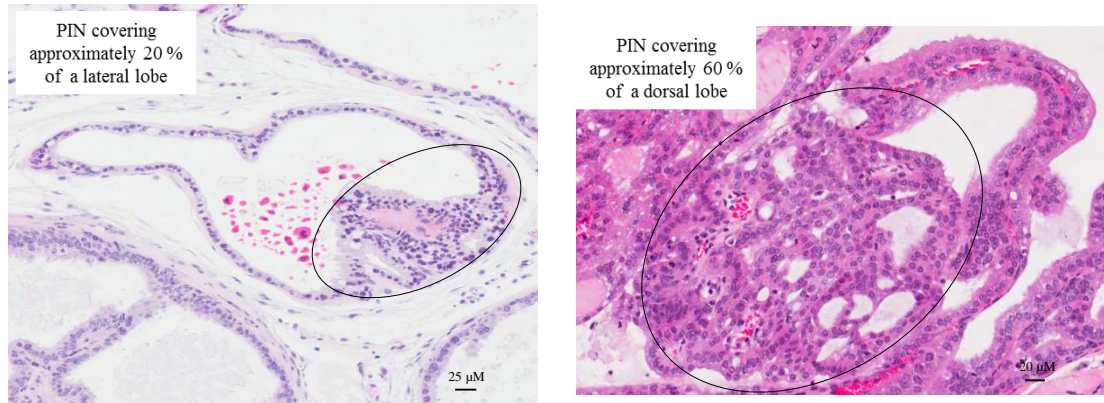
Figure 5.3: Area of prostatic lobe covered with PIN lesions in PB^{Cre4}**p53**^{flox}**Rb**^{flox} **mice on 0.2 % TMFol diet or control diet from age 4 to 27 weeks.** All prostatic lobes for each mouse on the slides were scored. As the sections contain variable amounts of prostatic tissues, the columns represent the mean ± SD of approximate estimates of % area with PIN within the prostatic lobes of 10 mice per group. The group means were not significantly different based on analysis using the Student's T-test. The images illustrate how the % area with PIN was estimated. Magnification x20. The circles indicate the area of PIN.
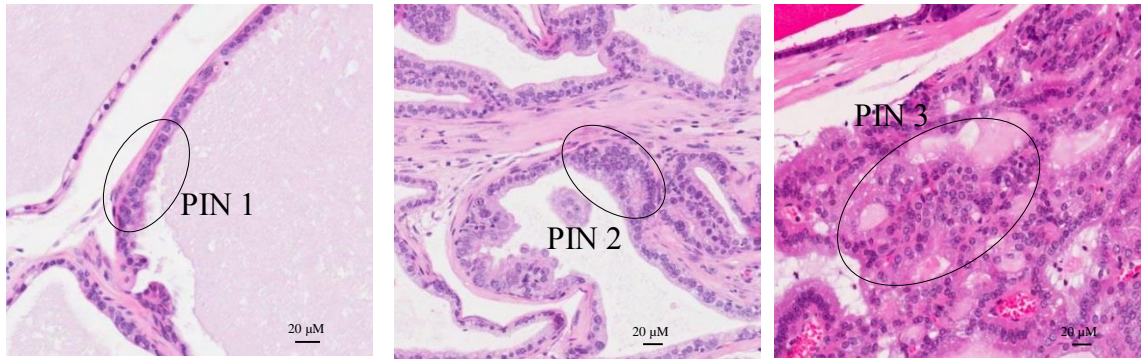
Figure 5.4: Histological appearance of PIN1, PIN2 and PIN3 in prostatic lobes from representative PB^{Cre4}**p53**^{flox}**Rb**^{flox} **mice.** The level of PIN development was classified as described by Park *et al.* (2002). Magnification x20. The circles indicate the region of PIN.

Interestingly, tumours were detected in the urethra rather than in the prostatic lobes of the PB^{Cre4}p53^{flox}Rb^{flox} mice in both groups. However histological analysis of the urethra was complicated by the fact 4 animals from the control group and 2 animals from the TMFol group could not be analysed. This was because the urethrae from these animals were lost during processing of the tissue-embedded paraffin blocks for staining with H&E. Therefore, it is difficult to judge if the result obtained from the current urethral analysis is representative of the effect of TMFol on the animals. Tumour formation was evident in the urethra of 4 out of 6 animals (67%) in the control group and 5 out of 8 animals (63 %) in the TMFol group (Table 4.1). The tumours generally occupied approximately 50 % of the lumen of the urethra in both groups (Figure 4.5 A).

Very few PB^{Cre4}p53^{flox}Rb^{flox} mice developed liver metastasis (2 out of 10 in the control group and 1 out of 10 in the TMFol group) (Table 4.1). There were several sites of tumour growth visible within the liver in both groups (Figure 4.5 B). It is difficult to determine if tumour formation and tumour size in the urethra correlate with liver metastasis, since the 2 cases of liver metastasis detected in the control group were found in animals without a urethra available for histological analysis.

Region	Lesion	Number of animals (% of the total)	
		Control	TMFol
Dorsal prostate	PIN 1	10 (100)	10 (100)
	PIN 2	6 (60)	6 (60)
	PIN 3	3 (30)	4 (40)
Lateral prostate	PIN 1	10 (100)	9 (100)
	PIN 2	5 (50)	5 (56)
	PIN 3	1 (10)	1 (11)
Anterior prostate	PIN 1	8 (80)	9 (90)
	PIN 2	6 (60)	5 (50)
	PIN 3	4 (40)	3 (30)
Ventral prostate	PIN 1	10 (100)	9 (100)
	PIN 2	7 (70)	6 (67)
	PIN 3	1 (10)	4 (44)
Urethra	Adenocarcinoma	4 (67)	5 (63)
Liver	Metastasis of adenocarcinoma	2 (20)	1 (10)

Table 5.1: Distribution of PIN and adenocarcinoma in PB^{Cre4}p53^{flox}Rb^{flox} mice on 0.2 % TMFol diet or control diet from age 4 to 27 weeks. The occurrence of the lesions was based on H&E staining in the prostatic lobes, urethra and liver for each mouse. All sections of the of prostatic lobes on the slides were analysed. In those cases where the region of interest was not visible for histological analysis it was reflected in the % of the total.

(A)

Control diet   TMFol diet

adenocarcinoma
inside the urethra

adenocarcinoma
inside the urethra

(B)

Control diet   TMFol diet

Liver with arrows
indicating adenocarcinoma

Liver with arrows
indicating adenocarcinoma

50 μm

50 μm
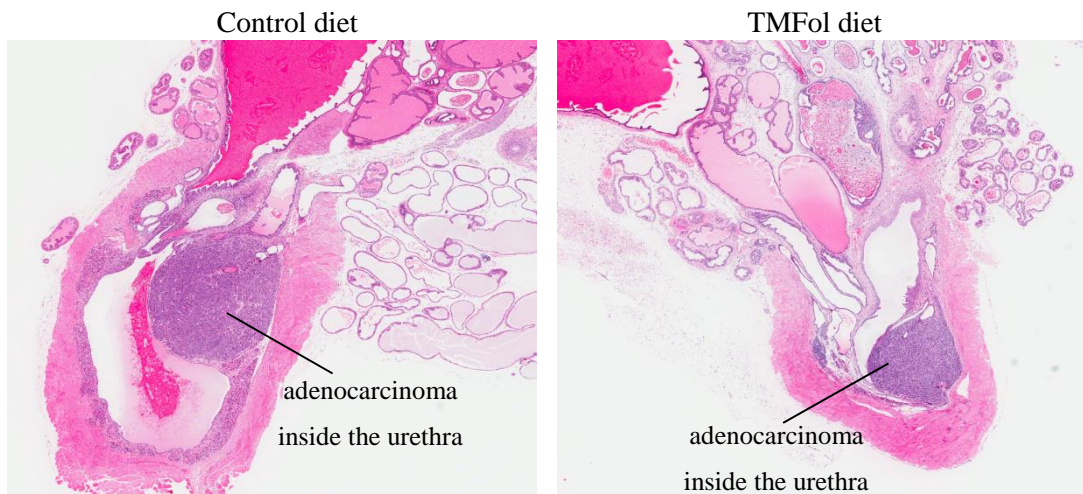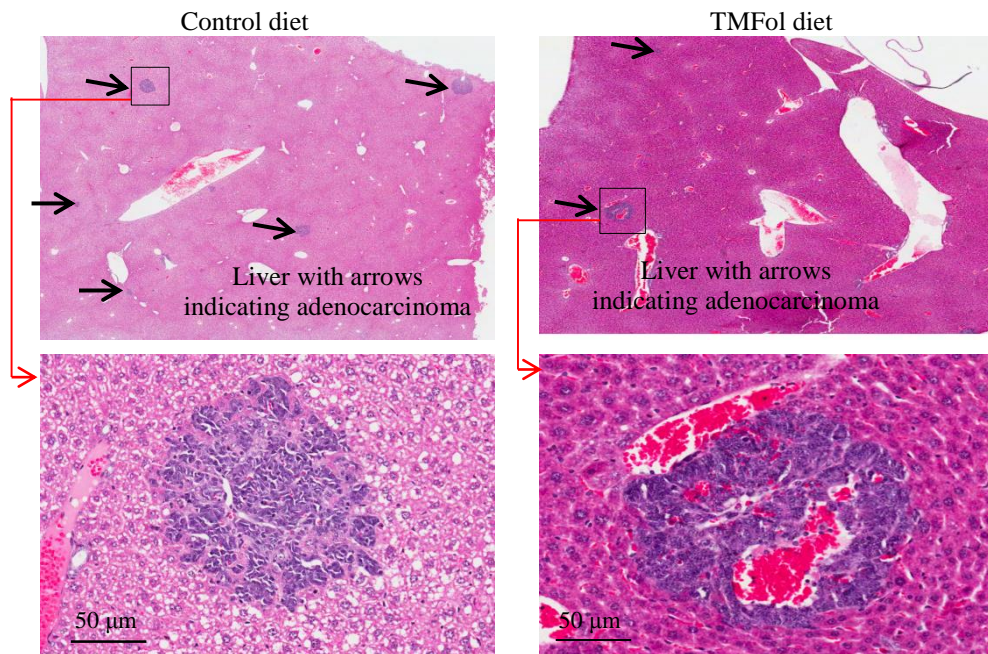
Figure 5.5: Histological appearance of (A) urethra and (B) liver (H&E stain) from representative PB^{Cre4}p53^{flox}Rb^{flox} mice on 0.2 % TMFol diet or control diet from age 4 to 27 weeks. Magnification x20. Areas of adenocarcinoma are indicated in the urethra and liver.

For the animals in the survival study, Kaplan-Meier analysis was used to compare the survival of PB^{Cre4}p53^{flox}Rb^{flox} mice on the control and TMFol diets (Figure 4.6). The median survival for animals on the TMFol diet (261 days) was modestly higher than that of animals on the control diet (224 days) but the Log-rank test indicated that statistically, the TMFol diet was not associated with any survival advantage (p = 0.6342). There were 10 animals in each group and at the end of the study there was only 1 animal alive in the control group and 2 animals in the TMFol group. This study was terminated earlier than originally planned due to the closure of the laboratory. One case of a non-prostate cancer death was found in the control group and an autopsy indicated obstruction within the stomach. Histological analysis of the animals in the survival study revealed larger tumours in the urethra and liver compared to the 23 week study, along with lymph node and lung metastases (Figure 4.7). Again there was no evidence of tumour formation within the prostatic lobes.

Median survival

Control diet: 224 days

TMFol diet: 261 days
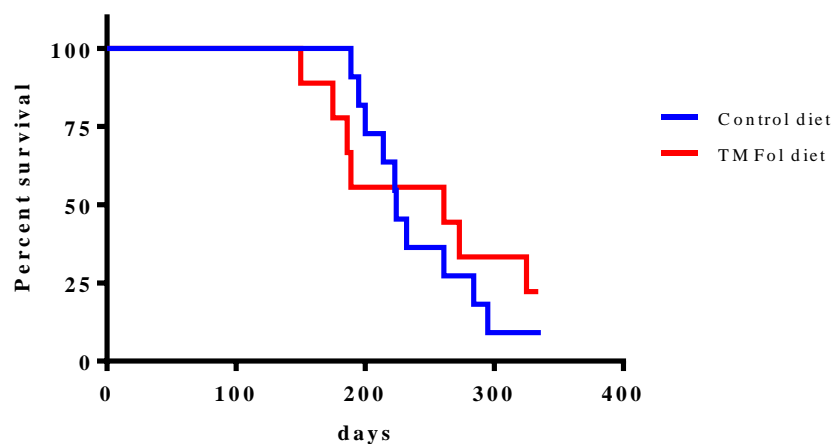
Figure 5.6: Kaplan-Meier survival curves of all cases of mortality for PB^{Cre4}p53^{flox}Rb^{flox} mice on 0.2% TMFol diet or control diet from age 4 to 44 weeks. N = 10 mice per group. There was only 1 animal alive in the control group and 2 animals in the TMFol group at the end of the study. Log-rank (Mantel-Cox) test showed no statistically significant difference (p = 0.6342) between the survival of animals on the control and TMFol diet.
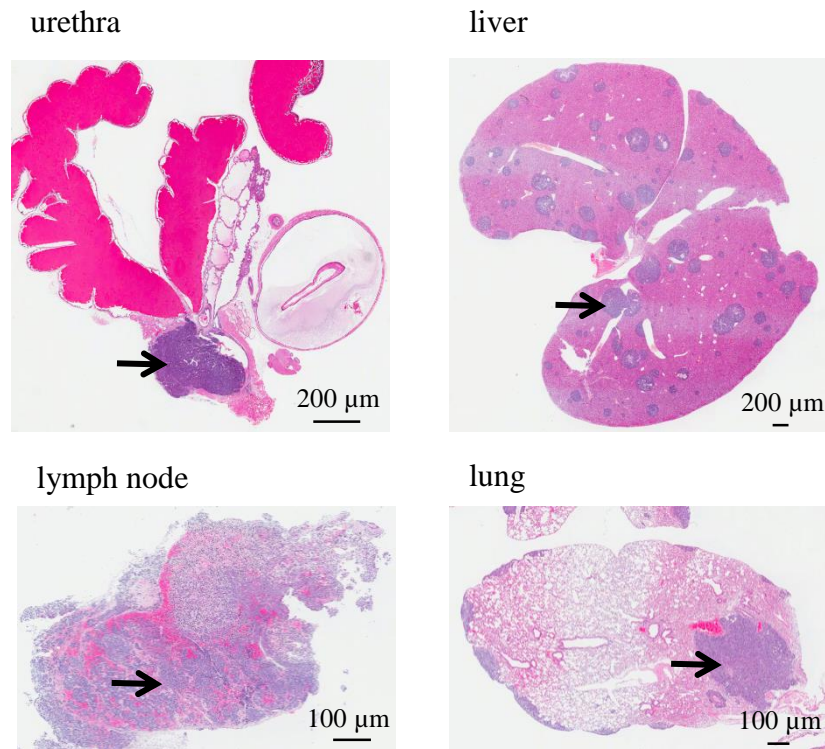
Figure 5.7: Typical histological appearance (H&E) of urethra, liver, lymph node and lungs in PB^{Cre4}**p53**^{flox}**Rb**^{flox} **mice on 0.2 % TMFol diet or control diet for 40 weeks.** These mice were exposed to the diets from age 4 weeks to 44 weeks of age. Magnification x10. Arrows indicate the adenocarcinoma.

5.3. Effect of TMFol consumption on PB^{Cre4}Pten^{flox} mice

As previously indicated there is no mouse model currently available that accurately reflects the entire spectrum of human prostate cancer, therefore, in this study the effect of TMFol on a second mouse model of prostate cancer, PB^{Cre4}Pten^{flox}, was included. Mutations in *Pten* are common in human prostate cancer (Wang et al., 2003). Hence, the efficacy of TMFol in modulating prostate carcinogenesis of different genetic origins would indicate its potential value in the management of prostate cancer. The investigation into the effect of TMFol on the growth of prostate cancer in PB^{Cre4}Pten^{flox} mice was performed over a period of 12 weeks, during which time animals consumed *ad libitum* AIN93G control diet or AIN93G diet supplemented with 0.2 % TMFol. The animals were enrolled in the study at about 3.5 months of age. At this stage these mice are expected to be already displaying PIN lesions (personal communication, Dr.Sérgio Felisbino). Therefore, the TMFol dietary intervention was assessing the ability of TMFol to delay the progression of PIN lesions to invasive adenocarcinoma. In this animal model, invasive adenocarcinoma is usually detectable, at least in the lateral prostate, at age 6 months (unpublished data, Dr. Sérgio Felisbino and Dr. Chiranjeevi Sandi, Cancer Research UK Cambridge Institute).

Over the course of the 12-week study, the body weights of the animals on the TMFol diet were marginally significantly higher than those on the control diet (p = 0.05) (Figure 4.8). The significant difference in body weights was first observed at week 10 of the study. On average, the animals in the TMFol group were 7.1 ± 1.8 % heavier than those in the control. Like the previous model in this study, there was also a significant increase in the body weights of the animals over time (p < 0.001).

H&E stained sections of the prostate gland, kidney, spleen, pancreas and liver from each animal were reviewed and analysed by Dr. Peter Greaves, pathologist within the Department of Cancer Studies, University of Leicester. PIN lesions were widespread throughout the prostatic lobes in all of the animals. Figure 4.9 is representative of the extensive PIN development in the dorsolateral prostate tissues in the control and TMFol groups. The assessment of PIN was according to the consensus report from the Bar Harbor meeting, where it was recommended to evaluate the area of the prostate involved rather than the cell differentiation pattern (Shappell et al., 2004). The

151

percentage area of the prostate with PIN was almost identical (approximately 70 %) in both groups (Figure 4.9). Furthermore there was no evidence of invasive adenocarcinoma or metastatic growth in the other tissues.
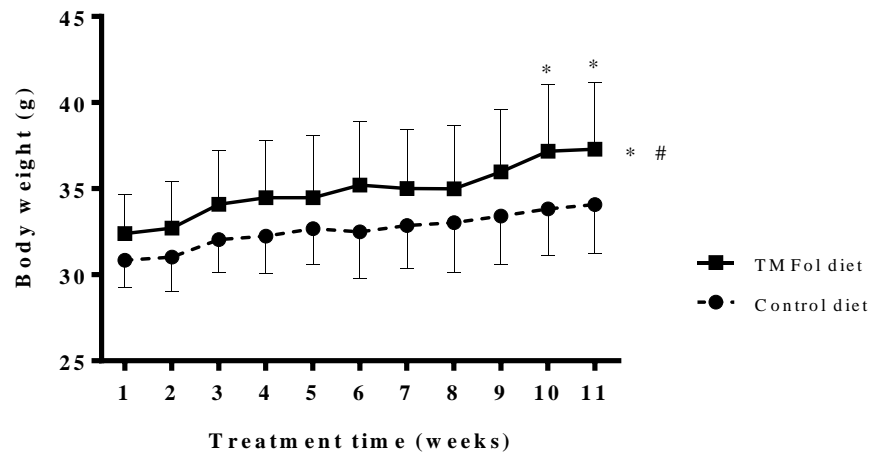
Figure 5.8: Body weights of PB^{Cre4}$Pten^{flox}$ mice on 0.2 % TMFol diet or control diet. Values represent mean ± SD for 10 mice per group. * indicates that the difference between the control and TMFol diets was statistically significant ($p < 0.05$), while # indicates that the difference between the body weights over time was statistically significant ($p < 0.001$). Statistical comparison was by a mixed effects linear regression. Student's T-test was used to compare the differences in body weights between the mice on the control and TMFol diets for each week. Significant difference is indicated as * ($p < 0.05$) on the graph above weeks 10 and 11.

Control diet

- **Dorsolateral prostate with many areas of PIN.**
- **Arrows indicate a few of the PIN.**

20 μm
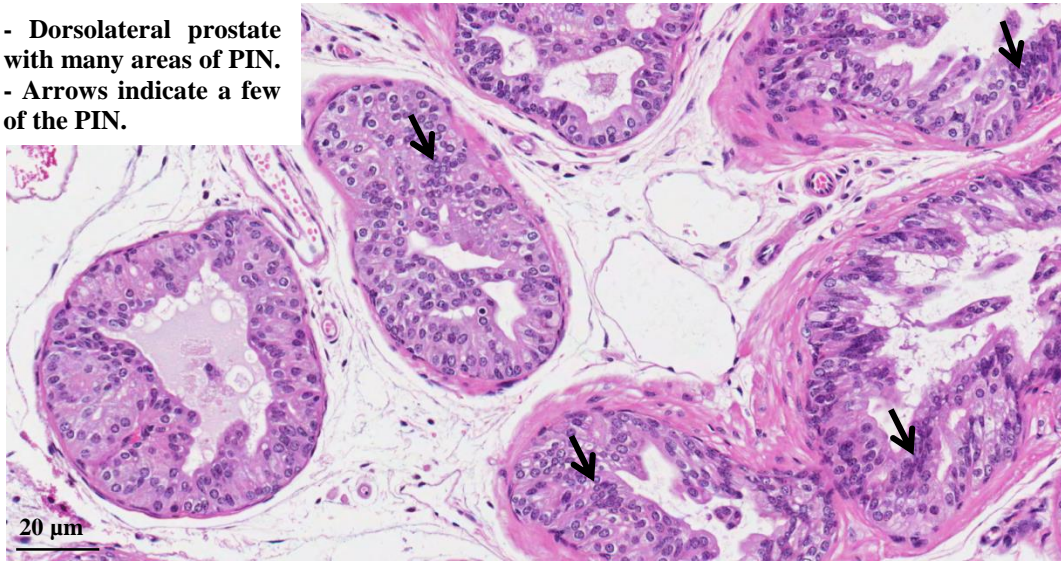
TMFol diet

- **Dorsolateral prostate with many areas of PIN.**
- **Arrows indicate a few of the PIN.**

20 μm
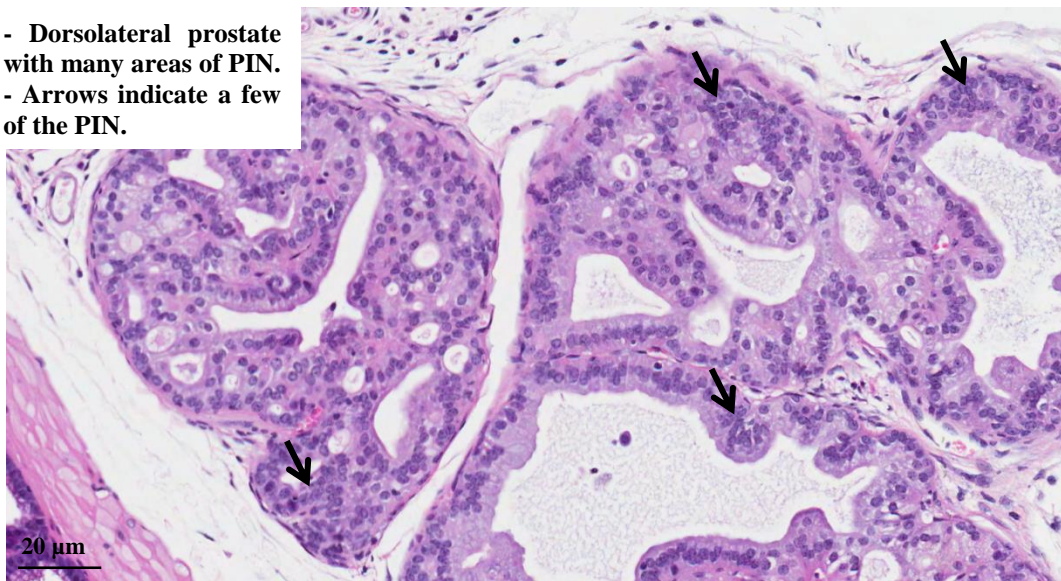
Figure 5.9: Histological appearance of dorsolateral prostate tissue (H&E) in PB^{Cre4}Pten^{flox} mice on 0.2 % TMFol diet or control diet for 12 weeks. Magnification x20. There was no evidence of adenocarcinoma.
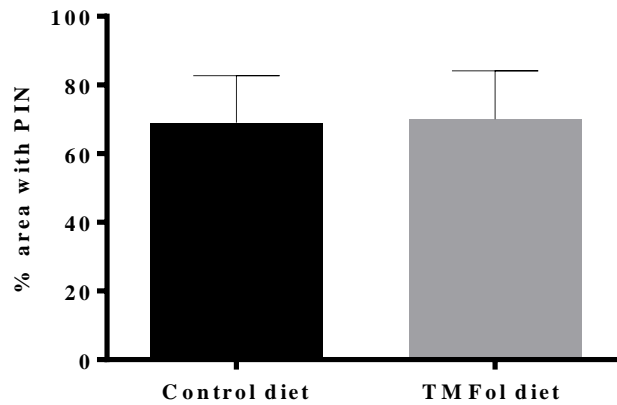
Figure 5.10: Area of the prostate with PIN in PB^{Cre4}***Pten***^{flox} **mice on 0.2% TMFol diet or control diet.** The prostatic tissues for each mouse on the slides were scored. No distinction was made between the prostatic lobes. As the sections contain variable amounts of prostatic tissues, the columns represent the mean ± SD of approximate estimates of % area with PIN within the prostatic tissues of 10 mice per group. Means were not significantly different based on Student's T-test.

5.4. Discussion

The primary focus of this chapter was to determine the *in vivo* efficacy of TMFol in two distinct conditional knockout mouse models that closely represent events in the development and progression of human prostate cancer. Since prostate cancer is a multigenic disease, the use of mouse models with different genetic profiles were considered the most effective tools for determining the ability of TMFol to prevent the development and progression of prostate cancer with different molecular origins. In the $PB^{Cre4}p53^{flox}Rb^{flox}$ model the *p53* and *Rb* genes are knocked out in the prostate, while in the $PB^{Cre4}Pten^{flox}$ model only the *Pten* gene is knocked out in the prostate. Mutations in *p53*, *Rb* and *Pten* genes are often implicated in the development and progression of human prostate cancer (Cooney et al., 1996; Downing et al., 2003; Pourmand et al., 2007; Sharma et al., 2010; Yoshimoto et al., 2006), but the frequency of these mutations in prostate cancer is less than 10 % (Catalogue of somatic mutations in cancer [COSMIC], 2015). Nevertheless, conditional knockout of these genes in the prostate of mice results in the development and progression of prostate cancer.

Overall, none of the mice on the 0.2 % TMFol diet developed adenocarcinoma in the prostate. However, PIN development was extensive and there was no significant difference between the percentage of PIN lesions observed in the prostatic lobes of the mice on the control diet and those on the TMFol diet. Therefore, the TMFol diet failed to demonstrate an *in vivo* efficacy in either mouse models of prostate cancer. In the $PB^{Cre4}p53^{flox}Rb^{flox}$ animals, histological analysis revealed the presence of adenocarcinoma in the urethra and liver metastases in both the control and TMFol-fed groups. Nevertheless, there was a 37-day difference in median survival in favour of the TMFol-fed animals in the survival study but it was considered not to be statistically significant. In the $PB^{Cre4}Pten^{flox}$ model TMFol had no effect on the progression of PIN lesions. Within the 12 week study period it was still too early to detect the presence of invasive adenocarcinoma. Nevertheless, given the extensive coverage of PIN lesions within the prostatic lobes of the control and TMFol-fed groups, it seems unlikely that TMFol would have delayed the progression to adenocarcinoma if the study had been extended.

In our laboratory, dietary intervention studies with TMFol in two independent mouse xenograft models of prostate cancer using human cell lines have resulted in significant inhibition of tumour growth (Saad, 2011; unpublished). Therefore, on the premise that TMFol has been well tolerated and efficacious, with no evidence of toxicity in these animal models, TMFol dietary interventions were expected to be efficacious in the conditional knockout models. Furthermore, both $PB^{Cre4}p53^{flox}Rb^{flox}$ and $PB^{Cre4}Pten^{flox}$ models display genetic features that TMFol has been shown to be effective against in *in vitro* studies. For example, TMFol can inhibit the growth of PC-3 cells (Figure 3.2), which harbour mutations in *p53* and *Pten* genes. To our knowledge, only the $PB^{Cre4}Pten^{flox}$ model has been used previously in drug efficacy studies (Berguin et al., 2007; Li et al., 2013; Ming et al., 2014). For example, in the study described by Berquin *et al.* (2007), omega-3 fatty acids were found to reduce prostate tumour growth and increase survival in the $PB^{Cre4}Pten^{flox}$ mice by modulating proteins involved in apoptosis. Therefore, $PB^{Cre4}Pten^{flox}$ mice have been used successfully in drug efficacy studies, while $PB^{Cre4}p53^{flox}Rb^{flox}$ mice display genetic features of human prostate cancer that when found in prostate cancer cell lines responded favourably to TMFol intervention.

There are two main factors that could have contributed to the lack of efficacy in the mouse models used in this current study. Firstly, the dose of TMFol used in this study could have been too low to have any meaningful effect on the prostate cancer phenotypes in the mouse models. However, the concentration of TMFol administered in the diet in this study (0.2 %) is identical to that which has been successfully used in all previous *in vivo* xenograft studies with TMFol, where significant efficacy has been observed (Howells et al., 2010; Saad, 2011). Saad (2011) demonstrated that the level of TMFol detected in the prostate tissue of the mice was approximately 6-fold higher than that achievable in the TRAMP C2 xenograft tumour. Therefore, it is unlikely that the level of TMFol uptake in the prostate tissues of the $PB^{Cre4}p53^{flox}Rb^{flox}$ and $PB^{Cre4}Pten^{flox}$ mice had any role in the lack of efficacy of TMFol in these mice. Secondly, if these animal models did not display the genetic or metabolic transformations targeted by TMFol to inhibit growth, then there would similarly be a lack of efficacy. There is no model that accurately represents all of the genetic and metabolic transformations of normal prostate cells to malignant cells in the development and progression of prostate cancer. Among patients there is much molecular variability in prostate tumours. cDNA

microarrays have been used to profile gene expression in primary prostate tumours and have led to the identification of tumour subtypes that require different treatment strategies (Lapointe et al., 2004). Therefore, it is important that the genetic or metabolic targets of chemopreventive/chemotherapeutic agents be present in the prostate tumours to facilitate efficacy. Apart from the genetic basis for prostate cancer development and the histological changes associated with cancer progression, the metabolic features of the PB^{Cre4}p53^{flox}Rb^{flox} and PB^{Cre4}Pten^{flox} models have not been fully characterised. Hence, the metabolic transformations that drive human prostate cancer may not be accurately represented in these models. The most enduring metabolic feature in human prostate cancer is the ZIP1/zinc/citrate relationship previously described in chapter 1 and so far this relationship has only been characterised in the TRAMP prostate cancer mouse model (Costello et al., 2011). From the *in vitro* studies (see chapters 3 and 4), TMFol is capable of modulating ACO2, which is the key enzyme regulating the ZIP1/zinc/citrate relationship of human prostate cancer. The activity of ACO2 is inhibited in normal human prostate but it exhibits high activity in malignant prostate (see chapter 1). As previously outlined in chapter 3, inhibition of ACO2 activity may be an integral part of the inhibitory effect of TMFol on prostate cancer cells. Hence, for TMFol to be effective in mouse models, the ZIP1/zinc/citrate relationship of human prostate cancer must be part of the metabolic feature of the mice. The potential importance of the ZIP1/zinc/citrate relationship for the efficacy of TMFol was not apparent prior to selection of the mouse models and execution of the animal studies. Hence, it is advisable that before embarking on *in vivo* efficacy studies with putative chemopreventive or chemotherapeutic agents in prostate cancer it is essential to thoroughly investigate the potential mechanisms of action *in vitro*, not only for the usual cell cycle, apoptosis and senescence features, but to also include any potential metabolic biomarkers, if there are any previous indicators of metabolic involvement. This would help to ensure that the mouse model with the most appropriate genetic and metabolic features is selected for the specific chemopreventive/chemotherapeutic agent. Unpublished RNA sequencing data from the laboratory of Dr. Sérgio Felisbino in Brazil has subsequently found that the levels of ACO2 mRNA remain unchanged in the prostate of PB^{Cre4}p53^{flox}Rb^{flox} and PB^{Cre4}Pten^{flox} mice as they progressed from the normal to the malignant state (personal communication, Dr. Felisbino). These data support the view that the mouse models used in this current study did not display the necessary metabolic features of human prostate cancer required for TMFol to be

effective. In contrast, TRAMP mice display the desired ZIP1/zinc/citrate relationship and would be worth investigating in any future dietary interventions with TMFol in prostate cancer. Taken together, the lack of efficacy of TMFol in the PB^{Cre4}$p53^{flox}Rb^{flox}$ and PB^{Cre4}$Pten^{flox}$ mouse models in this study may not be a true reflection of its inhibitory activity in prostate cancer but a case of inappropriate mouse model selection for the drug under consideration.

Chapter 6. Final Discussion

Prostate cancer is the second most common malignancy in men worldwide. Generally, prostate cancer has a long latency of progression from the initiation and development of PIN to the invasive form of the disease; PIN is often evident in the 40-50 age group, leading to the malignant form of the disease at around age 70. For many men the premalignant lesions do not progress to the malignant disease but there is no available test to distinguish between tumours that are indolent and those that are aggressive. The highly heterogeneous nature of prostate cancer has made it difficult to accurately identify biomarkers that can distinguish indolent from aggressive disease at an early stage in the pathogenesis of prostate cancer.

In the management of this disease, several treatment regimens are in use, including prostatectomy, radiotherapy, hormonal therapy and chemotherapy. High morbidity and cost are associated with these treatment protocols. For reasons previously highlighted (see chapter 1) prostate cancer is a suitable candidate for chemoprevention. Several nutritional and pharmaceutical interventions have been tested but none have been approved for prostate cancer chemoprevention. Hence, there is a need for the development and use of novel agents in the management of prostate cancer. Flavonoids and their synthetic analogues have been identified as a potential source of putative prostate cancer chemopreventive/chemotherapeutic agents. TMFol, a synthetic analogue of the dietary flavonol quercetin, has demonstrated potent anti-cancer effects in some prostate models, in comparison to its dietary congener (Saad, 2011), but the mechanisms used to generate these effects have not been systematically analysed. Therefore, the research undertaken in this thesis was designed to:

1. Identify the mechanisms of growth inhibition induced by TMFol in prostate cancer cells
2. Determine the effects of TMFol on prostate cancer metabolism
3. Examine the effects of TMFol as a potential chemopreventive/chemotherapeutic agent in two transgenic mouse models of prostate cancer, $PB^{Cre4}p53^{flox}Rb^{flox}$ and $PB^{Cre4} Pten^{flox}$.

As part of the preclinical evaluation of potential chemopreventive/chemotherapeutic agents, it is important to assess the impact of these agents on normal cells. The work

described in chapter 3 shows that the immortalised normal human prostate epithelial cells (PNT2) were only slightly less sensitive to the anti-proliferative effects of TMFol when compared to the malignant 22Rv1 and PC-3 cells. This is unlike its dietary congeners, quercetin and fisetin, which have been suggested not to cause any quantifiable growth inhibition in normal prostate epithelial cells (Aalinkeel et al., 2008; Haddad et al., 2006; Khan et al., 2008). Rather, the activity of TMFol resembles that of the soy isoflavone genistein and equol, the biologically active metabolite of another soy isoflavone daidzein (Hedlund et al., 2003). Reasons for this are unknown and it is unlikely to be explained by any structure-activity relationship, since TMFol is methylated while the isoflavones are not methylated. Both genistein and equol can be found in high concentrations in the serum or prostatic fluid of men after consumption of a soy-rich diet. A high-soy diet, and by extension, high levels of equol and genistein are believed to be a major reason for the low incidence of prostate cancer among Asians (Akaza et al., 2004; Hsing et al., 2000; Hedlund et al., 2003). Interestingly, these two isoflavonoids, at concentrations found in the serum or prostatic fluid of Asians consuming a traditional soy-rich diet, significantly inhibit the proliferation of both normal and malignant prostate epithelial cells (Hedlund et al., 2003, Rao et al., 2002). This growth inhibition is also evident in *in vivo* studies and is not associated with any adverse side effects in mice (Lund et al., 2004; Wang et al., 2007). Since the proliferation of normal or benign prostatic cells could increase the risk of oncogenic events, including the inactivation or loss of tumour suppressor genes (Preston-Martin et al., 1993), an anti-proliferative effect on normal prostate epithelial cells could reduce the risk of malignancy. Therefore, the investigation into TMFol as a potential agent in the management of prostate cancer was continued.

The p53 tumour suppressor gene is often mutated in prostate cancer (Gumerlock et al., 1997). Therefore, it is important that chemopreventive/chemotherapeutic agents can inhibit the growth of prostate cancer cells independent of their p53 status. The experiments outlined in chapter 3 suggest that TMFol may exert its anti-prostate cancer activity through p53-independent mechanisms. TMFol caused S-phase arrest in the p53-deficient PC-3 cells. p53 is only critical for growth arrest in G1 and G2/M, but not in S phase arrest (Agarwal et al., 1995). Furthermore, the PNT2 cells were arrested in S phase, but the expression of p53 initially remained unchanged and then decreased significantly. Hence, p53 involvement is not suspected here. The cell cycle genes that

are modulated by TMFol should be analysed in future experiments to determine how cell cycle arrest is achieved. The 22Rv1 prostate cancer cells which displayed a significant upregulation of p53 expression at all of the time points in response to TMFol intervention, showed no signs of cell cycle arrest. The proliferative potential of the S phase arrested cells after the removal of TMFol was not measured in chapter 3 and should be investigated in the future to determine if the cell cycle arrest is reversible or not. Instead, SA-β-galactosidase activity was measured to determine if TMFol induced senescence as a potential antiproliferative mechanism. If the significant increase in SA-β-galactosidase activity seen in the PC-3 cells is indeed a reliable indicator of senescence, one may deduce that TMFol again engages a p53-independent mechanism to induce growth arrest.

A prominent characteristic of many dietary flavonoids such as quercetin and their synthetic analogues, is the ability to induce apoptosis in cancer cells (Aalinkeel et al., 2008; Haddad et al., 2010). However, TMFol did not induce apoptosis in prostate cancer cells *in vitro*. In contrast, in the 22Rv1 *in vivo* model, TMFol caused a significant increase in the proportion of cells expressing the apoptosis indicator cleaved caspase-3. It was proposed in chapter 4 that TMFol may have the potential to trigger an increase in the uptake of zinc, which can induce apoptosis. The level of zinc in the growth medium of the cells was too low to facilitate the induction of apoptosis but was more than sufficient in the 22Rv1 xenografts. Hence, the *in vitro* system appears inadequate for creating the necessary environment that could result in TMFol-induced apoptosis in the cancer cells. It is interesting to note that the 22Rv1 prostate cancer cells were the most sensitive to the growth inhibitory effect of TMFol *in vitro* whilst they were resistant to TMFol-induced cell cycle arrest and apoptosis. Therefore, other growth inhibitory mechanisms seem to be involved in mediating the *in vitro* anti-proliferative effect of TMFol.

Targeting cancer cell metabolism is a relatively recent area of research in cancer chemoprevention/chemotherapy. Hence, studies exploring the ability of dietary flavonoids to modulate metabolic pathways are on the increase. As a consequence, it was realised that the inhibitory effect of quercetin on the proliferation of prostate cancer cells is due in part to the downregulation of ACC and FAS (Noori-Daloii et al., 2011). The investigation of TMFol described here suggests that it is also capable of

downregulating the expression of ACC at the level of protein and mRNA. Once again, the PC-3 cells were more sensitive, exhibiting enhanced downregulation of ACC compared to the 22Rv1 cells. While p53 has been shown to modulate fatty acid metabolism via a number of pathways (Puzio-Kuter, 2011), some therapeutic agents can modulate the metabolism without p53 involvement (Guseva et al., 2011). The work conducted in this current study indicates that mechanisms used by TMFol seem to be more striking in prostate cancer cells lacking p53, tentatively hinting at the possibility that TMFol might be effective against prostate cancers with p53 mutations.

Precision medicine in cancer is a recent and growing practice which tries to optimise treatment strategies based on genetic classification of the cancer. There is much genetic variation among the prostate tumours of patients. Much of the focus has been on the typical genomic alterations including *Rb*, *Pten* and *AR* (Roychowdhury and Chinnaiyan, 2013). Classification of the metabolic features has not been a priority despite the fact that downregulation of zinc transporters is a persistent feature in prostate cancer cells and that it correlates with the decline in zinc levels, the increase in ACO2 activity and prostate malignancy (Costello et al., 1997; Desouki et al., 2007; Franklin et al., 2005; Rishi et al., 2003). TMFol has the unique ability to significantly reduce ACO2 in prostate cancer cells *in vitro* (see chapter 4). This places TMFol in a position where it can potentially inhibit the growth of prostate tumours regardless of its other genetic features. Whether TMFol directly inhibits ACO2 or increases the expression of zinc transporters so that there is an increase in zinc uptake to inhibit ACO2, is not yet known. Therefore, determination of this mechanism should be a priority in future experiments.

Arguably, the most striking result described in chapter 4 is the ability of TMFol to inhibit ACO2 expression and activity. The increase in ACO2 activity is a persistent hallmark of prostate cancer and according to the literature, no dietary flavonoid or synthetic analogue has previously demonstrated an ability to inhibit ACO2 activity in prostate cancer cells. 22Rv1 cells did not demonstrably undergo apoptosis or cell cycle arrest, yet were found to be the most sensitive to inhibition of ACO2 activity. It is very likely that this is a major mechanism accounting for the anti-proliferative activity of TMFol. Whether or not p53 is involved in triggering this mechanism is unknown as both p53 deficient and p53 wild type cells were similarly affected by TMFol. This

appears to be a unique mechanism of TMFol as it modulates a characteristic that is prostate specific. The inhibition of ACO2 activity essentially halts citrate oxidation and potentially could result in a cascade of changes in connected signalling pathways that ultimately inhibits growth or triggers cell death (Zinchenko et al., 2007). Nevertheless, in normal prostate cells ACO2 is inactivated (Costello et al., 1996; Liu et al 1996) but inactivation of ACO2 has been shown to inhibit the growth of prostate cancer cells (Juang, 2004). The previous mouse xenograft studies and the current transgenic studies with TMFol suggest the possibility that inhibition of ACO2 activity induced by TMFol is prostate specific. One may argue that without this specificity the animals in the treatment groups would have most likely died at a faster rate than the control mice. This did not happen in any of the *in vivo* studies. Therefore, the ability of TMFol to inhibit ACO2 activity in prostate cancer cells may well be a specific mechanistic feature that should be investigated further for potential use of TMFol as a single agent or in combination with other chemopreventive/chemotherapeutic agents.

Chapter 5 of this study attempted to demonstrate the *in vivo* efficacy of TMFol in two separate transgenic mouse models of prostate cancer. Despite convincing evidence for efficacy of TMFol in prostate xenograft models, and evidence for its accumulation in prostatic tissue, no efficacy was observed in the chosen transgenic mouse models. Whilst this is clearly not a positive outcome, as discussed in chapter 5, the transgenic models did not demonstrate the metabolic feature that is now believed to be essential for the *in vivo* efficacy of TMFol. Nevertheless, future *in vivo* efficacy studies should be considered using the TRAMP mouse as an alternative and potentially more appropriate model. Such studies should incorporate experiments to identify the optimum dosing protocol and to measure chronic toxicity, so that TMFol is not prematurely disregarded as a potential chemopreventive/chemotherapeutic agent for prostate cancer.

The findings outlined in this thesis demonstrate the potential mechanisms through which TMFol can inhibit the growth of prostate cancer cells and also highlight the challenges associated with the preclinical evaluation of putative chemopreventive/chemotherapeutic agents for prostate cancer. The findings of this study can be summarised in the schematic diagram below (Figure 6.1).
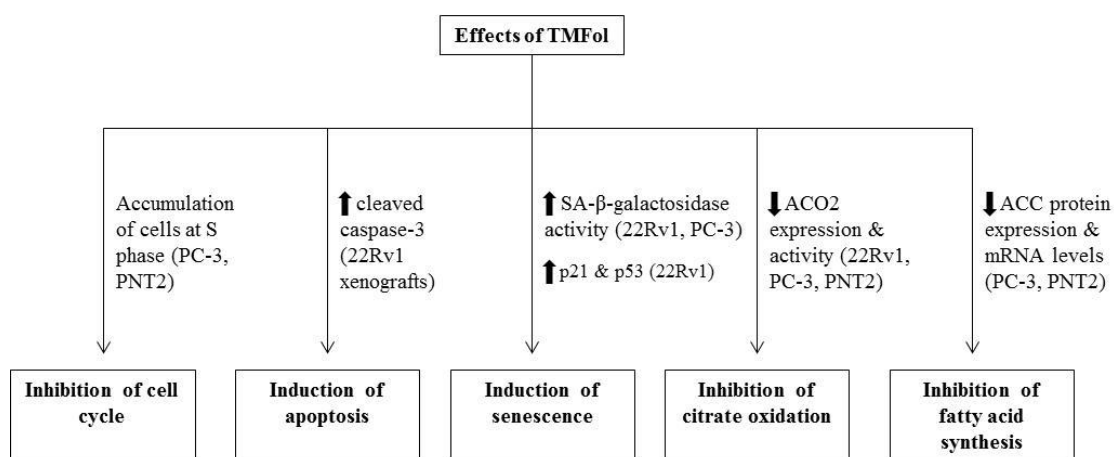
Figure 6.1: Schematic diagram summarising the potential mechanisms of action used by TMFol in the inhibition of prostate cancer. The cell signalling or metabolic pathways that are potentially induced or inhibited upon exposure to TMFol can inhibit the proliferation of prostate cancer.

The changes identified in the prostate cancer cells in response to TMFol exposure affect cell cycle progression, apoptosis, senescence, fatty acid synthesis and citrate oxidation, in ways that could inhibit the proliferation of prostate cancer (Figure 6.1). However, it is important that specific *in vitro* and *in vivo* experiments discussed throughout this thesis be pursued to establish the significance of each mechanism in the inhibition of prostate cancer. Therefore, in conclusion, TMFol exhibits some mechanistic features that could be beneficial in the chemoprevention/chemotherapy of prostate cancer, but further evaluation will determine the future of TMFol in the management of human prostate cancer.

References

Aalinkeel, R., Bindukumar, B., Reynolds, J. L., Sykes, D. E., Mahajan, S. D*., et al.* (2008). The dietary bioflavonoid, quercetin, selectively induces apoptosis of prostate cancer cells by down-regulating the expression of heat shock protein 90. *Prostate,* 68**:** 1773-89.

Aaltomaa, S., Lipponen, P., Eskelinen, M., Ala-Opas, M. & Kosma, V. M. (1999). Prognostic value and expression of p21(waf1-cip1) protein in prostate cancer. *Prostate,* 39**:** 8-15.

Abrahamsson, P. (1999). Neuroendocrine differentiation in prostatic carcinoma. *Prostate,* 39**:** 135-148.

Abremski, K. & Hoess, R. (1984). Bacteriophage P1 site-specific recombination. Purification and properties of the Cre recombinase protein. *J Biol Chem,* 259**:** 1509-1514.

Adhami, V. M., Malik, A., Zaman, N., Sarfaraz, S., Siddiqui, I. A*., et al.* (2007). Combined inhibitory effects of green tea polyphenols and selective cyclooxygenase-2 inhibitors on the growth of human prostate cancer cells both in vitro and in vivo. *Clin Cancer Res,* 13**:** 1611-9.

Adhami, V. M., Siddiqui, I. A., Sarfaraz, S., Khwaja, S. I., Hafeez, B. B*., et al.* (2009). Effective prostate cancer chemopreventive intervention with green tea polyphenols in the TRAMP model depends on the stage of the disease. *Clin Cancer Res,* 15**:** 1947-53.

Agarwal, M. L., Agarwal, A., Taylor, W. & Stark, G. R. (1995). p53 controls both the G2/M and the G1 cell cycle checkpoints and mediates reversible growth arrest in human fibroblasts. *Proc. Natl. Acad. Sci. USA,* 92**:** 8493-8497.

Ahmad, I., Sansom, O. J. & Leung, H. Y. (2008). Advances in mouse models of prostate cancer. *Expert Rev Mol Med,* 10**:** e16.

Ahmad, N., Feyes, D. K., Nieminen, A.-L., Agarwal, R. & Mukhtar, H. (1997). Green tea constituent epigallocatechin-3-gallate and induction of apoptosis and cell cycle arrest in human carcinoma cells. *J Natl Cancer Inst,* 89**:** 1881-1886.

Ahuja, D., Saenz-Robles, M. T. & Pipas, J. M. (2005). SV40 large T antigen targets multiple cellular pathways to elicit cellular transformation. *Oncogene,* 24**:** 7729-45.

Akaza, H., Miyanaga, N., Takashima, N., Naito, S., Hirao, Y*., et al.* (2004). Comparisons of percent equol producers between prostate cancer patients and controls:

case-controlled studies of isoflavones in Japanese, Korean and American residents. *Jpn J Clin Oncol,* 34**:** 86-89.

Albrecht, D. S., Clubbs, E. A., Ferruzzi, M. & Bomser, J. A. (2008). Epigallocatechin-3-gallate (EGCG) inhibits PC-3 prostate cancer cell proliferation via MEK-independent ERK1/2 activation. *Chem Biol Interact,* 171**:** 89-95.

American Cancer Society, 2015. *Prostate cancer* [Online]. Available: http://www.cancer.org/cancer/prostatecancer/ [Accessed 03/09/2015].

Amling, G., Blute, M. L., E.J., B., Seay, T. M., Slezak, J.*, et al.* (2000). Long-term hazard of progression after radical prostatectomy for clinically localized prostate cancer: continued risk of biochemical failure after 5 years. *J Urol,* 164**:** 101-105.

Anai, S., Goodison, S., Shiverick, K., Iczkowski, K., Tanaka, M.*, et al.* (2006). Combination of PTEN Gene Therapy and Radiation Inhibits the Growth of Human Prostate Cancer Xenografts. *Hum Gene Ther,* 17**:** 975-984.

Andriole, G. L., Bostwick, D. G., Brawley, O. W., Gomella, L. G., Marberger, M.*, et al.* (2010). Effect of Dutasteride on the Risk of Prostate Cancer. *N Engl J Med,* 362**:** 1192-1202.

Andriole, G. L., Crawford, E. D., Grubb III, R. L., Buys, S. S., Chia, D.*, et al.* (2009). Mortality results from a randomized prostate-cancer screening trial. *N Engl J Med,* 360**:** 1310-1319.

Applewhite, J. C., Matlaga, B. R., Mccullough, D. L. & Hall, M. C. (2001). Transrectal ultrasound and biopsy in the early diagnosis of prostate cancer. *Cancer Control,* 8**:** 141-150.

Arellano, M. & Moreno, S. (1997). Regulation of CDK/cyclin complexes during the cell cycle. *Int J Biochem Cell Biol,* 29**:** 559-573.

Azvolinsky, A. (2014). Repurposing to fight cancer: the metformin-prostate cancer connection. *J Natl Cancer Inst,* 106**:** dju030.

Azzouni, F., Godoy, A., Li, Y. & Mohler, J. (2012). The 5 alpha-reductase isozyme family: a review of basic biology and their role in human diseases. *Adv Urol,* 2012**:** 530121.

Badal, V., Ménendez, S., Coomber, D. & Lane, D. P. (2014). Regulation of the p14ARF promoter by DNA methylation. *Cell Cycle,* 7**:** 112-119.

Bartholomew, J. N., Volonte, D. & Galbiati, F. (2009). Caveolin-1 regulates the antagonistic pleiotropic properties of cellular senescence through a novel Mdm2/p53-mediated pathway. *Cancer Res,* 69**:** 2878-86.

166

Bauer, D. E., Hatzivassiliou, G., Zhao, F., Andreadis, C. & Thompson, C. B. (2005). ATP citrate lyase is an important component of cell growth and transformation. *Oncogene,* 24**:** 6314-22.

Beauséjour, C. M., Krtolica, A., Galimi, F., Narita, M., Lowe, S. W*., et al.* (2003). Reversal of human cellular senescence: roles of the p53 and p16 pathways. *EMBO J,* 22**:** 4212-4222.

Beckers, A., Organe, S., Timmermans, L., Scheys, K., Peeters, A*., et al.* (2007). Chemical inhibition of acetyl-CoA carboxylase induces growth arrest and cytotoxicity selectively in cancer cells. *Cancer Res,* 67**:** 8180-7.

Ben Sghaier, M., Skandrani, I., Nasr, N., Franca, M. G., Chekir-Ghedira, L*., et al.* (2011). Flavonoids and sesquiterpenes from Tecurium ramosissimum promote antiproliferation of human cancer cells and enhance antioxidant activity: a structure-activity relationship study. *Environ Toxicol Pharmacol,* 32**:** 336-48.

Ben-Porath, I. & Weinberg, R. A. (2005). The signals and pathways activating cellular senescence. *Int J Biochem Cell Biol,* 37**:** 961-76.

Ben-Shlomo, Y., Evans, S., Ibrahim, F., Patel, B., Anson, K*., et al.* (2008). The risk of prostate cancer amongst black men in the United Kingdom: the PROCESS cohort study. *Eur Urol,* 53**:** 99-105.

Berger, A. H. & Pandolfi, P. P. (2011). Haplo-insufficiency: a driving force in cancer. *J Pathol,* 223**:** 137-46.

Bernardes De Jesus, B. & Blasco, M. A. (2012). Assessing cell and organ senescence biomarkers. *Circ Res,* 111**:** 97-109.

Bernstein, C., Holubec, H., Bhattacharyya, A. K., Nguyen, H., Payne, C. M., et al. (2011). Carcinogenicity of deoxycholate, a secondary bile acid. *Arch Toxicol,* 85: 863-71.

Berquin, I. M., Min, Y., Wu, R., Wu, J., Perry, D*., et al.* (2007). Modulation of prostate cancer genetic risk by omega-3 and omega-6 fatty acids. *J Clin Invest.,* 117**:** 1866-1875.

Berthon, P., Cussenot, O., Hopwood, L., Leduc, A. & Maitland, N. J. (1995). Functional expression of sv40 in normal human prostatic epithelial and fibroblastic cells - differentiation pattern of nontumorigenic cell-lines. *Int J Oncol.,* 6**:** 333-343.

Bettuzzi, S., Brausi, M., Rizzi, F., Castagnetti, G., Peracchia, G*., et al.* (2006). Chemoprevention of human prostate cancer by oral administration of green tea catechins in volunteers with high-grade prostate intraepithelial neoplasia: a preliminary report from a one-year proof-of-principle study. *Cancer Res,* 66**:** 1234-40.

Bhavsar, A. & Verma, S. (2014). Anatomic imaging of the prostate. *Biomed Res Int,* 2014**:** 728539.

Bishara, T., Ramnani, D. M. & Epstein, J. I. (2004). High-grade prostatic intraepithelial neoplasia on needle biopsy. Risk of cancer on repeat biopsy related to number of involved cores and morphologic pattern. *Am J Surg Pathol,* 28**:** 629-633.

Biswas, S., Lunec, J. & Bartlett, K. (2012). Non-glucose metabolism in cancer cells--is it all in the fat? *Cancer Metastasis Rev,* 31**:** 689-98.

Bokhorst, L. P., Bangma, C. H., Van Leenders, G. J., Lous, J. J., Moss, S. M.*, et al.* (2014). Prostate-specific antigen-based prostate cancer screening: reduction of prostate cancer mortality after correction for nonattendance and contamination in the Rotterdam section of the European Randomized Study of Screening for Prostate Cancer. *Eur Urol,* 65**:** 329-36.

Bolla, M., Van Tienhoven, G., Warde, P., Dubois, J. B., Mirimanoff, R.-O.*, et al.* (2010). External irradiation with or without long-term androgen suppression for prostate cancer with high metastatic risk: 10-year results of an EORTC randomised study. *The Lancet Oncology,* 11**:** 1066-1073.

Bradford, T. J., Tomlins, S. A., Wang, X. & Chinnaiyan, A. M. (2006). Molecular markers of prostate cancer. *Urol Oncol,* 24**:** 538-51.

Brausi, M., Rizzi, F. & Bettuzzi, S. (2008). Chemoprevention of human prostate cancer by green tea catechins: two years later. A follow-up update. *Eur Urol,* 54**:** 472-3.

Brawer, M. K. (2005). Prostatic intraepithelial neoplasia: an overview. *Rev Urol,* 7**:** S11-S18.

Brawley, O. W. & Barnes, S. T. (2001). Potential Agents for Prostate Cancer Chemoprevention. *Epidemiol Rev,* 23**:** 168-172.

Bray, F., Lortet-Tieulent, J., Ferlay, J., Forman, D. & Auvinen, A. (2010). Prostate cancer incidence and mortality trends in 37 European countries: an overview. *Eur J Cancer,* 46**:** 3040-52.

Brehm, A., Miska, E. A., Mccance, D. J., Reid, J. L., Bannister, A. J.*, et al.* (1998). Retinoblastoma protein recruits histone deacetylase to repress transcription. *Nature,* 39**:** 597-601.

Bringold, F. & Serrano, M. (2000). Tumor suppressors and oncogenes in cellular senescence. *Exp Gerontol,* 35**:** 317-329.

Britton, R. G., Fong, I., Saad, S., Brown, K., Steward, W. P.*, et al.* (2009). Synthesis of the flavonoid 3',4',5'-trimethoxyflavonol and its determination in plasma and tissues of

mice by HPLC with fluorescence detection. *J Chromatogr B Analyt Technol Biomed Life Sci,* 877**:** 939-42.

Britton, R. G., Horner-Glister, E., Pomenya, O. A., Smith, E. E., Denton, R.*, et al.* (2012). Synthesis and biological evaluation of novel flavonols as potential anti-prostate cancer agents. *Eur J Med Chem,* 54**:** 952-8.

Brusselmans, K., De Schrijver, E., Verhoeven, G. & Swinnen, J. V. (2005a). RNA interference-mediated silencing of the acetyl-CoA-carboxylase-alpha gene induces growth inhibition and apoptosis of prostate cancer cells. *Cancer Res,* 65**:** 6719-25.

Brusselmans, K., Vrolix, R., Verhoeven, G. & Swinnen, J. V. (2005a). Induction of cancer cell apoptosis by flavonoids is associated with their ability to inhibit fatty acid synthase activity. *J Biol Chem,* 280**:** 5636-45.

Burton, D. G., Giribaldi, M. G., Munoz, A., Halvorsen, K., Patel, A.*, et al.* (2013). Androgen deprivation-induced senescence promotes outgrowth of androgen-refractory prostate cancer cells. *PLoS One,* 8**:** e68003.

Cai, H., Sale, S., Schmid, R., Britton, R. G., Brown, K.*, et al.* (2009). Flavones as colorectal cancer chemopreventive agents--phenol-o-methylation enhances efficacy. *Cancer Prev Res (Phila),* 2**:** 743-50.

Campisi, J. & D'adda Di Fagagna, F. (2007). Cellular senescence: when bad things happen to good cells. *Nat Rev Mol Cell Biol,* 8**:** 729-40.

Campisi, J. (2001). Cellular senescence as a tumor-suppressor mechanism. *Trends Cell Biol,* 11**:** S27-31.

Cancer Research UK, 2014a. *Prostate cancer* [Online]. Available: http://www.cancerresearchuk.org/health-professional/cancer-statistics/worldwide-cancer [Accessed 03/09/2015].

Cancer Research UK 2014b. *Prostate cancer statistics* [Online]. Available: http://www.cancerresearchuk.org/health-professional/cancer-statistics/statistics-by-cancer-type/prostate-cancer [Accessed 05/03/2015].

Cantor, J. R. & Sabatini, D. M. (2012). Cancer cell metabolism: one hallmark, many faces. *Cancer Discov,* 2**:** 881-98.

Cao, Y. & Ma, J. (2011). Body mass index, prostate cancer-specific mortality, and biochemical recurrence: a systematic review and meta-analysis. *Cancer Prev Res (Phila),* 4**:** 486-501.

Capecchi, M. R. (1994). Targeted gene replacement. *Sci Am,* 270**:** 52-59.

Carracedo, A., Cantley, L. C. & Pandolfi, P. P. (2013). Cancer metabolism: fatty acid oxidation in the limelight. *Nat Rev Cancer,* 13**:** 227-32.

Carter, B. S., Beaty, T. H., Steinberg, G. D., Childs, B. & Walsh, P. C. (1992). Mendelian inheritance of familial prostate cancer. *Proc Natl Acad Sci U S A,* 89**:** 3367-3371.

Carter, H. B., Albertsen, P. C., Barry, M. J., Etzioni, R., Freedland, S. J*., et al.* 2013. Early detection of prostate cancer: AUA guideline [Online]. Available: http://www.auanet.org.

Catz, S. D. & Johnson, J. L. (2003). BCL-2 in prostate cancer: a minireview. *Apoptosis,* 8**:** 29-37.

Chan, J. M., Stampfer, M. J., Ma, J., Rimm, E. B., Willett, W. C*., et al.* (1999). Supplemental vitamin E intake and prostate cancer risk in a large cohort of men in the United States. *Cancer Epidemiol Biomarkers Prev,* 8**:** 893-899.

Chandler, J. D., Williams, E. D., Slavin, J. L., Best, J. D. & Rogers, S. (2003). Expression and localization of GLUT1 and GLUT12 in prostate carcinoma. *Cancer,* 97**:** 2035-42.

Chen, D., Banerjee, S., Cui, Q. C., Kong, D., Sarkar, F. H*., et al.* (2012). Activation of AMP-activated protein kinase by 3,3'-Diindolylmethane (DIM) is associated with human prostate cancer cell death in vitro and in vivo. *PLoS One,* 7**:** e47186.

Chen, Y. C., Page, J. H., Chen, R. & Giovannucci, E. (2008). Family history of prostate and breast cancer and the risk of prostate cancer in the PSA era. *Prostate,* 68**:** 1582-91.

Chen, Z., Trotman, L. C., Shaffer, D., Lin, H. K., Dotan, Z. A*., et al.* (2005). Crucial role of p53-dependent cellular senescence in suppression of Pten-deficient tumorigenesis. *Nature,* 436**:** 725-30.

Chhipa, R. R., Wu, Y., Mohler, J. L. & Ip, C. (2010). Survival advantage of AMPK activation to androgen-independent prostate cancer cells during energy stress. *Cell Signal,* 22**:** 1554-61.

Chien, C. S., Shen, K. H., Huang, J. S., Ko, S. C. & Shih, Y. W. (2010). Antimetastatic potential of fisetin involves inactivation of the PI3K/Akt and JNK signaling pathways with downregulation of MMP-2/9 expressions in prostate cancer PC-3 cells. *Mol Cell Biochem,* 333**:** 169-80.

Chiu, F. L. & Lin, J. K. (2008). Downregulation of androgen receptor expression by luteolin causes inhibition of cell proliferation and induction of apoptosis in human prostate cancer cells and xenografts. *Prostate,* 68**:** 61-71.

Choan, E., Segal, R., Jonker, D., Malone, S., Reaume, N.*, et al.* (2005). A prospective clinical trial of green tea for hormone refractory prostate cancer: an evaluation of the complementary/alternative therapy approach. *Urol Oncol,* 23**:** 108-13.

Choi, J., Shendrik, I., Peacocke, M., Peehl, D., Buttyan, R.*, et al.* (2000). Expression of senescence-associated beta-galactosidase in enlarged prostates from men with benign prostatic hyperplasia. *Urology,* 56**:** 160-166.

Chueh, F. Y., Leong, K. F., Cronk, R. J., Venkitachalam, S., Pabich, S.*, et al.* (2011). Nuclear localization of pyruvate dehydrogenase complex-E2 (PDC-E2), a mitochondrial enzyme, and its role in signal transducer and activator of transcription 5 (STAT5)-dependent gene transcription. *Cell Signal,* 23**:** 1170-8.

Chuu, C. P., Chen, R. Y., Kokontis, J. M., Hiipakka, R. A. & Liao, S. (2009). Suppression of androgen receptor signaling and prostate specific antigen expression by (-)-epigallocatechin-3-gallate in different progression stages of LNCaP prostate cancer cells. *Cancer Lett,* 275**:** 86-92.

Clark, L. C., Dalkin, B., Krongrad, A., Combs, G. F., Turnbull, B. W.*, et al.* (1998). Decreased incidence of prostate cancer with selenium supplementation: results of a double-blind cancer prevention trial. *Br J Urol,* 81**:** 730-734.

Collado, M., Gil, J., Efeyan, A., Guerra, C., Schuhmacher, A. J.*, et al.* (2005). Tumour biology: senescence in premalignant tumours. *Nature,* 436**:** 642.

Cooney, K. A., Wetzel, J. C., Merajver, S. D., Macoska, J. A., Singleton, T. P.*, et al.* (1996). Distinct Regions of Allelic Loss on 13q in Prostate Cancer. *Cancer Res,* 56**:** 1142-1145.

Cooper, G. M. 2000. The development and causes of cancer. *In: The cell: A molecular Approach. 2nd edition.* Sunderland, MA: Sinauer Associates.

Coppe, J. P., Kauser, K., Campisi, J. & Beausejour, C. M. (2006). Secretion of vascular endothelial growth factor by primary human fibroblasts at senescence. *J Biol Chem,* 281**:** 29568-74.

Coppe, J. P., Patil, C. K., Rodier, F., Sun, Y., Munoz, D. P.*, et al.* (2008). Senescence-associated secretory phenotypes reveal cell-nonautonomous functions of oncogenic RAS and the p53 tumor suppressor. *PLoS Biol,* 6**:** 2853-68.

Coppé, J.-P., Patil, C. K., Rodier, F., Krtolica, A., Beauséjour, C. M.*, et al.* (2010). A Human-Like Senescence-Associated Secretory Phenotype Is Conserved in Mouse Cells Dependent on Physiological Oxygen. *PLoS One,* 5**:** e9188.

Corcoran, M. P., Mckay, D. L. & Blumberg, J. B. (2012*)*. Flavonoid basics: chemistry, sources, mechanisms of action, and safety. *J Nutr Gerontol Geriatr,* 31**:** 176-89.

COSMIC, 2015. *Prostate cancer* [Online]. Available: http://cancer.sanger.ac.uk/cosmic [Accessed 03/09/2015].

Costello, L. C. & Franklin, R. B. (1989). Prostate epithelial cells utilize glucose and aspartate as the carbon sources for net citrate production. *Prostate,* 15**:** 335-342.

Costello, L. C. & Franklin, R. B. (1998). Novel role of zinc in the regulation of prostate citrate metabolism and its implications in prostate cancer. *Prostate,* 35**:** 285-296.

Costello, L. C. & Franklin, R. B. (2000). The intermediary metabolism of the prostate: A key to understanding the pathogenesis and progression of prostate malignancy. *Oncology,* 59**:** 269-282.

Costello, L. C. & Franklin, R. B. (2006). The clinical relevance of the metabolism of prostate cancer; zinc and tumor suppression: connecting the dots. *Mol Cancer,* 5**:** 17.

Costello, L. C., Feng, P., Milon, B., Tan, M. & Franklin, R. B. (2004). Role of zinc in the pathogenesis and treatment of prostate cancer: critical issues to resolve. *Prostate Cancer Prostatic Dis,* 7**:** 111-7.

Costello, L. C., Franklin, R. B. & Feng, P. (2005). Mitochondrial function, zinc, and intermediary metabolism relationships in normal prostate and prostate cancer. *Mitochondrion,* 5**:** 143-53.

Costello, L. C., Franklin, R. B. & Narayan, P. (1999). Citrate in the Diagnosis of Prostate Cancer. *Prostate,* 38**:** 237-245.

Costello, L. C., Franklin, R. B., Zou, J., Feng, P., Bok, R.*, et al.* (2011). Human prostate cancer ZIP1/zinc/citrate genetic/metabolic relationship in the TRAMP prostate cancer animal model. *Cancer Biol Ther,* 12**:** 1078-84.

Costello, L. C., Guan, Z., Kukoyi, B., Feng, P. & Franklin, R. B. (2004). Terminal oxidation and the effects of zinc in prostate versus liver mitochondria. *Mitochondrion,* 4**:** 331-8.

Costello, L. C., Liu, Y. & Franklin, R. B. (1996). Testosterone and prolactin stimulation of mitochondrial aconitase in pig prostate epithelial cells. *Urology,* 48**:** 654-659.

Costello, L. C., Liu, Y., Franklin, R. B. & Kennedy, M. C. (1997). Zinc Inhibition of Mitochondrial Aconitase and Its Importance in Citrate Metabolism of Prostate Epithelial Cells. *J. Biol. Chem.,* 272**:** 28875-28881.

Critz, F. A., Benton, J. B., Shrake, P. & Merlin, M. L. (2013). 25-Year disease-free survival rate after irradiation for prostate cancer calculated with the prostate specific antigen definition of recurrence used for radical prostatectomy. *J Urol,* 189**:** 878-883.

Cross, A. J. & Sinha, R. (2004). Meat-related mutagens/carcinogens in the etiology of colorectal cancer. *Environ Mol Mutagen,* 44**:** 44-55.

Cross, A. J., Peters, U., Kirsh, V. A., Andriole, G. L., Reding, D.*, et al.* (2005). A prospective study of meat and meat mutagens and prostate cancer risk. *Cancer Res,* 65**:** 11779-84.

Crowell, J. A. (2005). The chemopreventive agent development research program in the Division of Cancer Prevention of the US National Cancer Institute: an overview. *Eur J Cancer,* 41**:** 1889-910.

Cunningham, F. H., Fiebelkorn, S., Johnson, M. & Meredith, C. (2011). A novel application of the Margin of Exposure approach: segregation of tobacco smoke toxicants. *Food Chem Toxicol,* 49: 2921-33.

Currie, E., Schulze, A., Zechner, R., Walther, T. C. & Farese, R. V., Jr. (2013). Cellular fatty acid metabolism and cancer. *Cell Metab,* 18**:** 153-61.

Dahan, A. & Altman, H. (2004). Food-drug interaction: grapefruit juice augments drug bioavailability--mechanism, extent and relevance. *Eur J Clin Nutr,* 58**:** 1-9.

Dakubo, G. D., Parr, R. L., Costello, L. C., Franklin, R. B. & Thayer, R. E. (2006). Altered metabolism and mitochondrial genome in prostate cancer. *J Clin Pathol,* 59**:** 10-6.

D'amico, A. V., Chen, M.-H., Renshaw, A. A., Loffredo, M. & Kantoff, P. W. (2008). Androgen suppression and radiation vs radiation alone for prostate cancer A randomized trial. *JAMA,* 299**:** 289-295.

D'amico, A. V., Whittington, R., Malkowicz, B., Schultz, D., Blank, K.*, et al.* (1998). Biochemical outcome after radical prostatectomy, external beam radiation therapy, or interstitial radiation therapy for clinically localized prostate cancer. *JAMA,* 280**:** 969-974.

Dang, C. V. & Semenza, G. L. (1999). Oncogenic alterations of metabolism. *Trends Biochem Sci,* 24**:** 68-72.

Dang, C. V. (2012). Links between metabolism and cancer. *Genes Dev,* 26**:** 877-90.

De Kok, J. B., Verhaegh, G. W., Roelofs, R. W., Hessels, D., Kiemeney, L. A.*, et al.* (2002). DD3(PCA3), a very sensitive and specific marker to detect prostate tumors. *Cancer Res,* 62**:** 2695-2698.

De Schrijver, E., Brusselmans, K., Heyns, W., Verhoeven, G. & Swinnen, J. V. (2003). RNA interference-mediated silencing of the fatty acid synthase gene attenuates growth and induces morphological changes and apoptosis of LNCaP prostate cancer cells. *Cancer Res,* 63**:** 3799-3804.

De Stefani, E., Deneo-Pellegrini, H., Boffetta, P., Ronco, A. & Mendilaharsu, M. (2000). α-Linolenic Acid and Risk of Prostate Cancer: A Case-Control Study in Uruguay. *Cancer Epidemiol Biomarkers Prev,* 9**:** 335-338.

Debacq-Chainiaux, F., Erusalimsky, J. D., Campisi, J. & Toussaint, O. (2009). Protocols to detect senescence-associated beta-galactosidase (SA-betagal) activity, a biomarker of senescent cells in culture and in vivo. *Nat Protoc,* 4**:** 1798-806.

Deberardinis, R. J., Lum, J. J., Hatzivassiliou, G. & Thompson, C. B. (2008). The biology of cancer: metabolic reprogramming fuels cell growth and proliferation. *Cell Metab,* 7**:** 11-20.

Desouki, M. M., Geradts, J., Milon, B., Franklin, R. B. & Costello, L. C. (2007). hZip2 and hZip3 zinc transporters are down regulated in human prostate adenocarcinomatous glands. *Mol Cancer,* 6**:** 37.

Di Cristofano, A. & Pandolfi, P. P. (2000). The Multiple Roles of PTEN in Tumor Suppression. *Cell,* 100**:** 387-390.

Di Cristofano, A., Pesce, B., Cordon-Cardo, C. & Pandolfi, P. P. (1998). Pten is essential for embryonic development and tumour suppression. *Nat Genet,* 19**:** 348-355.

Di Leonardo, A., Linke, S. P., Clarkin, K. & Wahl, G. M. (1994). DNA damage triggers a prolonged p53-dependent G1 arrest and long-term induction of Cip1 in normal human fibroblasts. *Genes Dev,* 8**:** 2540-2551.

Discacciati, A., Orsini, N. & Wolk, A. (2012). Body mass index and incidence of localized and advanced prostate cancer--a dose-response meta-analysis of prospective studies. *Ann Oncol,* 23**:** 1665-71.

Djavan, B., Zlotta, A., Schulman, C., Teillac, P., Iversen, P.*, et al.* (2004). Chemotherapeutic prevention studies of prostate cancer. *J Urol,* 171**:** S10-S13.

Djulbegovic, M., Beyth, R. J., Neuberger, M. M., Stoffs, T. L., Vieweg, J.*, et al.* (2010). Screening for prostate cancer: systematic review and meta-analysis of randomised controlled trials. *BMJ,* 341**:** c4543.

Downing, S. R., Russell, P. J. & Jackson, P. (2003). Alterations of p53 are common in early stage prostate cancer. *Can J Urol.,* 10**:** 1924-1933.

Draisma, G., Etzioni, R., Tsodikov, A., Mariotto, A., Wever, E.*, et al.* (2009). Lead time and overdiagnosis in prostate-specific antigen screening: importance of methods and context. *J Natl Cancer Inst,* 101**:** 374-83.

Duffield-Lillico, A. J., Dalkin, B. L., Reid, M. E., Turnbull, B. W., Slate, E. H.*, et al.* (2003). Selenium supplementation, baseline plasma selenium status and incidence of prostate cancer: an analysis of the complete treatment period of the Nutritional Prevention of Cancer Trial. *BJU Int,* 91**:** 608-612.

Edwards, S. M., Kote-Jarai, Z., Meitz, J., Hamoudi, R., Hope, Q.*, et al.* (2003). Two Percent of Men with Early-Onset Prostate Cancer Harbor Germline Mutations in the *BRCA2* Gene. *The American Journal of Human Genetics,* 72**:** 1-12.

Effert, P., Beniers, A. J., Tamimi, Y., Handt, S. & Jakse, G. (2004). Expression of Glucose Transporter 1 (Glut-1) in Cell Lines and Clinical Specimens from Human Prostate Adenocarcinoma. *Anticancer Res,* 24**:** 3057-3064.

El-Deiry, W. S., Tokino, T., Velculescu, V. E., Levy, D. B., Parsons, R.*, et al.* (1993). WAF1, a potential mediator of p53 tumor suppression. *Cell,* 75**:** 817-825.

Elo, J. P. & Visakorpi, T. (2001). Molecular genetics of prostate cancer. *Ann Med,* 33**:** 130-141.

Epstein, J. I., Allsbrook, J. W. C., Amin, M. B., Egevad, L. L. & Committee, I. G. (2005). The 2005 International Society of Urological Pathology (ISUP) Consensus Conference on Gleason Grading of Prostatic Carcinoma. *Am J Surg Pathol,* 29**:** 1228-1242.

Etzioni, R., Penson, D. F., Legler, J. M., Di Tommaso, D. & Boer, R. (2002). Overdiagnosis due to prostate-specific antigen screening: lessons from U.S. prostate cancer incidence trends. *J Natl Cancer Inst,* 94**:** 981-90.

Ewald, J. A., Desotelle, J. A., Wilding, G. & Jarrard, D. F. (2010). Therapy-induced senescence in cancer. *J Natl Cancer Inst,* 102**:** 1536-46.

Falzarano, S. M. & Magi-Galluzzi, C. (2010). Staging prostate cancer and its relationship to prognosis. *Diagnostic Histopathology,* 16**:** 432-438.

Faubert, B., Boily, G., Izreig, S., Griss, T., Samborska, B.*, et al.* (2013). AMPK is a negative regulator of the Warburg effect and suppresses tumor growth in vivo. *Cell Metab,* 17**:** 113-24.

Feil, R., Brocard, J., Mascrez, B., Lemeur, M., Metzger, D.*, et al.* (1996). Ligand-activated site-specific recombination in mice. *Proc Natl Acad Sci U S A,* 93**:** 10887-10890.

Feldman, B. J. & Feldman, D. (2001). The development of androgen-independent prostate cancer. *Nat Rev Cancer,* 1**:** 34-45.

Feng, P., Li, T. L., Guan, Z. X., Franklin, R. B. & Costello, L. C. (2002). Direct effect of zinc on mitochondrial apoptogenesis in prostate cells. *Prostate,* 52**:** 311-8.

Feng, P., Liang, J., Li, T., Guan, Z., Zou, J.*, et al.* (2000). Zinc induces mitochondria apoptogenesis in prostate cells. *Mol Urol,* 4**:** 31-36.

Ferlay, J., Soerjomataram, I., Ervik, M., Dikshit, R., Eser, S.*, et al.* 2013. *GLOBOCAN 2012 v1.0, Cancer Incidence and Mortality Worldwide: IARC CancerBase No. 11 [Internet]* [Online]. Lyon, France: International Agency for Research on Cancer. Available: http://globocan.iarc.fr [Accessed 05/03/2015].

Fiorani, M., Accorsi, A. & Cantoni, O. (2003). Human Red Blood Cells as A Natural Flavonoid Reservoir. *Free Radical Research,* 37**:** 1331-1338.

Fiorentino, M., Zadra, G., Palescandolo, E., Fedele, G., Bailey, D.*, et al.* (2008). Overexpression of fatty acid synthase is associated with palmitoylation of Wnt1 and cytoplasmic stabilization of beta-catenin in prostate cancer. *Lab Invest,* 88**:** 1340-8.

Flavin, R., Zadra, G. & Loda, M. (2011). Metabolic alterations and targeted therapies in prostate cancer. *J Pathol,* 223**:** 283-94.

Fleshner, N., Bagnell, P. S., Klotz, L. & Venkateswaran, V. (2004). Dietary fat and prostate cancer. *J Urol,* 171**:** S19-S24.

Fogarty, S. & Hardie, D. G. (2010). Development of protein kinase activators: AMPK as a target in metabolic disorders and cancer. *Biochim Biophys Acta,* 1804**:** 581-91.

Forman, D. & Ferlay, J. 2014. The global and regional burden of cancer. *In:* STEWART, B. W. & WILD, C. P. (eds.) *World Cancer Report 2014.* International Agency for Research on Cancer.

Franklin, R. B. & Costello, L. C. 2009. Citrate metabolism in prostate and other cancers. *In:* SINGH, K. K. & COSTELLO, L. C. (eds.) *Mitochondria and cancer.*

Franklin, R. B., Feng, P., Milon, B., Desouki, M. M., Singh, K. K.*, et al.* (2005). hZIP1 zinc uptake transporter down regulation and zinc depletion in prostate cancer. *Mol Cancer,* 4**:** 32.

Franklin, R. B., Ma, J., Zou, J., Guan, Z., Kukoyi, B. I.*, et al.* (2003). Human ZIP1 is a major zinc uptake transporter for the accumulation of zinc in prostate cells. *Journal of Inorganic Biochemistry,* 96**:** 435-442.

Franklin, R. B., Zou, J., Yu, Z. & Costello, L. C. (2006). EAAC1 is expressed in rat and human prostate epithelial cells; functions as a high-affinity L-aspartate transporter; and is regulated by prolactin and testosterone. *BMC Biochem,* 7**:** 10.

Freedland, S. J., Humphreys, E. B., Mangold, L. A., Eisenberger, M., Dorey, F. J.*, et al.* (2005). Risk of prostate cancer-specific mortality following biochemical recurrence after radical prostatectomy. *294***:** 433-439.

Frigo, D. E., Howe, M. K., Wittmann, B. M., Brunner, A. M., Cushman, I.*, et al.* (2011). CaM kinase kinase beta-mediated activation of the growth regulatory kinase AMPK is required for androgen-dependent migration of prostate cancer cells. *Cancer Res,* 71**:** 528-37.

Frost, P., Moatamed, F., Hoang, B., Shi, Y., Gera, J.*, et al.* (2004). In vivo antitumor effects of the mTOR inhibitor CCI-779 against human multiple myeloma cells in a xenograft model. *Blood,* 104**:** 4181-7.

Gálvez, M. (2003). Cytotoxic effect of Plantago spp. on cancer cell lines. *J Ethnopharmacol,* 88**:** 125-130.

Gao, X., Lavalley, M. P. & Tucker, K. L. (2005). Prospective studies of dairy product and calcium intakes and prostate cancer risk: a meta-analysis. *J Natl Cancer Inst,* 97**:** 1768-77.

Gao, Y., Islam, M. S., Tian, J., Lui, V. W. & Xiao, D. (2014). Inactivation of ATP citrate lyase by Cucurbitacin B: A bioactive compound from cucumber, inhibits prostate cancer growth. *Cancer Lett,* 349**:** 15-25.

Gary, R. K. & Kindell, S. M. (2005). Quantitative assay of senescence-associated beta-galactosidase activity in mammalian cell extracts. *Anal Biochem,* 343**:** 329-34.

Gayther, S. A., De Foy, K. a. F., Harrington, P., Pharoah, P., Dunsmuir, W. D.*, et al.* (2000). The frequency of germ-line mutations in the breast cancer predisposition genes *BRCA1* and *BRCA2* in familial prostate cancer. *Cancer Res,* 60**:** 4513-4518.

Gennaro, L., Leonardi, C., Esposito, F., Salucci, M., Maiani, G.*, et al.* (2002). Flavonoid and carbohydrate contents in Tropea red onions: Effects of homelike peeling and storage. *J Agric Food Chem,* 50**:** 1904-1910.

Gerhauser, C., Bartsch, H., Crowell, J., De Flora, S., D'incalci, M.*, et al.* (2006). Development of novel cancer chemopreventive agents in Europe--neglected Cinderella or rising phoenix? A critical commentary. ESF Workshop on Cancer Chemoprevention, DKFZ, Heidelberg, September 18-20, 2005. *Eur J Cancer,* 42**:** 1338-43.

Ghosh, J. (2004). Rapid induction of apoptosis in prostate cancer cells by selenium: reversal by metabolites of arachidonate 5-lipoxygenase. *Biochem Biophys Res Commun,* 315**:** 624-35.

Gingrich, J. R., Barrios, R. J., Morton, R. A., Boyce, B. F., Demayo, F. J.*, et al.* (1996). Metastatic prostate cancer in a transgenic mouse. *Cancer Res,* 56**:** 4096-4102.

Giono, L. E. & Manfredi, J. J. (2006). The p53 tumor suppressor participates in multiple cell cycle checkpoints. *J Cell Physiol,* 209**:** 13-20.

Giovannucci, E., Liu, Y., Platz, E. A., Stampfer, M. J. & Willett, W. C. (2007). Risk factors for prostate cancer incidence and progression in the health professionals follow-up study. *Int J Cancer,* 121**:** 1571-8.

Gleason, D. F. Histologic grading of prostate cancer. *Hum Pathol,* 23**:** 273-279.

Goetzl, M. A. & Holzbeierlein, J. M. (2006). Finasteride as a chemopreventive agent in prostate cancer: impact of the PCPT on urologic practice. *Nat Clin Pract Urol,* 3**:** 422-9.

Gong, Z., Agalliu, I., Lin, D. W., Stanford, J. L. & Kristal, A. R. (2007). Obesity is associated with increased risks of prostate cancer metastasis and death after initial cancer diagnosis in middle-aged men. *Cancer,* 109**:** 1192-202.

Gown, A. M. & Willingham, M. C. (2002). Improved Detection of Apoptotic Cells in Archival Paraffin Sections: Immunohistochemistry Using Antibodies to Cleaved Caspase 3. *J Histochem Cytochem,* 50**:** 449-454.

Graña, X. & Reddy, E. P. (1995). Cell cycle control in mammalian cells: role of cyclins, cyclin dependent kinases (CDKs), growth suppressor genes and cyclin-dependent kinase inhibitors (CKIs). *Oncogene,* 11**:** 211-219.

Gray, P. J., Lin, C., Jemal, A. & Efstathiou, J. A. (2014). Recent Trends in the Management of Localized Prostate Cancer: Results From the National Cancer Data Base. *International Journal of Radiation Oncology*Biology*Physics,* 90**:** S431-S432.

Greenberg, N. M., Demayo, F., Finegold, M. J., Medina, D., Tilley, W. D.*, et al.* (1995). Prostate cancer in a transgenic mouse. *Proc Natl Acad Sci U S A,* 92**:** 3439-3443.

Greenwald, P. (2002). Cancer chemoprevention. *BMJ,* 324**:** 714-718.

Gumerlock, P. H., Chi, S.-G., Shi, X.-B., Voeller, H. J., Jacobson, J. W.*, et al.* (1997). p53 Abnormalities in Primary Prostate Cancer: Single-Strand Conformation Polymorphism Analysis of Complementary DNA in Comparison With Genomic DNA. *J. Natl. Cancer Inst,* 89**:** 66-71.

Gunawardena, K., Murray, D. K. & Meikle, A. W. (2000). Vitamin E and other antioxidants inhibit human prostate cancer cells through apoptosis. *Prostate,* 44**:** 287-295.

Guo, Y., Sklar, G. N., Borkowski, A. & Kyprianou, N. (1997). Loss of the cyclin-dependent kinase inhibitor p27(Kip1) protein in human prostate cancer correlates with tumor grade. *Clin Cancer Res,* 3**:** 2269-2274.

Gupta, S., Ahmad, N., Nieminen, A. L. & Mukhtar, H. (2000). Growth inhibition, cell-cycle dysregulation, and induction of apoptosis by green tea constituent (-)-epigallocatechin-3-gallate in androgen-sensitive and androgen-insensitive human prostate carcinoma cells. *Toxicol Appl Pharmacol,* 164**:** 82-90.

Gupta, S., Hastak, K., Ahmad, N., Lewin, J. S. & Mukhtar, H. (2001). Inhibition of prostate carcinogenesis in TRAMP mice by oral infusion of green tea polyphenols. *Proc Natl Acad Sci U S A,* 98**:** 10350-5.

Gupta, S., Hussain, T. & Mukhtar, H. (2003). Molecular pathway for (-)-epigallocatechin-3-gallate-induced cell cycle arrest and apoptosis of human prostate carcinoma cells. *Arch Biochem Biophys,* 410**:** 177-185.

Guseva, N. V., Rokhlin, O. W., Glover, R. A. & Cohen, M. B. (2011). TOFA (5-tetradecyl-oxy-2-furoic acid) reduces fatty acid synthesis, inhibits expression of AR, neuropilin-1 and Mcl-1 and kills prostate cancer cells independent of p53 status. *Cancer Biol Ther,* 12**:** 80-5.

Haas, G. P. & Sakr, W. A. (1997). Epidemiology of Prostate Cancer. *CA Cancer J Clin,* 47**:** 273-287.

Habib, F. K., Mason, M. K., Smith, P. H. & Stitch, S. R. (1979). Cancer of the prostate: early diagnosis by zinc and hormone analysis? *Br J Cancer,* 39**:** 700-704.

Haddad, A. Q., Fleshner, N., Nelson, C., Saour, B., Musquera, M.*, et al.* (2010). Antiproliferative mechanisms of the flavonoids 2,2'-dihydroxychalcone and fisetin in human prostate cancer cells. *Nutr Cancer,* 62**:** 668-81.

Haddad, A. Q., Venkateswaran, V., Viswanathan, L., Teahan, S. J., Fleshner, N. E.*, et al.* (2006). Novel antiproliferative flavonoids induce cell cycle arrest in human prostate cancer cell lines. *Prostate Cancer Prostatic Dis,* 9**:** 68-76.

Hagen, R. M., Chedea, V. S., Mintoff, C. P., Bowler, E., Morse, H. R.*, et al.* (2013). Epigallocatechin-3-gallate promotes apoptosis and expression of the caspase 9a splice variant in PC3 prostate cancer cells. *Int J Oncol,* 43**:** 194-200.

Hail, Jr. N. (2005). Mitochondria: A novel target for the chemoprevention of cancer. *Apoptosis,* 10**:** 687-705.

Hamdy, F. C. (2001). Prognostic and predictive factors in prostate cancer. *Cancer Treat Rev,* 27**:** 143-151.

Hanahan, D. & Weinberg, R. A. (2000). The hallmarks of cancer. *Cell,* 100**:** 57-70.

Hanahan, D. & Weinberg, R. A. (2011). Hallmarks of cancer: the next generation. *Cell,* 144**:** 646-74.

Harper, C. E., Patel, B. B., Wang, J., Eltoum, I. A. & Lamartiniere, C. A. (2007). Epigallocatechin-3-Gallate suppresses early stage, but not late stage prostate cancer in TRAMP mice: mechanisms of action. *Prostate,* 67**:** 1576-89.

Harris, R. A., Bowker-Kinley, M. M., Huang, B. & Wu, P. (2002). Regulation of the activity of the pyruvate dehydrogenase complex. *Advan Enzyme Regul,* 42**:** 249-259.

Hastak, K., Agarwal, M. K., Mukhtar, H. & Agarwal, M. L. (2005). Ablation of either p21 or Bax prevents p53-dependent apoptosis induced by green tea polyphenol epigallocatechin-3-gallate. *FASEB J,* 19**:** 789-791.

Hedlund, T. E., Johannes, W. U. & Miller, G. J. (2003). Soy isoflavonoid equol modulates the growth of benign and malignant prostatic epithelial cells in vitro. *Prostate,* 54**:** 68-78.

Heinonen, O. P., Albanes, D., Virtamo, J., Taylor, P. R., Huttunen, J. K*., et al.* (1998). Prostate cancer and supplementation with alpha-tocopherol and beta-carotene: incidence and mortality in a controlled trial. *J Natl Cancer Inst,* 90**:** 440-446.

Hemminki, K. & Chen, B. (2005). Familial association of prostate cancer with other cancers in the Swedish Family-Cancer Database. *Prostate,* 65**:** 188-94.

Hemminki, K. & Czene, K. (2002). Age specific and attributable risks of familial prostate carcinoma from the family-cancer database. *Cancer,* 95**:** 1346-53.

Hensley, P. J. & Kyprianou, N. (2012). Modeling prostate cancer in mice: limitations and opportunities. *J Androl,* 33**:** 133-44.

Hessels, D., Smit, F. P., Verhaegh, G. W., Witjes, J. A., Cornel, E. B*., et al.* (2007). Detection of TMPRSS2-ERG fusion transcripts and prostate cancer antigen 3 in urinary sediments may improve diagnosis of prostate cancer. *Clin Cancer Res,* 13**:** 5103-8.

Hiipakka, R. A., Zhang, H., Dai, W., Dai, Q. & Liao, S. (2002). Structure-activity relationships for inhibition of human 5alpha-reductases by polyphenols. *Biochem Pharmacol,* 63**:** 1165-1176.

Ho, P.C., D.J. Saville and S. Wanwimolruk, 2001. Inhibition of human CYP3A4 activity by grapefruit flavonoids, furanocoumarins and related compounds. J. Pharm. Pharmaceut. Sci., 4: 217-227

Holubova, M., Axmanova, M., Gumulec, J., Raudenska, M., Sztalmachova, M*., et al.* (2014). KRAS NF-κB is involved in the development of zinc resistance and reduced curability in prostate cancer. *Metallomics,* 6**:** 1240-53.

Howells, L. M., Britton, R. G., Mazzoletti, M., Greaves, P., Broggini, M*., et al.* (2010). Preclinical colorectal cancer chemopreventive efficacy and p53-modulating activity of 3',4',5'-trimethoxyflavonol, a quercetin analogue. *Cancer Prev Res (Phila),* 3**:** 929-39.

Hsing, A. W., Reichardt, J. K. & Stanczyk, F. Z. (2002). Hormones and prostate cancer: current perspectives and future directions. *Prostate,* 52**:** 213-35.

Hsing, A. W., Tsao, L. & Devesa, S. S. (2000). International trends and patterns of prostate cancer incidence and mortality. *Int. J. Cancer,* 85**:** 60-67.

Huang, M., Narita, S., Numakura, K., Tsuruta, H., Saito, M*., et al.* (2012). A high-fat diet enhances proliferation of prostate cancer cells and activates MCP-1/CCR2 signaling. *Prostate,* 72**:** 1779-88.

Hughes, C., Murphy, A., Martin, C., Sheils, O. & O'leary, J. (2005). Molecular pathology of prostate cancer. *J Clin Pathol,* 58**:** 673-84.

Hur, H.-G., Lay Jr, J. O., Beger, R. D., Freeman, J. P. & Rafii, F. (2000). Isolation of human intestinal bacteria metabolizing the natural isoflavone glycosides daidzin and genistin. *Archives of Microbiology,* 174**:** 422-428.

Huss, W. J., Barrios, R. J. & Greenberg, N. M. (2003). SU5416 selectively impairs angiogenesis to induce prostate cancer-specific apoptosis. *Mol Cancer Ther,* 2**:** 611-616.

Iannolo, G., Conticello, C., Memeo, L. & De Maria, R. (2008). Apoptosis in normal and cancer stem cells. *Crit Rev Oncol Hematol,* 66**:** 42-51.

IARC 2015. GLOBOCAN 2012 v 1.2. Lyon, France: International Agency for Research on Cancer.

Jagerstad, M. & Skog, K. (2005). Genotoxicity of heat-processed foods. *Mutat Res,* 574**:** 156-72.

Jarrard, D. F., Sarkar, S., Shi, Y., Yeager, T. R., Magrane, G*., et al.* (1999). p16/pRb Pathway Alterations Are Required for Bypassing Senescence in Human Prostate Epithelial Cells. *Cancer Res,* 59**:** 2957-2964.

Jayakumar, A., Tai, M.-H., Huang, W.-Y., Al-Feel, W., Hsu, M.*, et al.* (1995). Human fatty acid synthase: Properties and molecular cloning. *Proc Natl Acad Sci U S A,* 92**:** 8695-8699.

Jennings, D., Hatton, B. N., Guo, J., Galons, J. P., Trouard, T. P.*, et al.* (2002). Early response of prostate carcinoma xenografts to docetaxel chemotherapy monitored with diffusion MRI. *Neoplasia,* 4**:** 255-62.

Jiang, Z., Woda, B. A., Rock, K. L., Xu, Y., Savas, L.*, et al.* (2001). P504S a new molecular marker for the detection of prostate carcinoma. *Am J Surg Pathol,* 25**:** 1397-1404.

Johnson, J. J., Bailey, H. H. & Mukhtar, H. (2010). Green tea polyphenols for prostate cancer chemoprevention: a translational perspective. *Phytomedicine,* 17**:** 3-13.

Joshi, A. D., Corral, R., Catsburg, C., Lewinger, J. P., Koo, J.*, et al.* (2012). Red meat and poultry, cooking practices, genetic susceptibility and risk of prostate cancer: results from a multiethnic case-control study. *Carcinogenesis,* 33**:** 2108-18.

Juang, H. H. (2004). Modulation of mitochondrial aconitase on the bioenergy of human prostate carcinoma cells. *Mol Genet Metab,* 81**:** 244-52.

Julin, B., Wolk, A., Johansson, J. E., Andersson, S. O., Andren, O.*, et al.* (2012). Dietary cadmium exposure and prostate cancer incidence: a population-based prospective cohort study. *Br J Cancer,* 107**:** 895-900.

Jurmeister, S., Ramos-Montoya, A., Neal, D. E. & Fryer, L. G. D. (2014). Transcriptomic analysis reveals inhibition of androgen receptor activity by AMPK in prostate cancer cells. *Oncotarget,* 5**:** 3785-3799.

Kaighn, M. E., Narayan, K. S., Ohnuki, Y., Lechner, J. F. & Jones, L. W. (1979). Establishment and characterization of a human prostatic carcinoma cell line (PC-3). *Invest Urol,* 17**:** 16-23.

Kanavy, H. E. & Gerstenblith, M. R. (2011). Ultraviolet radiation aand melanoma. *Semin Cutan Med Surg,* 30: 222-228.

Kaplan-Lefko, P. J., Chen, T. M., Ittmann, M. M., Barrios, R. J., Ayala, G. E.*, et al.* (2003). Pathobiology of autochthonous prostate cancer in a pre-clinical transgenic mouse model. *Prostate,* 55**:** 219-37.

Kenfield, S. A., Van Blarigan, E. L., Dupre, N., Stampfer, M. J., Giovannucci, E.L., *et al.* (2015). Selenium supplementation and prostate cancer mortality. *J Natl Cancer Inst,* 107**:** 360.

Khan, N., Adhami, V. M. & Mukhtar, H. (2010). Apoptosis by dietary agents for prevention and treatment of prostate cancer. *Endocr Relat Cancer,* 17**:** R39-52.

Khan, N., Afaq, F., Syed, D. N. & Mukhtar, H. (2008). Fisetin, a novel dietary flavonoid, causes apoptosis and cell cycle arrest in human prostate cancer LNCaP cells. *Carcinogenesis,* 29**:** 1049-56.

Kiciński, M., Vangronsveld, J. & Nawrot, T. S. (2011). An Epidemiological Reappraisal of the Familial Aggregation of Prostate Cancer: A Meta-Analysis. *PLoS One,* 6**:** e27130.

Kim, J. W., Tchernyshyov, I., Semenza, G. L. & Dang, C. V. (2006). HIF-1-mediated expression of pyruvate dehydrogenase kinase: a metabolic switch required for cellular adaptation to hypoxia. *Cell Metab,* 3**:** 177-85.

Klein, E. A., Thompson, I. M., Tangen, C. M., Crowley, J. J., Lucia, M. S.*, et al.* (2011). Vitamin E and the risk of prostate cancer. The Selenium and Vitamin E Cancer Prevention Trial (SELECT). *JAMA,* 306**:** 1549-1556.

Klein, R. D. (2005). The use of genetically engineered mouse models of prostate cancer for nutrition and cancer chemoprevention research. *Mutat Res,* 576**:** 111-9.

Knekt, P., Kumpulainen, J., Järvinen, R., Rissanen, H., Heliövaara, M.*, et al.* (2002). Flavonoid intake and risk of chronic diseases. *Am J Clin Nutr,* 76**:** 560-568.

Konishi, N., Nakamura, M., Kishi, M., Nishimine, M., Ishida, E.*, et al.* (2002). Heterogeneous Methylation and Deletion Patterns of the INK4a/ARF Locus Within Prostate Carcinomas. *Am J Pathol,* 160**:** 1207-1214.

Koukourakis, M. I., Giatromanolaki, A., Sivridis, E., Gatter, K. C. & Harris, A. L. (2005). Pyruvate Dehydrogenase and Pyruvate Dehydrogenase Kinase Expression in Non Small Cell Lung Cancer and Tumor-Associated Stroma. *Neoplasia,* 7**:** 1-6.

Kridel, S. J., Axelrod, F., Rozenkrantz, N. & Smith, J. W. (2004). Orlistat is a novel inhibitor of fatty acid synthase with antitumor activity. *Cancer Res,* 64**:** 2070-2075.

Kristal, A. R., Darke, A. K., Morris, J. S., Tangen, C. M., Goodman, P. J.*, et al.* (2014). Baseline selenium status and effects of selenium and vitamin E supplementation on prostate cancer risk. *J Natl Cancer Inst,* 106**:** djt456.

Krtolica, A., Parrinello, S., Lockett, S., Desprez, P. Y. & Campisi, J. (2001). Senescent fibroblasts promote epithelial cell growth and tumorigenesis: a link between cancer and aging. *Proc Natl Acad Sci U S A,* 98**:** 12072-7.

Kuhajda, F., Jenner, K., Wood, F. D., Hennigar, R. A., Jacobs, L. B.*, et al.* (1994). Fatty acid synthesis: A potential selective target for antineoplastic therapy. *Proc Natl Acad Sci U S A,* 91**:** 6379-6383.

Kumar, S. & Pandey, A. K. (2013). Chemistry and biological activities of flavonoids: an overview. *Scientific World Journal,* 2013**:** 162750.

Kumar, S., Shelley, M., Harrison, C., Coles, B., Wilt, T. J.*, et al.* (2006). Neo-adjuvant and adjuvant hormone therapy for localised and locally advanced prostate cancer. *Cochrane Database Syst Rev,* 18**:** CD006019.

Kumar-Sinha, C., Shah, R. B., Laxman, B., Tomlins, S. A., Harwood, J.*, et al.* (2004). Elevated α-Methylacyl-CoA Racemase Enzymatic Activity in Prostate Cancer. *Am J Pathol,* 164**:** 787-793.

Kuno, T., Tsukamoto, T., Hara, A. & Tanaka, T. (2012). Cancer chemoprevention through the induction of apoptosis by natural compounds. *Journal of Biophysical Chemistry,* 03**:** 156-173.

Kurata, T., Oguri, T., Isobe, T., Ishioka, S.-I. & Yamakido, M. (1999). Differential expression of facilitative glucose transporter (*GLUT*) genes in primary lung cancers and their liver metastases. *Jpn J Cancer Res,* 90**:** 1238-1243.

Lapointe, J., Li, C., Higgins, J. P., Van De Rijn, M., Bair, E.*, et al.* (2004). Gene expression profiling identifies clinically relevant subtypes of prostate cancer. *Proc Natl Acad Sci U S A,* 101**:** 811-6.

Lee, B. Y., Han, J. A., Im, J. S., Morrone, A., Johung, K.*, et al.* (2006). Senescence-associated beta-galactosidase is lysosomal beta-galactosidase. *Aging Cell,* 5.

Lee, D. H., Szczepanski, M. & Lee, Y. J. (2008). Role of Bax in quercetin-induced apoptosis in human prostate cancer cells. *Biochem Pharmacol,* 75**:** 2345-55.

Lefevre, M. (2013). A role for finasteride in the prevention of prostate cancer. *N Engl J Med,* 369**:** 670-671.

Lehtonen, R., Kiuru, M., Rökman, A., Ikonen, T., Cunningham, J. M.*, et al.* (2003). No fumarate hydratase (FH) mutations in hereditary prostate cancer. *J Med Genet,* 40**:** e19.

Lexander, H., Palmberg, C., Auer, G., Hellstrom, M., Franzen, B.*, et al.* (2005). Proteomic analysis of protein expression in prostate cancer. *Anal Quant Cytol Histol,* 27**:** 263-272.

Li, G., Rivas, P., Bedolla, R., Thapa, D., Reddick, R. L.*, et al.* (2013). Dietary resveratrol prevents development of high-grade prostatic intraepithelial neoplastic lesions: involvement of SIRT1/S6K axis. *Cancer Prev Res (Phila),* 6**:** 27-39.

Li, H., Stampfer, M. J., Giovannucci, E. L., Morris, J. S., Willett, W. C.*, et al.* (2004). A Prospective Study of Plasma Selenium Levels and Prostate Cancer Risk. *J Natl Cancer Inst,* 96**:** 696-703.

Liang, J., Liu, Y., Zou, J., Franklin, R. B., Costello, L. C.*, et al.* (1999). Inhibitory effect of zinc on human prostatic carcinoma cell growth. *Prostate,* 40**:** 200-207.

Lin, V. C., Tsai, Y. C., Lin, J. N., Fan, L. L., Pan, M. H.*, et al.* (2012). Activation of AMPK by pterostilbene suppresses lipogenesis and cell-cycle progression in p53 positive and negative human prostate cancer cells. *J Agric Food Chem,* 60**:** 6399-407.

Lippman, S. M., Benner, S. E. & Hong, W. K. (1994). Cancer chemoprevention. *J Clin Oncol,* 12**:** 851-873.

Lippman, S. M., Klein, E. A., Goodman, P. J., Lucia, M. S., Thompson, I. M.*, et al.* (2009). Effect of selenium and vitamin E on risk of prostate cancer and other cancers. The Selenium and Vitamin E Cancer Prevention Trial (SELECT). *JAMA,* 301**:** 39-51.

Litman, H. J., Bhasin, S., Link, C. L., Araujo, A. B. & Mckinlay, J. B. (2006). Serum Androgen Levels in Black, Hispanic, and White Men. *The Journal of Clinical Endocrinology & Metabolism,* 91**:** 4326-4334.

Little, J. L., Wheeler, F. B., Fels, D. R., Koumenis, C. & Kridel, S. J. (2007). Inhibition of fatty acid synthase induces endoplasmic reticulum stress in tumor cells. *Cancer Res,* 67**:** 1262-9.

Liu, Y. (2006). Fatty acid oxidation is a dominant bioenergetic pathway in prostate cancer. *Prostate Cancer Prostatic Dis,* 9**:** 230-4.

Liu, Y., Costello, L. C. & Franklin, R. B. (1996). Prolactin Specifically Regulates Citrate Oxidation and m-Aconitase of Rat Prostate Epithelial Cells. *Metabolism,* 45**:** 442-449.

Liu, Y., Franklin, R. B. & Costello, L. C. (1997). Prolactin and testosterone regulation of mitochondrial zinc in prostate epithelial cells. *Prostate,* 30**:** 26-32.

Liu, Y., Zuckier, L. S. & Ghesani, N. V. (2010). Dominant Uptake of Fatty Acid over Glucose by Prostate Cells: A Potential New Diagnostic and Therapeutic Approach. *Anticancer Res,* 30**:** 369-374.

Locke, J. A., Guns, E. S., Lubik, A. A., Adomat, H. H., Hendy, S. C.*, et al.* (2008). Androgen levels increase by intratumoral de novo steroidogenesis during progression of castration-resistant prostate cancer. *Cancer Res,* 68**:** 6407-15.

Lopez-Lazaro, M., Willmore, E. & Austin, C. A. (2010). The dietary flavonoids myricetin and fisetin act as dual inhibitors of DNA topoisomerases I and II in cells. *Mutat Res,* 696**:** 41-7.

Lund, T. D., Munson, D. J., Haldy, M. E., Setchell, K. D., Lephart, E. D*., et al.* (2004). Equol is a novel anti-androgen that inhibits prostate growth and hormone feedback. *Biol Reprod,* 70**:** 1188-95.

Luo, J., Zha, S., Gage, W. R., Dunn, T. A., Hicks, J. L*., et al.* (2002). Alpha-methylacyl-CoA racemase a new molecular marker for prostate cancer. *Cancer Res,* 62**:** 2220-2226.

Luo, Z., Zang, M. & Guo, W. (2010). AMPK as a metabolic tumor suppressor: control of metabolism and cell growth. *Future Oncol,* 6**:** 457-70.

Maddison, L. A., Nahm, H., Demayo, F. & Greenberg, N. M. (2000). Prostate specific expression of Cre recombinase in transgenic mice. *Genesis,* 26**:** 154-156.

Maddison, L. A., Sutherland, B. W., Barrios, R. J. & Greenberg, N. M. (2004). Conditional deletion of Rb causes early stage prostate cancer. *Cancer Res,* 64**:** 6018-6025.

Majumder, P. K., Grisanzio, C., O'connell, F., Barry, M., Brito, J. M*., et al.* (2008). A prostatic intraepithelial neoplasia-dependent p27 Kip1 checkpoint induces senescence and inhibits cell proliferation and cancer progression. *Cancer Cell,* 14**:** 146-55.

Manach, C., Scalbert, A., Morand, C., Rémésy, C. & Jiménez, L. (2004). Polyphenols food sources and bioavailability. *Am J Clin Nutr,* 79**:** 727-747.

Manach, C., Williamson, G., Morand, C., Scalbert, A. & Rémésy, C. (2005). Bioavailability and bioefficacy of polyphenols in humans. I. Review of 97 bioavailability studies. *Am J Clin Nutr,* 81**:** 230S-242S.

Margel, D., Urbach, D. R., Lipscombe, L. L., Bell, C. M., Kulkarni, G*., et al.* (2013). Metformin use and all-cause and prostate cancer-specific mortality among men with diabetes. *J Clin Oncol,* 31**:** 3069-75.

Martin, S. J., Reutelingsperger, C. P. M., Mcgahon, A. J., Rader, J. A., Van Schie, R. C. a. A*., et al.* (1995). Early redistribution of plasma membrane phosphatidylserine is a general feature of apoptosis regardless of the initiating stimulus: inhibition by overexpression of Bcl-2 and Abl. *J Exp Med,* 182**:** 1545-1556.

Mathon, N. F. & Lloyd, A. C. (2001). Cell senescence and cancer. *Nat Rev Cancer,* 1**:** 203-213.

Mawhinney, M. & Mariotti, A. (2013). Physiology pathology and pharmacology of the male reproductive system. *Periodontology 2000,* 61**:** 232-251.

Mazaris, E. & Tsiotras, A. (2013). Molecular pathways in prostate cancer. *Nephrourol Mon,* 5**:** 792-800.

McCarthy, S., Caporali, A., Enkemann, S., Scaltriti, M., Eschrich, S.*, et al.* (2007). Green tea catechins suppress the DNA synthesis marker MCM7 in the TRAMP model of prostate cancer. *Mol Oncol,* 1**:** 196-204.

McCarty, M. F. (2004). Targeting multiple signaling pathways as a strategy for managing prostate cancer: multifocal signal modulation therapy. *Integr Cancer Ther,* 3**:** 349-80.

Mcintosh, H. (1997). Why do African-American men suffer more prostate cancer? *J Natl Cancer Inst,* 89**:** 188-189.

Meeran, S. M. & Katiyar, S. K. (2008). Cell cycle control as a basis for cancer chemoprevention through dietary agents. *Front Biosci,* 13**:** 2191-2202.

Menendez, J. A. & Lupu, R. (2007). Fatty acid synthase and the lipogenic phenotype in cancer pathogenesis. *Nat Rev Cancer,* 7**:** 763-77.

Menter, D. G., Sabichi, A. L. & Lippman, S. M. (2000). Selenium effects on prostate cell growth. *Cancer Epidemiol Biomarkers Prev,* 9**:** 1171-1182.

Messina, M. J., Persky, V., Setchell, K. D. & Barnes, S. (1994). Soy intake and cancer risk: a review of the in vitro and in vivo data. *Nutr Cancer,* 21**:** 113-31.

Messing, E. M., Manola, J., Yao, J., Kiernan, M., Crawford, D.*, et al.* (2006). Immediate versus deferred androgen deprivation treatment in patients with node-positive prostate cancer after radical prostatectomy and pelvic lymphadenectomy. *The Lancet Oncology,* 7**:** 472-479.

Metcalfe, C., Patel, B., Evans, S., Ibrahim, F., Anson, K.*, et al.* (2008). The risk of prostate cancer amongst South Asian men in southern England: the PROCESS cohort study. *BJU Int,* 102**:** 1407-12.

Michalides, R. J. a. M. (1999). Cell cycle regulators: mechanisms and their role in aetiology, prognosis, and treatment of cancer. *J Clin Pathol,* 52**:** 555-568.

Ming, D. S., Pham, S., Deb, S., Chin, M. Y., Kharmate, G.*, et al.* (2014). Pomegranate extracts impact the androgen biosynthesis pathways in prostate cancer models in vitro and in vivo. *J Steroid Biochem Mol Biol,* 143**:** 19-28.

Mizuma, T., Ohta, K., Hayashi, M. & Awazu, S. (1993). Comparative study of active absorption by the intestine and disposition of anomers of sugar-conjugated compounds. *Biochem Pharmacol,* 45**:** 1520-1523.

Modica-Napolitano, J. S. & Singh, K. K. (2004). Mitochondrial dysfunction in cancer. *Mitochondrion,* 4**:** 755-62.

Montironi, R., Mazzucchelli, R., Lopez-Beltran, A., Scarpelli, M. & Cheng, L. (2011). Prostatic intraepithelial neoplasia: its morphological and molecular diagnosis and clinical significance. *BJU Int,* 108**:** 1394-1399.

Moore, S., Knudsen, B., True, L. D., Hawley, S., Etzioni, R.*, et al.* (2005). Loss of stearoyl-CoA desaturase expression is a frequent event in prostate carcinoma. *Int J Cancer,* 114**:** 563-71.

Moyer, V. A. (2012). Screening for prostate cancer: U.S. Preventive Services Task Force recommendation statement. *Ann Intern Med,* 157**:** 120-134.

Mycielska, M. E., Patel, A., Rizaner, N., Mazurek, M. P., Keun, H.*, et al.* (2009). Citrate transport and metabolism in mammalian cells: prostate epithelial cells and prostate cancer. *Bioessays,* 31**:** 10-20.

National Cancer Intelligence Network and Cancer Research UK 2009. Cancer incidence and survival by major ethnic group, England 2002-2006.

Navone, N. M., Troncoso, P., Pisters, L. L., Goodrow, T. L., Palmer, J. L.*, et al.* (1993). p53 protein accumulation and gene mutation in the progression of human prostate carcinoma. *J Natl Cancer Inst,* 85**:** 1657-1669.

Nemeth, K. & Piskula, M. K. (2007). Food content, processing, absorption and metabolism of onion flavonoids. *Crit Rev Food Sci Nutr,* 47**:** 397-409.

NHS, 2015. *Prostate cancer screening* [Online]. Available: http://www.cancerscreening.nhs.uk/prostate/ [Accessed 03/09/2015].

Nice 2014. Prostate cancer: diagnosis and treatment. *NICE clinical guideline 175.*

Nickoloff, B. J., Lingen, M. W., Chang, B., Shen, M., Swift, M.*, et al.* (2004). Tumor suppressor maspin is up-regulated during keratinocyte senescence, exerting a paracrine antiangiogenic activity. *Cancer Res,* 64**:** 2956-2961.

Nomura, A. M. Y., Lee, J., Stemmermann, G. N. & Combs, J. G. F. (2000). Serum selenium and subsequent risk of prostate cancer. *Cancer Epidemiol Biomarkers Prev,* 9**:** 883-887.

Noori-Daloii, M. R., Momeny, M., Yousefi, M., Shirazi, F. G., Yaseri, M.*, et al.* (2011). Multifaceted preventive effects of single agent quercetin on a human prostate

adenocarcinoma cell line (PC-3): implications for nutritional transcriptomics and multi-target therapy. *Med Oncol,* 28**:** 1395-404.

Norbury, C. & Nurse, P. (1992). Animal cell cycles and their control. *Ann Rev Biochem,* 61**:** 441-470.

Nurmi, T., Mursu, J., Heinonen, M., Nurmi, A., Hiltunen, R.*, et al.* (2009). Metabolism of berry anthocyanins to phenolic acids in humans. *J Agric Food Chem,* 57**:** 2274-2281.

Paller, C. J. & Antonarakis, E. S. (2013). Management of biochemically recurrent prostate cancer after local therapy: evolving standards of care and new directions. *Clin Adv Hematol Oncol,* 11**:** 14-23.

Pan, C., Potter, S. R., Partin, A. W. & Epstein, J. I. (2000). The prognostic significance of tertiary Gleason patterns of higher grade in radical prostatectomy specimens. A proposal to modify the Gleason grading system. *Am J Surg Pathol,* 24**:** 563-569.

Pannek, J., Berges, R. R., Sauvageot, J., Lecksell, K. L., Epstein, J. I.*, et al.* (1999). Cell turnover in human seminal vesicles and the prostate: an immunohistochemical study. *Prostate Cancer Prostatic Dis,* 2**:** 200-203.

Parisotto, M. & Metzger, D. (2013). Genetically engineered mouse models of prostate cancer. *Mol Oncol,* 7**:** 190-205.

Park, H. U., Suy, S., Danner, M., Dailey, V., Zhang, Y.*, et al.* (2009). AMP-activated protein kinase promotes human prostate cancer cell growth and survival. *Mol Cancer Ther,* 8**:** 733-41.

Park, J.-H., Walls, J. E., Galvez, J. J., Kim, M., Abate-Shen, C.*, et al.* (2002). Prostatic Intraepithelial Neoplasia in Genetically Engineered Mice. *The American Journal of Pathology,* 161**:** 727-735.

Park, S. H., Chang, S. N., Baek, M. W., Kim, D. J., Na, Y. R.*, et al.* (2013). Effects of dietary high fat on prostate intraepithelial neoplasia in TRAMP mice. *Lab Anim Res,* 29**:** 39-47.

Parnes, H. L., House, M. G. & Tangrea, J. A. (2013). Prostate cancer prevention: strategies for agent development. *Curr Opin Oncol,* 25**:** 242-51.

Paschka, A. G., Butler, R. & Young, C. Y-F. (1998). Induction of apoptosis in prostate cancer cell lines by the green tea component, (-)-epigallocatechin-3-gallate. *Cancer Lett,* 130**:** 1-7.

Pashayan, N., Duffy, S. W., Pharoah, P., Greenberg, D., Donovan, J.*, et al.* (2009). Mean sojourn time, overdiagnosis, and reduction in advanced stage prostate cancer due

to screening with PSA: implications of sojourn time on screening. *Br J Cancer,* 100**:** 1198-204.

Patel, M. S. & Korotchkina, L. G. (2006). Regulation of the pyruvate dehydrogenase complex. *Biochem Soc Trans,* 34**:** 217-222.

Paweletz, C. P., Charboneau, L., Bichsel, V. E., Simone, N. L., Chen, T. M*., et al.* (2001). Reverse phase protein microarrays which capture disease progression show activation of pro-survival pathways at the cancer invasion front. *Oncogene,* 20**:** 1981-1989.

Peehl, D. M. (2005). Primary cell cultures as models of prostate cancer development. *Endocr Relat Cancer,* 12**:** 19-47.

Pelicano, H., Martin, D. S., Xu, R. H. & Huang, P. (2006). Glycolysis inhibition for anticancer treatment. *Oncogene,* 25**:** 4633-46.

Pelser, C., Mondul, A. M., Hollenbeck, A. R. & Park, Y. (2013). Dietary fat, fatty acids, and risk of prostate cancer in the NIH-AARP diet and health study. *Cancer Epidemiol Biomarkers Prev,* 22**:** 697-707.

Philip, J., Dutta Roy, S., Ballal, M., Foster, C. S. & Javle, P. (2005). Is a digital rectal examination necessary in the diagnosis and clinical staging of early prostate cancer? *BJU Int,* 95**:** 969-71.

Phillips, S. M. A., Barton, C. M., Lee, S. J., Morton, D. G., Wallace, D. M. A*., et al.* (1994). Loss of the retinoblastoma susceptibility gene (RB1) is a frequent and early event in prostatic tumorigenesis. *Br J Cancer,* 70**:** 1252-1257.

Pienta, K. J., Abate-Shen, C., Agus, D. B., Attar, R. M., Chung, L. W*., et al.* (2008). The current state of preclinical prostate cancer animal models. *Prostate,* 68**:** 629-39.

Pinto, J. T., Sinha, R., Papp, K., Facompre, N. D., Desai, D*., et al.* (2007). Differential effects of naturally occurring and synthetic organoselenium compounds on biomarkers in androgen responsive and androgen independent human prostate carcinoma cells. *Int J Cancer,* 120**:** 1410-7.

Podsypanina, K., Ellenson, L. H., Nemes, A., Gu, J., Tamura, M*., et al.* (1999). Mutation of Pten/Mmac1 in mice causes neoplasia in multiple organ systems. *Proc Natl Acad Sci U S A,* 96**:** 1563-1568.

Pourmand, G., Ziaee, A.-A., Abedi, A. R., Mehrsai, A., Alavi, H. A*., et al.* (2007). Role of PTEN gene in progression of prostate cancer. *Urol J,* 4**:** 95-100.

Powell, W. C., Cardiff, R. D., Cohen, M. B., Miller, G. J. & P., R.-B. (2003). Mouse strains for prostate tumorigenesis based on genes altered in human prostate cancer. *Curr Drug Targets,* 4**:** 263-279.

Pratheeshkumar, P., Budhraja, A., Son, Y.-O., Wang, X., Zhang, Z.*, et al.* (2012). Quercetin Inhibits Angiogenesis Mediated Human Prostate Tumor Growth by Targeting VEGFR- 2 Regulated AKT/mTOR/P70S6K Signaling Pathways. *PLoS One,* 7**:** e47516.

Prensner, J. R., Rubin, M. A., Wei, J. T. & Chinnaiyan, A. M. (2012). Beyond PSA: the next generation of prostate cancer biomarkers. *Sci Transl Med,* 4**:** 127rv3.

Preston-Martin, S., Pike, M. C., Ross, R. K. & Henderson, B. E. (1993). Epidemiologic evidence for the increased cell proliferation model of carcinogenesis. *Environ Health Perspect,* 101**:** 137-138.

Prieur, A., Besnard, E., Babled, A. & Lemaitre, J. M. (2011). p53 and p16(INK4A) independent induction of senescence by chromatin-dependent alteration of S-phase progression. *Nat Commun,* 2**:** 473.

Priulla, M., Calastretti, A., Bruno, P., Azzariti, A., Paradiso, A.*, et al.* (2007). Preferential chemosensitization of PTEN-mutated prostate cells by silencing the Akt kinase. *Prostate,* 67**:** 782-9.

Puzio-Kuter, A. M. (2011). The Role of p53 in Metabolic Regulation. *Genes Cancer,* 2**:** 385-91.

Rabbani, F., Stroumbakis, N., Kava, B. R., Cookson, M. S. & Fair, W. R. (1998). Incidence and clinical significance of false-negative sextant prostate biopsies. *J Urol,* 159**:** 1247-1250.

Ramírez De Molina, A., Rodríguez-González, A., Gutiérrez, R., Martínez-Piñeiro, L., Sánchez, J. J.*, et al.* (2002). Overexpression of choline kinase is a frequent feature in human tumor-derived cell lines and in lung, prostate, and colorectal human cancers. *Biochem Biophys Res Commun,* 296**:** 580-583.

Rao, A., Woodruff, R. D., Wade, W. N., Kute, T. E. & Cramer, S. D. (2002). Genistein and Vitamin D Synergistically Inhibit Human Prostatic Epithelial Cell Growth. *J Nutr,* 132**:** 3191-3194.

Redman, M. W., Tangen, C. M., Goodman, P. J., Lucia, M. S., Coltman, C. A., Jr.*, et al.* (2008). Finasteride does not increase the risk of high-grade prostate cancer: a bias-adjusted modeling approach. *Cancer Prev Res (Phila),* 1**:** 174-81.

Resende, F. A., Vilegas, W., Dos Santos, L. C. & Varanda, E. A. (2012). Mutagenicity of flavonoids assayed by bacterial reverse mutation (Ames) test. *Molecules,* 17**:** 5255-68.

Rietjens, I. M., Boersma, M. G., Van Der Woude, H., Jeurissen, S. M., Schutte, M. E.*, et al.* (2005). Flavonoids and alkenylbenzenes: mechanisms of mutagenic action and carcinogenic risk. *Mutat Res,* 574**:** 124-38.

Rishi, I., Baidouri, H., Abbasi, J. A., Bullard-Dillard, R., Kajdacsy-Balla, A.*, et al.* (2003). Prostate cancer in African American men is associated with downregulation of zinc transporters. *App. Immunohistochem. Mol. Morph.,* 11**:** 253-260.

Rodier, F. & Campisi, J. (2011). Four faces of cellular senescence. *J Cell Biol,* 192**:** 547-56.

Roehl, K. A., Han, M., Ramos, C. G., Antenor, J. A. & Catalona, W. J. (2004). Cancer progression and survival rates following anatomical radical retropubic prostatectomy in 3,478 consecutive patients: long-term results. *J Urol,* 172**:** 910-914.

Roehrborn, C. G., Nickel, J. C., Andriole, G. L., Gagnier, R. P., Black, L.*, et al.* (2011). Dutasteride improves outcomes of benign prostatic hyperplasia when evaluated for prostate cancer risk reduction: secondary analysis of the REduction by DUtasteride of prostate Cancer Events (REDUCE) trial. *Urology,* 78**:** 641-6.

Roninson, I. B. (2003). Tumor Cell Senescence in Cancer Treatment. *Cancer Res,* 63**:** 2705-2715.

Rossi, M., Bosetti, C., Negri, E., Lagiou, P. & La Vecchia, C. (2010). Flavonoids, proanthocyanidins, and cancer risk: a network of case-control studies from Italy. *Nutr Cancer,* 62**:** 871-7.

Rossi, S., Graner, E., Febbo, P., Weinstein, L., Bhattacharya, N.*, et al.* (2003). Fatty acid synthase expression defines distinct molecular signatures in prostate cancer. *Mol Cancer Res,* 1**:** 707-715.

Roth-Kauffman, M. (2011). Prostate cancer. *Clinician Reviews,* 21**:** 28-34.

Roudier, E. & Perrin, A. (2009). Considering the role of pyruvate in tumor cells during hypoxia. *Biochim Biophys Acta,* 1796**:** 55-62.

Roychowdhury, S. & Chinnaiyan, A. M. (2013). Advancing precision medicine for prostate cancer through genomics. *J Clin Oncol,* 31**:** 1866-73.

Rubin, M. A., Zhou, M., Dhanasekaran, S. M., Barrette, T. R., Sanda, M. G.*, et al.* (2002). alpha-Methylacyl coenzyme A racemase as a tissue biomarker for prostate cancer. *JAMA,* 287**:** 1662-1670.

Saad, S. E. A. 2011. *Preclinical evaluation of TMFol for the management of prostate cancer.* PhD, University of Leicester.

Saad, S. E., Jones, D. J., Norris, L. M., Horner-Glister, E., Patel, K. R*., et al.* (2012). Tissue distribution and metabolism of the putative cancer chemopreventive agent 3',4',5'-trimethoxyflavonol (TMFol) in mice. *Biomed Chromatogr,* 26**:** 1559-66.

Saad, S., Howells, L., Britton, R. G., Steward, W. P., Gescher, A*., et al.* (2010). 3', 4', 5'-Trimethoxyflavonol (TMFol), a novel putative prostate cancer chemopreventive agent: In vitro and in vivo preclinical activity *Cancer Prev Res,* 3**:** A104.

Sarveswaran, S., Liroff, J., Zhou, Z., Nikitin, A. Y. & Ghosh, J. (2010). Selenite triggers rapid transcriptional activation of p53, and p53-mediated apoptosis in prostate cancer cells: Implication for the treatment of early-stage prostate cancer. *Int J Oncol,* 36**:** 1419-1428.

Schröder, F. H., Hugosson, J., Roobol, M. J., Tammela, T. L., Ciatto, S*., et al.* (2009). Screening and prostate-cancer mortality in a randomized European study. *N Engl J Med,* 360**:** 1320-1328.

Schröder, F. H., Hugosson, J., Roobol, M. J., Tammela, T. L., Ciatto, S*., et al.* (2012). Prostate-cancer mortality at 11 years of follow-up. *N Engl J Med,* 366**:** 981-990.

Schwarze, S. R., Fu, V. X., Desotelle, J. A., Kenowski, M. L. & Jarrard, D. F. (2005). The Identification of Senescence-Specific Genes during the Induction of Senescence in Prostate Cancer Cells. *Neoplasia,* 7**:** 816-823.

SEER 18. (2014). *SEER Stat Fact Sheets: Prostate Cancer* [Online]. Available: http://seer.cancer.gov/statfacts/html/prost.html [Accessed 05/03/2015].

Selley, S., Donovan, J., Faulkner, A., Coast, J. & Gillat, D. (1997). Diagnosis, management and screening of early localised prostate cancer. *Health Technology Assessment,* 1**:** 1-96.

Shappell, S. B., Thomas, G. V., Roberts, R. L., Herbert, R., Ittman, M. M*., et al.* (2004). Prostate pathology of genetically engineered mice: definitions and classification. The consensus report from the Bar Harbor Meeting of the mouse models of human cancer consortium prostate pathology committee. *Cancer Res,* 64**:** 2270-2305.

Sharma, A., Yeow, W.-S., Ertel, A., Coleman, I., Clegg, N*., et al.* (2010). The retinoblastoma tumor suppressor controls androgen signaling and human prostate cancer progression. *J Clin Invest.,* 120**:** 4478-4492.

Shaw, R. J. (2009). LKB1 and AMP-activated protein kinase control of mTOR signalling and growth. *Acta Physiol (Oxf),* 196**:** 65-80.

Shen, J., Klein, R. D., Wei, Q., Guan, Y., Contois, J. H*., et al.* (2000). Low-dose genistein induces cyclin-dependent kinase inhibitors and G1 cell-cycle arrest in human prostate cancer cells. *Mol Carcinog,* 29**:** 92-102.

Sherr, C. J. & Roberts, J. M. (1995). Inhibitors of mammalian G1 cyclin-dependent kinases. *Genes Dev,* 9**:** 1149-1163.

Sherr, C. J. (1994). G1 phase progression: Cycling on cue. *Cell,* 79**:** 551-555.

Shiau, C. W., Huang, J. W., Wang, D. S., Weng, J. R., Yang, C. C*., et al.* (2006). alpha-Tocopheryl succinate induces apoptosis in prostate cancer cells in part through inhibition of Bcl-xL/Bcl-2 function. *J Biol Chem,* 281**:** 11819-25.

Shimizu, H., Ross, R. K., Bernstein, L., Yatani, R., Henderson, B. E*., et al.* (1991). Cancers of the prostate and breast among Japanese and white immigrants in Los Angeles County. *Br J Cancer,* 63**:** 963-966.

Shirai, T., Sano, M., Tamano, S., Takahashi, S. & Hirose, M. (1997). The prostate a target for carcinogenicity of 2-amino-1-methyl-6-phenylimidazo[4,5-b]pyridine (PhIP) derived from cooked foods. *Cancer Res,* 57**:** 195-198.

Shukla, S. & Gupta, S. (2005). Dietary agents in the chemoprevention of prostate cancer. *Nutr Cancer,* 53**:** 18-32.

Shukla, S. & Gupta, S. (2014). Apigenin-induced Cell Cycle Arrest is Mediated by Modulation of MAPK, PI3K-Akt, and Loss of Cyclin D1 Associated Retinoblastoma Dephosphorylation in Human Prostate Cancer Cells. *Cell Cycle,* 6**:** 1102-1114.

Siddiqui, I. A., Adhami, V. M., Saleem, M. & Mukhtar, H. (2006). Beneficial effects of tea and its polyphenols against prostate cancer. *Mol Nutr Food Res,* 50**:** 130-43.

Siddiqui, I. A., Asim, M., Hafeez, B. B., Adhami, V. M., Tarapore, R. S*., et al.* (2011). Green tea polyphenol EGCG blunts androgen receptor function in prostate cancer. *FASEB J,* 25**:** 1198-207.

Siddiqui, I. A., Malik, A., Adhami, V. M., Asim, M., Hafeez, B. B*., et al.* (2008). Green tea polyphenol EGCG sensitizes human prostate carcinoma LNCaP cells to TRAIL-mediated apoptosis and synergistically inhibits biomarkers associated with angiogenesis and metastasis. *Oncogene,* 27**:** 2055-63.

Siler, U., Barella, L., Spitzer, V., Schnorr, J., Lein, M*., et al.* (2004). Lycopene and vitamin E interfere with autocrine/paracrine loops in the Dunning prostate cancer model. *FASEB J,* 18**:** 1019-1021.

Simmons, M. N., Berglund, R. K. & Jones, J. S. (2011). A practical guide to prostate cancer diagnosis and management. *Cleve Clin J Med,* 78**:** 321-31.

Simon, E., Bartlett, K. & Pourfarzam, M. (1996). Mammalian mitochondrial beta-oxidation. *Biochem J,* 320**:** 345-357.

Singh, K. K., Desouki, M. M., Franklin, R. B. & Costello, L. C. (2006). Mitochondrial aconitase and citrate metabolism in malignant and nonmalignant human prostate tissues. *Mol Cancer,* 5**:** 14.

Singh, R. P. & Agarwal, R. (2006). Mechanisms of action of novel agents for prostate cancer chemoprevention. *Endocr Relat Cancer,* 13**:** 751-78.

Sinha, R., Park, Y., Graubard, B. I., Leitzmann, M. F., Hollenbeck, A.*, et al.* (2009). Meat and meat-related compounds and risk of prostate cancer in a large prospective cohort study in the United States. *Am J Epidemiol,* 170**:** 1165-77.

Sirovich, B. E., Schwaztz, L. M. & Woloshin, S. (2003). Screening men for prostate and colorectal cancer in the United States. Does practice reflect the evidence? *JAMA,* 289**:** 1414-1420.

Society, A. C. 2015. *Prostate Cancer* [Online]. Available: http://www.cancer.org/cancer/prostatecancer/ [Accessed 05/03/2015].

Sramkoski, R. M., Pretlow Ii, T. G., Giaconia, J. M., Pretlow, T. P., Schwartz, S.*, et al.* (1999). A new human prostate carcinoma cell line, 22Rv1. *In vitro Cell Dev Biol Anim,* 35**:** 403-409.

Stein, G. H., Drullinger, L. F., Soulard, A. & Dulic, V. (1999). Differential roles for cyclin-dependent kinase inhibitors p21 and p16 in the mechanisms of senescence and differentiation in human fibroblasts. *Mol Cell Biol,* 19**:** 2109-2117.

Steward, W. P. & Brown, K. (2013). Cancer chemoprevention: a rapidly evolving field. *Br J Cancer,* 109**:** 1-7.

Suganuma, N., Segade, F., Matsuzu, K. & Bowden, D. W. (2007). Differential expression of facilitative glucose transporters in normal and tumour kidney tissues. *BJU Int,* 99**:** 1143-9.

Sugimura, T., Wakabayashi, K., Nakagama, H. & Nagao, M. (2004). Heterocyclic amines: Mutagens carcinogens produced during cooking of meat and fish. *Cancer Sci,* 95**:** 290-299.

Suh, Y., Afaq, F., Khan, N., Johnson, J. J., Khusro, F. H.*, et al.* (2010). Fisetin induces autophagic cell death through suppression of mTOR signaling pathway in prostate cancer cells. *Carcinogenesis,* 31**:** 1424-33.

Sun, S. Y., Hail, N. & Lotan, R. (2004). Apoptosis as a Novel Target for Cancer Chemoprevention. *J Natl Cancer Inst,* 96**:** 662-672.

Surh, Y. (1999). Molecular mechanisms of chemopreventive effects of selected dietary and medicinal phenolic substances. *Mutat Res,* 428: 305-327.

Suzuki, A., Luis De La Pompa, J., Stambolic, V., Elia, A. J., Sasaki, T*., et al.* (1998). High cancer susceptibility and embryonic lethality associated with mutation of the PTEN tumor suppressor gene in mice. *Curr Biol,* 8**:** 1169-1178.

Swinnen, J. V., Roskams, T., Joniau, S., Van Poppel, H., Oyen, R*., et al.* (2002). Overexpression of fatty acid synthase is an early and common event in the development of prostate cancer. *Int J Cancer,* 98**:** 19-22.

Swinnen, J. V., Vanderhoydonc, F., Elgamal, A. A., Eelen, M., Vercaeren, I*., et al.* (2000). Selective activation of the fatty acid synthesis pathway in human prostate cancer. *Int J Cancer,* 88**:** 176-179.

Swords, K., Wallen, E. M. & Pruthi, R. S. (2010). The impact of race on prostate cancer detection and choice of treatment in men undergoing a contemporary extended biopsy approach. *Urol Oncol,* 28**:** 280-4.

Syed, D. N., Suh, Y., Afaq, F. & Mukhtar, H. (2008). Dietary agents for chemoprevention of prostate cancer. *Cancer Lett,* 265**:** 167-76.

Tennant, D. A., Duran, R. V. & Gottlieb, E. (2010). Targeting metabolic transformation for cancer therapy. *Nat Rev Cancer,* 10**:** 267-77.

Thilakarathna, S. H. & Rupasinghe, H. P. (2013). Flavonoid bioavailability and attempts for bioavailability enhancement. *Nutrients,* 5**:** 3367-87.

Thomas, L. N., Douglas, R. C., Lazier, C. B., Gupta, R., Norman, R. W*., et al.* (2008). Levels of 5alpha-reductase type 1 and type 2 are increased in localized high grade compared to low grade prostate cancer. *J Urol,* 179**:** 147-151.

Thompson, D., Easton, D. F. & Consortium, T. B. C. L. (2002). Cancer Incidence in BRCA1 mutation carriers. *J Natl Cancer Inst,* 94**:** 1358-1365.

Thompson, I. M. J., Cabang, A. B. & Wargovich, M. J. (2014). Future directions in the prevention of prostate cancer. *Nat Rev Clin Oncol,* 11**:** 49-60.

Thompson, I. M., Pauler Ankerst, D., Chi, C., Lucia, M. S., Goodman, P. J*., et al.* (2005). Operating Characteristics of Prostate-Specific Antigen in Men With an Initial PSA Level of 3 0 ng/mL or Lower *JAMA,* 294**:** 66-70.

Thompson, I. M., Pauler, D. K., Goodman, P. J., Tangen, C. M., Lucia, M. S*., et al.* (2004). Prevalence of Prostate Cancer among Men with a Prostate-Specific Antigen Level ≤4.0 ng per Milliliter. *N Engl J Med,* 350**:** 2239-2246.

Toivanen, R., Taylor, R. A., Pook, D. W., Ellem, S. J. & Risbridger, G. P. (2012). Breaking through a roadblock in prostate cancer research: an update on human model systems. *J Steroid Biochem Mol Biol,* 131**:** 122-31.

Tomlinson, I. P., Alam, N. A., Rowan, A. J., Barclay, E., Jaeger, E. E.*, et al.* (2002). Germline mutations in FH predispose to dominantly inherited uterine fibroids, skin leiomyomata and papillary renal cell cancer. *Nat Genet,* 30**:** 406-10.

Trock, B. J. (2001). Validation of surrogate endpoint biomarkers in prostate cancer chemoprevention trials. *Urology,* 57**:** 241-247.

Trotman, L. C., Niki, M., Dotan, Z. A., Koutcher, J. A., Di Cristofano, A.*, et al.* (2003). Pten dose dictates cancer progression in the prostate. *PLoS Biol,* 1**:** E59.

Tsugane, S. & Sawada, N. (2014). The JPHC study: design and some findings on the typical Japanese diet. *Jpn J Clin Oncol,* 44**:** 777-82.

Tsui, K. H., Feng, T. H., Lin, Y. F., Chang, P. L. & Juang, H. H. (2011). p53 downregulates the gene expression of mitochondrial aconitase in human prostate carcinoma cells. *Prostate,* 71**:** 62-70.

Valkenberg, K. C. & Williams, B. O. (2011). Mouse models of prostate cancer. *Prostate Cancer,* 2011: 895238.

Van Bokhoven, A., Varella-Garcia, M., Korch, C., Johannes, W. U., Smith, E. E.*, et al.* (2003). Molecular characterization of human prostate carcinoma cell lines. *Prostate,* 57**:** 205-25.

van den Brandt, P. A., Zeegers, M. P. A., Bode, P. & Goldbohm, R. A. (2003). Toenail selenium levels and the subsequent risk of prostate cancer: A prospective cohort study. *Cancer Epidemiol Biomarkers Prev,* 12**:** 866-871.

Vander Heiden, M. G., Cantley, L. C. & Thompson, C. B. (2009). Understanding the Warburg effect: The metabolic requirements of cell proliferation. *Science,* 324**:** 1029-1033.

Vaz, C. V., Alves, M. G., Marques, R., Moreira, P. I., Oliveira, P. F.*, et al.* (2012). Androgen-responsive and nonresponsive prostate cancer cells present a distinct glycolytic metabolism profile. *Int J Biochem Cell Biol,* 44**:** 2077-84.

Venkateswaran, V., Fleshner, N. E., Sugar, L. M. & Klotz, L. H. (2004). Antioxidants Block Prostate Cancer in *Lady* Transgenic Mice. *Cancer Res,* 64**:** 5891-5896.

Venkateswaran, V., Klotz, L. H., Ramani, M., Sugar, L. M., Jacob, L. E.*, et al.* (2009). A combination of micronutrients is beneficial in reducing the incidence of prostate

cancer and increasing survival in the Lady transgenic model. *Cancer Prev Res (Phila),* 2**:** 473-83.

Ventura, A., Kirsch, D. G., Mclaughlin, M. E., Tuveson, D. A., Grimm, J.*, et al.* (2007). Restoration of p53 function leads to tumour regression in vivo. *Nature,* 445**:** 661-5.

Vermes, I., Haanen, C., Steffens-Nakken, H. & Reutelingsperger, C. (1995). A novel assay for apoptosis. Flow cytometric detection of phosphatidylserine expression on early apoptotic cells using fluorescein labelled Annexin V. *J Immunol Methods,* 184**:** 39-51.

Walle, T., Ta, N., Kawamori, T., Wen, X., Tsuji, P. A.*, et al.* (2007). Cancer chemopreventive properties of orally bioavailable flavonoids--methylated versus unmethylated flavones. *Biochem Pharmacol,* 73**:** 1288-96.

Wang, J., Eltoum, I. E. & Lamartiniere, C. A. (2007). Genistein chemoprevention of prostate cancer in TRAMP mice. *J Carcinog,* 6**:** 3.

Wang, S., Gao, J., Lei, Q., N., R., Pritchard, C.*, et al.* (2003). Prostate-specific deletion of the murine Pten tumor suppressor gene leads to metastatic prostate cancer. *Cancer Cell,* 4**:** 209-221.

Wang, S., Gao, J., Lei, Q., Rozengurt, N., Pritchard, C.*, et al.* (2003). Prostate-specific deletion of the murine Pten tumor suppressor gene leads to metastatic prostate cancer. *Cancer Cell,* 4**:** 209-221.

Wang, Y., Xue, H., Cutz, J. C., Bayani, J., Mawji, N. R.*, et al.* (2005). An orthotopic metastatic prostate cancer model in SCID mice via grafting of a transplantable human prostate tumor line. *Lab Invest,* 85**:** 1392-404.

WCRF 2014. Diet, Nutrition, Physical Activity, and Prostate Cancer. *World Cancer Research Fund International/American Institute for Cancer Research Continuous Update Project Report.*

Weston, A. & Harris, C. C. 2003. Multistage carcinogenesis. *In:* KUFE, D. W., POLLOCK, R. E., WEICHSELBAUM, R. R., BAST, J., R.C., GANSLER, T. S. et al (eds.) *Holland-Frei Cancer Medicine. 6th edition.* Hamilton, ON: BC Decker.

Wilson, J. D., Griffin, J. E., Leshin, M. & George, F. W. (1981). Role of gonadal hormones in development of the sexual phenotypes. *Hum Genet,* 58**:** 78-84.

Wolf, A. M., Wender, R. C., Etzioni, R. B., Thompson, I. M., D'amico, A. V.*, et al.* (2010). American Cancer Society guideline for the early detection of prostate cancer: update 2010. *CA Cancer J Clin,* 60**:** 70-98.

Workman, P., Aboagye, E. O., Balkwill, F., Balmain, A., Bruder, G.*, et al.* (2010). Guidelines for the welfare and use of animals in cancer research. *Br J Cancer,* 102**:** 1555-77.

Wu, X., Wu, J., Huang, J., Powell, W. C., Zhang, J.*, et al.* (2001). Generation of a prostate epithelial cell-specific Cre transgenic mouse model for tissue-specific gene ablation. *Mech Dev,* 101**:** 61-69.

Xu, R., Zhang, Y., Ye, X., Xue, S., Shi, J.*, et al.* (2013). Inhibition effects and induction of apoptosis of flavonoids on the prostate cancer cell line PC-3 in vitro. *Food Chem,* 138**:** 48-53.

Xue, W., Zender, L., Miething, C., Dickins, R. A., Hernando, E.*, et al.* (2007). Senescence and tumour clearance is triggered by p53 restoration in murine liver carcinomas. *Nature,* 445**:** 656-60.

Yokota, J. (2000). Tumor progression and metastasis. *Carcinogenesis,* 21: 497-503.

Yoshimoto, M., Cutz, J. C., Nuin, P. A., Joshua, A. M., Bayani, J.*, et al.* (2006). Interphase FISH analysis of PTEN in histologic sections shows genomic deletions in 68% of primary prostate cancer and 23% of high-grade prostatic intra-epithelial neoplasias. *Cancer Genet Cytogenet,* 169**:** 128-37.

Yu, H. & Berkel, H. (1999). Insulin-like growth factors and cancer. *J La State Med Soc.,* 151**:** 218-223.

Yu, H., Harris, R. E., Gao, Y.-T., Gao, R. & Wynder, E. L. (1991). Comparative epidemiology of cancers of the colon, rectum, prostate and breast in Shanghai, China versus the United States. *Int J Epidemiol,* 20**:** 76-81.

Yuan-Jing, F., Nan-Shan, H. & Lian, X. (2009). Genistein synergizes with RNA interference inhibiting survivin for inducing DU-145 of prostate cancer cells to apoptosis. *Cancer Lett,* 284**:** 189-97.

Zadra, G., Photopoulos, C. & Loda, M. (2013). The fat side of prostate cancer. *Biochim Biophys Acta,* 1831**:** 1518-32.

Zadra, G., Photopoulos, C., Tyekucheva, S., Heidari, P., Weng, Q. P.*, et al.* (2014). A novel direct activator of AMPK inhibits prostate cancer growth by blocking lipogenesis. *EMBO Mol Med,* 6**:** 519-38.

Zheng, J., Yang, B., Huang, T., Yu, Y., Yang, J.*, et al.* (2011). Green tea and black tea consumption and prostate cancer risk: an exploratory meta-analysis of observational studies. *Nutr Cancer,* 63**:** 663-72.

Zhivotovsky, B. & Orrenius, S. (2006). Carcinogenesis and apoptosis: paradigms and paradoxes. *Carcinogenesis,* 27**:** 1939-45.

Zhong, W. & Oberley, T. D. (2001). Redox-mediated effects of selenium on apoptosis and cell cycle in the LNCaP human prostate cancer cell line. *Cancer Res,* 61**:** 7071-7078.

Zhou, P., Chen, M. H., Mcleod, D., Carroll, P. R., Moul, J. W.*, et al.* (2005). Predictors of prostate cancer-specific mortality after radical prostatectomy or radiation therapy. *J Clin Oncol,* 23**:** 6992-8.

Zhou, Z., Flesken-Nikitin, A., Corney, D. C., Wang, W., Goodrich, D. W.*, et al.* (2006). Synergy of p53 and Rb deficiency in a conditional mouse model for metastatic prostate cancer. *Cancer Res,* 66**:** 7889-98.

Zijp, I. M., Korver, O. & Tijburg, L. B. (2000). Effect of tea and other dietary factors on iron absorption. *Crit Rev Food Sci Nutr,* 40**:** 371-98.

Zinchenko, V. P., Goncharov, N. V., Teplova, V. V., Kasymov, V. A., Petrova, O. I.*, et al.* (2007). Interaction of intracellular signalling and metabolic pathways at inhibition of mitochondrial aconitase by fluoroacetate. *Cell and Tissue Biology,* 1**:** 541-550.

Zu, K. & Ip, C. (2003). Synergy between selenium and vitamin E in apoptosis induction is associated with activation of distinctive initiator caspases in human prostate cancer cells. *Cancer Res,* 63**:** 6988-6995.